Ascending and Descending Projections of Cholinergic, GABAergic and Glutamatergic Basal Forebrain Neurons and their Role in Cortical Activity and Sleep-Wake States

Pablo Henny V.

Department of Neurology and Neurosurgery

Montreal Neurological Institute

McGill University

Montreal, August 2006

Supervisor

Barbara E. Jones, Ph.D.

A thesis submitted to McGill University in partial fulfillment of the requirements of the degree of Doctor of Philosophy, Ph.D., in Neurological Sciences

Your file Votre référence
ISBN: 978-0-494-32357-1
Our file Notre référence
ISBN: 978-0-494-32357-1

To those who gave me life and those that

have continuously changed it since then

My beloved wife Isabel

My parents Enrique and Fresia

My sister Alejandra

My grandmothers Fresia and Lucía

My friends Nicolás, Claudio, Myrna,

Andrés, Maricarmen, Alex, Daniel

My teachers Sonia, Jorge and Barbara

Acknowledgments

I would like to express my utmost gratitude to my supervisor and exceptional mentor, Dr. Barbara E. Jones, for her kind, coherent, continuous and fruitful guidance over these years, since my arrival in Montreal on September 2001.

I am also thankful to all my colleagues with which I have shared a constructive, non-competitive, unselfish and friendly everyday collaborative experience. Names come easily to mind, Dr. Ian Manns, Dr. Maan Gee Lee, Dr. Mandana Modirrousta as well as current colleagues Dr. Thomas Stroh, Dr. Frédéric Brischoux, Amélie Perron, Dr. Oum Hassani, Soufiane Boucetta and Dr. Chris Córdova.

I also take this opportunity to thank my advisory committee members, the late Dr. Angel Alonso, Dr. Alain Beaudet and Dr. Edith Hamel for their guidance during my graduate years.

Finally, my deepest gratitude goes to Naomi Takeda and Lynda Mainville, our administrative assistant and technician for their helpful support, indisputable professionalism and kind spirit which, without any doubt, I will truly miss after my departure.

NOTE TO REVIEWERS

This thesis work consists of four manuscripts, whose authorship, title, status and corresponding chapters are provided as follow:

1. Ivana Gritti, Pablo Henny, Francesca Galloni, Lynda Mainville, Maurizio Mariotti and Barbara E. Jones: "Stereological estimates of the basal forebrain cell population in the rat, comprising neurons containing choline acetyltransferase, glutamic acid decarboxylase and phosphate-activated glutaminase and colocalizing vesicular glutamate transporters", in revision. **Chapter I.**
2. Pablo Henny and Barbara E. Jones: "Basal Forebrain Axon Terminals Containing Vesicular Transporters for Acetylcholine (VAChT), GABA (VGAT) or Glutamate (VGluT) in Rat Prefrontal Cortex", in preparation. **Chapter II.**
3. Pablo Henny and Barbara E. Jones: "Vesicular glutamate (VGluT), GABA (VGAT), and acetylcholine (VAChT) transporters in basal forebrain axon terminals innervating the lateral hypothalamus". The Journal of Comparative Neurology, 496(4):453-67. (2006). **Chapter III.**
4. Pablo Henny and Barbara E. Jones: "Innervation of Orexin/Hypocretin Neurons by GABAergic, Glutamatergic or Cholinergic Basal Forebrain Terminals Evidenced by Immunostaining for Presynaptic Vesicular Transporter and Postsynaptic Scaffolding Proteins". The Journal of Comparative Neurology, 499(4):645-61. (2006). **Chapter IV.**

PERSONAL CONTRIBUTION TO CHAPTERS

Chapter I: As a co-author in the first manuscript I got involved in part of the data analysis presented in Table 1. In addition, I was in full charge of the acquisition and posterior analysis of data concerning double immunohistochemistry for the synthetic enzymes and VGluT3.

Chapters II, III and IV: As a first author in the rest of the manuscripts, I was in charge of almost all the generation, acquisition, analysis and presentation of data provided. That included: animal surgery, brain tissue processing, double and triple immunohistochemical procedures, stereological and other quantitative analysis from tissue processed for light, epifluorescent and confocal microscopy as well as the generation of all tables and figures. I was also involved in the writing of all the manuscript drafts, under the direction and guidance of my supervisor.

TABLE OF CONTENTS

Ascending and Descending Projections of Cholinergic, GABAergic and Glutamatergic Basal Forebrain Neurons and their Role in Cortical Activity and Sleep-Wake States

Pablo Henny V.

Department of Neurology and Neurosurgery

Montreal Neurological Institute

McGill University

Montreal, August 2006

When I'm in the middle of a dream

Stay in bed, float up stream

Please, don't wake me, no, don't shake me

Leave me where I am ...

"I'm Only Sleeping" by Lennon/McCartney

(Album Revolver, The Beatles, 1966)

ABSTRACT

The basal forebrain (BF) plays multiple and divergent roles in the modulation of cortical activity and the control of sleep-wake states. BF neurons project to cortex, where they promote cortical activation during wakefulness (W) and paradoxical sleep (PS). Other neurons may conversely promote the appearance of slow wave activity (SWA) that occurs during slow wave sleep (SWS). BF neurons also send projections to the lateral hypothalamus (LH), a wake- and arousal-promoting region and whose inhibition by the BF is thought to facilitate the appearance of behavioral quiescence and sleep. It is likely that these multiple roles are carried out by the heterogeneous population that comprises the BF, which include cholinergic, GABAergic and as yet putative glutamatergic neurons which, as shown by retrograde tracing, innervate these areas. To better understand the mechanisms through which BF neurons modulate cortical activity and sleep-wake states, research was carried out to determine the numbers of cholinergic, GABAergic and putative glutamatergic neurons in the BF, and to examine their respective efferent projections to the cortex and LH. Following stereological quantification of immunohistochemically identified ACh-, GABA- and glutamate-synthesizing neurons, anterograde transport of biotinylated dextran amine 10,000 MW (BDA) in magnocellular BF neurons was combined with immunohistochemistry for vesicular transporter proteins (VTPs) for ACh (VAChT), GABA (VGAT) or glutamate (VGluT) for identification of BF terminals in prefrontal cortex (PFC) and LH. Subsequent stereological analysis was used to determine contributions of cholinergic, GABAergic and newly identify glutamatergic BF axon terminals to these areas. There, triple fluorescent

staining was performed to describe the innervation by BF terminals of pyramidal and interneuronal cell groups in the PFC and of the orexin/hypocretin cell population in the LH. Additional triple staining with postsynaptic markers was used to provide evidence for synaptic contacts. Together, these findings demonstrate the existence of at least three neuronal contingents of BF neurons, which may have the capacity to modulate the activity of cortical or LH neurons and thus, to control different aspects of cortical activity and sleep-wake states.

RÉSUMÉ

Le télencéphale basal (TB) joue des rôles multiples et divergents dans la modulation de l'activité corticale et le contrôle des états de veille-sommeil. Certains neurones du TB projètent dans le cortex cérébral, où ils promeuvent l'activation corticale durant l'éveil et le sommeil paradoxal alors que d'autres neurones peuvent au contraire promouvoir l'apparition de l'activité à ondes lentes qui se produit durant le sommeil lent. Par ailleurs, des neurones du TB envoient des projections dans l'hypothalamus latéral, une région promouvant l'éveil et dont l'inhibition par le TB semble faciliter l'apparition de la passivité comportementale et du sommeil. Il est probable que ces multiples rôles sont exécutés par la population neuronale hétérogène que comprend le TB et qui inclut des neurones cholinergiques, GABAergiques et encore présumés glutamatergiques dont on sait par des techniques de traçage rétrograde des voies nerveuses qu'ils innervent le cortex cérébral et l'hypothalamus latéral. Afin de mieux comprendre les mécanismes à travers lesquels ces neurones modulent l'activité corticale et les états de veille-sommeil, nous avons cherché à déterminer le nombre de neurones cholinergiques, GABAergiques et présumés glutamatergiques dans le TB et à examiner leurs projections respectives dans le cortex cérébral et de l'hypothalamus latéral. Ainsi, après avoir quantifié par stéréologie les neurones identifiés par immunohistochimie dans le TB comme synthétisant l'acétylcholine, le GABA ou le glutamate, le transport antérograde du dextran amine biotinylé de 10000 Da dans les neurones magnocellulaires du TB a été combiné avec une détection immunohistochimique des transporteurs vésiculaires de l'acétylcholine, du GABA ou du glutamate afin d'en identifier les axones terminaux dans le cortex

préfrontal et l'hypothalamus latéral. Ultérieurement, une analyse stéréologique dans ces régions a été utilisée pour déterminer la contribution des axones terminaux cholinergiques, GABAergiques et nouvellement identifiés glutamatergiques. En outre, des triples marquages fluorescents ont été effectués pour décrire l'innervation par les axones du TB des cellules pyramidales et des interneurones dans le cortex préfrontal et des neurones à orexine/hypocrétine dans l'hypothalamus latéral. Enfin, d'autres triples marquages avec des marqueurs postsynaptiques ont été utilisés pour indiquer de possibles contacts synaptiques. En conclusion, nos travaux démontrent l'existence d'au moins trois contingents de neurones du TB qui peuvent avoir la capacité de moduler l'activité des neurones du cortex cérébral ou de l'hypothalamus latéral et ainsi de contrôler les différents aspects de l'activité corticale et des états de veille-sommeil.

INTRODUCTION

Mammals continuously alternate between three unique and distinctive behavioral states: wakefulness (W), slow wave sleep (SWS) and paradoxical sleep (PS). Each of these states is characterized by a particular combination of behavioral features and physiological correlates. W is behaviorally characterized by alertness, responsiveness, movement and goal directed behavior, which are physiologically paralleled by a low sensory threshold, high muscle tone, a relatively high sympathetic tone and, as indicated by the electroencephalogram (EEG), the presence of low voltage/high frequency activity. Conversely, SWS (also known as non-rapid eye movement sleep, NREM) is distinguished by behavioral quiescence, higher sensory thresholds, lower muscle tone, increased parasympathetic tone and an EEG comprised by high amplitude/low frequency activity (~0.5 to 4 Hz), generally known as slow wave activity (SWA). PS (also called rapid eye movement sleep, REM) is also characterized by behavioral sleep, higher sensory threshold, absence of muscle tone (or atonia) and yet, by an activated EEG exhibiting low voltage/high frequency activity, "paradoxically" resembling that of W (Jouvet, 1965; Jones, 2005b, c; Steriade, 2005).

The generation of these states and associated phenomena are controlled by different regions and systems within the central nervous system (CNS) and whose dysfunction has been proposed to underlie the appearance of sleep- or sleep related-disorders including insomnia, restless legs syndrome, REM sleep behavior disorder and narcolepsy (Mignot et al., 2002; Jones, 2005b). Therefore, the study of the mechanisms by which these CNS regions promote and coordinate their

occurrence is relevant in the design of therapies and drugs aimed to treat them (Mignot et al., 2002; Jones, 2005a).

Among CNS regions, the basal forebrain (BF, Figure 1) has been shown to play a critical role in the expression of cortical activation that occurs during W and PS (Buzsaki et al., 1988; Berntson et al., 2002; Jones, 2004) as well as on the direct promotion of sleep (Sterman and Clemente, 1962a, 1962b; Szymusiak and McGinty, 1986a; Jones, 2005a). Through widespread projections to the cortical mantle (Kievit and Kuypers, 1975; Luiten et al., 1987; Gritti et al., 1997) BF neurons promote theta (~5 to 10 Hz) and gamma activity (>30 Hz) (Stewart et al., 1984; Lee et al., 1994; Cape and Jones, 2000; Berntson et al., 2002; Jones, 2004), both correlates of cortical activation and associated with other various cortical functions including neuronal plasticity, sensory processing, sensory binding, memory formation and consciousness (Llinas and Ribary, 1993; Buzsaki and Chrobak, 1995; Jefferys et al., 1996; Sarter et al., 2003; Jones, 2004).

Reciprocally, the BF promotes the appearance of cortical SWA that occurs during SWS as well as the generation of sleep itself, as stimulation of the BF leads to SWA and sleep (Sterman and Clemente, 1962a, 1962b; Szymusiak and McGinty, 1986a; Jones, 2005a), and conversely, lesions of the BF are associated with sleep loss and insomnia (von Economo, 1930; Nauta, 1946; McGinty and Sterman, 1968; Szymusiak and McGinty, 1986a).

It is likely that these various and divergent roles are carried out by chemically differentiated groups of neurons that populate the BF (Jones, 2005a). As suggested by several early studies (Krnjevic, 1967; Shute and Lewis, 1967; Johnston et al., 1979; Lehmann et al., 1980), and confirmed by many others

(Kimura et al., 1980; Rye et al., 1984; Wainer and Rye, 1984; Gritti et al., 1997), there is a population of cholinergic neurons in the BF which send prominent projections to the cortex (Figure 2). These neurons have been shown to participate in cortical activation that occurs during W and PS (Jasper and Tessier, 1971; Stewart et al., 1984; Manns et al., 2000a; Berntson et al., 2002; Lee et al., 2005b), as well as in cognitive and behavioral processes that are mediated by the cortex (Everitt and Robbins, 1997; Sarter et al., 2003), as most evidently demonstrated by the deficits of cortical and cognitive function seen in Alzheimer's disease, which is associated with loss of cholinergic activity in the cortex (Davies and Maloney, 1976; Rossor et al., 1982) and a decrease in cortical activation (Jeong, 2004).

Another major population of neurons that project to the cortex is GABAergic (Figure 2) (Zaborszky et al., 1986; Fisher et al., 1988; Gritti et al., 1997), which is part of a numerous population of GABAergic neurons that exist in the BF (Young et al., 1984; Brashear et al., 1986; Gritti et al., 1993). Although less is known about their role in cortical function, anatomical and physiological studies have suggested that subgroups of GABAergic BF neurons may play divergent roles in cortical activity, either by promoting cortical activation of W and PS (Freund and Gulyas, 1991; Manns et al., 2000b, 2003a) or SWA of SWS (Manns et al., 2000b; Jones, 2005a).

In addition to cortical projections, GABAergic and a few cholinergic neurons provide a descending projection to the lateral hypothalamus (LH, Figure 3) (Gritti et al., 1994). It has been proposed that this inhibitory projection may facilitate the appearance of behavioral quiescence and sleep (Gritti et al., 1994;

Manns et al., 2003b; Jones, 2005a), given the long known role of the LH in the behavioral display of arousal and the promotion of wakefulness (Nauta, 1946; Hess, 1957; Lin et al., 1989; Sakai et al., 1990). Critically, it has been recently shown that neurons in the LH, which contain the peptide Orexin (Orx, or Hypocretin), play a cardinal role in the maintenance of W, as their absence leads to narcolepsy (de Lecea et al., 1998; Peyron et al., 1998; Sakurai et al., 1998; Chemelli et al., 1999; Lin et al., 1999). Thus, it is plausible that the sleep promoting role of the BF may be carried out by direct inhibition of the LH and Orx neurons (Jones, 2005a).

In spite this relatively vast knowledge about BF organization, there are several aspects of its anatomy that remain unsolved and may be relevant to our understanding of the mechanisms by which the BF modulates cortical activity and sleep-wake states.

Retrograde tracing studies have estimated that cholinergic and GABAergic neurons represent ~25% and ~45% of the total contingent of BF neurons projecting to the cortex (Gritti et al., 1997) and ~3% and ~20% of those projecting to the LH (Gritti et al., 1994), respectively. These results indicate that another non-cholinergic, non-GABAergic population must also participate in these projections and thus be part of the influence that the BF has over the cortex and LH (Figures 2 and 3). As recently proposed, they may comprise glutamate-synthesizing neurons given the presence of the enzyme phosphate activated glutaminase (PAG), which is thought to participate in the synthesis of the neurotransmitter glutamate (Bradford et al., 1978; Kaneko and Mizuno, 1988) in a large, yet unknown, number of BF neurons and in ~80% of those projecting to the

cortex (Manns et al., 2001). However, it is not known whether BF neurons may have the actual mechanisms to release glutamate from their axon terminals. Moreover, since PAG is also coexpressed in the vast majority of cholinergic (~95%) and a large proportion of GABAergic (~60%) neurons, these results also indicate that in addition to purely glutamatergic neurons, cholinergic and GABAergic neurons might synthesize glutamate as well (Manns et al., 2001). Similarly, whether cholinergic and GABAergic neurons have the capacity to release glutamate is as yet unknown.

In addition, while the proportions of cholinergic, GABAergic and putative glutamatergic neurons that participate in these projections are known, the proportions of axon terminals that each of these groups provides to cortex and LH are not. This is a critical point since the pattern of innervation, in terms of axonal collateralization and density of synaptic terminals per volume may differ considerably among components and therefore may not necessarily reflect the proportion of neurons from which they appear.

Finally, the innervation that each of these contingents provide to specific cortical cell groups, including principal and interneuronal cell types is relatively unknown. Likewise, the innervation that cholinergic, GABAergic and putative glutamatergic neurons provide to LH neurons, including Orx neurons, has not been established.

To clarify these important issues about BF organization, research was carried out to study in detail the BF neurochemical groups and their projections to cortex and LH. In this aim, the main of objectives of this project were: 1) to determine the number of glutamate-synthesizing neurons, as well as those

synthesizing ACh and GABA in the BF, 2) to assess in those neurons the presence of markers for glutamate release, 3) to examine the presence of markers for ACh, GABA and glutamate release in BF terminals innervating the cortex and LH, as well as their proportions and 4) to study the innervation that these groups provide to cortical and hypothalamic cell groups.

In the first place, the number of BF neurons immunohistochemically positive for choline acetyltransferase (ChAT, the synthetic enzyme for ACh), glutamic acid decarboxylase (GAD, the synthetic enzyme for GABA) and PAG, was determined by stereological analysis in serial sections of the rat BF. In addition, the presence of the recently identified vesicular transporter proteins (VTPs) for glutamate (VGluTs), as definitive markers for glutamatergic neurons (Bellocchio et al., 2000; Fremeau et al., 2001; Herzog et al., 2001; Fremeau et al., 2002; Gras et al., 2002; Kaneko and Fujiyama, 2002; Schafer et al., 2002) was assessed in each BF population by dual immunohistochemical fluorescent staining.

Second, axonal transport of the anterograde neuronal tracer biotinylated dextran amine 10,000 MW (BDA) from magnocellular BF neurons was combined with immunohistochemistry for the VTPs for ACh, VAChT (Gilmor et al., 1996; Arvidsson et al., 1997), GABA, VGAT (McIntire et al., 1997; Chaudhry et al., 1998) or glutamate, VGluT (subtypes 1, 2 or 3) (Bellocchio et al., 2000; Fremeau et al., 2001; Fujiyama et al., 2001; Fremeau et al., 2002), as markers for neurotransmitter-specific releasing terminals, and examined in prefrontal cortex (PFC). There, estimates of the contribution of cholinergic, GABAergic and glutamatergic BF axon terminals were determined by unbiased sampling

procedures in serial sections of the rat PFC. By using triple fluorescence staining for BDA, VTPs and the postsynaptic proteins (PSPs) gephyrin (Geph), as a marker for inhibitory synapses (Sassoe-Pognetto and Fritschy, 2000; Sassoe-Pognetto et al., 2000) and PSD-95, as a marker for excitatory synapses (Kornau et al., 1995; Sheng and Pak, 2000; Sassoe-Pognetto et al., 2003), the capacity of BF terminals to form synapses was assessed. Finally, triple fluorescence staining for BDA, VTPs and the cell-specific markers non-phosphorylated neurofilament (NPNF) for pyramidal cells (Campbell and Morrison, 1989; Kirkcaldie et al., 2002), and the calcium binding proteins (CBP) parvalbumin (PV) and calbindin (CB) for interneurons (Celio, 1986, 1990) was used to examine the relation of BF terminals to subpopulations of cortical neurons.

Third, by single staining of BDA and dual fluorescence staining of BDA and VTPs, the projection to LH was also studied. Proportions of LH neurons innervated, as well as the number and proportions of BF cholinergic, GABAergic and glutamatergic terminals present in the LH, were estimated by stereological analysis. Additionally, triple fluorescence staining of BDA, VTPs and PSPs was used to examine the capacity of BF GABAergic and glutamatergic axons to form synapses with LH neuronal elements.

Finally, the specific innervation of the orexin/hypocretin (Orx) neuronal population in the hypothalamus was analyzed. By dual staining for BDA and Orx, the innervation of Orx neurons by BF afferents was examined and quantitatively described. Then, triple fluorescent staining of BDA, VTPs and Orx was used to examine the innervation of Orx neurons and determine quantitatively the contribution of each BF contingent to it. Finally, triple fluorescent stained

material for BDA, PSPs and Orx was performed to assess the synaptic nature of the innervation.

Figure 1: Basal forebrain nuclei. Depicted are five antero-posterior levels (~9.8 to ~7.0 anterior to interaural zero) across the forebrain of the rat. The basal forebrain (BF, orange contours) consists of several telencephalic nuclei (blue contours) which include the medial septum (MS), the nucleus of the diagonal band (DBB), the magnocellular preoptic nucleus (MCPO), the anterior (or subcommissural) and posterior (or sublenticular) parts of the substantia innominata (SIa and SIp, respectively) and the globus pallidus (GP). What is common to these nuclei and here defines the BF is the presence of cortically projecting cholinergic neurons. BF nuclei also send prominent projections to subcortical regions (see text). Other abbreviations: A, amygdala; ac, anterior commissure; Acb, accumbens nucleus; BST, bed nucleus of the stria terminalis; cc, corpus callosum; CPu, caudate putamen; Cx, cerebral cortex; EP, entopeduncular nucleus; f, fornix; ic, internal capsule; lo, lateral olfactory tract; LPO, lateral preoptic area; LS, lateral septum; ot, optic tract; OTu, olfactory tubercle; Rt, reticular thalamic nucleus.

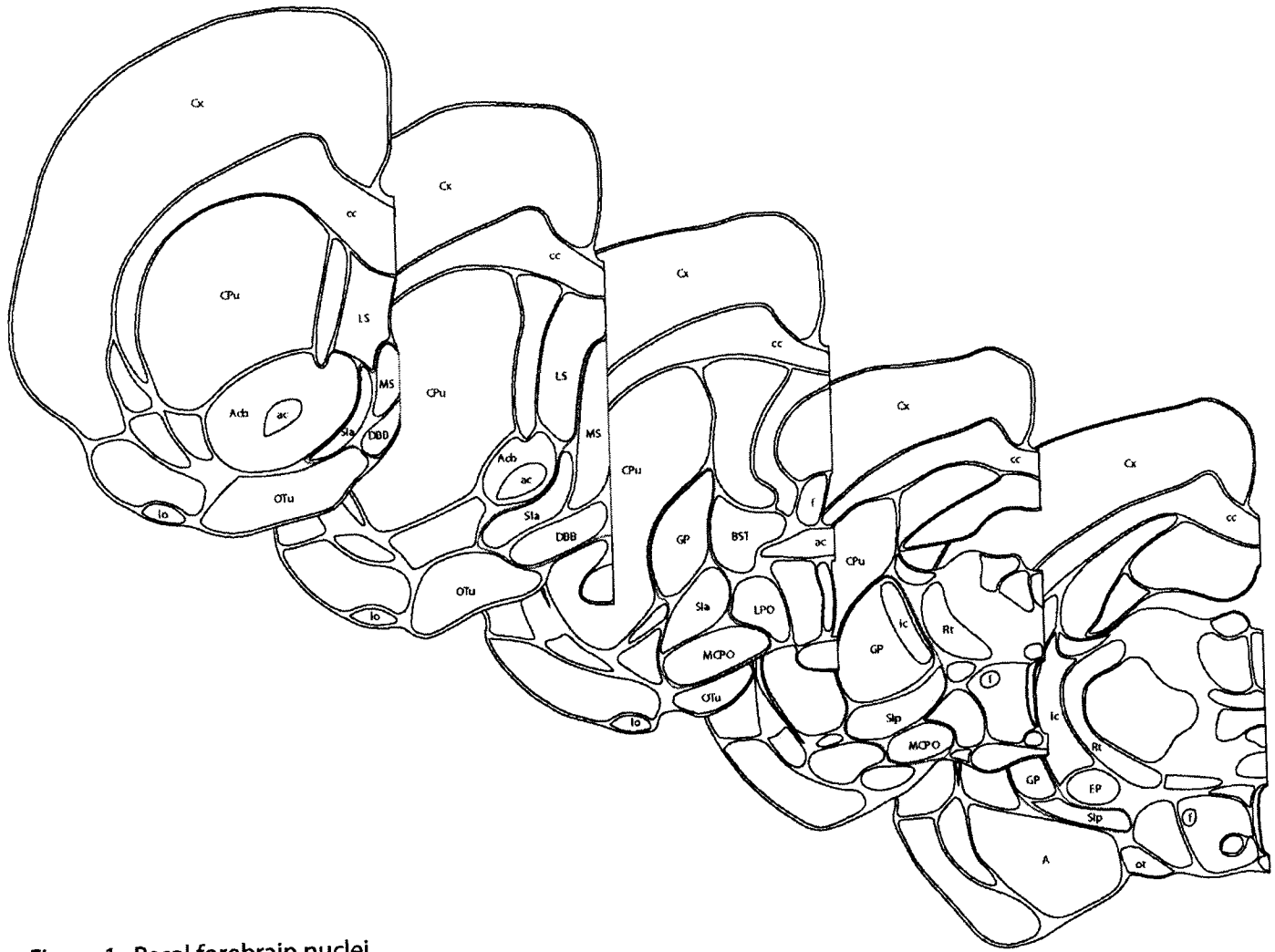

Figure 1. Basal forebrain nuclei

Figure 2: Ascending projections of the basal forebrain. As part of an ascending activating system which originates in the reticular formation (grey arrows), the basal forebrain (BF, here represented by the substantia innominata, SI) provides a prominent innervation to the cerebral cortex (Cx) through which it promotes cortical activation during wakefulness (W) and paradoxical sleep (PS), as exemplified in the activated (low voltage, fast) EEG on the upper left. Constituents of this projection are BF neurons that synthesize acetylcholine (ACh, in blue), GABA (in red) and possibly glutamate (in green contours), as evident from the presence of the synthetic enzymes, choline acetyltransferase (ChAT, blue circle), glutamic acid decarboxylase (GAD, red triangle) and phosphate activated glutaminase (PAG, green open rhombus), respectively. Some GABAergic neurons may also promote slow wave activity during slow wave sleep (SWS). Other abbreviations: ac, anterior commissure; CPu, caudate putamen; Gi, gigantocellular reticular formation; GiA, gigantocellular reticular formation, alpha part; GiV, gigantocellular reticular formation, ventral part; GP, globus pallidus; Hi, hippocampus; ic, internal capsule; LC, locus coeruleus; LDTg, laterodorsal tegmental nucleus; LH, lateral hypothalamus; Mes RF, mesencephalic reticular formation; ot, optic tract; PnC, pontine reticular formation, caudal part; PnO, pontine reticular formation, oral part; POA, preoptic area; PPTg, pedunculopontine tegmental nucleus; Rt, reticular thalamic nucleus; SN, substantia nigra; Sol, solitary tract nucleus; Th, thalamus; TM, tuberomammillary nucleus; VTA, ventral tegmental area. Modified with permission from Jones BE (2005a), Figure 1.

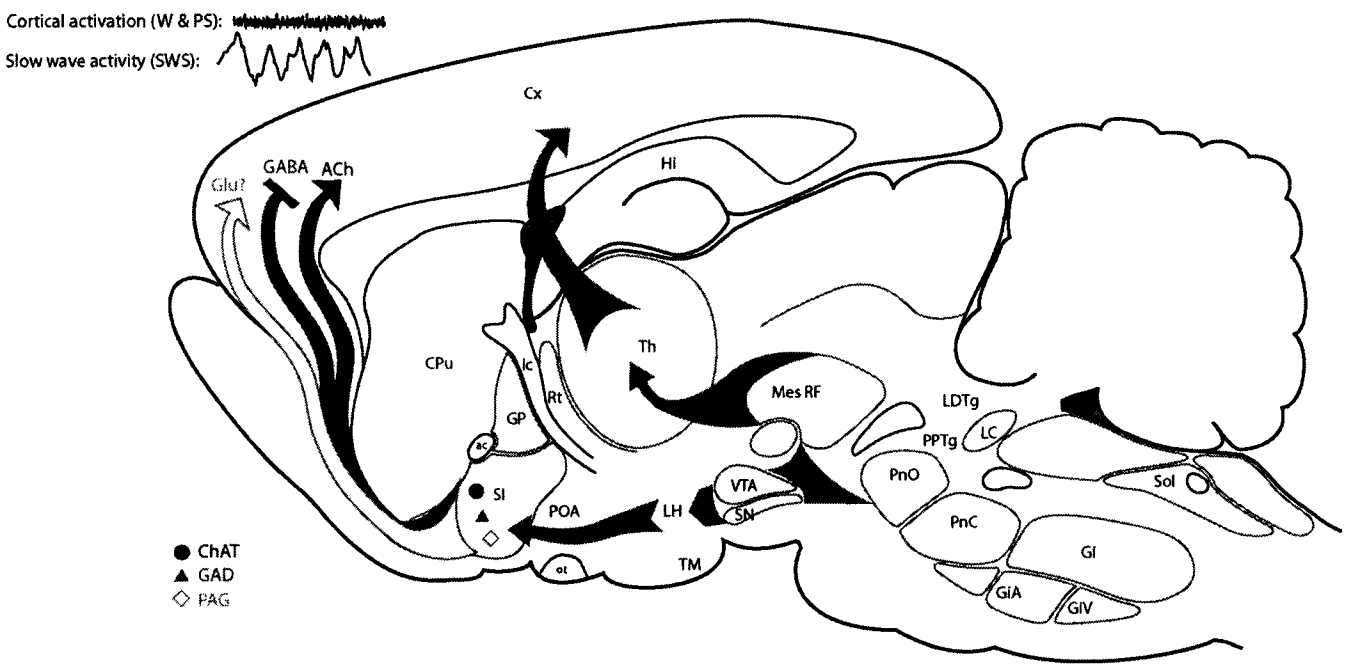

Figure 2. Ascending projections of the basal forebrain

Figure 3: Descending projections of the basal forebrain. As part of a descending system involved in the suppression of arousal, the basal forebrain (BF, here represented by the substantia innominata, SI) provides a prominent innervation to the lateral hypothalamus (LH) and brainstem. The activity of this system would be involved in the promotion of sleep, along with the disfacilitation of muscle tone, which occurs during SWS, and its suppression, which occurs during paradoxical sleep (PS), as exemplified by the decreasing amplitude of electromyographic activity (EMG) on the lower right. This projection is comprised by neurons that synthesize GABA (in red) as indicated by the presence of glutamic acid decarboxylase (GAD, red triangles) in neurons retrogradely labeled from the LH. In addition, a few cholinergic (in blue) and a large number of neurons that are neither GABAergic nor cholinergic (non-ChAT/non-GAD, green open rhombus) which could use glutamate (Glu, in green contours) contribute to this projection. Other abbreviations: ac, anterior commissure; ChAT, choline acetyltransferase; CPu, caudate putamen; Gi, gigantocellular reticular formation; GiA, gigantocellular reticular formation, alpha part; GiV, gigantocellular reticular formation, ventral part; GP, globus pallidus; Hi, hippocampus; ic, internal capsule; LC, locus coeruleus; LDTg, laterodorsal tegmental nucleus; Mes RF, mesencephalic reticular formation; ot, optic tract; PnC, pontine reticular formation, caudal part; PnO, pontine reticular formation, oral part; POA, preoptic area; PPTg, pedunculopontine tegmental nucleus; Rt, reticular thalamic nucleus; SN, substantia nigra; Sol, solitary tract nucleus; Th, thalamus; TM, tuberomammillary nucleus; VTA, ventral tegmental area. Modified with permission from Jones BE (2005a), Figure 1.

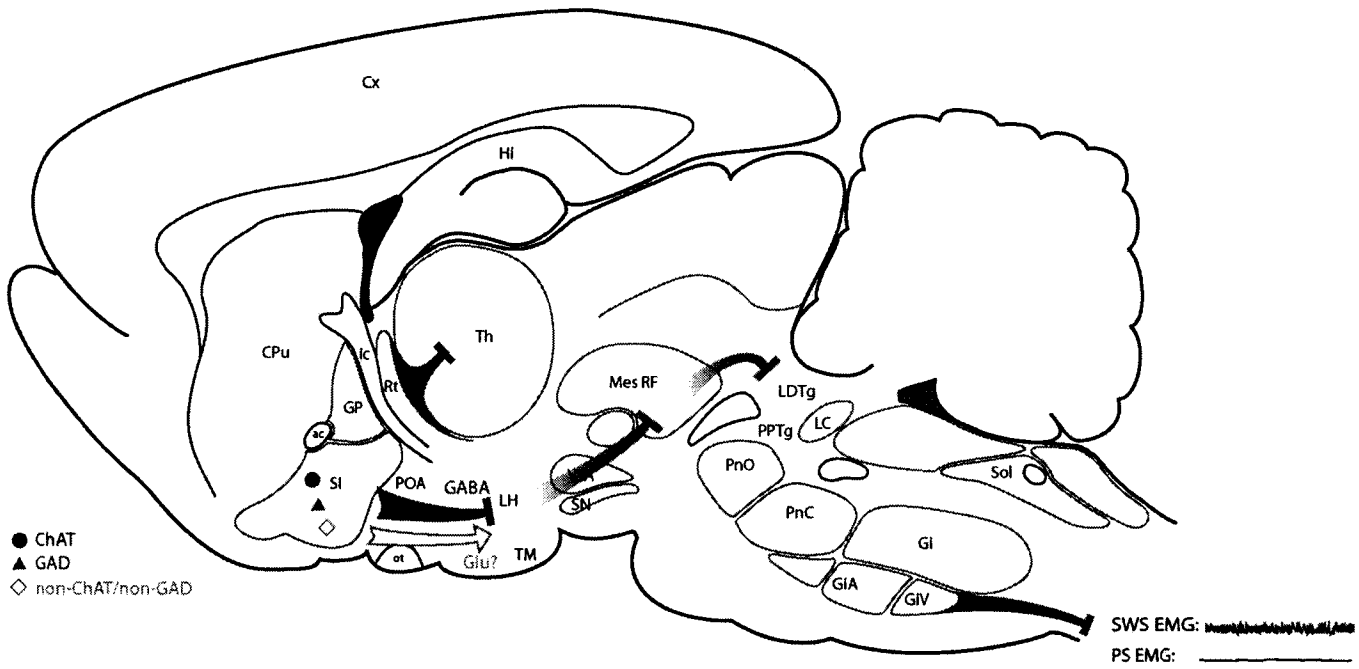

Figure 3. Descending projections of the basal forebrain

REVIEW OF THE LITERATURE

The BF has been proposed to play a role in the modulation of cortical activity and in the control of behavioral states. Through its direct projections to cortex and descending projections to LH, the diverse populations of cells that comprise the BF might contribute and regulate these processes. In this part, the most relevant anatomical and physiological data supporting a direct role of the BF in cortical activation and SWA, as well as on the direct control over the generation of sleep and related phenomena are reviewed. Special attention is paid to unsolved issues and open questions, which are summarized in a separate section. The review is then finalized by a brief revision of the literature on the core basic techniques used in this project.

1. General description

Historically, the term basal forebrain has referred to a group of structures located in the medio-ventral aspect of the telencephalon, often including cell groups of rather diverse anatomical as well as functional identity (Alheid and Heimer, 1988). More recently, however, the term basal forebrain has been applied to the forebrain region that contains a population of cortically projecting cholinergic neurons (Butcher and Semba, 1989). In the rat, these telencephalic structures form a continuum that from rostral to caudal includes the medial septum (MS), the nucleus of the diagonal band of Broca (DBB), the magnocellular preoptic nucleus (MCPO), the anterior (or subcommissural) and posterior (or sublenticular) parts of the substantia innominata (SIa and SIp, respectively) and the globus pallidus (GP). These structures share many anatomical and functional

characteristics, yet as we will see later, differ in the preponderance to which they project to different cortical structures. Here and in most of the chapters (II, III and IV) and unless specified, we generally use the term BF to refer to the magnocellular region of the MCPO, SI and GP, from where the major projections to the neocortex originate (Mesulam et al., 1983b; Mesulam et al., 1983a; Gritti et al., 1997).

Limited dorsally by the striatum, laterally by the piriform cortex and medially by the lateral preoptic area, the BF lays within or just adjacent to the path of the medial forebrain bundle (MFB), the most important communicating pathway of the anterior brain (Nieuwenhuys et al., 1982; Veening et al., 1982; Geeraedts et al., 1990). This critical location allows BF neurons to receive multiple inputs arising from the ascending reticular activating system of the brainstem to relay such inputs to the cerebral cortex and promote cortical activation (Jones and Cuello, 1989; Gritti et al., 1997). It is through this pathway too, that the BF can influence reciprocally the LH and brainstem regions to promote, as seen previously and discussed more extensively in the next section, behavioral quiescence and sleep (Swanson, 1976; Grove, 1988; Gritti et al., 1994).

2. Role of the basal forebrain in modulation of cortical activity

2.1 Central mechanisms responsible for arousal and cortical activation

Experiments done during the first half of the last century showed that ascending signals of the brainstem are critical for the appearance of cortical activation, a phenomenon that occurs in association with aroused states and wakefulness and characterized by the presence of low voltage and high frequency activities in the EEG (Jones, 2005b). As clearly shown by Bremer in his pioneering *cerveau isolé* preparation (Bremer, 1929), transections at the level of the mesencephalon eliminate cortical activation and leave the forebrain in a continuous sleep state, similar to that normally observed during SWS, as indicated by the presence of SWA in the cortical EEG. This observation led to the conclusion that afferent sensory signals, which enter or travel through the brainstem, were responsible for the appearance and maintenance of a waking and aroused state, and conversely, that their absence was the cause of sleep. Subsequent experiments showed, however, that the generalized activation of the EEG was evoked by stimulation of the brainstem reticular formation (RF) and could occur independently of sensory inputs, as lesions of the sensory pathways that ascend through the brainstem did not eliminate its occurrence (Moruzzi and Magoun, 1949). These results clearly indicated that wakefulness and the phenomenon of cortical activation (later also shown to occur during PS (Dement, 1958; Jouvet, 1965)) depended upon the brainstem reticular formation.

The ascending pathways by which the RF stimulates the cortex were thought to rely in part on the so-called diffuse thalamic projection system, formed by a collection of midline and intralaminar thalamic nuclei that, by mean of long

and widespread projections, would activate the cortical mantle (Moruzzi and Magoun, 1949). Nonetheless, since thalamic ablations did not completely eliminate cortical activation, either evoked by stimulation of the RF (Starzl et al., 1951) or occurring spontaneously across the sleep-wake cycle (Villablanca and Salinas-Zeballos, 1972), the existence of another, extrathalamic pathway involved in this phenomenon was suggested (Starzl et al., 1951). This alternative pathway to the cortex was shown to involve a ventral route, through the hypothalamus and up to the BF from where signals were then transmitted to the cortex (Jones, 2005b).

2.2 Basal forebrain projections to cortex

Although previously suggested by several studies (Starzl et al., 1951; Shute and Lewis, 1967), the requisite of a direct projection from the BF neurons to the cortex was first proven by Kievit and Kuypers (Kievit and Kuypers, 1975) using injections of the retrograde tracer horseradish peroxidase (HRP) into frontal and parietal cortices. They accordingly described a large group of cortically projecting neurons that were distributed ventrally across the BF as well as the hypothalamus. These projections, as subsequently shown by anterograde tracing from BF neurons, travel in association with subjacent white matter to then provide innervation to all cortical layers, yet clear regional differences in the laminar distribution of BF axons have been observed (Saper, 1984; Gaykema et al., 1990; Freund and Gulyas, 1991). The projections from the BF to cortex were shown to present some degree of topography, in that more anterior regions of the BF project to more anterior and medial cortical areas, whereas more posterior levels of the

BF project to more caudal and lateral cortical areas (Lamour et al., 1982; Saper, 1984; Luiten et al., 1987). Still, the basalo-projection was also shown to be widespread since single neurons were found to innervate different cortical regions (Adams et al., 1986) and reciprocally, specific cortical regions may be innervated by BF neurons located in different nuclei (Price and Stern, 1983; Fisher et al., 1988; Gritti et al., 1997). Through widespread projections, the BF and other extrathalamic forebrain regions may promote the simultaneous activation of the EEG in several and distant cortical areas as occurring during cortical activation (Moruzzi and Magoun, 1949; Starzl et al., 1951; Cape and Jones, 2000).

In parallel to anatomical evidence, projections from BF neurons to cortex were shown to be critical for the appearance of cortical activation, as electrolytic (Lo Conte et al., 1982) or neurotoxic (Stewart et al., 1984; Buzsaki et al., 1988) lesions of the BF resulted in EEG changes from high frequency activity (over ~20 Hz) toward lower frequency activity (in the delta range, ~0.5 to 4 Hz). This evidence supported thus the view of the BF as an anatomical and functional extrathalamic extension of the ascending reticular activating system (Buzsaki et al., 1988; Jones, 2005b), as originally inferred by Magoun and colleagues (Moruzzi and Magoun, 1949; Starzl et al., 1951). Consonant with this concept, microinjections in the BF of glutamate agonists (Cape and Jones, 2000) or noradrenaline (Cape and Jones, 1998), two important neurotransmitters used by the brainstem arousal system (Jones, 1991, 1995), were accompanied by increases in high frequency activity and active waking, with concomitant decreases in SWA and total suppression of sleep.

2.3 Cholinergic mechanisms in cortical activity and function

2.3.1 Morphological aspect of the BF cholinergic population and their innervation to cortex

Several neuronal groups carry out the influence of the BF over cortical activity, of which the most known is that formed by neurons that synthesize ACh. The existence of this population was suggested almost 40 years ago by Shute and Lewis (Lewis and Shute, 1967; Shute and Lewis, 1967) who using histochemical staining for the catabolic enzyme for ACh, AChE, described cells of the MS, DBB, MCPO and GP, as well as other forebrain areas. However, as evidence indicated that the sole presence of AChE did not necessarily indicate a cholinergic phenotype (Butcher, 1995), it was only with the advent of antibodies against the synthetic enzyme for acetylcholine, ChAT, that the presence of ACh-synthesizing neurons in the BF was unequivocally demonstrated (Kimura et al., 1980; Houser et al., 1983; Butcher, 1995).

BF cholinergic neurons, as determined by ChAT immunohistochemistry (Kimura et al., 1981; Mesulam et al., 1983a; Wainer and Rye, 1984; Brashear et al., 1986; Gritti et al., 1993), distribute across BF nuclei where they can be generally classified as bipolar or multipolar cells, with a small number of radiating dendrites that, as for reticular neurons in the brainstem, are oriented perpendicular to the major passing fiber systems in the forebrain (Gritti et al., 1993; Jones, 1995). As intermingled with other non-cholinergic cells (see below), cholinergic neurons represent only a portion of the total neuronal BF population, being estimated as ~15,000 across BF nuclei (including the MS and DBB) (Gritti

et al., 1993). More recently, studies based on stereology estimated their number to be ~26,000 (Miettinen et al., 2002).

The projection that BF cholinergic neurons provide to the cortex was also proposed based on the existence of neurons and emerging axons stained for AChE (Shute and Lewis, 1967), findings that were confirmed by subsequent studies combining ChAT immunostaining with retrograde tracing (Rye et al., 1984; Wainer and Rye, 1984). The cholinergic projection was also shown to present some degree of topography since cholinergic neurons of different BF areas innervated preponderantly, yet not exclusively, certain cortical areas (Rye et al., 1984; Gritti et al., 1997). Thus, cholinergic neurons of the medial septum and vertical limb of the DBB provide innervation mainly to the hippocampal formation; cholinergic neurons in more ventral aspects of DBB innervate retrosplenial as well as occipital cortex; whereas cholinergic neurons of the magnocellular area, including MCPO, SI and GP gave rise to projections to neocortex (Rye et al., 1984; Zaborszky et al., 1986; Gritti et al., 1997). Neurons in the MCPO also provide a prominent projection to olfactory bulb and olfactory cortices (Rye et al., 1984; Zaborszky et al., 1986). Cholinergic neurons are intermingled with other cortically projecting neurons (see below) and represent only a portion of the cortically projecting cells. Indeed, BF cholinergic neurons represent ~20% of the projection to neocortex (Gritti et al., 1997).

In the cortex, cholinergic axons have been observed that form a dense mesh innervating all layers, as shown by a large number of studies using

immunohistochemistry for ChAT in cortical structures*. Differences in laminar distribution have been observed yet they are largely dependent on the cortical region studied (Lysakowski et al., 1986; Eckenstein et al., 1988; Lysakowski et al., 1989; Mechawar et al., 2000), and as proposed, they may reflect the functional role of ACh in each particular functional system (Lysakowski et al., 1986; Lysakowski et al., 1989; Beaulieu and Somogyi, 1991). Regional differences in density of innervation also exist, with frontal cortex presenting a higher density of cholinergic axons than parietal or occipital cortices (Mechawar et al., 2000).

Cholinergic axons in the cortex have a relatively small diameter with small varicosities (Houser et al., 1985; Stichel and Singer, 1985; Mechawar et al., 2000). They have been reported to form synaptic complexes, most often of the symmetric type (Wainer et al., 1984; Houser et al., 1985; Beaulieu and Somogyi, 1991). While synapses have been shown to be formed on dendrites of pyramidal cells and interneurons (Wainer et al., 1984; Houser et al., 1985; De Lima and Singer, 1986), detailed analysis of postsynaptic elements has indicated that cholinergic axons provide a richer innervation to dendrites of interneurons, as identified by the presence of GABA immunostaining, than to pyramidal cells (Beaulieu and Somogyi, 1991), indicating that part of their control over principal cell activity may be inhibitory. Yet, discrepancies exist concerning the frequency

* In most mammals, cholinergic axons originate subcortically in the BF (Semba, 2004). However, an intrinsic population of cholinergic neurons has been described in the cortex of the rat (Houser et al., 1983; Houser et al., 1985), a portion of which has been shown to belong to the group of bipolar interneurons which express the vasoactive intestinal polypeptide (VIP) (Bayraktar et al., 1997). Still, it has been considered that their contribution to cortical cholinergic innervation should be relatively minor in comparison to subcortical afferents, as neurotoxic lesions in the cortex (which would only eliminate cortical cells but not subcortical axons), produced a decrease of less than ~8% in ChAT activity (Lehmann et al., 1980).

with which cholinergic axon terminals form synapses and therefore the main mechanism through which they influence cortical neurons of either type. Thus, whereas some authors have claimed that most cholinergic varicosities form synapses (Turrini et al., 2001), others have reported that they do so infrequently (De Lima and Singer, 1986; Mechawar et al., 2000), suggesting a prominent contribution of non-synaptic released of ACh (Descarries et al., 2004).

2.3.2 Cholinergic neurons in the basal forebrain modulate cortical activity

As shown by early studies, ACh had a facilitatory effect on cortical activity, since intracerebroventricular injections of muscarinic or nicotinic agonists (Domino et al., 1968) promoted the appearance of high frequency as well as theta activity in the cortex and conversely, injections of muscarinic antagonists produced SWA (Domino et al, 1968; Stewart et al., 1984). Moreover, ACh was shown to be released maximally during W and PS (Jasper and Tessier, 1971), two states distinguished by the presence of high frequency as well as theta activity on the EEG (Jones, 2005b). This facilitatory action of ACh could be in part explained by the slow and persistent excitatory effect that ACh had on pyramidal cells (Krnjevic, 1967), which as shown later depended on slow muscarinic currents (McCormick and Prince, 1985; McCormick, 1993). Similarly, this effect may also involve excitation of interneurons, whose high frequency spiking might contribute to fast EEG activity (McCormick and Prince, 1985; McCormick, 1993).

Another determinant on the influence that the cholinergic system has on cortical activity may be the activity of BF cholinergic neurons *per se*, which as

shown by recordings of immunohistochemically identified cholinergic neurons from BF slices *in vitro*, have the intrinsic capacity to discharge in high frequency burst of action potentials, which appear rhythmically at slow frequencies (Khateb et al., 1992), similar to those of theta activity. This activity has also been recorded from cholinergic neurons in *in vivo* anaesthetized rats, and shown to occur in parallel with high frequency and theta activity recorded on the EEG (Manns et al., 2000a). Recently, it has also been shown that in unanaesthetized rats BF cholinergic neurons discharge similarly during active W and PS (Lee et al., 2005b).

The influence of the cholinergic system in the cortex has been shown to be critical for various processes that depend on the cortex, in particular those related to cognitive processes such as attention, learning and memory (Everitt and Robbins, 1997; Sarter et al., 2003). These influences may relate to the role of the cholinergic system in promoting cortical fast activity, as the most clear hallmark in patients suffering from Alzheimer's disease is a decrease in cortical fast activity (Jeong, 2004), which has been attributed to loss of cholinergic activity in both the BF (Rossor et al., 1982) and the cortex (Davies and Maloney, 1976).

2.4 GABAergic neurons in the basal forebrain in the control of cortical activity

2.4.1 Existence of a GABAergic population in the BF with ascending projections to cortex

Another group of BF neurons which provide massive projections to cortex is that comprised by GABA-synthesizing neurons. Following the development of antibodies against the synthetic enzyme for GABA, GAD, and their availability

for immunocytochemical studies in brain tissue (McLaughlin et al., 1974; Oertel et al., 1981), it was soon found that a large population of neurons in the BF were immunopositive for GAD (Young et al., 1984; Brashear et al., 1986). Although GABAergic and cholinergic neurons present similar morphology and distribution through the BF, it was determined that ChAT+ and GAD+ cells form two mutually exclusive groups with no (Gritti et al., 1993) or only minimal (Brashear et al., 1986) numbers of neurons showing colocalization of cholinergic and GABAergic markers. GAD+ cells in the BF represented approximately twice the number for ChAT+ neurons (Brashear et al., 1986; Zaborszky et al., 1986), according to their number estimated as ~31,000 (including those in the MS and DBB) (Gritti et al., 1993).

Like cholinergic neurons, GAD+ neurons contribute significantly to cortical projections (Zaborszky et al., 1986; Fisher et al., 1988). Cortically projecting GABAergic neurons intermingle with and are also structurally and morphologically similar to cortically projecting cholinergic neurons (Fisher et al., 1988; Gritti et al., 1997). As for their numbers, cortically projecting GABAergic neurons outnumber cholinergic ones in projections to cortex (Fisher et al., 1988; Gritti et al., 1997), as they represent ~30% of the total projecting population, in contrast to the ~20% originated from cholinergic neurons (Gritti et al., 1997).

Whereas most studies have relied on retrograde transport to examine the BF GABAergic projection to cortex, yielding knowledge about the distribution, number and proportions of GABAergic neurons in the BF, only a few have attempted to reveal the GABAergic cortical projection by use of anterograde tracing techniques. By combining transport of *Phaseolus vulgaris* leucoagglutinin

(PHA-L) from BF neurons with immunohistochemistry for GABA, ultrastructural analysis as well as morphological criteria, Freund and colleagues (Freund and Gulyas, 1991; Freund and Meskenaite, 1992) reported a population of BF axon terminals of relatively large size that were immunoreactive for GABA and formed symmetrical synapses. Although immunohistochemical staining for ChAT was not performed, this axonal type was assumed to represent non-cholinergic axons, since the cholinergic type was previously suggested to be formed by thin fibers and varicosities (Nyakas et al., 1987; Gaykema et al., 1990). The GABA stained axons formed synapses on morphologically identified interneurons, many of which also contained GABA. As assessed by light microscopic analysis and relying on morphological criteria, these axons were found, in the cat, to innervate interneurons that expressed the calcium binding proteins (CBP) parvalbumin (PV) or the peptide somatostatin. Contrastingly, in the rat brain, BF axons innervated only interneurons containing the CBP calbindin (CB) and also those containing the peptide somatostatin.

2.4.2 Role of basal forebrain GABAergic neurons in cortical activity

Based on the prominent innervation of interneurons by GABAergic BF neurons (see above), Freund and colleagues proposed that a major role of GABAergic BF neurons could be the disinhibition of pyramidal cells (Freund and Meskenaite, 1992) and thus, in synergism with cholinergic neurons, the promotion of cortical activation.

However, neurons in the BF that have been recorded, labeled and identified immunohistochemically as GABAergic in the *in vivo* anaesthetized rat, form a

heterogeneous group in their discharge profiles in relation to cortical activity (Manns et al., 2000b). One of the main groups comprises neurons that increase their discharge during cortical activation induced by somatosensory stimulation. These neurons, some of which could be antidromically activated from the prefrontal cortex, discharge tonically at frequencies in the gamma range and simultaneously with gamma activity in the EEG. Therefore, these neurons have been proposed to promote cortical activation (Manns et al., 2000b, 2003a). However, another main group, which also includes neurons antidromically activated from the prefrontal cortex, comprises neurons that discharge maximally in association with irregular SWA and actually decrease their firing with cortical activation. Some of these neurons discharge phasically in bursts of action potentials at low (<1 Hz) frequencies, similar to the SWA recorded in the EEG. Given the profile of activity, and that similar units have been recorded in the freely moving rat during SWS, this group has been proposed to comprise SWS-active neurons (Lee et al., 2004; Jones, 2005a).

2.5 Glutamatergic neurons in the basal forebrain

Retrograde tracing studies from olfactory bulb (Zaborszky et al., 1986) or cortex (Fisher et al., 1988; Gritti et al., 1994) have shown that the number of projecting neurons is larger than the sum of cholinergic and GABAergic projecting neurons, indicating the existence of another population of neurons in the BF whose identity is unknown. Based on the presence of phosphate activated glutaminase (PAG) in a large proportion (~80%) of BF neurons projecting to entorhinal cortex, it has been proposed that this population may be glutamatergic (Manns et al., 2001).

PAG, which is thought to participate in the synthesis of the neurotransmitter pool of glutamate (Bradford et al., 1978), is present in identified glutamatergic neurons, including pyramidal as well cortically projecting thalamic cells (Kaneko and Mizuno, 1988). Hence, PAG neurons in the BF might also synthesize and use glutamate for neurotransmission. However, PAG is also coexpressed in a high proportion of ChAT (~95%) and GAD (~60%) BF neurons, suggesting that cholinergic and some GABAergic neurons could synthesize and release glutamate as well (Manns et al., 2001).

Putative glutamatergic neurons, which are positive for PAG and negative for ChAT and GAD, have also been recorded *in vivo* in the anaesthetized rat (Manns et al., 2003a). These neurons, which by antidromic activation were shown to project to cortex or olfactory bulb, increase their firing rate with cortical activation and discharge rhythmically at slow theta-like frequencies in clusters of action potentials (with intracluster frequencies in the beta, ~20 Hz, range). Interestingly, the rhythmic activity of these neurons is coherent with slow rhythmic activity recorded from olfactory bulb and prefrontal cortex. These results thus show that putative glutamatergic neurons might contribute, in parallel to cholinergic and some GABAergic neurons, to cortical activation by promoting cortical synchronization at theta and/or beta frequencies.

3. Role of the basal forebrain in sleep-wake states

3.1 Forebrain regions involved in sleep promotion

Following the epidemic of *Encephalitis lethargica* that spanned Europe during the second and third decade of the last century, Constantin von Economo documented disruption in the sleep-wake organization of a group of patients previously affected by *Encephalitis* (von Economo, 1930). Based on the post-mortem observation that lesions located in the preoptic area, which included part of the BF, were associated with severe insomnia, whereas lesions located caudally in the posterior hypothalamus and upper brainstem were associated with somnolence, he postulated the existence of a sleep-controlling center formed by an anterior sleep-promoting zone and a posterior wake-promoting one (von Economo, 1930).

Years later, Nauta studied experimentally the location and functional interconnections of these two areas in the rat, by performing transections at levels from the preoptic area down to the posterior hypothalamus, while leaving the connections between the RF and the thalamus intact. By these means, he allowed sensory inputs to reach the thalamus and cortex. Like von Economo, he observed that transections isolating the preoptic region from the rest of the hypothalamus resulted in severe insomnia and hyperactivity. Conversely, transections that isolated the posterior hypothalamus from anterior portions, lead to somnolence, adynamia and increases in behavioral sleep (Nauta, 1946). These results supported the hypothesis that sleep is an active process requiring of an intact anterior hypothalamic/preoptic region to appear and not resulting simply from the absence of sensory input.

In line with Nauta's observations, Hess, who was studying autonomic as well as motor functions of the forebrain and brainstem (Hess, 1957), found that electrical stimulation of anterior hypothalamus and preoptic region results consistently in parasympathetic responses, such as pupil contraction and decreases in heart rate, arterial blood pressure and muscle tone with the appearance of quiescent behaviors, including most commonly adynamia and sleep. In contrast, stimulation of the posterior-lateral hypothalamus produced arousal and autonomic responses associated with a sympathetic activation.

3.2 Basal forebrain role in sleep

3.2.1 Lesions of the basal forebrain leads to insomnia

To localize more precisely the forebrain regions that elicited sleep in the cat, Sterman and Clemente mapped the full extent of the BF and preoptic region, and found that brief periods of electrical stimulation in these regions triggered behavioral quiescence and sleep (Sterman and Clemente, 1962b). The appearance of sleep was also accompanied by cortical SWA of the same characteristics as those observed during normal SWS (Sterman and Clemente, 1962a). Accordingly, subsequent studies involving electrolytic (McGinty and Sterman, 1968) or neurotoxic lesions (Szymusiak and McGinty, 1986a) of the BF were associated with sleep loss.

3.2.1 Sleep active neurons in the basal forebrain

The sleep promoting action of the BF could be carried out by neurons that have been recently shown to be selectively active during sleep, as indicated by the

expression of c-Fos in BF neurons following sleep deprivation and rebound (Modirrousta et al., 2004). Even more, since many of these neurons also express GAD, they could directly participate in the inhibitory processes that, as discussed in the next section, permit sleep to appear. Hence, this sleep active population may correspond to neurons that in the BF discharge maximally with SWS (Szymusiak and McGinty, 1986b, 1989; Lee et al., 2004; Jones, 2005a) and that, as SWA-active GABAergic neurons (Manns et al., 2000b), project to cortex and may be involved in the promotion of cortical SWA during SWS (Manns et al., 2000b; Jones, 2005a).

Sleep active GABAergic neurons may also correspond to neurons that in the BF increase their discharge rates continuously from W to SWS to be maximally active with PS (Lee et al., 2004; Jones, 2005a). The discharge of these sleep active neurons is negatively correlated with muscle tone amplitude, and they may accordingly participate in the decrease and suppression of muscle tone which occur during SWS and PS (Jones, 2005a). In fact, a role of the BF in promoting suppression of muscle tone along with promotion of PS has been previously suggested from experiments showing that stimulation of the BF with cholinergic agonists is able to evoke PS in cats (Hernandez Peon and Chavez Ibarra, 1963) or loss of muscle tone in dogs (Nishino et al., 1995). Similarly, selective stimulation of the BF cholinergic system with the peptide neurotensin evokes quiet waking state and PS, which occurs along with increases in theta activity and reduction of muscle tone (Cape et al., 2000).

3.2.3 Descending projections of the basal forebrain to the posterior and lateral hypothalamus

One of the mechanisms through which the BF may promote sleep is through their massive descending projections to the LH which, as pointed out previously and discussed extensively in the next section, is important for arousal and generation of W. As known from many studies, the BF sends prominent projections to subcortical regions, which include the hypothalamus and brainstem (Swanson, 1976; Grove, 1988). By using the autoradiographic method, Swanson described fibers that descended through the MFB and gave rise to collaterals to the LH on their way to more posterior regions, such as the supramammillary bodies, ventral tegmental area and locus coeruleus (Swanson, 1976). These results were also confirmed by Grove, who by using anterograde and retrograde tracing techniques, described projections that reached posterior lateral hypothalamus, supramammillary regions and the brainstem (Grove, 1988).

In contrast to the cortical projection, almost the totality of the BF subcortical projection arises from non-cholinergic neurons (Grove, 1988; Semba et al., 1989; Gritti et al., 1994). Importantly, this projection was shown to comprise a significant proportion of GABAergic neurons, as indicated by the presence of GAD staining in ~20% of BF neurons retrogradely labeled from the posterior lateral hypothalamus (Gritti et al., 1994).

3.3 The lateral hypothalamus in the control of wakefulness

As described, Nauta attributed a wake-promoting role to the posterior hypothalamus and Hess found this region to promote arousal. Subsequent studies

have confirmed these observations by showing that electrolytic lesions of the posterior hypothalamus lead to a somnolent state (Swett and Hobson, 1968) and similarly, that chemical inactivation of the posterior hypothalamus produces sleep (Lin et al., 1989). The neurochemical identity of the neurons that may be responsible for these functions was unknown until the recent discovery of two excitatory neuropeptides, called orexin-1 and -2 (Orx, or also hypocretin-A and -B). These peptides are expressed in a discrete population of neurons in the tuberal hypothalamus, including LH, perifornical region (PF) and dorsomedial hypothalamus (DMH) (de Lecea et al., 1998; Sakurai et al., 1998) and innervate most of CNS regions (Peyron et al., 1998). Orx neurons have been shown to be critical for arousal and W, since their absence, or that of the peptide, or the receptor resulted in narcolepsy in experimental animals (Chemelli et al., 1999; Lin et al., 1999). Narcolepsy is a human, equine and canine disease characterized by excessive sleepiness and is in most cases present together with cataplexy (narcolepsy-cataplexy), a sudden loss of muscle tone that in humans is triggered by strong emotions (Nishino and Mignot, 1997). In humans, narcolepsy-cataplexy is the results of a degeneration of orexin-containing neurons whereas in dogs it is the result of a mutation in the receptor for Orexin 2 (Lin et al., 1999; Siegel, 1999; Peyron et al., 2000). The orexinergic system has been shown to have a strong facilitatory role on sympathetic (Kayaba et al., 2003; Zhang et al., 2006) and hypothalamo-pituitary-adrenal (HPA) (Winsky-Sommerer et al., 2005) systems, as well as on muscle tone (Lin et al., 1999; Yamuy et al., 2004). Consonant with these findings, Orx neurons have been shown to discharge maximally during active W and to be silent during behavioral quiescence, SWS

and PS (Lee et al., 2005a). As Orx neurons have been shown to be endowed with mechanisms that allow them to be continuously active (Eggermann et al., 2003), it is therefore inferred that they must be under strong inhibition during behavioral quiescence and sleep. Part of this inhibitory drive may come from BF GABAergic neurons that provide a prominent innervation to the LH (Gritti et al., 1994).

4. Unsolved issues and open questions

In the previous sections, we have reviewed the organization of the BF and constitutive cellular groups and discussed their involvement in regulation of cortical activity and sleep wake states. Although our knowledge about the BF anatomy and function is vast, it is evident that many critical issues about BF neuronal constituency and organization of its projection system are still unsolved and therefore open for investigation. First, what type of cells constitute the BF? Are cholinergic and GABAergic cells the only efferent contingents of the BF? Is there another neuronal population that contributes to BF output? Secondly, do BF axons have the capacity to release the neurotransmitters they are supposed to synthesize? Can they release more than one neurotransmitter? Finally, are BF projecting contingents organized in the same way? Do they project to the same regions, and within regions, do they form contacts with different cell types?

These and other related questions form the core of this thesis project. We believe that by answering them we will significantly contribute to the knowledge of BF organization and function.

5. Methodologies in the study of BF cell groups and projections

The ascending and descending projections of the BF have been examined in great detail with the use of anterograde and retrograde transport of tracers (Saper, 1984; Zaborszky et al., 1986; Luiten et al., 1987; Grove, 1988; Gritti et al., 1994). Although providing detailed information on morphology and spatial distribution of efferent fibers, anterograde tracing studies have generally not been able to unequivocally identify the neurochemical phenotype of those fibers, nor their neurochemically-specific distribution, morphology, number or targeted cell populations (Luiten et al., 1987; Grove, 1988; Gaykema et al., 1990). In fact, it is only from the use of retrograde tracing methods that, in combination with immunohistochemistry, most of the knowledge about neurochemical identity and contribution of cortically or caudally projecting BF cell groups has come (Rye et al., 1984; Zaborszky et al., 1986; Gritti et al., 1994; Gritti et al., 1997; Manns et al., 2001). In spite of these advances, the lack of more definitive markers for neurotransmitter usage by BF neurons, along with the apparent overlap in cell body phenotype, makes necessary the examination and identification of the neurochemical identity of BF axon terminals.

Following this rationale, the core of this project has relied on the use of anterograde tracing techniques in combination with immunohistochemistry for definitive neurochemical markers of neurotransmitters in BF axon terminals.

5.1 Anterograde transport of biotinylated dextran amines for axonal tracing

Biotinylated dextran amine 10,000 MW (BDA-10,000; BDA) is a highly stable and non-toxic hydrophilic polysaccharide (dextran) conjugated to biotin and an

amine group. In its 10,000 MW form, BDA is a reliable anterograde tracer, which as PHA-L, labels axon fibers and terminals with a Golgi-like quality with preservation of morphology at both the light microscopic and ultrastructural level (Veenman et al., 1992; Wouterlood and Jorritsma-Byham, 1993; Reiner et al., 2000). However, the most critical advantage of BDA is that in contrast to PHA-L, it does not require an immunohistochemical procedure for revelation, but only the avidin-biotin reaction, which may be done with a routine ABC protocol (Veenman et al., 1992; Wouterlood and Jorritsma-Byham, 1993). In addition to providing quicker and simpler means of revelation, the single staining of BDA does not require the use of high concentrations of detergent for permeabilization, given the high affinity between avidin and biotin molecules and the relatively small size of the ABC complex (180,000 MW). Due to these advantages, BDA has been reliably used in combination with other staining techniques, including immunohistochemistry, for double or triple staining (Lanciego et al., 2000; Reiner et al., 2000; Wouterlood et al., 2002a).

5.2 Vesicular transporter proteins as neurochemically specific markers.

Vesicular transporter proteins (VTPs) are recently identified molecules involved in the uptake of neurotransmitter (or in some cases its substrate) from the cytosol to the synaptic vesicle lumen (Roghani et al., 1994; Peter et al., 1995; McIntire et al., 1997; Reimer et al., 1998; Bellocchio et al., 2000; Fremeau et al., 2001). As differentiated by their protein structure, uptake mechanism and substrate affinity, they represent markers for neurochemical phenotype and most notably, capacity

for neurotransmitter-specific synaptic release (Reimer et al., 1998; Fremeau et al., 2004)

The vesicular ACh transporter, VAChT, was originally identified from the unc-17 gene in *Caenorabhditis elegans* (Alfonso et al., 1993; Roghani et al., 1994). This gene expresses a protein involved in the vesicular uptake of ACh and shows homology with the vesicular transporter for monoamines (VMAT) (Peter et al., 1995; Reimer et al., 1998). In the rat, the VAChT protein is present in all cholinergic cells groups described previously to express ChAT and localizes in somatic, dendritic as well as axonal compartments of cholinergic neurons in the CNS and peripheral ganglia (Gilmor et al., 1996; Arvidsson et al., 1997; Garzon and Pickel, 2000). In the cortex, VAChT has been found to be present in axonal varicosities forming synapses onto pyramidal cells which, as also observed with ChAT immunohistochemistry, are often of the symmetric type (Turrini et al., 2001). Since it is involved in the vesicular release of ACh, VAChT represents a marker for cholinergic axon terminals.

The vesicular GABA transporter (VGAT, or vesicular inhibitory amino acid transporter, VIAAT) was originally identified from the unc-47 gene in *C. elegans*, as a protein involved in the uptake of GABA and glycine for synaptic release and found to present no homology to VMAT or VAChT (McIntire et al., 1997; Sagne et al., 1997). In mammals, VGAT is expressed at symmetric synapses where it colocalizes with GABA and/or glycine (Chaudhry et al., 1998). In contrast to the synthetic enzyme for GABA, GAD, VGAT is absent in most cell bodies within the CNS.

The vesicular glutamate transporters (VGluT1, 2 or 3, VGluTs) were identified and cloned recently (Bellocchio et al., 2000; Fremeau et al., 2001; Herzog et al., 2001; Fremeau et al., 2002; Gras et al., 2002; Schafer et al., 2002). In contrast to VMAT, VAChT or VGAT, VGluTs do not show homology with any of previously identified VTPs (Fremeau et al., 2004). Indeed, VGluT1 and 2 had been already described in the brain as proteins involved in the transport of phosphate (as the brain-specific Na(+)-dependent inorganic phosphate co-transporter (BNPi) and the differentiation-associated Na(+)-dependent inorganic phosphate cotransporter (DNPi), respectively) without a direct role in glutamate uptake (Ni et al., 1994; Ni et al., 1995; Aihara et al., 2000; Hisano et al., 2000; Fujiyama et al., 2001). VGluT1 and VGluT2 neurons are profuse within the CNS and, as identified by *in situ* hybridization, exhibit a complementary distribution throughout the CNS. In the forebrain, VGluT1 neurons are abundant in the cortex and hippocampus, whereas VGluT2 neurons appear predominant in subcortical structures. Like VGAT, neither VGluT1 nor VGluT2 accumulate in cell bodies but are found exclusively in axon terminals (Fremeau et al., 2001; Fujiyama et al., 2001). Both VGluT1 and VGluT2 have been found present in axon terminals forming synapses of the asymmetric type (Bellocchio et al., 1998; Fremeau et al., 2001; Fujiyama et al., 2001). VGluT3, on the other hand, was originally described as being expressed by restricted populations of neurons in the CNS, which surprisingly included cholinergic neurons in the striatum and serotonergic neurons of raphe nuclei (Fremeau et al., 2002; Gras et al., 2002; Kaneko and Fujiyama, 2002; Herzog et al., 2004). Yet, as recent reports suggest, VGluT3 may be expressed more ubiquitously (Harkany et al., 2003; Harkany et al., 2004).

In contrast to VGluT1 and VGluT2, VGluT3 is not only found in axon terminals but also in cell bodies and dendrites (Fremeau et al., 2002; Harkany et al., 2004). Remarkably, somato-dendritic VGluT3 has been shown to participate in the release of glutamate from the soma and dendrites of pyramidal cells (Harkany et al., 2004).

These markers were accordingly utilized for the definitive identification of BF axon terminals and varicosities that have the capacity to release ACh, GABA or glutamate.

Contingent upon the presence of these markers, additional evidence for synaptically mediated transmission was sought by the presence of postsynaptic proteins in association with identified BF axon terminals. To this end, the presence of PSD-95, a protein constituent of postsynaptic densities of excitatory synapses and involved in the anchoring of NMDA and AMPA glutamate receptors at these synapses (Kornau et al., 1995; Chen et al., 2000; Sheng and Pak, 2000; Sassoe-Pognetto et al., 2003) was examined in relation to BF axons having the capacity to release glutamate, ACh or GABA. Similarly, the presence of Gephyrin, (Geph) a protein involved in the synaptic clustering of $GABA_AR$ and glycine receptors and present at inhibitory synapses (Giustetto et al., 1998; Sassoe-Pognetto and Fritschy, 2000; Sassoe-Pognetto et al., 2000) was examined in relation to GABAergic, cholinergic and glutamatergic terminals.

PREFACE TO CHAPTER I

The numerous roles that the BF plays in modulating cortical function and behavioral state are likely carried out by neurochemically differentiated groups of neurons that comprise the BF. ACh- and GABA-synthesizing cell groups have been well described in the BF, yet together they do not account for the total BF neuronal population, nor for those contingents projecting to cortex or caudally to the hypothalamus. It has been recently proposed that a third population of BF neurons might comprise glutamate-synthesizing neurons, based on the expression of PAG in the cell bodies of a large proportion of BF neurons. As a first step in identifying and characterizing this putative population, the total number of neurons, including those containing PAG, plus those containing ChAT and GAD, was quantified in the BF using unbiased sampling procedures. In addition, the presence of a newly described family of proteins involved in the vesicular uptake and release of glutamate was examined in cells containing ChAT, GAD and PAG, as an independent, yet functionally complementary indication of a glutamatergic phenotype.

Chapter I

Stereological estimates of the basal forebrain cell population in the rat, comprising neurons containing choline acetyltransferase, glutamic acid decarboxylase and phosphate-activated glutaminase and colocalizing vesicular glutamate transporters

Ivana Gritti[a], Pablo Henny[b], Francesca Galloni[a],

Lynda Mainville[b], Maurizio Mariotti[a] and Barbara E. Jones[b]

[a]Dipartimento di Scienze Cliniche Luigi Sacco, Università degli Studi di Milano,

Via Giovan Battista Grassi 74, Milan, Italy 20157

[b]Department of Neurology and Neurosurgery, McGill University,

Montreal Neurological Institute, 3801 University Street, Montreal, Quebec,

Canada H3A 2B4

Abbreviations:

A	amygdala
ac	anterior commissure
Acb	accumbens nucleus
ACh	acetylcholine
AD	anterodorsal thalamic nucleus
AHA	anterior hypothalamic area
AM	anteromedial thalamic nucleus
Arc	arcuate hypothalamic nucleus
AV	anteroventral thalamic nucleus
BF	basal forebrain
BST	bed nucleus of the stria terminalis
ChAT	choline acetyltransferase
Cl	claustrum
CM	central medial thalamic nucleus
CPu	caudate putamen
DBB	diagonal band of Broca nucleus
En	endopiriform nucleus
EP	entopeduncular nucleus
f	fornix
FStr	fundus striati
G	gelatinosus thalamic nucleus
GAD	glutamic acid decarboxylase
Glu	glutamate

GP	globus pallidus
IAM	interanteromedial thalamic nucleus
ic	internal capsule
LD	laterodorsal thalamic nucleus
LH	lateral hypothalamic area
lo	lateral olfactory tract
LOT	nucleus of the lateral olfactory tract
LPO	lateral preoptic area
LS	lateral septal nucleus
MCPO	magnocellular preoptic nucleus
MD	mediodorsal thalamic nucleus
MPO	medial preoptic nucleus
MS	medial septal nucleus
NR	neutral red
oc	optic chiasm
ot	optic tract
OTu	olfactory tubercle
Pa	paraventricular hypothalamic nucleus
PAG	phosphate-activated glutaminase
PC	paracentral thalamic nucleus
Pe	periventricular hypothalamic nucleus
Pir	piriform cortex
PT	paratenial thalamic nucleus
PV	paraventricular thalamic nucleus

Re	reuniens thalamic nucleus
Rh	rhomboid thalamic nucleus
Rt	reticular thalamic nucleus
SCh	suprachiasmatic nucleus
SFi	septofimbrial nucleus
SI	substantia innominata
SIa	substantia innominata anterior
SIp	substantia innominata posterior
sm	stria medullaris of the thalamus
SO	supraoptic nucleus
st	stria terminalis
TT	tenia tecta
VAChT	vesicular acetylcholine transporter
VGAT	vesicular GABA transporter
VGluT	vesicular glutamate transporter
VL	ventrolateral thalamic nucleus
VM	ventromedial thalamic nucleus
VMH	ventromedial hypothalamic nucleus
ZI	zona incerta

ABSTRACT

The basal forebrain (BF) plays an important role in modulating cortical activity and influencing attention, learning and memory. These activities are fulfilled importantly yet not entirely by cholinergic neurons. Noncholinergic neurons also contribute and are comprised by GABAergic neurons and other possibly glutamatergic neurons. The aim of the present study was to estimate the total number of cells in the BF of the rat and the proportions of that total represented by cholinergic, GABAergic and glutamatergic neurons. For this purpose, cells were counted using unbiased stereological methods within the medial septum, diagonal band, magnocellular preoptic nucleus, substantia innominata and globus pallidus in sections stained for Nissl substance and/or the neurotransmitter enzymes, choline acetyltransferase (ChAT), glutamic acid decarboxylase (GAD) or phosphate-activated glutaminase (PAG). In Nissl-stained sections, the total number of neurons in the BF was estimated as ~355,000 and the numbers of ChAT-immuno-positive (+) as ~22,000, GAD+ ~119,000 and PAG+ ~316,000, corresponding to ~5%, ~35% and ~90% of the total. Thus, of the large population of BF neurons, only a small proportion has the capacity to synthesize acetylcholine (ACh), one third to synthesize GABA and the vast majority to synthesize glutamate (Glu). Moreover, through the presence of PAG, a proportion of ACh- and GABA-synthesizing neurons also have the capacity to synthesize Glu. In sections dual fluorescent immunostained for vesicular transporters, VGluT3 and not VGluT2 was present in the cell bodies of most PAG+ and ChAT+ and half the GAD+ cells. Given previous results showing that VGluT2 and not VGluT3 was present in BF axon terminals and not colocalized

with VAChT or VGAT, we conclude that the BF cell population influences cortical and subcortical regions through neurons which release ACh, GABA or Glu from their terminals but which in part can also synthesize and release Glu from their soma or dendrites.

INTRODUCTION

As evident from the devastating effects of lesions, the basal forebrain (BF) plays a critical role in cortical and state modulation, which influences sleep-wake states, attention, learning and memory (Damasio et al., 1985; Dunnett et al., 1991; Wenk, 1997; Sarter et al., 2003; Jones, 2004). This role has been attributed particularly to the cholinergic neurons and their widespread projections to the allo- and neo-cortex. Yet, selective neurotoxic lesions of the cholinergic neurons have not produced the same overwhelming effects as the total lesions of the BF (Lee et al., 1994; Baxter et al., 1995; Gerashchenko et al., 2001a), indicating that other BF neurons participate in cortical and state modulation. It is thus important to characterize and quantify the noncholinergic as well as cholinergic constituents of the BF cell population.

Acetylcholine (ACh)-synthesizing neurons are distributed across BF nuclei of the medial septum-diagonal band of Broca (MS-DBB), from where they give rise to prominent projections to hippocampus, and the magnocellular preoptic-substantia innominata-globus pallidus (MCPO-SI-GP), from where they give rise to prominent projections to neocortex (Rye et al., 1984). Another well-defined contingent of the BF cell population contains the synthetic enzyme for GABA. Neurons containing glutamic acid decarboxylase (GAD) are codistributed with the those containing choline acetyltransferase (ChAT), and large GAD-positive (+) neurons project in parallel with ChAT+ neurons from the MS-DBB to the allocortex and from the MCPO-SI-GP to the neocortex (Kohler et al., 1984; Brashear et al., 1986; Zaborszky et al., 1986; Fisher et al., 1988; Freund and Antal, 1988; Freund and Meskenaite, 1992; Gritti et al., 1993; Gritti et al., 1997).

In contrast to ChAT+ neurons, GAD+ neurons also give rise to important descending projections to the hypothalamus and brainstem (Semba et al., 1989; Gritti et al., 1994), and they likely also include local interneurons. In the BF, the GAD+ plus the ChAT+ neurons do not account for all the cortically projecting, nor for all the caudally projecting BF neurons (Gritti et al., 1997; Gritti et al., 2003). It was thus proposed that the nonGABAergic, noncholinergic BF neurons are likely glutamatergic neurons.

The synthesis of glutamate (Glu) as a neurotransmitter in neurons occurs from the substrate glutamine, which is taken up from glia, and by the mitochondrial enzyme phosphate-activated glutaminase (PAG) (Bradford et al., 1978). In immunohistochemical studies in the neocortex, PAG was found to be contained predominantly in pyramidal neurons and rarely in GABAergic interneurons (Donoghue et al., 1985; Kaneko and Mizuno, 1988; Akiyama et al., 1990; Kaneko et al., 1992; Kaneko and Mizuno, 1994; Van der Gucht et al., 2003). In a previous study, we thus utilized PAG to label Glu-synthesizing neurons in the BF (Manns et al., 2001). In that study, we found that a major proportion of neocortically projecting BF neurons contained PAG and would accordingly have the capacity to synthesize Glu as a neurotransmitter. By applying stereology, we sought in the present study to determine the total numbers of ChAT+, GAD+ and PAG+ neurons along with the total number of all, Nissl-stained, neurons in the BF of the rat.

Given that the numbers and proportions of PAG+ cells exceeded that of the ChAT-negative (-) and GAD- cells in the present study and that a proportion of ChAT+ and GAD+ cells were found to be PAG+ in a previous study (Manns et

al., 2001), we also examined in the present study whether ChAT+, GAD+ and/or PAG+ cells contained the vesicular transporters for Glu (VGluT) and could thus store and release Glu as a neurotransmitter (Fremeau et al., 2001; Fujiyama et al., 2001; Fremeau et al., 2002). Using RT-PCR or in situ for mRNA or immunohistochemistry for protein, VGluT2 has been found to be synthesized in BF neurons and transported along their axons to terminals from where it is released as a neurotransmitter and VGluT3 to be contained in BF nerve cell bodies and dendrites from where it can be released to act as a retrograde signal (Harkany et al., 2003; Hajszan et al., 2004; Colom et al., 2005; Danik et al., 2005; Hur and Zaborszky, 2005; Henny and Jones, 2006a). Employing colchicine treatment to block axonal transport, we examined dual immunostaining by fluorescence for the enzymes and VGluTs to determine the proportion of each cell type that would have the capacity to release Glu.

EXPERIMENTAL PROCEDURES

Animals and surgery

Results from six adult male Wistar rats (Charles River Canada, St. Constant, Quebec, Canada), weighing approximately 250 grams, are reported in this study. All procedures were approved by the McGill University Animal Care Committee and conform to standards of the Canadian Council on Animal Care. For surgery or euthanasia, the rats were anesthetized with sodium pentobarbital (Somnotol, 65 mg/kg, i.p.). Three rats were operated ~24 hours prior to killing for injections of colchicine (50 μg in 25 μl saline) into the lateral ventricle, as previously applied (Gritti et al., 1993; Gritti et al., 1997) for enhancing levels of GAD in cell bodies and here for also enhancing levels of VGluTs within dual-immunostained tissue (below). All rats were killed by perfusion with a fixative through the ascending aorta.

Perfusion and fixation

Brains were fixed with Zamboni's solution, according to a slight modification of the procedure developed by Kaneko for immunostaining of the PAG enzyme (Kaneko and Mizuno, 1988; Kaneko et al., 1989; Manns et al., 2001). Following a brief rinse with phosphate buffered saline, the animals were perfused through the ascending aorta with 500 ml of a modified Zamboni's solution of 0.3% paraformaldehyde and 75% saturated picric acid in 0.1 M sodium phosphate buffer (pH 7.0, over ~30 minutes). The brains were post-fixed overnight at 4°C in a solution of 3% paraformaldehyde with 75% saturated picric acid (pH 7.0). They

were subsequently immersed in a solution of 30% sucrose at 4°C for ~72 hours for cryoprotection. Brains were then frozen at -50°C and stored at -80°C.

Immunohistochemistry

Coronal sections were cut on a freezing microtome with a thickness of 20 μm, which was established as the thickest that allowed full and even penetration of antibodies (particularly for PAG). The sections were collected at 400 μm intervals in twenty adjacent series used for different immunostaining. For random starting and ordering of the series, a random number generator was employed to determine which series would be immunostained with ChAT, GAD or PAG in each brain. The sections were collected in phosphate buffer (pH 7.4; 0.1M).

For peroxidase immunostained series (from 3 untreated rats, G1, G2 and G3), sections were first incubated in a Tris-saline solution (TS, 0.1 M) containing bovine serum albumin (BSA) at 3% for prior blocking and at 1% for all other applications. As previously employed (Gritti et al., 2003), antisera for ChAT (from rabbit, 1:2000) were obtained from Chemicon International (Temecula, CA, USA: AB143). Also previously employed (Manns et al., 2001), antisera for PAG (from rabbit, 1:6000) were kindly supplied by Dr. T. Kaneko (Kyoto, Japan) who originally showed that the antisera recognizes two bands of peptides at 62 and 65 kD, corresponding to the two isoforms of rat brain PAG (Akiyama et al., 1990). Also previously employed (Gritti et al., 2003), antisera for GAD (from rabbit, 1:3000) were obtained from Chemicon (AB108) and shown by them using Western Blot to recognize a 67 kD band of protein from rat brain, corresponding to GAD67. Sections were incubated overnight at room temperature with primary

antibodies for ChAT and PAG or for three nights at 4° C with those for GAD. The sections were subsequently incubated with donkey anti-rabbit antiserum (1:100, Jackson ImmunoResearch Laboratories, West Grove, PA, USA) followed by rabbit peroxidase-antiperoxidase (PAP, 1:200, Jackson). PAP was revealed using diaminobenzidine (DAB) in the presence of 0.1% glucose oxidase in Tris-buffer (pH 7.4) during 15 min for ChAT, 13 min for PAG and 17 min for GAD. For the PAG series, DAB was intensified with nickel (DAB-Ni), and the sections were counterstained for Nissl using Neutral Red (NR).

For dual fluorescent immunostained series (from 3 colchicine treated rats, G5, G6 and G7), sections were incubated in a Tris-saline solution (0.1 M) containing Triton x-100 at 0.1% and normal donkey serum (NDS) at 3% for prior blocking and at 1% for the rest of the procedure. The primary antibodies for VGluT2 and VGluT3 (both from guinea pig) were obtained from Chemicon (AB5907 and AB5421, respectively) and were found in previous studies (Henny and Jones, 2006a) to provide staining similar to that published with other antibodies for these proteins (Fremeau et al., 2001; Fremeau et al., 2002). The primary antibody for GAD (from mouse) was obtained from Chemicon (MAB5406) and shown by them to recognize a 67 kD band in rat brain. Sections were co-incubated overnight at room temperature with the primary antibodies against 1) VGluT2 (1:5000) and PAG (as above), 2) VGluT3 (1:1000) and PAG (as above), 3) VGluT3 and ChAT (as above), or 4) VGluT3 and GAD67 (1:500). The sections were then co-incubated for 2 hours with Cy3-conjugated donkey anti-guinea pig (1:1000, Jackson, for VGluT2 or VGluT3) and Cy2-conjugated

donkey anti-rabbit (1:200, Jackson, for ChAT or PAG) or Cy2-conjugated donkey anti-mouse (1:200, Jackson, for GAD67).

Controls were routinely carried out by replacing the primary antisera with normal sera from the same species and at the same concentration to insure that nonspecific staining did not occur. After processing, all sections were washed in phosphate buffer, mounted out of TS, dehydrated through graded alcohols, delipidated in xylene and coverslipped using Permount (Fisher, Fair Lawn, NJ, USA).

Stereological analysis

Sections were viewed using a Leica DMLB microscope equipped with an x/y/z movement-sensitive stage and video camera connected to a computer. Cells were plotted and images acquired for figures using Neurolucida software (MicroBrightField, MBF, Williston, VT, USA). In three brains processed for peroxidase immunostaining, cells were counted using StereoInvestigator software (MBF). Plotting and counting were done using a computer resident atlas of the forebrain, which was designed according to cytoarchitectonic and chemoarchitectonic principles (Geeraedts et al., 1990; Gritti et al., 1993). For this purpose, outlines of sections and contours of the major nuclei were drawn in Neurolucida from series of sections which were collected at 400 μm intervals and stained for Nissl, Klüver-Barrera, ChAT and GAD. The levels of the atlas correspond approximately to those of the Paxinos and Watson atlas (Paxinos and Watson, 1986), although from anterior (A) 8.6 (from interaural zero), at which level our sections are matched to the Paxinos and Watson atlas, extending

rostrally and caudally, they differ slightly (~10% difference). For stereological estimates, cell counts were performed within the atlas contours of the BF nuclei in 12 sections at 400 μm intervals from A7.0 to A11.0. For plotting and illustrating the distribution of cells in the BF nuclei, cells were plotted in 6 sections at 800 μm intervals. In each case, histological sections of each series were matched to computer atlas templates using low magnification (5 or 10x) objectives. When necessary the contours of the atlas were slightly adjusted to fit the nuclei of the histology section. Plotting or counting was then performed within the contours at high magnification using a 63x Oil objective with a 1.4 numerical aperture and an oil condenser. For plotting cells for illustration of their distribution in figures using Neurolucida, all labeled neuronal cell profiles in the BF nuclei contours were marked through the full depth of individual (20 μm thick cut) sections.

In each series of three brains (G1, G2 and G3) immunostained by peroxidase, immuno-positive (+) or NR+ cells were counted by applying systematic unbiased sampling using the Optical Fractionator probe of StereoInvestigator. The cells were counted within 6 nuclei in the BF: MS, DBB, MCPO, SIa, SIp and GP. For each nucleus, labeled cells were counted on one side of the brain in at least 4 sections (4 – 7, depending upon the length of each nucleus) at 400 μm intervals (1/20 sections sampled). A counting frame of 89 x 89 μm (7921 μm^2) and a sampling grid of 200 x 200 μm (40,000 μm^2) were employed. Since the average thickness of the mounted sections was ~10 μm across series and brains, a dissector height of 8 μm below the surface was employed. From the top surface of each section, cells were counted if the top of

the cell came into focus beneath the surface and within the dissector height. The sampling thus included 5% of the sections, ~20% of the area of each nucleus and ~80% of the height of the section for an overall sampling of ~0.8% of the volume of each nucleus through the BF. Accordingly, an average of ~894 sampling sites were employed for counting cells in an average total volume for the six BF nuclei of ~11.34 mm^3. In initial sampling and for the duration of the counting, the precision of the estimates was checked by referring to Gundersen's Coefficient of Error (CE, m1). The average CE (in 3 brains) for the total number of cells across the BF was 0.08 for the ChAT+ cells, 0.04 for the GAD+ cells, 0.02 for the PAG+/NR+ cells and 0.06 for the PAG-/NR+ cells.

Additional series processed for dual fluorescent immunostaining for VGluTs and PAG, ChAT, or GAD were analyzed under epifluorescent microscopy on the Leica DMLB microscope equipped with filters appropriate for Cy2 (FITC) and Cy3 (rhodamine) detection. In each dual immunostained series of three brains (G5, G6 and G7), immuno-positive cells were counted by applying systematic unbiased sampling using the Optical Fractionator probe of StereoInvestigator for estimates of proportions of double-labeled cells within the MCPO at one level (~A8.2). The probe was run twice in each series, so as to sample the same population of cells but with different (Cy3 or Cy2) filters. A counting frame of 89 x 89 μm (7921 μm^2) and a sampling grid of 200 x 200 μm (40,000 μm^2) were employed, such as to sample an average of ~30 sites in each series. A dissector height of 8 μm was used in this series of mounted sections which had an average thickness of 8 μm.

Color photographs were prepared using Adobe Photoshop and schematic figures from the computer atlas images from Neurolucida using Adobe Illustrator (Adobe Systems, San Jose, CA, USA).

RESULTS

Distribution and estimates of ChAT+, GAD+ and PAG+ neurons

As evident in the MCPO (Fig. 1), ChAT+, GAD+ and PAG+ neurons were codistributed through the nuclei of the BF cholinergic cell area. Darkly stained with DAB, ChAT+ cells were most commonly medium to large in size, fusiform to polygonal in shape and in some regions grouped in clusters (Fig. 1A). Also darkly stained with DAB, GAD+ cells were variable in size from small to large, oval to polygonal in shape and relatively densely distributed through all areas where cholinergic cells were present (Fig. 1B). In some places, large GAD+ cells also formed small aggregates. Stained in a punctate manner with black DAB-Ni, PAG+ neurons were also variable in size from small to large, oval to polygonal in shape and more numerous than the ChAT+ or GAD+ cells (Fig. 1C). PAG+/NR+ cells were codistributed with less numerous NR+ cells that did not contain PAG+ punctate staining and were thus considered PAG-/NR+ cells. Like the PAG+/NR+, these were also variable in size and shape. Along with GAD+ cells, the PAG+ cells were evident across all the BF nuclei where cholinergic cells were located, including the MCPO (Fig. 1), the DBB (Fig. 2A), the SIa (Fig. 2B), the SIp (Fig. 2C) and the GP (Fig. 2D). In each of these areas, the PAG+/NR+ cells were codistributed with less numerous PAG-/NR+ cells (Fig. 2). All cell types were also present in the olfactory tubercle (OTu), but were not included in the present survey.

From rostral to caudal, ChAT+ cells were distributed through the MS, DBB, MCPO, SIa, SIp and GP (Fig. 3), in some places in aggregates, as described previously (Gritti et al., 1993). Ubiquitously, though not evenly, intermingled

with the ChAT+ cells, GAD+ cells were densely distributed through the same regions (Fig. 4). Throughout, PAG+/NR+ cells were present in the highest density along with less numerous PAG-/NR+ (Fig. 5).

Using the Optical Fractionator probe of StereoInvestigator, total cell numbers were estimated for each cell type across the BF nuclei from three rats (G1, G2 and G3; Table 1). The average total numbers of cells estimated in this manner were ~22,000 ChAT+ cells, ~119,000 GAD+ cells, ~315,000 PAG+ cells and 350,000 (PAG+/ and PAG-/) NR+ cells. According to these estimates the cell densities were ~2000 ChAT+, 11,000 GAD+ cells, 28,000 PAG+ and 31,000 NR+ cells per mm^3. The relative proportions of cells were ~5% ChAT+, 35% GAD+ and 90% PAG+ of the total (NR+) cell population. Except within the GP, these proportions were similar across nuclei of the BF.

Proportions of PAG+, ChAT+ and GAD+ neurons containing VGluT

In order to determine if PAG+, ChAT+ and/or GAD+ cells contained VGluTs, dual fluorescent immunostained series were examined from colchicine treated rats (G5, G6 and G7). In series dual immunostained for PAG and VGluT2 (Fig. 6A), the VGluT2 staining was prominent within axon terminals and varicosities (Fig. 6A2). In contrast, it was not evident at levels above background in cell bodies of neurons in the BF, despite colchicine pretreatment. Under these conditions, PAG+ nerve cell bodies were judged to be negative for VGluT2 immunostaining (Fig. 6A1 and A2).

In series dual immunostained for the synthetic enzymes and VGluT3 (Fig. 6B-D), the VGluT3 staining was prominent in a small number of axon terminals

and in many nerve cell bodies. In sections dual immunostained for PAG and VGluT3, most PAG+ cells contained VGluT3 (Fig. 6B1 and B2). Using unbiased estimates through the MCPO, approximately 70% of PAG+ cells were judged to be immuno-positive for VGluT3 (mean ± standard deviation from three rats, SD: 70.3% ± 26.7%). Reciprocally, almost all VGluT3+ neurons were positively stained for PAG (96.3% ± 4.4%). In sections dual immunostained for ChAT and VGluT3, the vast majority of ChAT+ neurons were judged immuno-positive for VGluT3 (Fig. 6C1 and C2). Indeed, VGluT3 was present in ~90% of the ChAT+ cells (88.9% ± 19.2%). In sections dual immunostained for GAD and VGluT3, about half of the GAD+ neurons were judged to be immuno-positive for VGluT3 (46.8% ± 21.6%) (Fig. 6D1 and D2).

DISCUSSION

The present stereological estimates reveal a very large cell population in the BF of the rat that is comprised of only a small proportion of ACh-synthesizing neurons together with a significant proportion of GABA-synthesizing neurons and major proportion of Glu-synthesizing neurons. Given the overlapping numbers, a proportion of ACh- and GABA-synthesizing neurons could also synthesize Glu. The vast proportion of Glu-synthesizing neurons also appear to have the capacity to store and release Glu either through VGluT2, which is present in axon terminals, or through VGluT3, which is present in most Glu- and ACh- and about half the GABA-synthesizing nerve cell bodies. These results indicate that glutamate can be synthesized in the cell bodies of a major proportion of BF cells and if not released from terminals, released from the soma or dendrites of glutamatergic but also many cholinergic and GABAergic neurons to contribute to the local processing as well as efferent output and consequential functional influence of the BF.

Numbers and proportions of neurons able to synthesize ACh, GABA and/or Glu

We employed stereological analysis for estimating total cell numbers through the volume of the BF nuclei in the present study. We first had to determine appropriate immunohistochemical processing and stereological procedures for counting immunostained cells. We learned that we could not use sections thicker than 20 μm in order to have full and even penetration of the antibodies for ChAT,

GAD and PAG through the full depth of the sections. We subsequently found that these sections were reduced to an average 10 μm thickness once they were dehydrated, delipidated and coverslipped. We were thus not able to apply what are otherwise considered to be optimal conditions for stereological counts which set guard zones at the top and bottom of the sections and count through more than 10 μm through the middle of the section (West, 1993). We adopted a strategy instead of counting the tops of cells which came into focus beneath the surface of the section and through 8 μm of the z axis. We moreover had to count cells based upon their immunostaining and thus of the cytoplasm, not the nucleus, which we thus did for the NR staining of the cytoplasm as well. Given several adjacent series of sections that were stained from each brain, we randomized the start of each series and collected sections at every 400 μm. This collection procedure thus provided for sampling of each series, 12 sections through the BF cholinergic cell area and 4 to 7 sections through each individual nucleus, depending upon its length. We subsequently selected a counting frame size that would provide >3 cells on average to be counted per frame per series across the BF. And finally we selected a grid size that provided >100 cells of each type to be counted per series across the BF. In practice, the sampling proved to be just adequate for the ChAT+ cells and more than adequate for the other cells, particularly the PAG+ cells.

We obtained an average estimate of ChAT+ cells of ~22,000 which is higher than the average estimate, ~15,000 (excluding the OTu), we previously calculated using counts corrected for double counting according to estimates of cell size and section thickness by the Abercrombie method (Abercrombie, 1946).

However, these two estimates are not statistically significantly different when compared between the two groups and thus support the contention that Abercrombie corrected counts can be successfully used to estimate cell numbers if applied appropriately (Guillery and Herrup, 1997). In the present sample, the variation across brains was relatively high with a coefficient of variation (CV: SD/mean) of 0.33. It is not known if this variation is due to sampling of what is an inhomogeneously distributed population of cells that tend to cluster in groups or to individual variation in the number of cells across rats. To our knowledge, there is one other published estimate of the total number of ChAT+ cells in the rat BF which is 26,390 (Miettinen et al., 2002).

The number of GAD+ cells, ~119,000, estimated here by stereology significantly and greatly exceeds the number, ~30,000 (excluding the OTu), previously estimated by us using Abercrombie corrected counts (Gritti et al., 1993). This three fold difference cannot be attributed to differences in counting method. It is undoubtedly due to the use of a different antibody for staining GAD. In our previous study, we employed the original sheep anti-GAD antiserum (Oertel et al., 1981), whereas in the current study we employed the more recent rabbit anti-GAD antiserum directed against the GAD67 isoform of the enzyme (Chemicon), which is present in the soma of most GABAergic cells and appears to provide greater sensitivity for staining cell bodies at least in the BF. We did also find a relatively large variation in the number of GAD+ cells across brains with a CV of 0.39. As for the ChAT+ cells, it could be due to the somewhat uneven distribution of GAD+ cells. It could also be due to individual differences in numbers of GAD+ cells. Such variation for GAD+ neurons (stained for

GAD67) has been noted by others using stereological estimates in the dentate gyrus and associated with a CV of 0.40 (Muller et al., 2001). In those studies, the variation was actually attributed to individual variation in the number of GAD+ cells across rats (see below). For comparison, we know of no other estimates for GAD+ cell numbers across the BF.

The number of PAG+ neurons was estimated here at ~316,000. This estimated number had the smallest CV of 0.14, indicating possibly that the large number and density as well as more even distribution of the PAG+ neurons was associated with more similar estimates across brains. Or it indicates that there is less variation in the number of PAG+ neurons. By adding the number of PAG-/NR+ neurons to those of the PAG+/NR+ neurons, we estimated the total population of cells in the BF as ~355,000 with a CV of 0.15. We know of no other published estimates of PAG+ or total BF cell population.

The PAG+ neurons represented ~90% of the BF cell population. Given that the ChAT+ cells represent ~5% and the GAD+ ~35%, it appears that there is an overlap in the three populations. We first employed PAG based upon immunohistochemical studies showing that it selectively labeled glutamatergic pyramidal cells and rarely labeled GABAergic interneurons in the cortex (Donoghue et al., 1985; Kaneko and Mizuno, 1988; Akiyama et al., 1990; Kaneko et al., 1992; Kaneko and Mizuno, 1994). On the other hand, in our previous study we found that PAG was present in ~95% of ChAT+ cells and ~60% of GAD+ (also >50% of parvalbumin+) cells in the BF (Manns et al., 2001; Gritti et al., 2003). As discussed in that original study on cortically projecting neurons, the colocalization of these neurotransmitter enzymes could indicate that Glu could be

synthesized and utilized together with ACh and GABA in the same neurons. PAG can also serve to provide Glu for the synthesis of GABA (Pow and Robinson, 1994). The clear presence of PAG- neurons in the BF, indicates that certain neurons do not contain this enzyme for the conversion of glutamine to Glu. In the cortex, evidence was presented that GABAergic interneurons do not contain PAG and contain instead high concentrations of soluble aspartate aminotransferase (sAAT) through which they could utilize α-ketoglutarate to produce Glu as a precursor for GABA (Kaneko and Mizuno, 1994). The numbers of the PAG-/NR+ cells (~39,000) correspond to approximately 40% of the GAD+ cell population that was the proportion of GAD+ cells found to be negative for PAG in our previous study (Manns et al., 2001). Together with our previous results, the present results suggest that some neurons contain PAG and GAD and have the capacity to synthesize both Glu and GABA or to utilize Glu synthesized by PAG for GABA synthesis, whereas others have the capacity to synthesize GABA alone through a different metabolic pathway for Glu. Perhaps the capacity for some PAG+ neurons to synthesize GABA from Glu through the presence of GAD is realized under certain conditions, as has been found for what are glutamatergic neurons in the dentate gyrus, which in addition to PAG, express GAD, and synthesize and release GABA following kindling (Kaneko and Mizuno, 1988; Sloviter et al., 1996; Gomez-Lira et al., 2005).

Proportions of neurons able to release Glu through VGluTs

Since implementation of immunohistochemical staining of the synthetic enzymes for ACh, GABA and Glu, the vesicular transporter proteins have been identified, which are responsible for the uptake, storage and release of ACh (VAChT) (Gilmor et al., 1996), GABA (VGAT) (Chaudhry et al., 1998) and Glu (VGluT 1 and 2) from nerve terminals (Fremeau et al., 2001; Fujiyama et al., 2001). Presence of specific vesicular transporters in terminals of neurons thus indicates use of the substrate as a neurotransmitter. Whereas VAChT is present in the soma and dendrites of cholinergic neurons, VGAT and VGluT1/2 are only found in the axonal varicosities and terminals. Some investigators have visualized VGluT2 in nerve cell bodies of neurons in the MS-DBB using very high doses (3 times those used in the present study) of colchicine (Hajszan et al., 2004; Colom et al., 2005), yet such doses also stimulate mRNA for many enzymes and peptides (Cortes et al., 1990). Using previously established and approved doses of colchicine which block axonal transport (Gritti et al., 1993), we were unable to detect VGluT2 in nerve cell bodies of neurons in the BF. It was thus not possible to employ immunohistochemical staining of cell bodies for this vesicular transporter to determine which BF neurons utilize Glu. In situ hybridization for mRNA of the vesicular transporters has been successfully employed in BF and revealed that some neurons contain mRNA for VGluT2 (Hur and Zaborszky, 2005). From RT-PCR studies, it also appeared that mRNA for VGluT2 can be colocalized with mRNA for ChAT and/or GAD in young and adult rats (Sotty et al., 2003; Danik et al., 2005). Thus, as for the presence of PAG, the presence of mRNA for VGluT2 in ChAT and GAD expressing neurons suggested that BF neurons have the

potential to synthesize Glu and the vesicular transporters necessary for its utilization along with ACh or GABA as neurotransmitters. In contrast, by immunohistochemical study of the vesicular transporters contained in anterogradely labeled BF terminals, we have found that the BF fibers are phenotypically distinct, containing VAChT, VGAT or VGluT2 in their terminals, and thus functionally cholinergic, GABAergic or glutamatergic (Henny and Jones, 2006a). In the descending projections to the hypothalamus, the VAChT+ terminals represented a small proportion (~10%), the VGAT+ terminals the largest proportion (~50%) and the VGluT2+ terminals ~25%. The estimate of glutamatergic BF projection neurons in our studies is similar to that recently estimated for the MS-DBB, though using different techniques, as representing 20-25% (Colom et al., 2005). On the other hand, these similar estimates leave in further question why such a large proportion of BF neurons contain PAG, including ChAT+ and GAD+ neurons.

In addition to VGluT1 and 2, a third type of VGluT was discovered and found to be present in cell bodies as well as terminals of neurons and moreover to be present within cholinergic neurons in the striatum (Gras et al., 2002) and GABAergic interneurons in the cortex (Fremeau et al., 2002; Herzog et al., 2004). VGluT3 was also reported to be present in many BF neurons, including both cholinergic and presumed GABAergic, parvalbumin-immunostained, neurons (Harkany et al., 2003). In the present study, we found that VGluT3 is present in the soma of BF neurons dual-immunostained for ChAT, GAD or PAG. In our previous studies, we did not find VGluT3 to be contained in terminals of BF projecting fibers to either hypothalamus (Henny and Jones, 2006a) or cortex

(Henny and Jones, in preparation). Its presence in the cell bodies thus presumably does not indicate that the cells have the capacity to release Glu from axon terminals. On the other hand, VGluT3 has been shown to endow the soma and dendrites of cells with the capacity to release Glu that can act as a retrograde signal upon afferent inputs (Fremeau et al., 2002; Harkany et al., 2003; Harkany et al., 2004). Here, the vast majority of ChAT+ cells and about half the GAD+ cells were judged immuno-positive for VGluT3. These proportions are very similar to those estimated for the ChAT+ and GAD+ cells that respectively contained PAG (Manns et al., 2001), indicating together with our previous results showing a lack of VGluT3 in BF terminals (above, (Henny and Jones, 2006a)), that these neurons would have the capacity to synthesize and release Glu not from axon terminals but from their cell bodies or dendrites. A large proportion (~70%) of PAG+ neurons were immunostained for VGluT3 and virtually all VGluT3+ neurons were immunostained for PAG, indicating that most Glu-synthesizing neurons would have the capacity to release Glu from their cell bodies or dendrites. It is thus possible that the presence of PAG in ChAT+ and GAD+ neurons (Manns et al., 2001) does reflect the capacity to synthesize Glu as a neurotransmitter or modulator, however one which is released through VGluT3 from the soma and dendrites of neurons which otherwise release ACh or GABA through VAChT or VGAT respectively from their axon terminals. The presence of PAG in ChAT- and GAD- neurons likely reflects the capacity of those neurons to synthesize Glu as a neurotransmitter that can be released from axon terminals presumably through VGluT2 and/or from cell bodies through VGluT3. Accordingly, the presence of PAG in the major proportion of BF neurons indicates that in addition

to ACh and GABA, Glu plays a major part in the distant and local influences of the BF neurons.

Given the large population of BF neurons and the small percentage comprised by the cholinergic cells, it is not surprising that nonselective lesions of the BF have had much more devastating effects upon cortical activity and behavioral state than selective cholinergic cell lesions (Damasio et al., 1985; Dunnett et al., 1991; Wenk, 1997; Sarter et al., 2003; Jones, 2004). Thus the important role played by the cholinergic cells must be viewed as contingent upon the influence of the predominant GABAergic and glutamatergic cells along with the potential modulation exerted by Glu, which can be synthesized and released from such a large proportion of BF neurons.

Acknowledgments—The research was supported by grants to IG and MM from the University of Milan and to BEJ from the Canadian Institutes of Health Research (CIHR, 13458) and the National Institute of Mental Health (NIMH, RO1 MH60119-01A1). We are most grateful to Dr. Takeshi Kaneko (Kyoto, Japan) for generously supplying the antibody for PAG. We would also like to thank Dr. Gianluca Vago (Department of Clinical Science Luigi Sacco, University of Milan, Milan, Italy) for his consultation.

Table 1. Stereological estimates of numbers and proportions of ChAT+, GAD+, PAG+ and total (NR+) cells in basal forebrain.

	Sections Sampled	Sites Sampled	Volume (mm3)	Cells Counted	Cell Number	Cell Density	% Total
Nucleus		**Mean ± SD**	**Mean ± SD**	**Mean ± SD**	**Mean ± SD**	**Mean ± SD**	**Mean ± SD**
ChAT+ cells							
MS	5	78.7 ± 1.5	0.939 ± 0.044	16.3 ± 15.0	2,062 ± 1,891	2,158 ± 1,954	4.4 ± 3.7
DBB	4	64.0 ± 5.3	0.738 ± 0.109	45.7 ± 13.2	5,765 ± 1,667	7,740 ± 1,379	14.5 ± 4.2
MCPO	5	104.7 ± 8.1	1.310 ± 0.112	43.0 ± 21.9	5,429 ± 2,769	4,147 ± 2,122	8.5 ± 4.3
SIa	7	187.0 ± 19.7	2.241 ± 0.245	17.0 ± 1.7	2,146 ± 219	969 ± 180	2.2 ± 0.2
SIp	4	100.0 ± 7.9	1.200 ± 0.094	21.7 ± 13.8	2,735 ± 1,742	2,275 ± 1,484	6.3 ± 3.4
GP	6	359.3 ± 10.2	4.941 ± 0.140	33.7 ± 13.7	4,250 ± 1,723	866 ± 364	6.1 ± 1.9
Total BF	**12**	**893.7 ± 23.0**	**11.369 ± 0.316**	**177.3 ± 57.7**	**22,388 ± 7,290**	**1,976 ± 661**	**6.2 ± 1.3**
GAD+ cells							
MS	5	79.7 ± 4.0	0.940 ± 0.046	120.7 ± 78.8	15,234 ± 9,946	16,279 ± 10,473	36.9 ± 24.1
DBB	4	66.0 ± 8.7	0.765 ± 0.136	62.7 ± 34.4	7,911 ± 4,347	9,891 ± 4,581	20.6 ± 12.4
MCPO	5	106.3 ± 7.5	1.313 ± 0.092	131.0 ± 78.1	16,538 ± 9,860	12,806 ± 8,074	26.2 ± 15.6
SIa	7	181.7 ± 12.5	2.173 ± 0.197	216.0 ± 130.0	27,269 ± 16,411	12,652 ± 8,138	29.2 ± 17.9
SIp	4	101.3 ± 4.7	1.210 ± 0.087	63.0 ± 26.5	7,954 ± 3,347	6,508 ± 2,429	20.6 ± 10.1
GP	6	358.7 ± 10.5	4.932 ± 0.135	353.0 ± 47.5	44,565 ± 5,992	9,052 ± 1,351	65.7 ± 6.8
Total BF	**12**	**893.7 ± 13.6**	**11.334 ± 0.276**	**946.3 ± 369.6**	**119,471 ± 46,657**	**10,528 ± 4,107**	**34.1 ± 12.8**
PAG+ cells							
MS	5	78.3 ± 2.3	0.939 ± 0.044	309.0 ± 56.6	39,010 ± 7,149	41,384 ± 5,832	90.5 ± 5.7
DBB	4	62.0 ± 7.8	0.738 ± 0.109	287.0 ± 64.0	36,233 ± 8,080	49,811 ± 12,461	89.6 ± 5.8
MCPO	5	103.7 ± 6.0	1.328 ± 0.088	470.0 ± 60.5	59,336 ± 7,639	44,571 ± 3,007	92.7 ± 2.0
SIa	7	185.0 ± 12.2	2.193 ± 0.163	653.3 ± 54.2	82,481 ± 6,848	37,881 ± 5,594	85.6 ± 7.8
SIp	4	100.7 ± 7.2	1.197 ± 0.096	292.0 ± 64.0	36,864 ± 8,083	30,979 ± 7,744	90.0 ± 0.7
GP	6	356.3 ± 4.7	4.910 ± 0.069	494.7 ± 115.9	62,450 ± 14,632	12,713 ± 2,920	90.8 ± 2.3
Total BF	**12**	**886.3 ± 15.0**	**11.304 ± 0.235**	**2,506.0 ± 347.4**	**316,374 ± 43,860**	**28,006 ± 3,992**	**89.4 ± 3.7**
NR+ cells (Total)							
MS	5	78.3 ± 2.3	0.939 ± 0.044	342.3 ± 65.3	43,218 ± 8,245	45,832 ± 6,829	100.0 ± 0.0
DBB	4	62.0 ± 7.8	0.738 ± 0.109	321.7 ± 74.5	40,609 ± 9,411	56,222 ± 16,845	100.0 ± 0.0
MCPO	5	103.7 ± 6.0	1.328 ± 0.088	508.0 ± 76.5	64,133 ± 9,663	48,129 ± 4,243	100.0 ± 0.0
SIa	7	185.0 ± 12.2	2.193 ± 0.163	769.7 ± 115.6	97,168 ± 14,591	44,777 ± 9,677	100.0 ± 0.0
SIp	4	100.7 ± 7.2	1.197 ± 0.096	324.7 ± 73.0	40,988 ± 9,216	34,438 ± 8,759	100.0 ± 0.0
GP	6	356.3 ± 4.7	4.910 ± 0.069	544.7 ± 124.1	68,762 ± 15,672	13,995 ± 3,113	100.0 ± 0.0
Total BF	**12**	**886.3 ± 15.0**	**11.304 ± 0.235**	**2,811.0 ± 432.2**	**354,879 ± 54,558**	**31,433 ± 5,132**	**100.0 ± 0.0**

Cells were counted and total cell numbers estimated using the Optical Fractionator probe of StereoInvestigator in the number of sections (every 400 μm) and sites (89 x 89 μm by 8 μm depth counting blocks) indicated along with the estimated volume and corresponding cell density (per mm^3) per nucleus. The % total represents the proportion that each cell type represents of the Nissl-stained (NR+) cells per nucleus, which was calculated as the total number of NR+ (PAG+/NR+ plus PAG-/NR+) cells.

Fig. 1. Images of ChAT+ (**A**), GAD+ (**B**) and PAG+ with NR+ (**C**) neurons in the magnocellular preoptic nucleus (MCPO, ~A8.5). ChAT and GAD are revealed with DAB (brown), and PAG is revealed with DAB-Ni (black) along with Nissl stained by Neutral Red (NR) (on right side in adjacent series from rat G3). Many cells are immuno-positive for PAG (PAG+/NR+, black arrowheads), evident as black granules over the cytoplasm, and are codistributed with fewer cells which are immuno-negative for PAG and stained for NR (PAG-/NR+, white arrowheads). Scale bar = 25 μm.

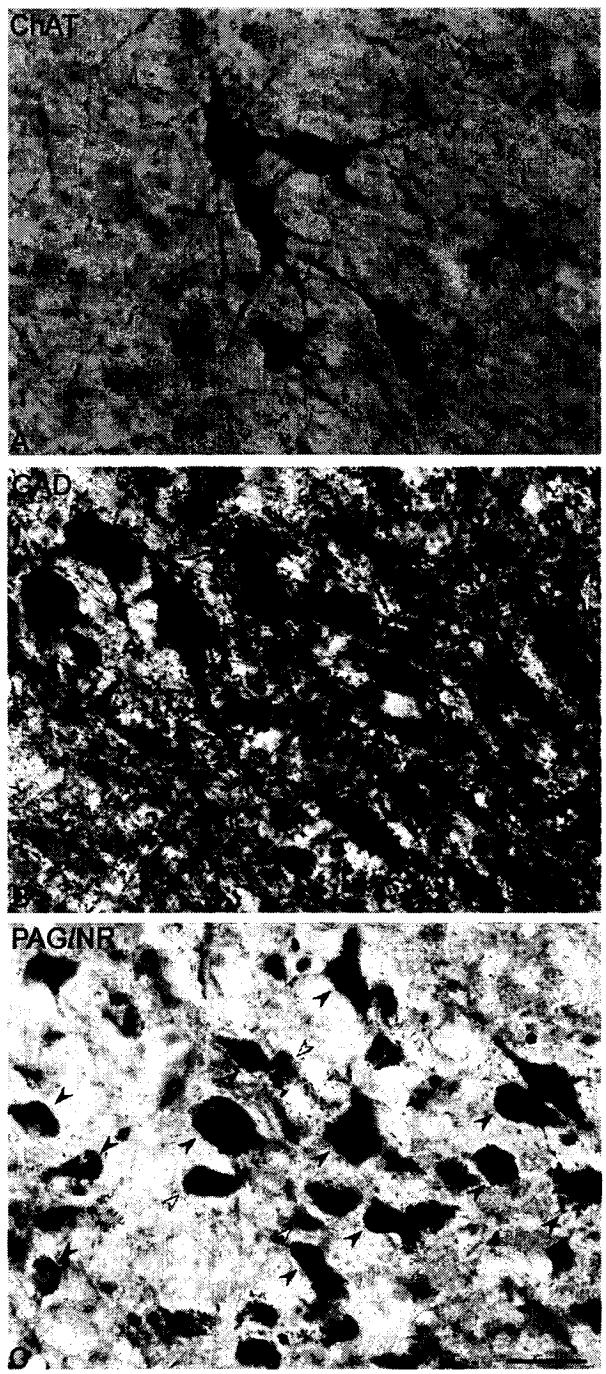

Fig. 1. Images of ChAT+ (A), GAD+ (B) and PAG+ with NR+ (C) neurons in the magnocellular preoptic nucleus (MCPO, ~A8.5)

Fig. 2. Images of PAG+/NR+ and PAG-/NR+ neurons in different BF nuclei. PAG+/NR+ cells (black arrowheads) are codistributed with PAG-/NR+ cells (white arrowheads) (on right side in same series from rat G3) in the nucleus of the diagonal band of Broca (DBB, ~A9.4, in **A**), the substantia innominata, pars anterior (SIa, ~A8.6 in **B**), the substantia innominata, pars posterior (SIp, A7.8 in **C**) and the globus pallidus (GP, ~A7.8 in **D**). Very small NR stained cells were judged to be glia and not counted as neurons. Scale bar = 25 μm.

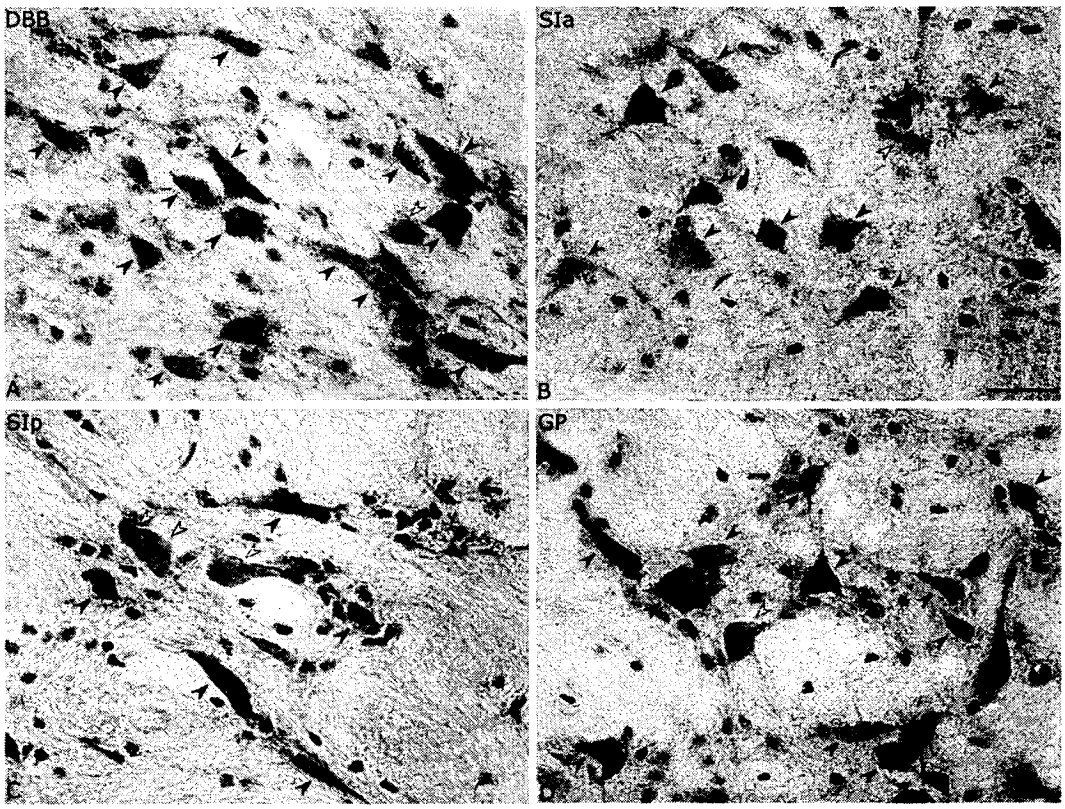

Fig. 2. Images of PAG+/NR+ and PAG-/NR+ neurons in different BF nuclei

Fig. 3. Distribution of ChAT+ neurons in the BF. Each symbol marks one ChAT+ cell plotted in one 20 μm thick section (from rat G3) on computer-based atlas templates. See list for abbreviations.

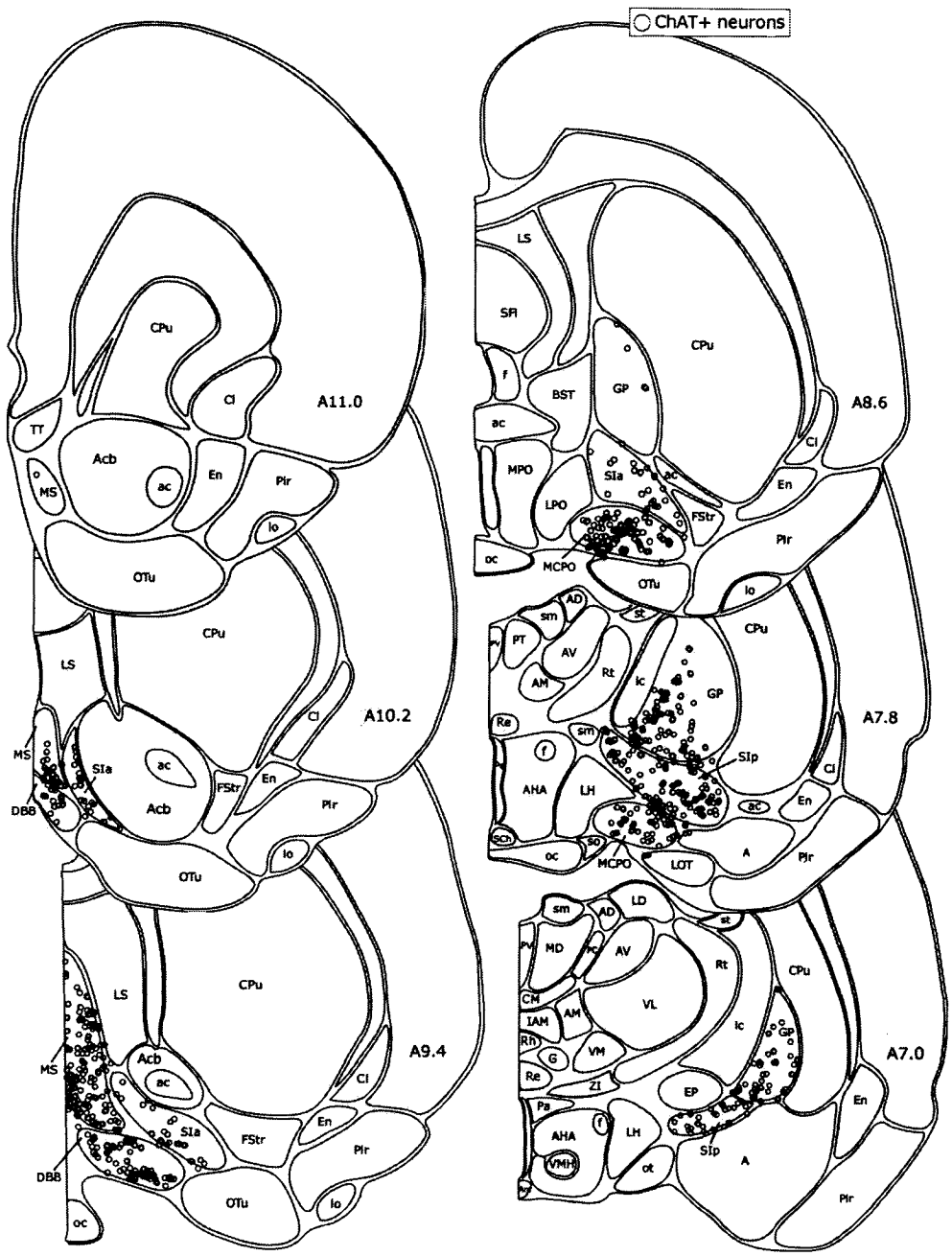

Fig. 3. Distribution of ChAT+ neurons in the BF

Fig. 4. Distribution of GAD+ neurons in the BF. Each symbol marks one GAD+ cell plotted in one 20 μm thick section (from rat G3) on computer-based atlas templates. See list for abbreviations.

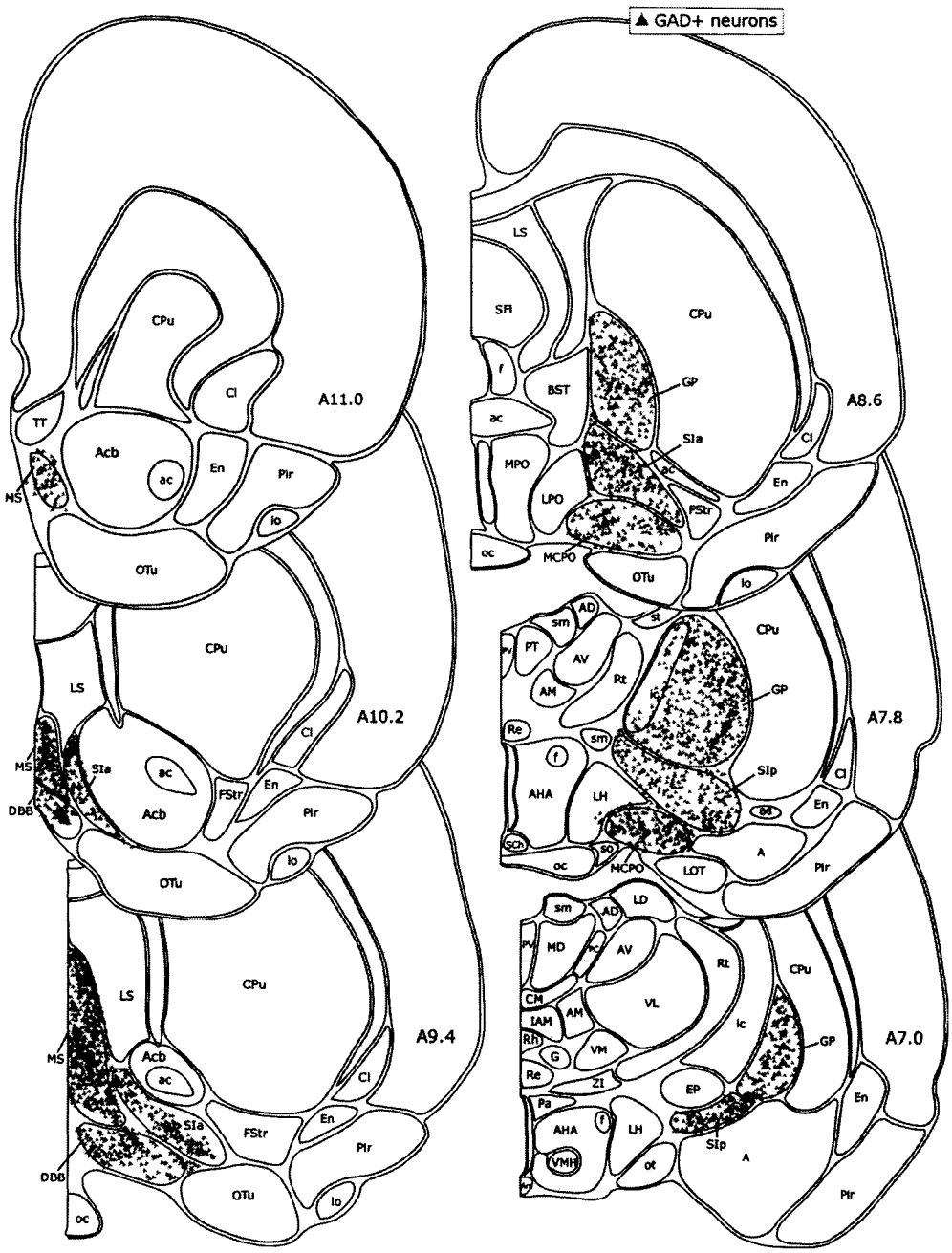

Fig. 4. Distribution of GAD+ neurons in the BF

Fig. 5. Distribution of PAG+/NR+ and PAG-/NR+ neurons in the BF. Each symbol marks one PAG+/NR+ or PAG-/NR+ cell plotted in one 20 μm thick section (from rat G3) on computer-based atlas templates. See list for abbreviations.

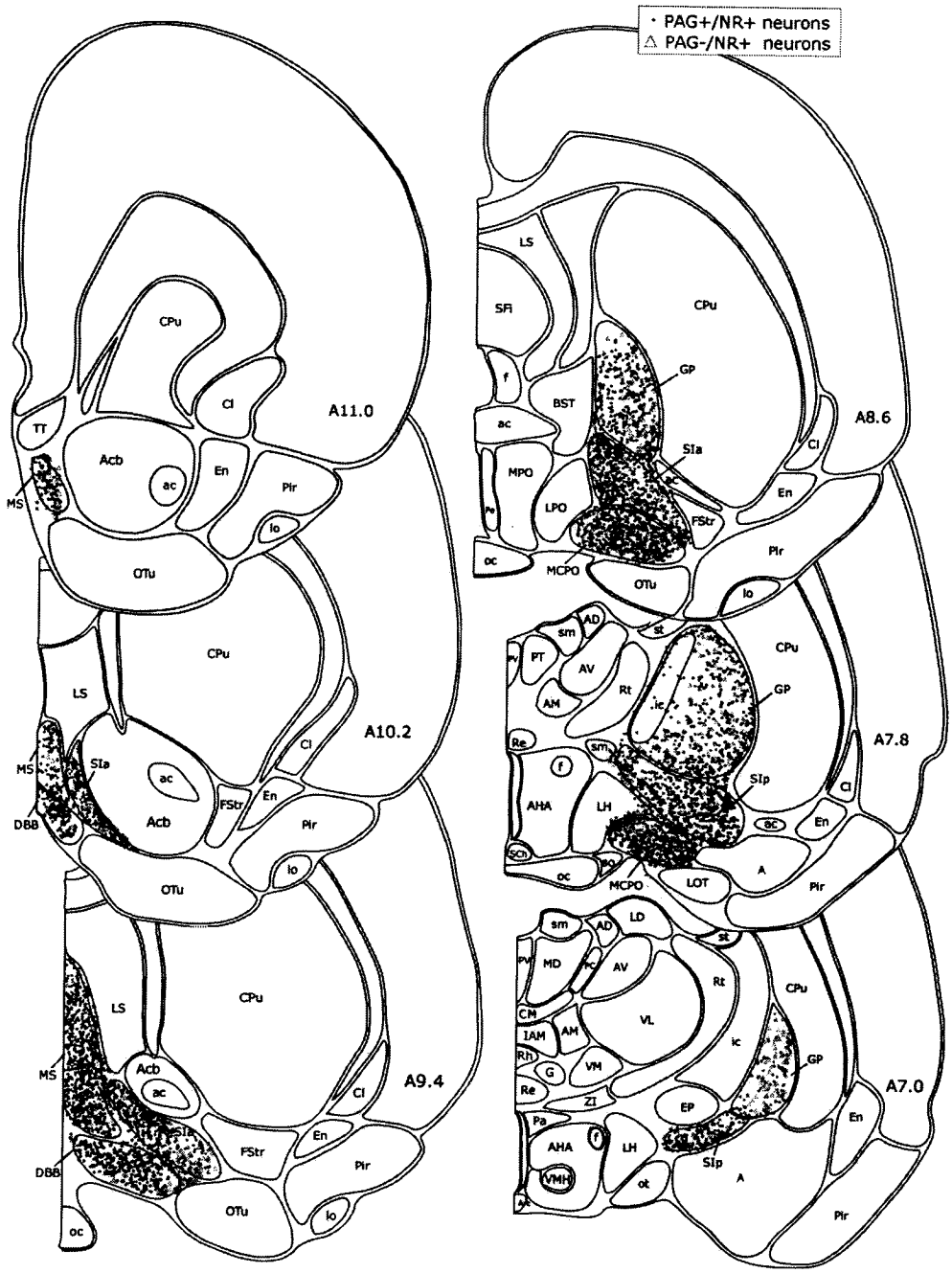

Fig. 5. Distribution of PAG+/NR+ and PAG-/NR+ neurons in the BF

Fig. 6. Presence of VGluT2 or VGluT3 in PAG+, ChAT+ or GAD+ cells in the MCPO of colchicine treated rats. **A**. PAG+ cells (in Cy2, solid arrowheads in **A1**) were not immunostained for VGluT2 (open arrowheads in **A2**), which was prominent in axon terminals (in Cy3, **A2**). **B**. Most PAG+ cells (in Cy2, solid arrowheads in **B1**) were positively immunostained for VGluT3 (in Cy3, solid arrowheads in **B2**). **C**. Most ChAT+ cells (in Cy2, solid arrowheads in **C1**) were immunostained for VGluT3 (in Cy3, solid arrowhead in **C2**). **D**. About half of GAD+ cells (in Cy2, solid arrowheads in **D1**) were judged immuno-positive (solid arrowheads in **D2**) and half immuno-negative (open arrowheads in **D2**) for VGluT3 immunostaining (in Cy3, **D2**). Scale bar = 25 μm.

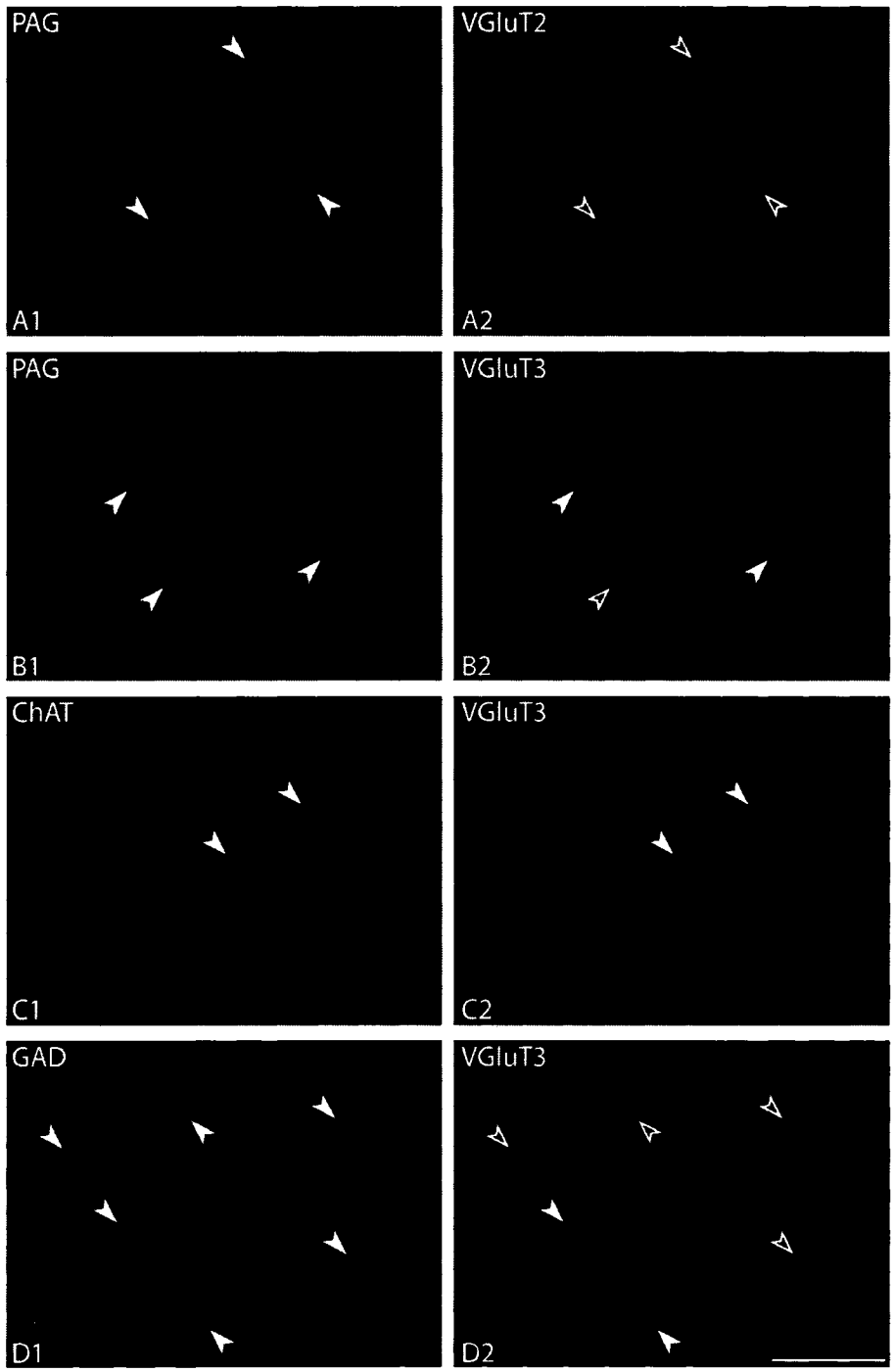

Fig. 6. Presence of VGluT2 or VGluT3 in PAG+, ChAT+ or GAD+ cells in the MCPO of colchicine treated rats

PREFACE TO CHAPTER II

In the previous chapter we showed that a large number of neurons in the BF contain PAG, and are thus able to synthesize glutamate. We also showed that PAG neurons also expressed VGluT3, indicating their capacity to take up and release glutamate. Critically, most of ChAT+ and half of the GAD+ cell population also contained VGluT3, in line with previous results showing the presence of PAG in these two neuronal populations. Nonetheless, the presence of PAG and VGluT3 in BF cell bodies leave many unanswered questions about the use of glutamate as a neurotransmitter by BF neurons. As discussed previously, VGluT3 expressed in the somato-dendritic compartment of neurons has been implicated in the retrograde signaling of glutamate (Harkany et al., 2004). Yet, if expressed in axon terminals, VGluT3 may also mediate axonal release of glutamate (Fremeau et al., 2004). Therefore, is VGluT3 only expressed in cell bodies and dendrites of BF neurons, or may it be also present in axon terminals and participate in the axonal release of glutamate? Second, based on the presence of PAG and VGluT3 in cholinergic and GABAergic neurons, may that be an indication of co-release of ACh or GABA with glutamate from axon terminals of those neurons? Finally, given the presence of a fraction of PAG neurons that does not express VGluT3, are other VGluTs used by BF neurons to release glutamate?

In the next two chapters, these questions will be addressed by combining anterograde transport from BF neurons with immunohistochemistry for VAChT, VGAT and VGluTs in order to assess the capacity of BF terminals for neurotransmitter release and/or co-release. We examined these terminals in the prefrontal cortex (PFC, chapter II) and the lateral hypothalamus (LH, chapter III),

two areas known to receive prominent projections and be critically influenced by the BF region.

Following the identification of cholinergic, GABAergic and glutamatergic contingents in PFC, their contribution to total innervation was estimated by unbiased sampling procedures. In addition, the capacity to form synapses as well as the relation of each contingent with cortical pyramidal and interneuronal cell populations was examined.

Given the diverse roles of the PFC in autonomic regulation, cognition and generation of SWA during sleep, the influence of cortically projecting BF neurons on these processes is discussed.

Chapter II

Basal Forebrain Axon Terminals Containing Vesicular Transporters for Acetylcholine (VAChT), GABA (VGAT) or Glutamate (VGluT) in Rat Prefrontal Cortex

Pablo Henny and Barbara E. Jones

Montreal Neurological Institute, McGill University,

Montreal, Quebec, Canada H3A 2B4

ABSTRACT

Through projections to cerebral cortex, the basal forebrain (BF) plays important roles in the modulation of cortical activity and function. Retrograde tracing studies have established that this projection comprises cholinergic, GABAergic and other unidentified neurons. Recent evidence suggests the latter could be glutamatergic. To examine the existence, contribution and organization of BF neurons that can release glutamate, the presence of vesicular transporters proteins (VTPs) for glutamate (VGluT), as well as for acetylcholine (ACh, VAChT) and GABA (VGAT), was examined in BF axon terminals innervating the prefrontal cortex (PFC). Following small injections of the anterograde tracer biotinylated dextran amine 10,000 MW (BDA) into the magnocellular region of the BF, brain serial sections were processed for dual and triple fluorescent staining. BDA-labeled axons were seen in the PFC, with a high density in the infralimbic cortex (IL), where they innervated deep layers. Axonal varicosities formed three independent populations containing VGluT2, VAChT or VGAT. In the IL, they accounted for ~15%, ~19% and ~52% of the total number of BF terminals, respectively. Glutamatergic and GABAergic axons appeared to form synapses, as assessed by the relation of the terminals with the postsynaptic proteins (PSPs) PSD-95 and Gephyrin (Geph), respectively. Some cholinergic axons were also associated with postsynaptic Geph profiles. Finally, it was found that PFC interneurons expressing the calcium binding protein (CBP) calbindin (CB) were apposed by glutamatergic, cholinergic and GABAergic axonal varicosities. VGAT+ varicosities also apposed interneurons containing the CBP parvalbumin (PV) as well as principal cells, as identified by non-phosphorylated

neurofilaments (NPNF). Through three independent cortically projecting contingents and specific efferent projections, the BF can modulate cortical activity in a diverse and complex manner.

INTRODUCTION

Through widespread projections to the cerebral cortex, the basal forebrain (BF) plays important and diverse roles in the modulation of cortical activity in association to behavioral states, cognitive processes and autonomic function (Buzsaki et al., 1988; Groenewegen and Uylings, 2000; Van Eden and Buijs, 2000; Sarter et al., 2001; Jones, 2004). The projections are comprised by heterogeneous yet not fully characterized populations of neurons that could contribute to different aspects of BF function.

Based on the presence of choline acetyltransferase (ChAT) and glutamic acid decarboxylase (GAD), the synthetic enzymes for acetylcholine (ACh) and GABA respectively, retrograde tracing studies have established that large contingents of ACh- and GABA-synthesizing BF neurons innervate the cortex (Zaborszky et al., 1986; Fisher et al., 1988; Gritti et al., 1997). They have nonetheless evidenced the existence of another non-cholinergic, non-GABAergic group of projecting neurons, since the proportions of ChAT (~20% to ~30%) and GAD (~40 to 45%) neurons retrogradely labeled from prefrontal or parietal cortex did not account for the total number of labeled cells (Gritti et al., 1997). This additional contingent might comprise glutamate-synthesizing neurons, since a prominent number of cortically projecting BF neurons (~80%) shows immunoreactivity for phosphate-activated glutaminase (PAG) (Manns et al., 2001), the enzyme involved in the synthesis of the neurotransmitter glutamate (Bradford et al., 1978; Kaneko and Mizuno, 1988). However, PAG is also present in a vast majority (~95%) of ChAT+ and large proportion (~60%) of GAD+ neurons, suggesting that in addition to purely glutamate-releasing neurons,

cholinergic and some GABAergic neurons might also synthesize and release glutamate (Manns et al., 2001).

In order to identify, quantify and describe the contribution of cholinergic, GABAergic and as yet putative glutamatergic BF neurons to the cortical projection, the presence of the vesicular transporter proteins (VTP) for ACh (VAChT) (Gilmor et al., 1996; Arvidsson et al., 1997), GABA (VGAT) (McIntire et al., 1997; Chaudhry et al., 1998) and glutamate (VGluTs) (Bellocchio et al., 2000; Fremeau et al., 2001; Fujiyama et al., 2001; Fremeau et al., 2002) as markers for neurotransmitter specific uptake and release, was examined in BF axon terminals in the prefrontal cortex (PFC), one of the major cortical targets of BF neurons (Luiten et al., 1987; Gaykema et al., 1990).

Following discrete deposits of biotinylated dextran amine 10,000 MW (BDA-10,000) in the magnocellular preoptic nucleus (MCPO) and substantia innominata (SI) and anterograde transport of the tracer, series were processed for dual staining of BDA and VAChT, VGAT or VGluT (1, 2 or 3) and examined in PFC. Additional series were processed for double-staining of VTP to assess colocalization of VTPs within the same varicosities. Subsequent stereological analysis was carried out to determine the number and proportion of terminals, in addition to their laminar distribution in the infralimbic cortex (IL). To assess whether the terminals formed synapses, sections were triple stained for BDA, VTPs and postsynaptic proteins (PSPs) gephyrin, a marker for inhibitory synapses (Sassoe-Pognetto and Fritschy, 2000; Sassoe-Pognetto et al., 2000), or PSD-95, a marker for excitatory synapses (Kornau et al., 1995; Sheng and Pak, 2000; Sassoe-Pognetto et al., 2003). Finally, triple stained material for BDA, VTP and

the cortical neuron markers non-phosphorylated neurofilament (NPNF) (Campbell and Morrison, 1989; Kirkcaldie et al., 2002) for pyramidal cells or the calcium binding proteins (CBP) parvalbumin (PV) or calbindin (CB) for interneurons (Celio, 1986, 1990) was examined to determine the relation with different cortical cell populations.

MATERIALS AND METHODS

Animals and Surgery

Procedures were in agreement with the guidelines of the Canadian Council on Animal Care and the U.S. NIH and were approved by the McGill University Animal Care committee.

As described previously (Henny and Jones, 2006a), Long-Evans rats (200-250 g, Charles River Canada, St. Constant, Quebec, Canada) were anaesthetized with ketamine/xylazine/acepromazine (65/5/1 mg/kg, i.p.) and placed in a stereotaxic frame (David Kopf Instruments, Tujunga, CA, U.S.A.) for surgery and holes were drilled in the skull on each side over the BF. Glass micropipettes (tip diameter 15 to 25 μm) were back-filled with a 0.5 M NaCl solution containing 2% 10,000 MW BDA (BDA-10,000, Molecular Probes, Eugene, Oregon, U.S.A.) and lowered into the BF on each side aimed at the magnocellular preoptic nucleus (MCPO, from *Bregma*: anterior-posterior (AP), -0.5 mm; Lateral (L), +/- 2.5 mm; Vertical (V), 8.5 mm) with the aid of a micropositioner (Model 660, David Kopf Instruments). A holding current of -300 nA was maintained (using a Microiontophoresis Dual Current Generator 260, World Precision Instruments (WPI), Sarasota, FL, U.S.A.) during the descent to avoid leakage of the solution. Microinjection of BDA was performed by iontophoresis applying positive current pulses (5 to 10 μA) in a duty cycle of 1 sec (0.5 s on, 0.5 s off) for a period of 25 to 30 min through a stimulator (Pulsemaster A300, WPI) and stimulus isolation unit (Iso-Flex, A.M.P.I., Israel). After the injection, the micropipette was held in place for 10 min and removed during renewed application of the holding current.

Rats were maintained for 5 or 6 days with food and water *ad libitum* to allow anterograde transport of the tracer. They were subsequently perfused transcardially under deep sodium pentobarbital anesthesia (100 mg/kg, i.p.) with ~500 ml 4% paraformaldehyde fixative solution. The brains were removed and put in a 30% sucrose solution for 2 to 3 days or until they sunk, after which they were frozen at -50° C and stored at -80° C for subsequent processing.

Immunohistochemistry

Forebrains, including cortex and BF, were cut in sections of 25 μm thickness and collected in eight series, using intervals of 200 μm between sections. The first series was processed for evaluation of the BDA injection site location and general BDA fiber distribution in the forebrain under light microscopy. For this purpose, sections were incubated and processed with the Vectastain ABC Elite kit (Vector Laboratories, Burlingame, CA, U.S.A.) with nickel-intensified diaminobenzidine (DAB-Ni) and counterstained with neutral red (NR).

Adjacent series containing PFC were processed for dual or triple fluorescent staining of BDA, VTPs, PSPs or cortical markers (see Table 1). Prior pilot studies were performed to determine the conditions necessary for antibody as well as streptavidin penetration through the full depth of the sections. As assessed under epifluorescent and confocal microscopy, we established that 0.1% and 0.3% Triton X-100 (TX) allowed full penetration of antibodies and streptavidin through the sections in double and triple fluorescent material, respectively. Free floating sections from each series were rinsed for 30 min in Trizma saline buffer (TS, 0.1

M, pH 7.4) followed by incubation for 30 min with a blocking solution of normal donkey serum (NDS, 6% in TS) containing 0.1% or 0.3% Triton X-100 (TX). Sections were subsequently incubated overnight at room temperature with one or two primary antibodies in TS containing NDS 1% and TX (0.1% or 0.3%). The sections were then rinsed for 30 min and incubated for three hours in appropriate secondary antibodies in NDS 1% and TX (0.1% or 0.3%) (Table 1). With the exception of double staining of two VTPs (see below), sections were then rinsed for 30 min and incubated for three hours in streptavidin for BDA revelation (Table 1).

For double labeling of BDA and one of the VTPs, sections were incubated (using 0.1% TX) first with primary antibodies against VAChT, VGAT or VGluT1, 2 or 3 (from Goat, Gt or Rabbit, Rb) and then with Cy3-conjugated secondary antibodies (from Donkey, Dky) followed by Cy2-conjugated streptavidin for revelation of BDA (see Table 1, Double BDA/VTP).

For double labeling of two VTPs, sections were incubated (using 0.1% TX) with two primary antibodies against VAChT, VGAT or VGluT2 (from different host species) and then with corresponding Cy2- and Cy3-conjugated secondary antibodies (from Dky) (see Table 1, Double VTP/VTP).

For triple labeling of BDA, VAChT and VGAT, sections were incubated (using 0.3% TX) with primary antibodies (from different host species) against VAChT and VGAT and then with corresponding Cy3 or Cy5 secondary antibodies (from Dky), respectively. The sections were subsequently incubated with Cy2-conjugated streptavidin for revelation of BDA (see Table 1, Triple BDA/VTP/VTP).

For triple labeling of BDA, the VTPs and PSPs, sections were incubated (using 0.3% TX) with two primary antibodies (from different host species) against VAChT, VGAT or VGluT2 and Geph or PSD-95 and then with corresponding Cy3 or Cy5 secondary antibodies (from Dky). Then, sections were subsequently incubated with Cy2-conjugated streptavidin for revelation of BDA (see Table 1, Triple BDA/VTP/PSP).

For triple labeling of BDA, the VTPs and the cortical markers, sections were incubated (using 0.3% TX) with two primary antibodies against VAChT, VGAT or VGluT2 and NPNF, PV or CB, respectively (from different host species) and then with appropriate Cy3 or Cy5 secondary antibodies (from Dky). They were subsequently incubated with Cy2-conjugated streptavidin for revelation of BDA (see Table 1, Triple BDA/VTP/Cortical markers).

All sections were mounted out of Trizma water, and the mounted sections dehydrated through alcohols, cleared in xylene and coverslipped with Permount.

Conventional microscopy and stereological analysis

Sections were examined under light and epifluorescent microscopy with a Leica DMLB microscope or Nikon Eclipse E800 which were equipped with x-y-z motorized stages, video or digital camera and filters appropriate for FITC (or Cy2), Rhodamine (or Cy3) fluorescence. Single as well as composite images were acquired using Neurolucida software (MicroBrightField, MBF, Colchester, VT, U.S.A.).

Injection sites from 8 rats (BDA 14, 15, 16, 18, 19, 20, 21 and 22) were examined under brightfield illumination in DAB-Ni/NR stained material. In 14

injection sites ('cases' on left and /or right sides), the labeled cells were centered in the MCPO-SI (on the left and/or right sides) and were used for analysis with double and triple fluorescent staining for BDA, VTP, PSPs or cortical markers. From these, 6 cases from 3 rats (BDA 16, 18 and 19) were selected for quantitative estimate of the proportions and layer distribution of BDA/VTP varicosities in PFC in fluorescent stained material (see text and Table 1).

Double labeling for VAChT, VGAT or VGluT2 was assessed under epifluorescent illumination on the Leica microscope (in 3 brains, Table 1).

Under epifluorescent illumination, fluorescent stained BDA-positive (+) varicosities were examined for double labeling with the VTPs in the PFC. Finding double labeling with VAChT, VGAT or VGluT2 (see Results), unbiased estimates of the total numbers of single BDA+ and double-labeled BDA+/VGluT2+, BDA+/ VAChT+ or BDA+/VGAT+ varicosities from 5 cases were estimated in the IL, a region from where projections from the BF have previously been described (Gritti et al., 1997). In all cases analyzed stereologically, all VTPs were stained using antibodies from Rabbit (Rb-Anti-VAChT, -VGAT and -VGluT2, see Table 1). Counts were performed under a 100x Oil objective (with 1.40 numerical aperture) using the Optical Fractionator probe of the Stereo Investigator software (MBF) on the Leica microscope. Varicosities were sampled in the IL, as delimited cytoarchitectonically by others (Krettek and Price, 1977), including all cortical layers, through 3 levels separated by 400 μm intervals (11.8, 11.4 and 11.0 μm anterior (A) to interaural zero (IA0)). The grid size (150 μm x 150 μm) was set to be larger than the counting

frame (75 μm x 75 μm) so as to sample 25% of the area in each of the regions. Counting was performed through ~8.5 μm of the section thickness (starting 1 μm from the surface of the mounted sections having an average thickness of ~10 μm). In each counting block, all BDA+ varicosities (in green, Cy2) were counted, including those which were or were not double-labeled for VTP (in red, Cy3) to allow an estimate of the proportion of double-labeled varicosities for each VTP. Additional estimations were performed at the same levels for the ventrolateral and lateral (VLO, LO) orbitofrontal cortex (OF), where a 900 x 900 μm^2 square was used as a sampling area.

To examine the distribution of BDA+ and BDA+/VTP+ axons across cortical layers, contours of the IL containing the mapped varicosities during the stereological procedure were overlaid on Nissl-stained rat brain sections. Molecular (I), superficial (II-III) and deep (V-VI) layers were delineated within the contours based onto cytoarchitectonic criteria (Krettek and Price, 1977; Hurley et al., 1991) and maps of the rat brain (Swanson, 1992), and the proportion of BDA+ and of each type of BDA+/VTP+ per layer over total BDA+ or BDA+/VTP+ in each series was estimated.

Confocal microscopy and image processing

To assess the presence of VGAT in BDA+/VAChT+, or the association of BDA+/VTP+ varicosities with postsynaptic elements or cortical neurons, triple stained sections for BDA/VAChT/VGAT, BDA/VTPs/PSPs or BDA/VTPs/Cortical markers were analyzed by confocal microscopy with a Zeiss

LSM 510 laser scanning microscope equipped with Argon 488 nm, helium-neon 543 nm and helium-neon nm 633 lasers for Cy2, Cy3 and Cy5 excitation as well as with appropriate filters for detection of Cy2 (bandpass 500 to 530 nm, green), Cy3 (bandpass 565 to 615 nm, red) and Cy5 (bandpass 697 to 719 nm, infrared). Scanning was performed through a Plan-Apochromat 100x (with 1.4 numerical aperture) objective and pinhole size of 1 (Airy Units) for each of the three channels. Images were acquired for the three chromogens using the resident LSM 510 software and consisted of stacks taken through the z-axis in optical slices of ~0.33 μm for PSP series or ~0.50 μm for cortical markers series.

Rendered 3D views of the image stacks were obtained using the image software Volocity 3.5.1 (Improvision Inc, Lexington, MA, U.S.A., www.improvision.com), which allowed interactive visualization, magnification and rotation of the 3D images in order to determine the relative location of each of the elements from the three channels.

Adjustments for brightness and contrast in brightfield images and tonal range for each individual RGB channel ("Adjust/levels" command) in fluorescent images were performed with Adobe Photoshop Creative Suite (Adobe System, San Jose, CA, U.S.A). Figures were mounted in Adobe Illustrator Creative Suite (Adobe).

RESULTS

BDA injection site and axonal labeling in the cortex

As described previously (Henny and Jones, 2006a), iontophoretic application of BDA-10,000 into the region of the MCPO-SI (Fig. 1A) produced a well restricted, round injection site (Fig. 1B) containing labeled cell bodies and dendrites (Fig. 1C). The average number of BDA-labeled neurons per injection was ~1400 (mean ± SEM, 1430.6 ± 315, n = 5), from which ~90% were located at the MCPO and ~6% at the SI (Henny and Jones, 2006a).

BDA-10,000 was found in axons within regions previously described to receive abundant projections from MCPO-SI, including cortical and subcortical regions (Luiten et al., 1987; Grove, 1988; Gritti et al., 1994; Gritti et al., 1997; Henny and Jones, 2006a). BDA-labeled axons reached the cortex through lateral and medial pathways, as previously described (Saper, 1984; Gaykema et al., 1990). In the lateral path, axons coursed laterally to reach and innervate piriform, entorhinal and perirhinal cortices caudally, and piriform cortex, the rhinal aspect of the agranular insular cortex, the claustrum and OF rostrally. Through the medial path, axons run rostrally through the diagonal band of Broca and medial septum, to innervate the tenia tecta, IL and prelimbic (PL) cortices.

Most prominently, the IL as well as VLO and LO cortices received abundant BDA-labeled axons, which could be seen across cortical layers yet more abundant in deep ones. Axonal fibers were morphologically diverse and bore both *boutons en passant*, as well as *boutons terminaux* (not shown).

VAChT, VGAT or VGluT within BDA-labeled varicosities in prefrontal cortex

Series that were double stained for BDA and the VTPs were examined to determine if BF axonal varicosities in the PFC were immunopositive (+) for VAChT, VGAT or VGluT1, 2 or 3.

In series processed for BDA and VAChT, a portion of the BDA-labeled terminals were double-labeled for VAChT (Fig. 2A and B). The BDA+/VAChT+ varicosities were relatively small and most often located along axons (Fig. 2A), yet at times they could be located at the end of axons as *boutons terminaux* (Fig. 2B).

In series stained for BDA and VGAT, VGAT was found in a large number of BDA+ axon terminals (Figure 2C, D). The BDA+/VGAT+ varicosities appeared somewhat larger and rounder than BDA+/VAChT+ ones and could be seen at the end of axons as *boutons terminaux* (Fig. 2C), yet most commonly along the axons as *boutons en passant*, (Fig. 2D).

In series processed for BDA and VGluT1, 2 or 3, only VGluT2 (Fig. 2E and F), and not VGluT1 or VGluT3 (not shown), was found to be present in BDA-labeled varicosities. The BDA+/VGluT2+ varicosities were most frequently seen as *boutons en passant* (Fig. 2E and F) though also seen as *boutons terminaux.*

To find evidence of colocalization of VGluT2 with VAChT or VGAT in BF terminals, dual stained material for VTPs was subsequently examined in IL and OF (Fig. 3). In dual-stained material for VAChT and VGluT2, no evidence for colocalization of the two markers was found (Fig. 3A). Similarly, in dual-stained material for VGAT and VGluT2 there was no evidence for colocalization

between these two populations (Fig. 3B). Thus, the results suggest that cholinergic or GABAergic BF axons do not express a glutamatergic phenotype in their terminals. Series dual stained for VAChT and VGAT were also examined. Most of VAChT+ varicosities were found to be negative for VGAT, and reciprocally, the vast majority of VGAT+ varicosities were found negative for VAChT (Fig. 3C). Yet, a very small proportion was found to be double labeled for VAChT and VGAT. To assess whether this small proportion could correspond to BDA-labeled cholinergic fibers coming from MCPO-SI neurons, triple staining was performed for BDA, VAChT and VGAT and analyzed in confocal microscopy. Of >290 BDA+/VAChT+ varicosities from several axons from 3 cases analyzed, less than 4% presented some staining for VGAT (not shown).

Proportion and laminar distribution of VAChT+, VGAT+ and VGluT2+ BDA-labeled varicosities

Having established the lack of colocalization by the different VTPs in BF axonal varicosities, the proportions of cholinergic, GABAergic and glutamatergic BF axon terminals were determined by stereological estimations of the total numbers of BDA+ and of BDA+/VTP+ varicosities in the IL and OF at three levels (~A11.8, A 11.4 and A11.0, Fig. 1, Table 2). In IL (n = 5), ~19% of BDA+ varicosities in the VAChT series were found BDA+/VAChT+, ~52% of the BDA+ varicosities in the VGAT series were BDA+/VGAT+ and ~15% of the BDA+ varicosities in the VGluT2 series were BDA+/VGluT2+ (see Table 2). In the OF (n = 6), ~23% of BDA+ varicosities in the VAChT series were found

BDA+/VAChT+, ~49% of the BDA+ varicosities in the VGAT series were BDA+/VGAT+ and ~8% of the BDA+ varicosities in the VGluT2 series were BDA+/VGluT2+. A two-way analysis of variance (ANOVA) for region and proportions of VTP (Region x VTP) yielded significant effects of VTP, but not for Region or the interaction ($F = 0.078$, $p > 0.05$ for Region; $F = 18.042$, $p < 0.001$ for VTP; $F = 0.291$, $p > 0.05$ for the interaction). Accordingly, raw data for both regions were pooled together (PFC), resulting in VAChT +, VGAT + and VGluT2+ proportions of ~21%, ~50% and ~11% of the BDA+ varicosities. The proportions of VTP differed significantly according to one-way ANOVA ($F=19.793$, $p < 0.001$).

To examine the laminar distribution of BF fibers, the proportions of BDA+ and BDA+/VTP+ varicosities located in layers I, II-III or V-VI of IL was determined. Of the total number of BDA+ varicosities sampled stereologically in the three series (see Methods), ~58% of them were found in layers V-VI, ~11% in layers II-III and ~31% in layer I. These proportions differed significantly (as assessed by one-way ANOVA, $F = 29.10$, $p < 0.001$) followed by post-hoc Bonferroni pairwise comparisons ($p < 0.05$ for each comparison). Of the total number of BDA+/VTP+ varicosities sampled in each series, proportions for each BDA+/VTP+ group were significantly higher in deep V-VI (~73%, ~71% and ~75% for BDA+/VAChT+, BDA+/VGAT+ and BDA+/VGluT2+ respectively) when compared to molecular I (~18%, ~27% and ~10%) or II-III (~9%, ~2%, and ~15%) layers (as assessed by two-way ANOVA, with Layer and VTP as factors: $F=23.4$, $p < 0.001$ for Layer; $F = 0.336$, $p > 0.05$ for VTP; $F = 0.416$, $p > 0.05$ for

the interaction and post-hoc Bonferroni pairwise comparisons, $p < 0.05$ for layer V-VI vs. layers I or II-III).

Presence of postsynaptic proteins Gephyrin or PSD-95 in relation to VAChT, VGAT or VGluT2 BDA-labeled terminals

To assess whether BF axon terminals might form synapses with postsynaptic elements in PFC, series were processed for triple staining of BDA, the VTPs and the PSPs Geph or PSD-95 (see Table 1). Material was examined and z-stacks of images (taken at 0.33 μm steps) acquired under confocal microscopy, to be subsequently analyzed as single raw images and 3D rendered reconstructions (Fig. 4). In series stained for BDA, VAChT and Geph (Fig. 4A), it was found that a moderate proportion of BDA+/VAChT+ profiles were found in association with Geph+ profiles (29.6% or 32 out of 108 varicosities observed). In series stained for BDA, VGAT and Geph (Fig. 4B), it was found that most of BDA+/VGAT+ varicosities were associated with Geph+ profiles (72.2% or 57 out of 79 varicosities observed). In contrast, only a relatively minor proportion of BDA+/VGluT2+ varicosities were associated with Geph profiles (16.7% or 2 out of 10 varicosities observed) in series stained for BDA, VGluT2 and Geph (Fig. 4C).

In series stained for BDA, VAChT and PSD-95 (Fig. 4D), only a small proportion of BDA+/VAChT+ varicosities were found associated with PSD-95+ profiles (13.9% or 5 out of 36 varicosities analyzed). Similarly, in series stained for BDA, VGAT and PSD-95 (Fig. 4E) a small proportion of BDA+/VGAT+

varicosities were in association with PSD-95 (13.3% or 2 out of 15 varicosities). In contrast, most of BDA+/VGluT2+ varicosities were associated with PSD-95+ profiles (53.3% or 16 out of 30 varicosities analyzed) in series stained for BDA, VGluT2 and PSD-95 (Fig. 4F).

VAChT+, VGAT+ and VGluT2+ BDA-labeled terminals in relation to NPNF pyramidal cells and PV or CB interneurons

Series that were triple-stained for BDA, the VTPs and cortical markers (n = 3 for each combination) were examined and acquired under confocal microscopy to examine if different BF contingents were located close to or in apposition to cortical neurons in PFC (Table 1, Fig. 5).

In BDA/VAChT/NPNF material, BDA+/VAChT+ axonal varicosities were often detected in the vicinity of NPNF+ cell bodies or dendrites (Fig. 5A), but not in direct apposition to the NPNF+ profiles. In BDA/VAChT/PV series, BDA+/VAChT+ varicosities could be seen in close proximity to PV+ cells (Fig. 5B). In BDA/VAChT/CB series, BDA+/VAChT+ terminals were seen in the vicinity of and sometimes in direct apposition to CB+ cells bodies (Fig. 5C).

In BDA/VGAT/NPNF material, BDA+/VGAT+ axonal varicosities were often detected in the vicinity of NPNF+ cell bodies or dendrites as well as in apparent contact with cell bodies (not shown) or dendrites (Fig. 5D). In BDA/VGAT/PV series, BDA+/VGAT+ varicosities could be seen in close proximity to PV+ cells and occasionally innervating perisomatically PV+ cell bodies (Fig. 5E). In BDA/VGAT/CB series, it was found that BDA+/VGAT+ varicosities could form appositions with CB+ cell bodies (Fig. 5F).

In BDA/VGluT2/NPNF series, BDA+/VGluT2+ varicosities were detected only in the vicinity of NPNF+ (Fig. 5G). Similarly, in BDA/VGluT2/PV series, BDA+/VGluT2+ varicosities were only seen in the vicinity of PV+ cells (Fig. 5H). In BDA/VGluT2/CB series, it was found that BDA+/VGluT2+ varicosities could form appositions with CB+ cell bodies (Fig. 5I).

DISCUSSION

The present study shows that the BF projection to PFC is formed by cholinergic, GABAergic and glutamatergic contingents. Through this projection, the BF may have a triple influence in the PFC and contribute differentially to cognitive, autonomic and behavioral functions executed by the PFC.

Glutamatergic BF cortically projecting neurons

The existence of glutamatergic neurons in the BF with projections to the cortex was postulated after retrograde tracing studies established that cholinergic and GABAergic neurons could not account for the total contingent of cortically projecting neurons (Gritti et al., 1997) and that a large proportion of BF neurons, including those with cortical projections, would have the capacity to synthesize neurotransmitter glutamate based on the presence of the enzyme PAG (Bradford et al., 1978; Kaneko and Mizuno, 1988; Manns et al., 2001). With the recent identification of VTPs for glutamate (VGluT1, 2 and 3) as proteins involved in the specific uptake of glutamate into synaptic vesicles, definitive markers for glutamatergic neurons have become available (Fremeau et al., 2001; Fujiyama et al., 2001; Fremeau et al., 2002). We report here that a set of cortically projecting BF neurons express the VGluT2 protein in their axon terminals, thus demonstrating the capacity of BF neurons to take up and release glutamate from their axon terminals in the cortex.

The presence of VGluT2 in axon terminals of BF neurons is in line with previous reports using *in situ* hybridization showing the presence of the mRNA for VGluT2 in BF neurons (Lin et al., 2003; Hur and Zaborszky, 2005). These

findings also conform to the principle that in contrast to VGluT1, VGluT2 expressing neurons predominate in subcortical regions (Fremeau et al., 2001; Kaneko and Fujiyama, 2002). On the other hand, neurons in the BF (Harkany et al., 2003), have also been shown to contain VGluT3 in their cell bodies. Yet, like BF neurons innervating the lateral hypothalamus (Henny and Jones, 2006a), cortically projecting glutamatergic neurons did not appear to express VGluT3 in their axon terminals. Since VGluT3 has been proposed to have a role in the somato-dendritic release of glutamate, our results indicate that BF neurons might release glutamate from axon terminals, using VGluT2, or from cell bodies and dendrites using VGluT3. Whether VGluT2 and VGluT3 could be expressed and utilized by the same neuronal population is as yet unknown.

Based on the colocalization of the synthetic enzymes ChAT and GAD with that of PAG in BF neurons, previous studies had suggested that cholinergic and GABAergic neurons might co-release glutamate (Manns et al., 2001). Given the lack of colocalization of VGluT2 with VAChT or VGAT, our results do not support the possibility of co-release of glutamate with ACh, or with GABA from the same terminals of BF neurons in the adult rat cortex. However, they do not exclude the possibility that cholinergic and some GABAergic neurons may synthesize glutamate and release it from their somato-dendritic compartments, indeed confirmed by the presence of VGluT3 protein in BF cholinergic and PV+, likely GABAergic, neurons (see above) (Harkany et al., 2003). Nor do the results exclude the rather unconventional idea that single neurons may give rise to axon terminals expressing different VTPs.

Previous studies have established that cholinergic and GABAergic BF populations do not overlap to a significant extent. We nonetheless examined the possibility of co-expression of VAChT and VGAT in BF terminals innervating the cortex, as it has been reported that ~8% of cholinergic synaptic terminals in the visual cortex of the cat present significant amounts of GABA immunoreactivity (Beaulieu and Somogyi, 1991). We found that of BF terminals expressing VAChT, less than 4% contained VGAT, indicating that whereas the BF may contribute some double-labeled terminals, another contribution must come from cortical cholinergic interneurons that are described in the rat, and are known to present both cholinergic and GABAergic phenotypes (Bayraktar et al., 1997). Together, these results show that in the adult rat, the BF projection to PFC is comprised by three independent, for the most part, non-overlapping, phenotypically distinct contingents.

Proportions and laminar distribution of cholinergic, GABAergic and glutamatergic BF axon terminals in PFC

We have found that cholinergic, GABAergic and glutamatergic BF terminals represent ~19%, ~52% and ~15% of the total BF terminals in their respective series in IL and similar proportions in OF. The proportions of cholinergic and GABAergic terminals are similar to the proportions of ChAT (23%) and GAD (43%) neurons retrogradely labeled in the MCPO after injections in the medial prefrontal cortex (Gritti et al., 1997). The proportion of glutamatergic terminals in IL (~15%) could not account for the total proportion of cortically projecting non-cholinergic, non-GABAergic neurons (~34%, from (Gritti et al., 2003)),

suggesting that another contingent, neither VAChT+, VGAT+, nor VGluT+, might be part of this projection.

In agreement with previous studies showing layer distribution of BF afferents to cortex (Saper, 1984), we found here that in IL all three contingents were mostly concentrated in deep layers. By innervating deep layers, cholinergic, GABAergic and glutamatergic BF fibers might influence the corticofugal output to BF itself (Gaykema et al., 1991), as well as subcortical autonomic and limbic areas (through layer V) to which IL projects (Vertes, 2004; Gabbott et al., 2005).

Postsynaptic proteins in relation to cholinergic, GABAergic and glutamatergic BF terminals

We have shown in this study that BF cholinergic, GABAergic and glutamatergic axon terminals, as identified by presynaptic VTPs, associate differentially with the PSPs Geph and PSD-95. Geph is a microtubule-associated protein that forms part of the molecular scaffolding of both glycine and $GABA_A$ receptors and is present at inhibitory synapses (Sassoe-Pognetto and Fritschy, 2000; Sassoe-Pognetto et al., 2000). PSD-95 is a scaffolding protein isolated from postsynaptic densities and shown to concentrate at asymmetrical excitatory synapses (Sheng and Pak, 2000; Sassoe-Pognetto et al., 2003). In addition, PSD-95 has been shown to interact directly and indirectly with NMDA and AMPA receptors, respectively. We have recently used both Geph and PSD-95 to show their association with BF GABAergic and glutamatergic descending axons in the lateral hypothalamus, respectively (Henny and Jones, 2006a).

Surprisingly, we observed a moderate incidence of cholinergic BF terminals with Geph. Although Geph has been shown not to associate with any known ACh receptor (AChR) type or play any known role in the assembling or clustering of AChR in avian peripheral ganglia (Allaire et al., 2000) , it should be noted that nicotinic receptors belong to the same family of glycinergic and $GABA_AR$ (Ortells and Lunt, 1995), both of which present association with Geph (Sassoe-Pognetto and Fritschy, 2000). Also of note is that cholinergic axon terminals in the cortex have been shown to form symmetric synapses (Houser et al., 1985; Beaulieu and Somogyi, 1991; Mechawar et al., 2000), which generally indicate inhibitory synapses. We observed that a large majority of BF GABAergic terminals were associated with Geph, thus confirming the capacity of BF neurons to form inhibitory synapses with cortical neuronal elements (Freund and Gulyas, 1991). In contrast, only a minor proportion of glutamatergic terminals were seen associated with Geph. Given the lack of colocalization between VGluT2 and VGAT in PFC, it is difficult at present to hypothesize what the functionality of that association might be. It should be noted, nonetheless, that CNS glutamatergic neurons have the capacity to change their phenotype to that of a GABAergic one under certain conditions (Gomez-Lira et al., 2005), of which the presence of Geph in association with some glutamatergic axons might be indicative.

Some cholinergic axon terminals were seen in association with PSD-95 but this proportion was minor as compared to those associated with Geph. PSD-95 has been reported to be present in peripheral nicotinic synapses and PSD-93, a close related protein, interacts directly with synaptic nicotinic receptors (Conroy

et al., 2003), suggesting that central cholinergic neurons may also do it. However, as far as we are concerned, the presence of PSD-95 in association with cholinergic central synapses has not been reported. Of note is that some, yet in marginal proportions, central cholinergic synapses have been shown to form asymmetrical synapses (Houser et al., 1985). Similarly, a very small proportion of BF GABAergic terminals presented some association with PSD-95. As no association of $GABA_AR$ with PSD-95 has been reported, the functional significance of this finding is difficult to interpret. In contrast, and in agreement with the prevalence of PSD-95 in glutamatergic synapses (Sheng and Pak, 2000; Sassoe-Pognetto et al., 2003), a majority of the VGluT2 BF varicosities associated with PSD-95, as was also previously shown for BF axonal varicosities in the lateral hypothalamus (Henny and Jones, 2006a).

Relation of cholinergic, GABAergic and glutamatergic BF terminals with cortical pyramidal and interneuronal cell populations

BF terminals innervated cortical pyramidal as well as interneurons identified by the cell-specific markers NPNF, PV and CB.

NPNF are neurofilaments in a non-phosphorylated state that have been reported to be present in pyramidal cell axons, dendrites and soma (Sternberger and Sternberger, 1983; Campbell and Morrison, 1989). In spite the relatively low intensity of NPNF staining in prefrontal cortex of the rat (Kirkcaldie et al., 2002), we were positively able to detect pyramidal cell profiles in both IL and OF with high magnification under confocal microscopy, indicating the feasibility of using the NPNF to detect pyramidal cells in this study. PV and CB are two calcium

binding proteins that together with calretinin have been shown to represent three, mostly non-overlapping, populations of cortical interneurons (Hendry et al., 1989; Celio, 1990; Kubota et al., 1994). It is assumed that both PV and CB interneurons modulate the activity of pyramidal neurons by direct inhibition, although through differential innervation of pyramidal cellular domains (Wang et al., 2004). Thus, evidence suggests that PV is generally present in basket or chandelier type of interneurons (DeFelipe, 1997), which encompass the group of neurons that provide somatic and proximal dendrite, as well as axonal innervation to pyramidal cells (Markram et al., 2004). Although CB may also be present in some basket cells (Markram et al., 2004) and a few layer III pyramidal cells (DeFelipe, 1997) it is usually present in double bouquet, Martinotti and/or Cajal-Retzius cells (DeFelipe, 1997), which in turn represent the group of neurons that provide dendritic innervation to pyramidal cells (Markram et al., 2004). In contrast to these cell populations, the action mode of calretinin neurons onto pyramidal cells is thought to occur indirectly through disinhibition, as they comprise interneuron-targeting interneurons (Wang et al., 2004).

BF cholinergic axons could be detected in apposition only to CB interneurons. They were seen close, but not in apposition, to pyramidal cells or PV interneurons. These results agree in general with studies showing a preferential innervation of interneurons (Beaulieu and Somogyi, 1991), in this case represented by CB cells, versus pyramidal cells by ChAT axons. The low incidence of appositions onto other cell types may also be indicative of the low incidence of synaptic specializations that cholinergic axons in the cortex have been reported to form (Mechawar et al., 2000). In that case, the cholinergic

influence may be by diffusion and thus more involved in modulation, rather than the driving of postsynaptic cell activity (Mechawar et al., 2000; Descarries et al., 2004). Among BF neurons, identified cholinergic neurons have been shown to discharge in association with cortical activation and during active wakefulness and paradoxical sleep (PS) (Manns et al., 2000a; Lee et al., 2005b). They have been shown to do so in bursts of action potentials at a theta frequency and in synchrony with cortical theta activity recorded in prefrontal and retrosplenial cortices (Manns et al., 2000a). In addition, ACh has been shown to produce a slow depolarization on pyramidal cells through muscarinic action. This effect is preceded by a fast inhibition mediated by fast muscarinic and nicotinic mediated excitation of interneurons which in turn inhibit the pyramidal cells (McCormick and Prince, 1985; McCormick, 1993). By excitation of CB interneurons, which can target soma/proximal dendrites of pyramidal cells, BF cholinergic neurons might indirectly pace their activity, to make them discharge in a theta frequency during cortical activation.

In contrast to cholinergic terminals, GABAergic terminals were seen in apposition with pyramidal as well as PV and CB interneurons. Given the association of BF GABAergic axons with the postsynaptic marker Geph, it is likely that the appositions on these cells represent synaptic specializations. If so, these results contrast with previous studies using anterograde tracing in combination with GABA immunohistochemistry and morphological criteria in EM, which showed an almost exclusive innervation by GABAergic BF afferents of CB interneurons, but not PV interneurons in the rat (Freund and Gulyas, 1991),

or of PV and somatostatin interneurons in the cat (Freund and Meskenaite, 1992), in both cases with no innervation of pyramidal cells.

GABAergic neurons in the BF comprise a physiologically heterogeneous group in the way they discharge in relation to cortical activity (Manns et al., 2000b, 2003a). On one hand, an important proportion of BF GABAergic neurons have been shown to increase their discharge during cortical activation induced by somatic stimulation under urethane anesthesia. These neurons, which as shown by antidromic activation also project to PFC, discharge tonically at frequencies in the gamma range. Innervating directly pyramidal neurons, GABAergic BF neurons of this type might pace high frequency firing of pyramidal cells during cortical activation. This influence might also be mediated through PV interneurons, which provide strong innervation of pyramidal cells, and have been suggested to contribute to the generation of gamma activity (Buzsaki and Chrobak, 1995; Jefferys et al., 1996) and do not adapt to high frequency input (Kawaguchi and Kubota, 1993), such as those which might be provided by BF high frequency spiking GABAergic neurons. By providing innervation to CB neurons, BF GABAergic neurons could also reduce the level of inhibition on pyramidal distal dendrites, in turn contributing to pyramidal cell excitability (Freund and Gulyas, 1991).

On the other hand, most of the GABAergic neurons identified under urethane anesthesia have been found to discharge maximally in association with irregular slow wave activity (of frequencies in the delta band, ~0.5 up to 4 Hz) and decrease their firing during cortical activation, and thus proposed to represent a population of neurons that could promote slow wave activity (Manns et al.,

2000b). Some of these neurons, which could be also activated antidromically from PFC, were shown to discharge phasically in bursts of action potentials at low (<1 Hz) frequencies, similar to the activity recorded in the cortex. By innervating pyramidal neurons, BF GABAergic neurons could promote the appearance of slow wave activity in PFC (see below). Innervation of interneurons may subserve a similar role in generation of slow wave activity, for example, by pacing activity of pyramidal cells through PV interneurons.

We found no evidence for a glutamatergic innervation of pyramidal or PV neurons in PFC. Glutamatergic axons could only be detected in apposition to CB interneurons. These appositions likely represent synaptic contacts given the association of glutamatergic axons with postsynaptic protein PSD-95. Putative glutamatergic neurons in the BF, as identified by the PAG enzyme and the lack of ChAT and GAD, have been shown to discharge in association with cortical activation in clusters of action potentials (Manns et al., 2003a). BF glutamatergic neurons might modulate the activity of pyramidal cells by reducing the influence of distal inputs if acting on dendrite-targeting CB interneurons or to pace pyramidal cell activity if representing CB soma- and proximal dendrite-targeting neurons.

Functional considerations

Acting as an extrathalamic relay from the reticular activating system to the cortex, the BF has been shown to promote cortical activation (Starzl et al., 1951; Kievit and Kuypers, 1975; Buzsaki et al., 1988; Jones, 2003). Yet, the variable and dissimilar influences that the BF imposes upon cortical activity (Sterman and

Clemente, 1962a; Manns et al., 2000b, 2003a; Jones, 2004) suggest that non-cholinergic inputs must also be of critical importance in other types of cortical activities and functions. We show here that the control the BF may have over PFC activity is carried out by three independent contingents of neurons, which may influence cortical activity through cholinergic, GABAergic or glutamatergic mechanisms.

The relevance of this varied influence of the BF over cortical, particularly PFC, activity is reflected in the effects that lesions of the BF have on cognitive processes, such as attention, short and long term memory and learning (Everitt and Robbins, 1997; Sarter et al., 2001; Sarter et al., 2003; Smith et al., 2004). These processes have been shown to depend on both cholinergic and non-cholinergic neurons, as the effect of total BF excitotoxic lesions are different, and commonly more deleterious, than those only targeting cholinergic neurons (Everitt and Robbins, 1997). In this regard, disruption of the cholinergic innervation of PFC primarily affects attention mechanisms, while having less direct influence on other processes, such as learning and memory (Sarter et al., 2003). It is suggested that those aspects primarily unaffected by cholinergic lesions might be carried out by the GABAergic system yet, as shown here, could also depend upon glutamatergic BF projection systems. OK

In relation to its influence over PFC cognitive processing, the BF may influence other aspects of PFC function. The PFC has been long known to play an important role in autonomic regulation, particularly in the control of the cardiovascular system (Verberne and Owens, 1998; Groenewegen and Uylings, 2000; Van Eden and Buijs, 2000; Resstel and Correa, 2006). In this regard, it is

interesting to note that ACh in the PFC has been shown to have a parasympathetic action, producing a significant decrease in arterial blood pressure when injected in the PFC of unanaesthetized rats (Crippa et al., 1999). This effect may be related to the parasympathetic activation that has been observed during attentive states, such as those during presentation of a conditioned stimulus (Hunt and Campbell, 1997), indicating that the role of ACh in attention (Sarter et al., 2003) may also be in part mediated through autonomic mechanisms. In contrast, microinjections of glutamate under the same behavioral conditions have been shown to elicit sympathoexcitatory pressor and tachycardic responses (Resstel and Correa, 2005, 2006), which suggest that the role of glutamate in PFC may be related to behavioral arousal. Although the sources of glutamate might also be other than the BF, glutamatergic BF neurons have been previously proposed to promote behavioral arousal through innervation of Orx neurons in the LH (Henny and Jones, 2006b). Through release of ACh or glutamate in deep layers of the PFC, BF neurons may mediate these autonomic effects by influencing the activity of PFC neurons that project to CNS areas involved in autonomic regulation, including the lateral hypothalamus, the nucleus of the tractus solitarius, the ventrolateral medulla and the thoracic spinal cord (Hurley et al., 1991; Vertes, 2004; Gabbott et al., 2005).

Finally, through innervation of the PFC, the BF may also promote sleep-related processes such as the appearance of slow wave activity that occurs during slow wave sleep (Sterman and Clemente, 1962a, 1962b). Exclusively sleep-related units have been identified in the subgenual prefrontal cortex of the monkey, which is homologous to IL in the rat (Rolls et al., 2003). The PFC has

been shown to be the cortical region where slow oscillations start in the course of SWS (Massimini et al., 2004). Also, anterior cortical regions, which would include the PFC show a maximal rebound in delta activity after SWS deprivation, suggesting a critical role in generation of these activities (Schwierin et al., 1999). It is proposed that these roles might depend, in part, on the activity of BF GABAergic neurons in the BF that project to the PFC and have been found to discharge during SWA at frequencies similar to those of the slow oscillation and of delta activity (Manns et al., 2000b).

Acknowledgments—We are grateful to Robert H. Edwards and Robert T. Fremeau (Departments of Neurology and Physiology, University of California San Francisco School of Medicine, San Francisco, CA 94143) for kindly supplying the antibodies for VGluT1 and 2. We thank Lynda Mainville for her excellent technical assistance.

Table 1. Primary antibodies (AB) for immunostaining of vesicular transporter proteins (VTPs), postsynaptic proteins (PSPs) or neuronal markers

Antigen	Host Sp.	Source[1]	Cat. #
VTPs			
VAChT	Rb	Sigma	V5387
VAChT	Gt	Chemicon	AB1578
VGAT	Rb	Chemicon	AB5062P
VGluT1	Rb	Gift RHE	-
VGluT2	Rb	Gift RHE	-
VGluT2	GP	Chemicon	AB5907
VGluT3	GP	Chemicon	AB5421
PSPs			
Geph	Ms	SY-SY	147 011
PSD-95	Ms	ABR	MA1-045
Neuronal markers			
NPNF	Ms	Sternberger	SMI32
PV	Ms	Sigma	P3088
CB	Ms	Sigma	C8666

[1]ABR: Affinity BioReagents, Golden, CO, U.S.A.; Chemicon International, Temecula, CA, U.S.A; Gift RHE: Gift from Robert H. Edwards, Fremeau et al (2001) "The expression of vesicular glutamate transporters defines two classes of excitatory synapse", Neuron 31(2):247-260; Sigma: Sigma, St. Louis, MO, U.S.A.; Sternberger: Sternberger Monoclonals Inc., Lutherville, MD, USA; SY-SY: Synaptic Systems, Göttingen, Germany. Abbreviations: GP, guinea pig; Gt, goat; Ms, mouse (monoclonal); Rb, rabbit.

Table 2. Combination and sequential processing of primary and secondary antibodies along with streptavidin (SA) used for triple fluorescent staining of vesicular transporter proteins (VTPs), postsynaptic proteins (PSPs), neuronal markers and biotinylated dextran amine (BDA)

	1[ry] AB (overnight)[1]			2[ry] AB (3 hours)		SA (3 hours)		
Series	**Antigen**	**Host sp**	**Dilution**	**IgG (Dky)[2,3]**	**Dilution**	**SA**	**Dilution**	**n[4]**
Double BDA/VTP								
BDA/VAChT	VAChT	Rb	1:1000	Anti-Rb-Cy3	1:800	SA-Cy2	1:800	6
BDA/VGAT	VGAT	Rb	1:250	Anti-Rb-Cy3	"	"	"	6
BDA/VGluT1	VGluT1	Rb	1:1000	Anti-Rb-Cy3	"	"	"	3
BDA/VGluT2	VGluT2	Rb	1:5000	Anti-Rb-Cy3	"	"	"	6
BDA/VGluT3	VGluT3	GP	1:1000	Anti-GP-Cy3	1:800	"	"	3
Double VTP/VTP								
VAChT/VGAT	VAChT	Gt	1:5000	Anti-Gt-Cy3	1:800			3
	VGAT	Rb	1:250	Anti-Rb-Cy2	1:200			
VAChT/VGluT2	VAChT	Gt	1:5000	"	"			3
	VGluT2	Rb	1:5000					
VGluT2/VGAT	VGluT2	GP	1:1000	Anti-GP-Cy3	1:800			3
	VGAT	Rb	1:250	Anti-Rb-Cy2	1:200			
Triple BDA/VTP/VTP								
BDA/VAChT/VGAT	VAChT	Gt	1:5000	Anti-Gt-Cy3	1:800	SA-Cy2	1:800	3
	VGAT	Rb	1:250	Anti-Rb-Cy5	1:800			
Triple BDA/VTP/PSP								
BDA/VAChT/Geph	VAChT	Rb	1:1000	Anti-Rb-Cy3	1:800	SA-Cy2	1:800	3
	Geph	Ms	1:100	Anti-Ms-Cy5	1:800			
BDA/VAChT/PSD-95	VAChT	Rb	1:1000	"	"	"	"	3
	PSD-95	Ms	1:100					
BDA/VGAT/Geph	VGAT	Rb	1:250	"	"	"	"	3
	Geph	Ms	1:100					
BDA/VGAT/PSD-95	VGAT	Rb	1:250	"	"	"	"	3
	PSD-95	Ms	1:100					
BDA/VGluT2/Geph	VGluT2	Rb	1:5000	"	"	"	"	3
	Geph	Ms	1:100					
BDA/VGluT2/PSD-95	VGluT2	Rb	1:5000	"	"	"	"	3
	PSD-95	Ms	1:100					
Triple BDA/VTP/Neuronal markers								
BDA/VAChT/NPNF	VAChT	Rb	1:1000	Anti-Rb-Cy3	1:800	SA-Cy2	1:800	3
	NPNF	Ms	1:800	Anti-Ms-Cy5	1:800			
BDA/VAChT/PV	VAChT	Rb	1:1000	"	"	"	"	3
	PV	Ms	1:1000					
BDA/VAChT/CB	VAChT	Rb	1:1000	"	"	"	"	3
	CB	Ms	1:200					
BDA/VGAT/NPNF	VGAT	Rb	1:250	"	"	"	"	3
	NPNF	Ms	1:800					
BDA/VGAT/PV	VGAT	Rb	1:250	"	"	"	"	3
	PV	Ms	1:1000					
BDA/VGAT/CB	VGAT	Rb	1:250	"	"	"	"	3
	CB	Ms	1:200					
BDA/VGluT2/NPNF	VGluT2	Rb	1:5000	"	"	"	"	3
	NPNF	Ms	1:800					
BDA/VGluT2/PV	VGluT2	Rb	1:5000	"	"	"	"	3
	PV	Ms	1:1000					
BDA/VGluT2/CB	VGluT2	Rb	1:5000	"	"	"	"	3
	CB	Ms	1:200					

[1] For sources and specificity of primary antibodies from different species refer to Table 1.
[2] Jackson Immuno Research Laboratories, West Grove, PA.
[3] For multiple labeling (ML) with minimal cross-reactivity (min X) to other species.
[4] n: number of cases (each case referring to an injection site and series from the same side of the brain, thus 1 or 2 per brain from 9 rats for a total of 16 injection sites selected for their placement in the MCPO/SI).
Abbreviations: AB, antibody; AMCA, aminomethylcoumarin acetate; Cy2, cyanine; Cy3, indocarbocyanine; Cy5, indodicarbocyanine; Dky, donkey; Geph, gephyrin; Gt, goat; Ms, mouse (monoclonal); Rb, rabbit; sp, species.

Table 3. Number (N°) and proportion of VAChT+, VGAT+ and VGluT2+ BDA-labeled BF axonal varicosities (var.) in infralimbic area (IL) based on stereology[1].

IL	VAChT	VGAT	VGluT2
N° BDA+ var.	6832 ± 1386	3344 ± 787	5456 ± 1508
N° BDA+/VTP+ var.	1168 ± 381	1728 ± 442	816 ± 334
% VTP+ var.	**19.2 ± 5.4**	**51.6 ± 9.9**	**14.6 ± 7.1**

[1]Numbers of varicosities were estimated by sampling from 3 levels per series per case in IL (see Fig. 1 and Methods). Mean values for estimated numbers of BDA+ var., for estimated numbers of double labeled BDA+/VTP+ var. and for percentages of BDA+VTP+ from 5 cases for IL (1 or 2 sides from 3 rat brains) are presented together with SEM. The proportions of the three VTP+ varicosities differed significantly ($p < 0.05$ according to one-way ANOVA) but not so the number of BDA+ sampled varicosities among cases. Post-hoc Bonferroni-corrected comparisons showed a significant difference ($p < 0.01$) between percentages for BDA+/VGAT+ and BDA+/VAChT+ or BDA+/VGluT2+ var. Abbreviations: Est., estimated; var., varicosities; VTP, vesicular transporter proteins.

Fig. 1. Localization of injection site and region of analysis in prefrontal cortex. A: Atlas of the basal forebrain area where biotin dextran amine (BDA) 10,000 MW was placed by microiontophoretic application into the MCPO-SI region. B: Image of one injection site containing BDA-labeled cells in MCPO. The small rectangle indicates the location of three labeled neurons shown at high magnification in *C*. C: High magnification image of three BDA-labeled neurons of the injection site. D: Contours of the rat forebrain at the level of the prefrontal cortex (~11.8, 11.4 and 11.0 mm anterior to interaural zero) where BF axons were observed in large amounts. The dashed contours depict the IL, where most of the quantitative analysis was carried out (see Table 2 and text). Abbreviations: AI, agranular insular cortex; ac, anterior commissure; Cg, cingulate cortex; Cl, claustrum; FS, fundus stratium; Fr, frontal cortex; IL, infralimbic cortex; LO, lateral orbital cortex; LPO, lateral preoptic area; MCPO, magnocellular preoptic nucleus; MPO, medial preoptic area; OTu, olfactory tubercle; Pir, piriform cortex; PL, prelimbic cortex; oc, optic chiasm; SI, substantia innominata; SO, supraoptic magnocellular nucleus; TT, taenia tecta; VLO, ventrolateral orbital cortex. Scale bar: B = 0.5 mm; C = 25 μm.

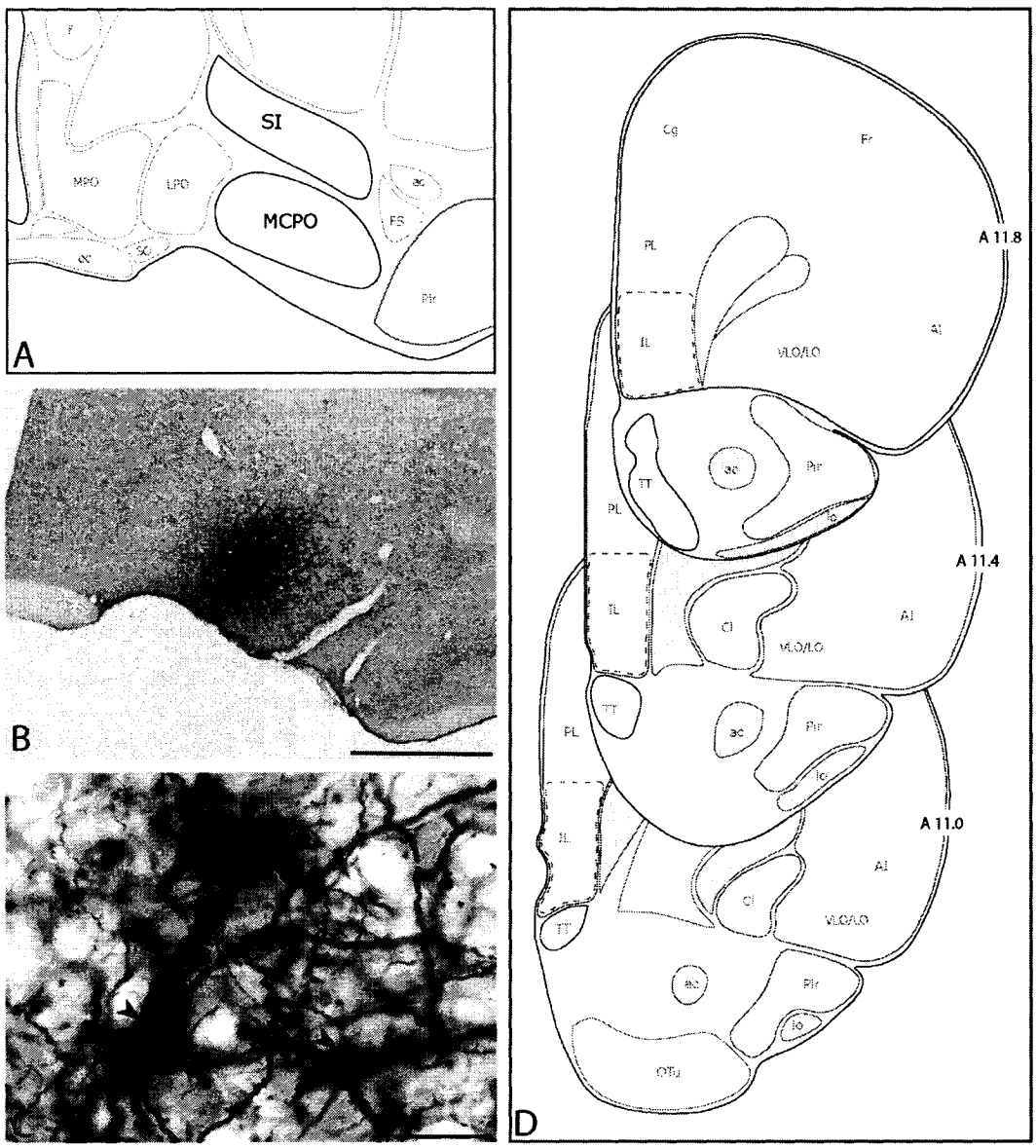

Fig. 1. Localization of injection site and region of analysis in prefrontal cortex

Fig. 2. Cholinergic, GABAergic and glutamatergic BF axons in prefrontal cortex. A, B: Epifluorescent microscopy images in the prefrontal cortex showing BDA-labeled axons (green A' and B') with varicosities (arrowheads) that are positive for the vesicular transporter for acetylcholine, VAChT (red in A" and B" and yellow in the merged image in A'" and B'"). C, D: Epifluorescent microscopy images of the prefrontal cortex that show BDA-labeled axons (green C' and D') with varicosities (arrowheads) that are positive for the vesicular transporter for GABA, VGAT (red in C" and D" and yellow in the merged image in C'" and D'"). E, F: Epifluorescent microscopy images of the prefrontal cortex of BDA-labeled axons (green E' and F') with varicosities (arrowheads) that are positive for the vesicular transporter for glutamate, VGluT2 (red in E" and F" and yellow in the merged image in E'" and F'"). Scale bar = 5 μm in F for all images.

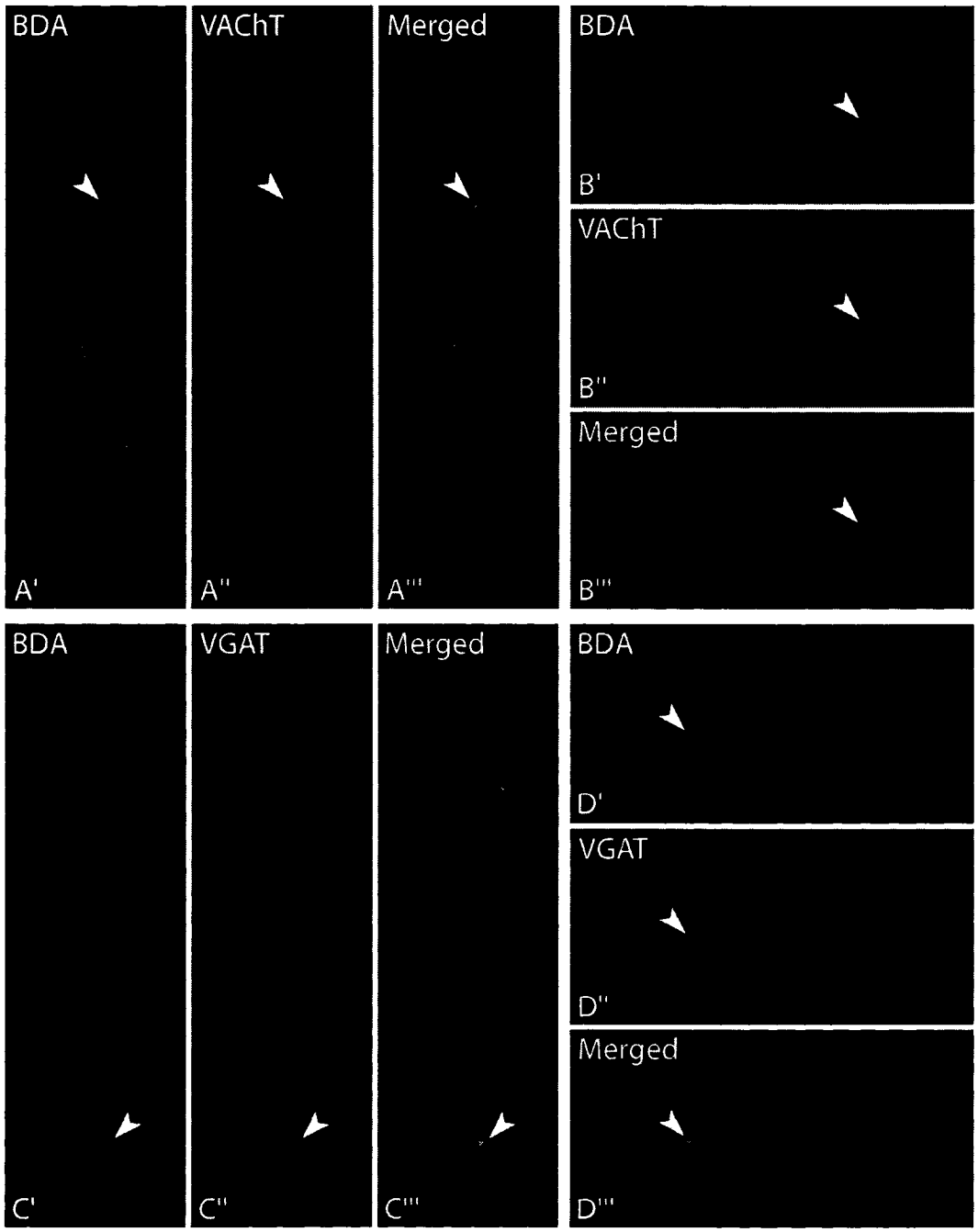

Fig. 2. Cholinergic, GABAergic and glutamatergic BF axons in prefrontal cortex

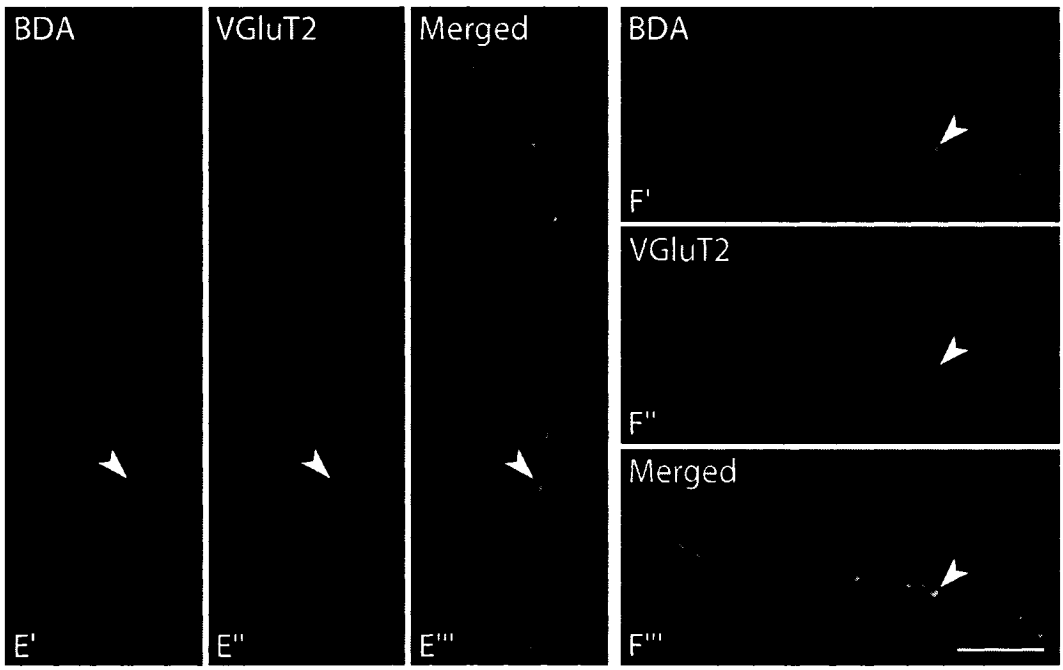

Fig. 2. Cholinergic, GABAergic and glutamatergic BF axons in prefrontal cortex (continued)

Fig. 3. Lack of colocalization of vesicular transporter proteins for ACh (VAChT), glutamate (VGluT2) or GABA (VGAT) in prefrontal cortex. A: Merged epifluorescent image from dual-stained material for VAChT (in red, Cy3) and VGluT2 (in green, Cy2) in prefrontal cortex. As shown by the open arrowheads, VAChT+ and VGluT2+ varicosities do not colocalize with each other. Some varicosities may appear close, but still appear distinguishable of each other, as seen in the two opposite arrowhead on the upper right. B: Merged epifluorescent image from dual-stained material for VGluT2 (in red, Cy3) and VGAT (in green, Cy2) in prefrontal cortex. As shown by the open arrowheads, VGluT2+ and VGAT+ varicosities do not colocalize with each other. C: Merged epifluorescent image from dual-stained material for VAChT (in red, Cy3) and VGAT (in green, Cy2) in prefrontal cortex. As shown by the open arrowheads, most of VAChT+ and VGAT+ varicosities do not colocalize with each other. Only few VAChT+/VGAT+ varicosities could be detected (solid arrowhead). Scale bar = 10 μm in C, for the three images.

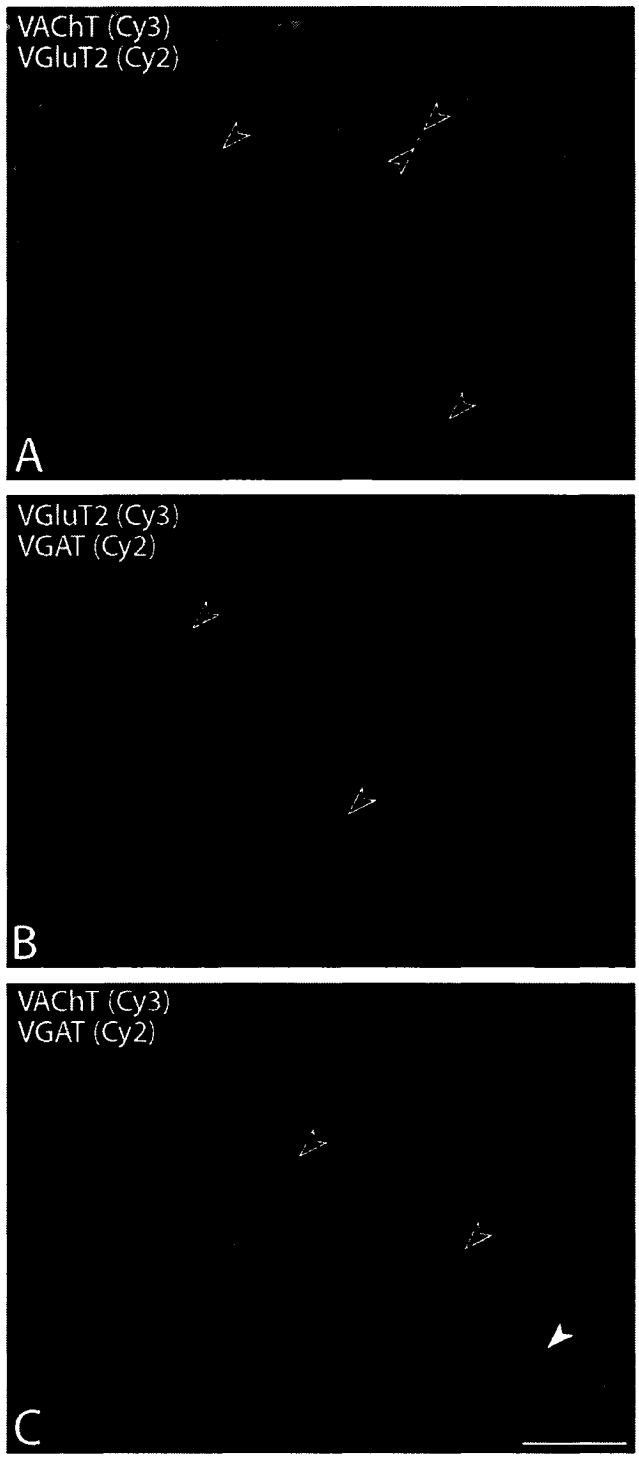

Fig. 3. Lack of colocalization of vesicular transporter proteins for ACh (VAChT), glutamate (VGluT2) or GABA (VGAT) in prefrontal cortex

Fig. 4. Postsynaptic proteins (PSPs) Gephyrin or PSD-95 in relation to cholinergic, GABAergic and glutamatergic BF terminals in prefrontal cortex. A-C: Rendered 3D confocal images (0.33 μm thick optical sections) of BDA-labeled axons (in blue, Cy2) that are positive for the VTPs (in red, Cy3) VAChT (A), VGAT (B) or VGluT2 (C) in relation to Geph (in green, Cy5). A: In the rendered 3D confocal image, some of the BDA+/VAChT+ varicosities appear in relation with Geph+ profiles (small and large solid arrowheads), whereas the majority do not (small and large open arrowheads), as evident in the insets (open and solid large arrowheads in panel). B: In the rendered image, most of the varicosities of the BDA+/VGAT+ axon (all solid arrowheads) associate with Geph+ profiles, as also evident in the varicosities shown in the inset (large arrowheads in the panel). C: Geph+ profiles do not usually associate with the BDA+/VGluT2+ axonal varicosities (open arrowhead), as evident in the rendered image at the inset (open arrowhead in the panel). D-F: Rendered 3D confocal images (0.33 μm thick optical sections) of BDA-labeled axons (in blue, Cy2) that are positive for the VTPs (in red, Cy3) VAChT (D), VGAT (E) or VGluT2 (F) in relation to PSD-95 (in green, Cy5). D: PSD-95+ profiles do not usually associate with the BDA+/VAChT+ axonal varicosities (all open arrowheads), as evident in the rendered image shown at the inset (open large arrowhead in the panel). E: As shown in the rendered 3D image, PSD-95+ profiles are not generally seen in association with the BDA+/VGAT+ axonal varicosities (open arrowheads), as evident in the rendered image at the inset (open arrowheads in large panel). F: As

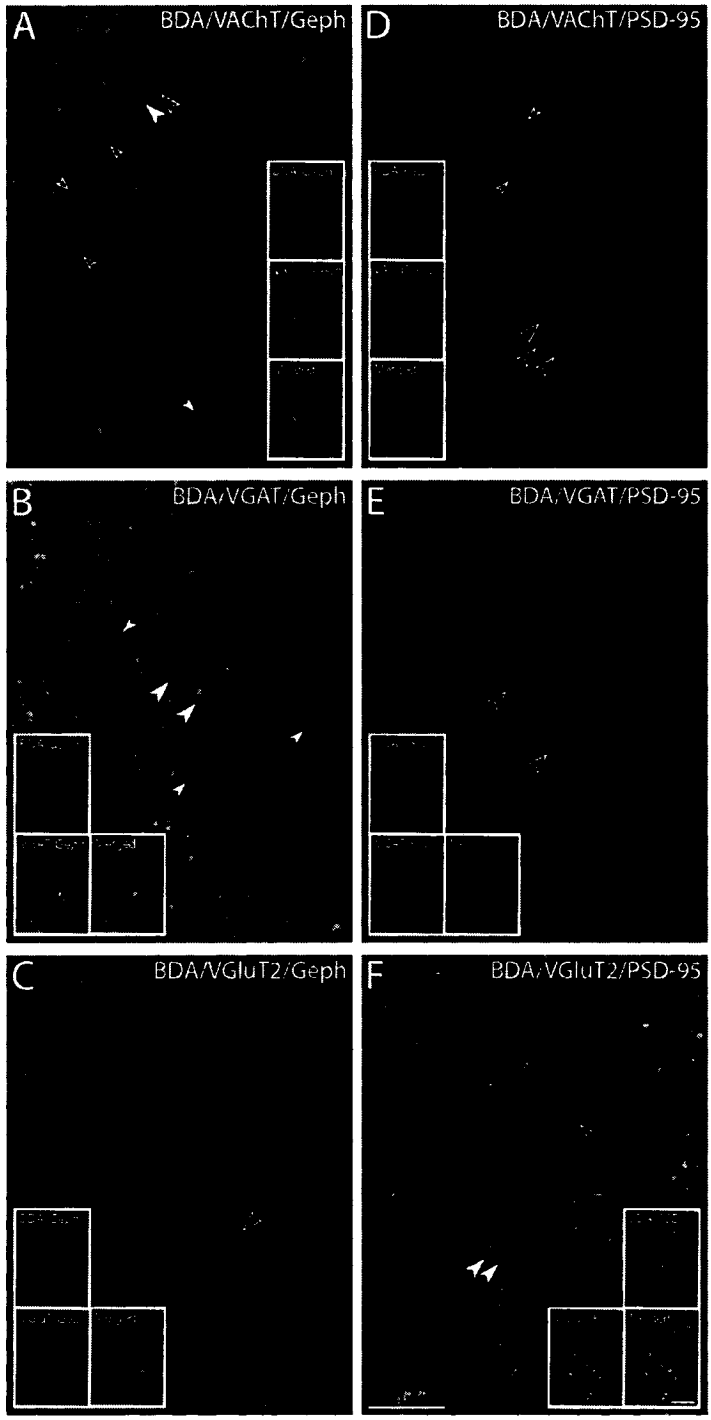

Fig. 4. Postsynaptic proteins (PSPs) Gephyrin or PSD-95 in relation to cholinergic, GABAergic and glutamatergic BF terminals in prefrontal cortex

shown in the rendered 3D image in F (solid arrowheads), many of the varicosities of BDA+/VGluT2+ axons associate with PSD-95+, as also evident in the rendered image in the inset (solid arrowheads in large panel). Yet, some BDA+/VGluT2+ varicosities did not show association with PSD-95+ profiles (small open arrowhead). Scale bar = 5 μm in F, for all large panels and 2 μm in F inset for all insets.

Fig. 5. BF cholinergic, GABAergic and glutamatergic axons in relation to pyramidal cells and interneurons in prefrontal cortex. A-C: Confocal 3D rendered reconstruction (large panels) of BDA-labeled axonal varicosities (in green) that are positive for the vesicular acetylcholine transporter protein VAChT (in red, arrowheads), which are shown in proximity (open arrowheads in A and B) or in apposition (solid arrowhead in C) to NPNF+ (A), PV+ (B) or CB+ (C) cells, as shown in the 3D reconstruction in the insets. D-F: Confocal 3D rendered reconstruction (large panels) of BDA-labeled axonal varicosities (in green) that are positive for the vesicular GABA transporter protein VGAT (in red, arrowheads), which are shown in apposition (solid arrowheads in D, E and F) to a NPNF+ dendrite (D), or a PV+ (E) or CB+ (F) neuron, as evident in the 3D reconstruction in the insets. Note in the inset D, the location of the VGAT staining inside the BDA+ varicosity pointing to the dendritic NPNF+ process. Note in E, the conspicuous innervation of the soma by the BDA+/VGAT+ varicosities. G-I: Confocal 3D rendered reconstruction (large panels) of BDA-labeled axonal varicosities (in green) that are positive for the vesicular glutamate transporter protein VGluT2 (in red, arrowheads), which are shown in the proximity (open arrowheads in G and H) or in apposition (solid arrowheads in I) to NPNF+ (G), PV+ (H) or CB+ (I) cells, as evident in the 3D reconstruction in the insets. Scale bar = 5 μm for large panels and 2 μm for insets.

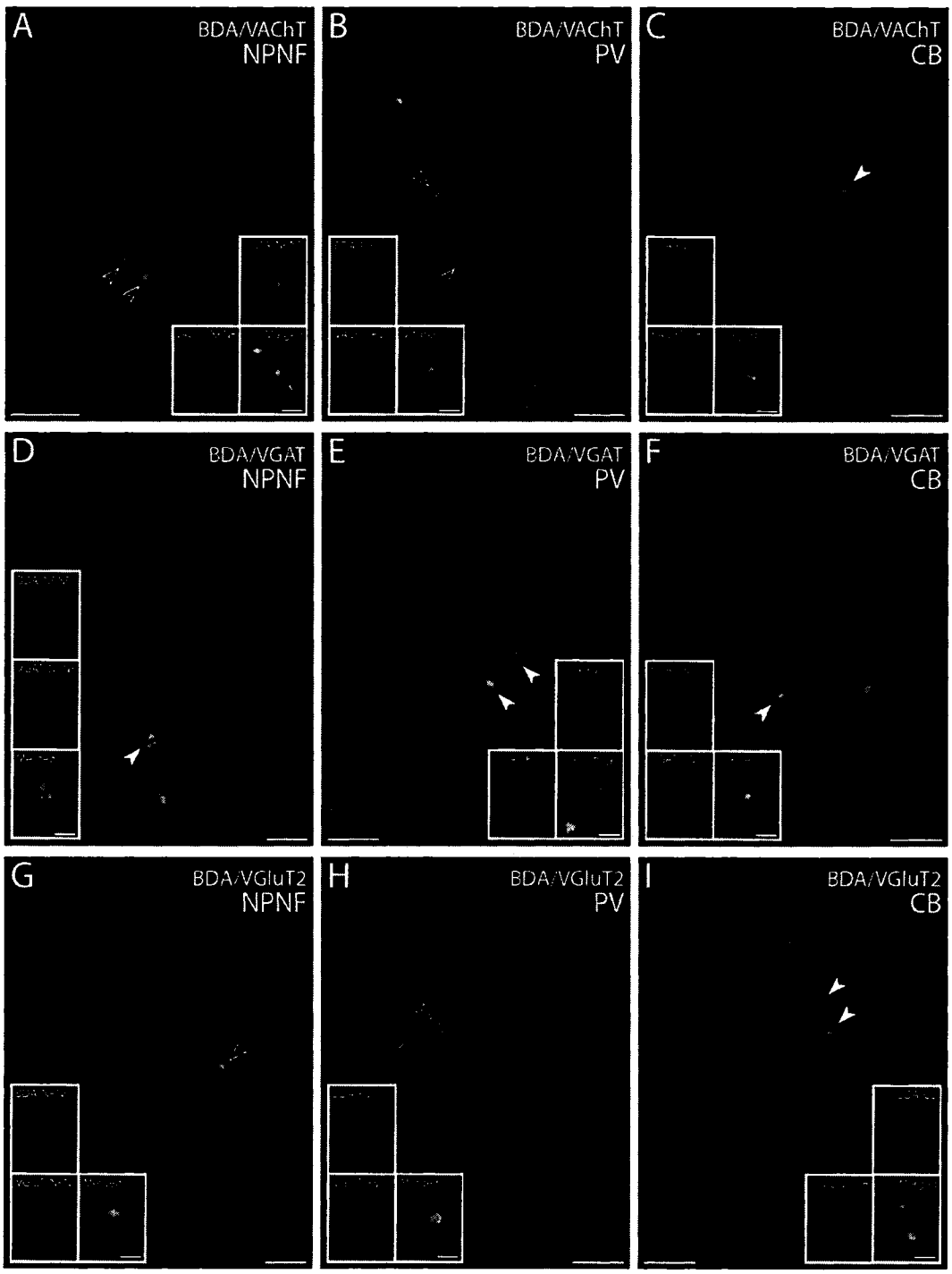

Fig. 5. BF cholinergic, GABAergic and glutamatergic axons in relation to pyramidal cells and interneurons in prefrontal cortex

PREFACE TO CHAPTER III

In addition to the cortex, the BF sends descending projections to the LH, a region long known to be involved in the maintenance of wakefulness as well as promotion of arousal and sympathetic activity. Retrograde tracing studies have determined that this projection is formed by an important number of GABAergic, few cholinergic and a large number of non-GABAergic non-cholinergic unidentified neurons, which may be glutamatergic. In order to establish whether the BF provides a glutamatergic innervation to the LH and whether this projection forms an independent contingent from that of GABAergic and cholinergic neurons, the presence of VGluTs, as well as of VGAT and VAChT was examined in anterogradely labeled BF axon terminals. The proportion and the distribution of axon terminals that each contingent provided to LH, was also determined. Finally, the capacity to form excitatory and inhibitory synapses was assessed by examining the presence of post-synaptic markers.

Based on the presence of state related neurons in the BF, including sleep-active GABAergic and putative wake-active glutamatergic cells, the capacity of BF neurons to inhibit or excite LH neurons is discussed in the context of the LH role in maintenance of waking and promotion of arousal.

Chapter III

Vesicular glutamate (VGluT), GABA (VGAT), and acetylcholine (VAChT) transporters in basal forebrain axon terminals innervating the lateral hypothalamus

Pablo Henny and Barbara E. Jones

Montreal Neurological Institute, McGill University,

Montreal, Quebec, Canada H3A 2B4

ABSTRACT

The basal forebrain (BF) is known to play important roles in cortical activation and sleep, which are likely mediated by chemically differentiated cell groups including cholinergic, GABAergic and other unidentified neurons. One important target of these cells is the lateral hypothalamus (LH), which is critical for arousal and the maintenance of wakefulness. In order to determine if chemically specific BF neurons provide an innervation to the LH, we employed anterograde transport of 10,000 MW biotinylated dextran amine (BDA) together with immunohistochemical staining of the vesicular transporter proteins (VTPs) for glutamate (VGluT1, 2 and 3), GABA (VGAT) or acetylcholine (ACh, VAChT). In addition, we applied triple staining for the postsynaptic proteins (PSPs), PSD-95 with VGluT or Gephyrin (Geph) with VGAT, to examine whether the BDA-labeled varicosities may form excitatory or inhibitory synapses in the LH. Axons originating from BDA-labeled neurons in the magnocellular preoptic nucleus (MCPO) and substantia innominata (SI) descended within the medial forebrain bundle and extended collateral varicose fibers to contact LH neurons. In the LH, the BDA-labeled varicosities were immunopositive (+) for VAChT (~10%), VGluT2 (25%) or VGAT (50%), revealing an important influence of newly identified glutamatergic together with GABAergic BF inputs. Moreover, in confocal microscopy, VGluT2+ and VGAT+ terminals were apposed to PSD-95+ and Geph+ profiles respectively, indicating that they formed synaptic contacts with LH neurons. The important inputs from glutamatergic and GABAergic BF cells could thus regulate LH neurons in an opposing manner to reciprocally stimulate vs. suppress cortical activation and behavioral arousal.

INTRODUCTION

The basal forebrain (BF) plays an important role in the modulation of cortical activity and regulation of sleep-wake states. As known from early studies, it serves as the ventral extrathalamic relay to the cerebral cortex from the brainstem reticular activating and arousal systems (Starzl et al., 1951; Jones, 2005b). Yet, it is also importantly involved in sleep, since lesions of the BF are associated with insomnia (von Economo, 1931; Nauta, 1946; McGinty and Sterman, 1968; Jones, 2005b). These opposing roles could be mediated by chemically differentiated cell groups in the BF that include cholinergic, GABAergic and non-cholinergic/non-GABAergic, presumed glutamatergic, neurons (Gritti et al., 1993, 1994; Gritti et al., 1997; Manns et al., 2001). According to multiple lines of evidence, cholinergic neurons actively stimulate cortical activation during waking and paradoxical sleep (PS, also called rapid eye movement, REM, sleep) (Buzsaki et al., 1988; Metherate et al., 1992; Duque et al., 2000; Manns et al., 2000a; Jones, 2004; Lee et al., 2005b). Some putative glutamatergic neurons can act in parallel with the cholinergic neurons in this process (Manns et al., 2003a). On the other hand, a majority of GABAergic BF neurons are minimally active during cortical activation (Manns et al., 2000b) and as reflected by c-Fos expression, many are maximally active during sleep (Modirrousta et al., 2004), indicating that they can promote sleep, including slow wave sleep (SWS). In addition to projections to the cerebral cortex (Gritti et al., 1997), BF neurons give rise to projections to the posterior lateral hypothalamus (LH) (Gritti et al., 1994), a region long known to be crucial for waking (von Economo, 1931; Nauta, 1946; Hess, 1957; Swett and Hobson, 1968; Jones, 2005c). Recently, neurons have been localized in the LH

which contain the peptide orexin (Orx, also called hypocretin) that is critical for sustaining waking, since absence of the peptide, its receptor or the Orx neurons results in narcolepsy (Chemelli et al., 1999; Lin et al., 1999; Peyron et al., 2000; Thannickal et al., 2000).

Although previous studies combining retrograde transport with immunohistochemical staining for neurotransmitter enzymes indicated that cholinergic, GABAergic and other BF neurons project to the LH (Gritti et al., 1994), they did not reveal the efferent BF fibers projecting into the LH nor did they prove the use of acetylcholine (ACh), GABA or as proposed, glutamate as neurotransmitters by the projection neurons. Recently, proof of the uptake, storage and release of specific neurotransmitters has become possible by immunohistochemical staining for specific vesicular transporter proteins (VTPs), including those for ACh (VAChT) (Gilmor et al., 1996), GABA (VGAT) (Chaudhry et al., 1998) and glutamate (VGluT1, 2 and 3) (Fremeau et al., 2001; Fujiyama et al., 2001; Fremeau et al., 2002). We thus combined anterograde transport of 10,000 MW biotinylated dextran amine (BDA) with immunohistochemical staining for VAChT, VGluT (1, 2 and 3) and VGAT to determine if cholinergic, glutamatergic or GABAergic neurons located in the magnocellular preoptic nucleus (MCPO) and substantia innominata (SI) project to the LH. To assess whether the VGluT+ and VGAT+ varicosities form synapses in the LH, we employed triple immunostaining for the postsynaptic proteins (PSPs) PSD-95, a marker for excitatory synapses (Sheng and Pak, 2000), or Gephryin (Geph), a marker for inhibitory synapses (Sassoe-Pognetto and Fritschy, 2000; Sassoe-Pognetto et al., 2000).

MATERIALS AND METHODS

Animals and Surgery

All procedures conformed to the guidelines of the Canadian Council on Animal Care and the U.S. NIH and were approved by the McGill University Animal Care committee.

Long-Evans rats (200-250 g, Charles River Canada, St. Constant, Quebec, Canada) were anesthetized with ketamine/xylazine/acepromazine (65/5/1 mg/kg, i.p.) and placed in a stereotaxic frame (David Kopf Instruments, Tujunga, CA, U.S.A.) for surgery. Anesthesia level was monitored during the experiment and augmented by boosters if necessary. Since previous studies based on retrograde as well as anterograde tracing showed no evidence of contralateral projections from BF to LH (Swanson, 1976; Gritti et al., 1994), injections of BDA were done on left and right sides of each brain. Holes were drilled in the skull and the *dura mater* removed on each side over the BF. Glass micropipettes (tip diameter 15 to 25 μm) were back-filled with a 0.5 M NaCl solution containing 2% 10,000 MW BDA (BDA-10,000, Molecular Probes, Eugene, Oregon, U.S.A.). With the aid of a micropositioner (Model 660, David Kopf Instruments), a BDA-filled pipette was lowered into the BF on each side aimed at the magnocellular preoptic nucleus (MCPO, from *Bregma*: anterior-posterior (AP), -0.5 mm; lateral (L), +/- 2.5 mm; vertical (V), 8.5 mm). A holding current of -300 nA was maintained (using a Microiontophoresis Dual Current Generator 260, World Precision Instruments (WPI), Sarasota, FL, U.S.A.) during the descent to avoid leakage of the solution. Once in the targeted site, microinjection of BDA was performed by iontophoresis

applying positive current pulses (5 to 10 μA) in a duty cycle of 1 sec (0.5 s on, 0.5 s off) for a period of 25 to 30 min through a stimulator (Pulsemaster A300, WPI) and stimulus isolation unit (Iso-Flex, A.M.P.I., Israel). After the injection, the micropipette was held in place for 10 min and removed during renewed application of the holding current.

Rats were maintained for 5 or 6 days with food and water *ad libitum* to allow anterograde transport of the tracer. They were subsequently perfused transcardially under deep sodium pentobarbital anesthesia (100 mg/kg, i.p.) with ~500 ml 4% paraformaldehyde fixative solution. The brains were removed and put in a 30% sucrose solution for 2 to 3 days or until they sunk, after which they were frozen at -50° C and stored at -80° C for subsequent processing.

Immunohistochemistry

Sections were cut using a freezing microtome in 25 μm thick coronal sections and collected in eight adjacent series at 200 μm intervals through the forebrain, including the magnocellular BF area and the tuberal-posterior hypothalamus. Series were processed for evaluation of the BDA injection site in the BF and BDA-labeled fibers in the LH by light microscopy. For this purpose, the avidin-biotin complex (ABC) procedure was performed using the Vectastain ABC Elite kit (Vector Laboratories, Burlingame, CA, U.S.A.) with nickel-intensified diaminobenzidine (DAB-Ni) and combined with a Nissl counterstain using neutral red (NR).

Adjacent series containing the tuberal-posterior LH region were processed for double or triple fluorescent staining (see Table 1). Prior pilot studies were

performed to determine the conditions necessary for antibody as well as streptavidin penetration through the full depth of the sections. As viewed through the z-axis under epifluorescent and confocal microscopy, we established that 0.1 or 0.3% Triton X-100 (TX) allowed full penetration of antibodies and streptavidin through 25 μm thick sections in double or triple stained series respectively. Free floating sections from each series were rinsed for 30 min in Trizma saline buffer (TS, 0.1 M, pH 7.4) followed by incubation for 30 min with a blocking solution of normal donkey serum (NDS, 6% in TS) containing TX (0.1 or 0.3%). Subsequent incubations and rinses (30 min between incubations) were done using TS containing NDS (1%) and TX (0.1 or 0.3%). Incubations were performed at room temperature overnight with primary antibodies and for 3 hours with secondary antibodies or streptavidin.

For double labeling of BDA and one of the VTPs, sections were incubated (using 0.1% TX) first with primary antibodies against VAChT, VGluT1, 2 or 3 or VGAT (from various species) and then with appropriate Cy3-conjugated secondary antibodies (from Donkey, Dky) followed by Cy2-conjugated streptavidin for revelation of BDA (see Table 1, Double BDA/VTP).

For double labeling of two VTPs, sections were incubated (using 0.1% TX) with two primary antibodies against VAChT, VGluT2 and/or VGAT (from different species) and then with appropriate Cy2- and Cy3-conjugated secondary antibodies (from Dky) (see Table 1, Double VTP/VTP).

For triple labeling of BDA, the VTPs and the PSPs, sections were incubated (using 0.3% TX) with two primary antibodies against VGluT2 or VGAT and

PSD-95 or Geph, respectively (from different species) and then with appropriate Cy3 or Cy5 secondary antibodies (from Dky). They were subsequently incubated with Cy2-conjugated streptavidin for revelation of BDA (see Table 1, Triple BDA/VTP:PSP).

All sections were mounted out of Trizma water, and the mounted sections dehydrated through alcohols, cleared in xylene and coverslipped with Permount.

Conventional microscopy, tracing and stereological analysis

Sections were examined under light and epifluorescent microscopy with a Leica DMLB microscope or Nikon Eclipse E800 which were equipped with x-y-z motorized stages, video or digital camera and filters appropriate for FITC (or Cy2), Rhodamine (or Cy3) and (on the Nikon) Cy5 fluorescence. Single as well as composite images were acquired and drawings performed using Neurolucida software (MicroBrightField, MBF, Colchester, VT, U.S.A.). Cells and varicosities were counted using the Optical Fractionator probe of Stereo Investigator software (MBF). For tracing or counting, a computer resident atlas of the rat brain was employed that has been developed and applied in our laboratory using standardized procedures for tissue processing (see (Gritti et al., 1993, 1994)). For each application, series of histology sections are matched to appropriate levels of the atlas (at 400 μm intervals) under low magnification (5 or 10x objective). At each level, the atlas image is then rotated if necessary, and the contours adjusted to optimally fit the relevant nuclei of the histology section.

Injection sites from 8 rats (BDA 14, 15, 16, 18, 19, 20, 21 and 22) were examined under brightfield illumination in DAB-Ni stained material. In 14 cases, the labeled cells were centered in the MCPO-SI (on the left and/or right sides). From these, 5 injection sites ('cases' on left and/or right sides) from 3 rats (BDA 16, 18 and 19) were selected for quantitative estimate of the cells in the injection sites. From the latter 14 cases, the innervation of the LH was studied qualitatively and quantitatively in DAB-Ni and fluorescent stained material (see text and Table 1).

Under brightfield illumination, unbiased estimates of the total number of DAB-Ni stained, BDA-labeled nerve cell bodies were performed using the Optical Fractionator probe of Stereo Investigator. Cells were counted within contours of the BF and surrounding nuclei, including the MCPO, SI, nucleus of the diagonal band of Broca (DBB), olfactory tubercle (OTu), lateral preoptic area (LPO), fundus of the striatum (FS), piriform cortex (Pir), nucleus of the lateral olfactory tract (LOT) and anterior amygdaloid area (AA). Counts were made under a 60x Oil objective (with 1.40 numerical aperture, NA) through 6 or 7 BF levels (at 200 μm intervals) using an x-y sampling grid size (of 120 μm x 120 μm) that was equal to the counting frame size, so as to sample 100% of each area. Counting was performed through 10 μm in the z-axis (starting 1 μm from the surface in mounted sections having an average of ~12 μm thickness following dehydration). Following the stereological procedures imposed in Stereo Investigator, cells were counted if their tops were contained within the defined counting block.

Projections of the DAB-Ni stained, BDA-labeled axons were examined through the tuberal-posterior LH and in relation to NR stained neurons viewed under brightfield illumination. The axons and neurons were drawn using a 100x Oil objective within a contour of the LH using Neurolucida software (MBF).

Given evidence for contacts of BF fibers on LH neurons, the total number of NR stained neurons which were or were not contacted by one or more DAB-Ni stained, BDA+ varicosities (NR+:BDA+ or NR+:BDA-) was estimated using the Optical Fractionator probe through the LH (n = 3 cases). Counts were performed under a 100x Oil objective (1.4 NA) on the Nikon microscope. The cells were sampled in the LH, as defined in the computer resident atlas, through 3 levels separated by 400 μm intervals (5800, 6200 and 6600 μm anterior (A) to interaural zero (IA0)). The sampling grid size (210 μm x 210 μm) was set to be larger than the counting frame (70 μm x 70 μm) so as to sample ~11% of the LH area. Counting was performed through 16 μm of the section thickness (starting 1 μm from the surface of the mounted sections which had an average thickness of ~19 μm following their minimal dehydration and differentiation for NR). As above, cells were counted if their tops were contained within the defined counting block.

Under epifluorescent illumination, fluorescent stained BDA-positive (+) varicosities were examined for double labeling with the VTPs in the LH. After finding double labeling with VAChT, VGluT2 and VGAT, unbiased estimates of the total numbers of single BDA+ and double-labeled BDA+/VAChT+, BDA+/VGluT2+ or BDA+/VGAT+ varicosities were estimated in the LH for each series using the Optical Fractionator probe of Stereo Investigator. In five

cases analyzed per series in stereology, all VTPs were stained using antibodies raised in Rabbit (Rb, VAChT, VGluT2 and VGAT, see Table 1). Counts were performed under a 100x Oil objective (with 1.40 NA) on the Leica microscope. The varicosities were sampled in the LH, as defined in the computer resident atlas, through 3 levels separated by 400 μm intervals (A 5800, A 6200 and A 6600) of the tuberal-posterior LH (in 4 cases per series, Table 2). The sampling grid size (180 μm x 180 μm) was set to be larger than the counting frame (90 μm x 90 μm) so as to sample 25% of the LH area. Counting was performed through 8 μm of the section thickness (starting 1 μm from the surface of the mounted sections having an average thickness of ~12 μm following dehydration). In each counting block and frame, all BDA+ varicosities (in green, Cy2) were counted, including those which were and were not double-labeled for the VTP (in red, Cy3) to obtain an estimate of the proportion of double-labeled varicosities for each VTP.

Double labeling for VAChT, VGluT2 and/or VGAT was assessed under epifluorescent illumination on the Leica microscope (in 4 cases per series, Table 1). In absence of any double labeling, no quantification was undertaken.

Confocal microscopy and image processing

To examine the presence of PSPs in association with BDA+/VTP+ varicosities, triple stained sections were analyzed by confocal microscopy with a Zeiss LSM 510 laser scanning microscope equipped with Argon 488 nm, helium-neon 543 nm and helium-neon nm 633 lasers for Cy2, Cy3 and Cy5 excitation as well as

with appropriate filters for detection of Cy2 (bandpass 500 to 530 nm, green), Cy3 (bandpass 565 to 615 nm, red) and Cy5 (bandpass 697 to 719 nm, infrared). Scanning was performed through a Plan-Apochromat 100x (with 1.4 NA) objective and pinhole size of 1 (Airy Units) for each of the three channels. Images were acquired for the three chromogens using the resident LSM 510 software and consisted of stacks taken through the z-axis in optical slices of ~0.33 μm. Rendered 3D views of the image stacks were obtained using the image software Volocity 3.5.1 (Improvision Inc, Lexington, MA, U.S.A., www.improvision.com) which allowed interactive visualization, magnification and rotation of the 3D images in order to determine the relative location of each of the elements from the three channels. In some images, a deconvolution procedure or iterative restoration in Volocity was applied using a 95% confidence level in order to maximize signal to noise ratio and better assess relationships among elements in the triple stained material. As assessed in 3 cases per series (Table 1), contacts between VTP+/BDA+ varicosities and PSP+ profiles were evaluated in the rotated images and validated by lack of separation between the pre- and postsynaptic elements.

Adjustments for brightness and contrast in brightfield images and tonal range for each individual RGB channel ("Adjust/levels" command in Photoshop) in fluorescent images were performed with Adobe Photoshop Creative Suite edition (Adobe System, San Jose, CA, U.S.A).

RESULTS

BDA injection site and cellular labeling

Iontophoretic application of BDA-10,000 into the region of the magnocellular preoptic area and substantia innominata (MCPO-SI, Fig. 1A) produced a small and well restricted, spherical injection site (Fig. 1B) containing labeled cell bodies and dendrites (Fig. 1C). The injection sites ranged in size from 300 to 500 μm in diameter and were consistently located primarily within the MCPO and secondarily in the overlying SI (n = 11 injection sites).

To appraise the number of cells labeled and their precise location in BF nuclei, stereological estimates were obtained through the BF. The average number of BDA-labeled neurons per injection was ~1400 (mean ± SEM, 1430.6 ± 315, n = 5 injection sites). The labeled cells were almost exclusively (96.2% ± 1.7%; range, 90 to 100%) located within the MCPO (90.2%) and SI (6.0%). A few scattered cells were variably found in immediately adjacent regions including the olfactory tubercle, lateral olfactory tract nucleus or anterior amygdaloid area (3.5% ± 1.8%). Isolated cells were found in the nearby fundus of the striatum or piriform cortex in some cases. No labeled cells were seen in the more rostral DBB. No labeled cells were seen in distant regions known to project to MCPO-SI, including the prefrontal cortex or importantly, the LH, indicating a lack of retrograde transport of the BDA-10,000 in these afferent systems.

BDA was found within axons in the diencephalon (n = 14 cases) and in cortical and subcortical telencephalic regions where different MCPO-SI neurons

are known to project from retrograde (Gritti et al., 1994; Gritti et al., 1997) and other anterograde tracing studies (Luiten et al., 1987; Grove, 1988).

BDA-labeled fibers and varicosities in the LH

In the diencephalon, thick fascicles of fibers were evident in the ventrolateral posterior LH (Fig. 2A). From these coarse fibers, collateral fine fibers extended out through the LH. Some fibers continued sparsely into the perifornical area but most remained within the LH. The fine fibers bore varicosities along their axons (*boutons en passant*, Fig. 2B') or occasionally at the end of their axons (*boutons terminaux,* Fig. 2B''). Although many varicose axons did not appear to contact nerve cell bodies in the region (Fig. 2B'), a significant number did appear to do so, innervating either small (Fig. 2B'') or large (Fig. 2B''') neurons by varicose processes that could entirely envelop the soma. To better visualize the fiber distribution and innervation of nerve cell bodies within the LH, high magnification tracing of the DAB-Ni stained axons and neutral red (NR+) stained cells was performed. As seen in Fig. 2C, the major axon fascicles were seen to course within the ventrolateral part of the medial forebrain bundle (MFB) from which they extended fine varicose fibers to contact and sometimes entirely surround cells in ventral, central and dorsal portions of the LH (Fig. 2D', 2D'' and 2D''').

To appraise the extent of the innervation of neurons in the LH, stereological estimates were obtained of the number and proportion of LH cells ostensibly contacted by BDA-labeled varicosities in the light microscope images. In three cases, the NR+ cells which were contacted (NR+:BDA+) together with those

which were not contacted (NR+:BDA-) were counted in random sampling through three levels of the LH (~A 5800, A 6200 and A 6600). The number of contacted cells (NR+:BDA+ = 8,027 ± 3,639 neurons) corresponded to ~14% (14.4 ± 5.3%) of the total number of NR+ cells (NR+:BDA+ plus NR+:BDA- = 52,495 ± 5,611 neurons) estimated in the LH.

VAChT, VGluT and VGAT within BDA-labeled varicosities in the LH

Series that were double stained for BDA and the VTPs were examined to determine if BF axonal varicosities in the LH were immunopositive (+) for VAChT, VGluT or VGAT.

VAChT+ varicosities were relatively sparse in the LH. Nonetheless, some BDA-labeled terminals were double-labeled for VAChT (Fig. 3A). The BDA+/VAChT+ varicosities were most often located along axons (Fig. 3A', A'' and A''').

Both VGluT1+ (not shown) and VGluT2+ varicosities were densely distributed through the LH, though the VGluT2 most densely so. VGluT3+ varicosities were also present though sparse (not shown). In adjacent series processed for BDA and VGluT1, 2 or 3, only VGluT2 was found to be present in BDA-labeled varicosities (Fig. 3B). The BDA+/VGluT2+ varicosities most frequently appeared to be *boutons en passant* (Fig. 3B', B'' and B'''), although some appeared to be *boutons terminaux.*

Varicosities that were VGAT+ were densely distributed within the LH area. Many of the BDA-labeled axonal varicosities were VGAT+ (Fig. 3C). The

BDA+/VGAT+ varicosities were most commonly *boutons en passant* (Fig. 3C', C'' and C'''), though some appeared to be *boutons terminaux.*

Double staining for different VTPs was subsequently examined (n = 4 cases per series) to determine if they might be colocalized in the BF terminals. Double-labeling for VAChT/VGluT2, VAChT/VGAT or VGluT2/VGAT was not detected in varicosities of the LH (not shown). These negative results indicated that multiple VTPs are not colocalized in the same BF axonal varicosities innervating the LH.

Proportion and distribution of VAChT+, VGluT2+ and VGAT+ BDA-labeled varicosities

To determine the proportions of cholinergic, glutamatergic and GABAergic BF axon terminals, stereological analysis was used for estimation of the total numbers of BDA+ and BDA+/VTP+ varicosities in the tuberal-posterior LH (~A 5800, A 6200 and A 6600, Table 2). In the double stained VAChT series, ~10% of the BDA+ varicosities were BDA+/VAChT+. In the VGluT2 series, ~23% of BDA+ varicosities were BDA+/VGluT2+. In the VGAT series, ~47% of the BDA+ varicosities were BDA+/VGAT+.

As evident in plots of the sampled BDA+/VAChT+, BDA+/VGluT2+ and BDA+/VGAT+ (Fig. 4, representing ~25% of the estimated total number of varicosities), the three types of terminals were codistributed across the LH. The three were commonly most dense within the ventral and central portions of the LH, though also scattered through more dorsal portions of the LH.

PSD-95 or Geph in relation to BDA+/VGluT2+ or BDA+/VGAT+ terminals

To assess whether PSPs were present in association with the numerous BDA+/VGluT2+ or BDA+/VGAT+ varicosities, triple fluorescent staining for BDA (Cy2), VGluT2 or VGAT (Cy3) and PSD-95 or Geph (Cy5) was performed in LH sections and analyzed by confocal microscopy using 3D reconstruction and rotation of the images (in 3 cases per series).

In the series stained for BDA, VGluT2 and PSD-95, the PSD-95 staining appeared punctate and smaller in size than VGluT2+ varicosities. As judged from magnified and rotated 3D images, PSD-95+ puncta were often seen closely associated with VGluT2+ varicosities (Fig. 5A, B and C, pointers). BDA+/VGluT2+ varicosities were commonly seen in close association with one or more PSD-95+ puncta (BDA+/VGluT2+:PSD-95+, Fig. 5 A and B, pointers opposite filled arrowheads). As confirmed in 3D rotations, the BDA+/VGluT2+ varicosities were apposed to the PSD-95+ profiles (Fig. 5A and B, insets). BDA+/VGluT2- varicosities were generally seen unassociated with PSD-95+ puncta (Fig. 5C), although some BDA+/VGluT2-:PSD-95+ profiles were admittedly seen (not shown).

In series stained for BDA, VGAT and Geph, Geph staining appeared punctate. The Geph+ puncta were generally larger that the PSD-95+ puncta. As judged from magnified and rotated 3D images, Geph+ puncta were frequently seen in close association with VGAT+ varicosities, and conversely VGAT varicosities were frequently seen in close association with Geph+ puncta (Fig. 5D, E and F, pointers). BDA+/VGAT+ axonal varicosities were apposed to Geph+ puncta (BDA+/VGAT+:Geph+), usually with one Geph+ profile per

BDA+/VGAT+ varicosity (Fig. 5D and E). Occasionally, unlabeled LH cells appeared to be surrounded by VGAT+ varicosities, including BDA+/VGAT+ ones that were apposed to Geph+ puncta, located on the inner side of the varicosities and thus presumably in the cell membrane of the innervated cell body (Fig. 5 D). BDA+/VGAT- varicosities were not seen in apposition to Geph+ profiles (Fig. 5F).

DISCUSSION

The present study provides evidence that cholinergic, glutamatergic and GABAergic BF neurons project to the LH. The quantitatively most important, glutamatergic and GABAergic fibers also appear to form excitatory and inhibitory synapses respectively on LH neurons. Through this projection, BF neurons can thus have a dual influence in the LH to excite or inhibit neurons involved in promoting cortical activation and behavioral arousal.

Technical considerations

Confirming its documented utility as an anterograde tracer (Veenman et al., 1992; Wouterlood and Jorritsma-Byham, 1993; Lanciego et al., 2000; Reiner et al., 2000), we found that BDA-10,000 provided discrete labeling of BF cell bodies and reliable anterograde labeling of BF fibers and varicosities. Although we noticed some labeled cells in areas surrounding the injection site in the MCPO-SI, which might have been retrogradely labeled, we did not find cells retrogradely labeled at a distance in the prefrontal cortex or LH, confirming that BDA-10,000, in contrast to BDA-3000 MW, results in neglible retrograde labeling (Wouterlood and Jorritsma-Byham, 1993; Reiner et al., 2000). Here from the labeled cells located predominantly (>90% on average) in the MCPO of the BF, the BDA-labeled axons were seen to course within the ventrolateral, "*a*" subdivision of the MFB, which has been known to carry descending fibers from the MCPO (Veening et al., 1982). In the posterior LH, the axons sent collateral branches through the LH region in a manner also previously described from the MCPO by application of other anterograde tracers, including *Phaseolus vulgaris*

leucoagglutinin (PHA-L) (Grove, 1988) and proteins synthesized from tritiated amino acids (Swanson, 1976). This distribution of efferent fibers to the LH from MCPO-SI fits within a lateral to medial topographic organization of projections to the tuberal-posterior hypothalamus from forebrain structures (Veening et al., 1982). Moreover, the BDA-labeled varicose fibers extended through a region in the LH from which neurons in the MCPO and SI had previously been retrogradely labeled with cholera toxin in large numbers in our laboratory (Gritti et al., 1994). Here, we labeled only a small proportion of these afferent neurons, according to their numbers and distribution (Gritti et al., 1993, 1994; Gritti et al., 2003), since our injection site was intentionally discrete so as to be maximally restricted to the MCPO and overlying SI. With this relatively small proportion of projection neurons labeled, we found nonetheless that an estimated ~22,000 terminals were labeled with BDA in the LH and ~8,000 cells (~15% of the estimated total LH cell population) were contacted by BDA+ terminals, thus providing a good sample of the basalo-hypothalamic projection to the LH.

Confirming the utility of BDA as an anterograde tracer that can be readily used along with immunostaining for elucidating complex neural circuits (Lanciego et al., 2000), we were able to apply double staining for BDA and the VTPs in order to identify the neurotransmitters utilized by the BF neurons projecting to the LH. We found that with use of Triton (0.1%), we obtained complete penetration in double stained material for VTP antibodies and streptavidin (through 25 μm thick sections). Such reliable, homogeneous staining thus permitted the application of stereological analysis to assess the proportions of

the different VTP+ terminals in the LH. We were moreover able to apply triple staining for BDA, the VTPs and PSPs (using 0.3% TX).

Double staining with the VTPs allowed unequivocal identification of the neurotransmitter utilized by the projecting neurons (Chaudhry et al., 1998; Bellocchio et al., 2000). VTP proteins form, together with other elements necessary for recycling, docking and fusion of synaptic vesicles, a critical component of the machinery for neurotransmitter release at presynaptic sites (Liu et al., 1999; Fremeau et al., 2004). Particularly in the case of VGAT and VGluT2, they have been found to be concentrated at symmetrical and asymmetrical synapses respectively, to co-purify with other synaptic proteins and to colocalize with synaptophysin and/or synaptobrevin in synaptic terminals (Chaudhry et al., 1998; Takamori et al., 2000; Gualix et al., 2003; Fremeau et al., 2004).

Triple staining with PSPs here confirmed that the BDA-labeled VGluT+ and VGAT+ terminals abutted excitatory and inhibitory postsynaptic elements, respectively. The PSPs, PSD-95 and Geph, form part of the postsynaptic scaffolding of excitatory (Kornau et al., 1995; O'Brien et al., 1999; Sheng and Pak, 2000) and inhibitory (Pfeiffer et al., 1984; Sassoe-Pognetto et al., 1995; Sassoe-Pognetto and Fritschy, 2000; Sassoe-Pognetto et al., 2000) synapses, respectively. Indeed, PSD-95 colocalizes with glutamate receptors by interacting directly with the C-terminus of synaptic NMDA receptor subunits (Kornau et al., 1995) and indirectly through the protein stargazin with AMPA receptors (Chen et al., 2000). Although not binding $GABA_A$ receptors directly, Geph colocalizes with the most common and synaptically located $GABA_A$ receptor subunits as well as the glycine receptor (Pfeiffer et al., 1984; Sassoe-Pognetto et al., 2000). We

employed laser scanning confocal microscopy and state-of-the-art 3D rendering technology to visualize appositions between BDA+/VTP+ terminals and PSP+ profiles, an approach that has been proposed to be suitable for judging the existence of synaptic contacts by confocal microscopy (Wouterlood et al., 2002b; Wouterlood et al., 2003), while recognizing that absolute proof of such contacts necessitates electron microscopy. Thus, we believe that the presynaptic enrichment of VTPs for glutamate and GABA in BDA+ terminals and their apposition with PSPs associated with excitatory and inhibitory synapses respectively, represents strong evidence for the synaptic contacts of glutamatergic and GABAergic BF terminals on LH neurons.

BF cholinergic, glutamatergic and GABAergic fibers in the LH

The immunohistochemical localization of VAChT, VGluT2 and VGAT in anterogradely labeled BF varicosities demonstrates that BF neurons have the capacity, endowed by the VTPs, to release ACh, glutamate or GABA respectively (Gilmor et al., 1996; Chaudhry et al., 1998; Bellocchio et al., 2000; Fremeau et al., 2001). Their neurotransmitter phenotypes would appear to be unambiguous, since in contrast to previous evidence for the presence of multiple mRNAs or proteins for synthetic enzymes of ACh, glutamate or GABA in BF cell bodies (Manns et al., 2001; Sotty et al., 2003), no evidence for colocalization of the VTP proteins was found here in terminals within the LH. BF neurons innervating the LH can thus be phenotypically identified as cholinergic, glutamatergic or GABAergic.

By demonstrating the presence of VGluT2 proteins in BF terminals, the present results provide the first proof for the existence of BF neurons that utilize glutamate as a neurotransmitter and can thus be considered glutamatergic. Another recent report showed by *in situ* hybridization that cortically projecting BF neurons contain mRNA for VGluT2 and accordingly have the capacity to synthesize the VGluT2 protein (Hur and Zaborszky, 2005). Previous results had also suggested the existence of glutamatergic BF neurons based upon the presence of phosphate-activated-glutaminase (PAG) (Manns et al., 2001), the enzyme utilized for the synthesis of glutamate from glutamine, yet possibly also used for the synthesis of GABA from the same substrate in some cells (Fujiyama et al., 2001). The presence of glutamatergic BF neurons that utilize VGluT2 follows the principle that in the forebrain, VGluT2 neurons are localized predominantly in subcortical structures, whereas VGluT1 neurons are localized predominantly in cortex (Fremeau et al., 2001). A third type of vesicular transporter for glutamate (VGluT3) has more recently been visualized in cell bodies within some cortical and subcortical neurons, including notably BF neurons (Fremeau et al., 2002; Schafer et al., 2002; Harkany et al., 2003; Herzog et al., 2004). In the present analysis, we did not find evidence for concentration of VGluT3 in BF varicosities within the LH. It would thus appear that BF neurons might contain VGluT3 in their cell bodies but not transport it to their terminals or alternatively that BF neurons which do transport VGluT3 to their terminals do not project caudally to the LH.

Of the total number of BF axonal varicosities in the LH, the smallest proportion was VAChT+ (<10%), a medium proportion VGluT2+ (~25%) and the

largest proportion VGAT+ (~50%). Previous studies employing retrograde transport with immunostaining for the synthetic enzymes of ACh (choline acetyltransferase, ChAT) and GABA (glutamic acid decarboxylase, GAD) found that of the BF cells within the MCPO projecting to LH, <5% were ChAT+, ~20% were GAD+ and up to ~75% were neither and thus presumed to be glutamatergic (Gritti et al., 1994). The higher proportions of anterogradely labeled VAChT+ and VGAT+ varicosities relative to retrogradely labeled ChAT+ and GAD+ cell bodies might be due to more axonal collateralization per neuron or more varicosities per axon length in GABAergic and cholinergic than non-GABAergic/non-cholinergic neurons, which would include the glutamatergic neurons. Irrespective of these possible differences, only 25% of the varicosities were found to be glutamatergic, and another ~15% of varicosities could not be accounted for as glutamatergic, cholinergic, or GABAergic. It is possible that this contingent might use another type of excitatory neurotransmitter, such as aspartate, which is not recognized as a substrate by the vesicular glutamate transporters (Bellocchio et al., 2000; Fremeau et al., 2001; Fremeau et al., 2002). Indeed, aspartate has been found in axon terminals forming asymmetric synapses in the hypothalamus (van den Pol, 1991). Or, this proportion might simply reflect negative immunohistochemical staining due to insufficient amounts of some or all of the VTPs in terminals.

By showing the presence of PSD-95 and Geph in apposition to BF identified glutamatergic and GABAergic terminals respectively in the LH, the results substantiate the synaptic nature of this projection and also corroborate the principle that glutamate and GABA terminals generally form synapses with

postsynaptic target neurons (Edwards, 1995). Given the small number and proportion of BDA+/VAChT+ varicosities in the LH and the less well known association of cholinergic terminals with specific PSPs (Parker et al., 2004) or synaptic specializations (Descarries et al., 1997), we did not examine the relationship of the BDA+/VAChT+ boutons to PSPs. ACh might act predominantly by diffuse transmission through ectopic release and extrasynaptic receptors (Levey et al., 1995; Coggan et al., 2005).

Functional significance of the cholinergic, glutamatergic and GABAergic BF projections to LH

Neurons in the LH project to brainstem arousal systems and/or spinal cord sympathetic and motor systems as well as forebrain limbic areas and the cerebral cortex (Saper et al., 1979; Saper, 1985; Holstege, 1987). By means of these multiple projections, the LH is well suited to play a central role in arousal. Indeed, the LH has been shown to positively influence several arousal-related processes such as sympathetic tone, locomotion and exploratory behavior, including food seeking, reward and cortical activation (Olds and Milner, 1954; Hess, 1957; Berthoud, 2002; DiLeone et al., 2003; Jones, 2005b). Recently, the diffusely projecting neurons have been identified in the LH that contain the peptide Orx (de Lecea et al., 1998; Peyron et al., 1998; Sakurai et al., 1998), which appears to be critical for arousal and postural muscle tone since in absence of the peptide or its receptor, narcolepsy with cataplexy occurs (Chemelli et al., 1999; Lin et al., 1999; Peyron et al., 2000; Thannickal et al., 2000; Gerashchenko et al., 2001b; Hara et al., 2001). Physiologically as well as anatomically and

chemically, the LH is comprised by different cell types, the vast majority of which discharge at high rates during active waking with behavioral arousal (Szymusiak et al., 1989; Sakai et al., 1990; Steininger et al., 1999; Koyama et al., 2003). Some discharge in association with cortical activation during both waking and PS. Identified Orx neurons have recently been found to discharge maximally during active wakefulness and to virtually cease firing during SWS and PS (Lee et al., 2005a; Mileykovskiy et al., 2005).

In the present study, we found that the LH received input from cholinergic BF terminals, which represented <10% of all BF varicosities. Since cholinergic BF neurons have been found to discharge in association with cortical activation during both waking and PS (Manns et al., 2000a; Lee et al., 2005b), they could possibly influence similar neurons in the LH which project selectively to the cerebral cortex and discharge with cortical activation during both waking and PS (Szymusiak et al., 1989; Sakai et al., 1990; Steininger et al., 1999; Koyama et al., 2003).

Glutamatergic terminals accounted for up to 25% of the total BF innervation of the LH, indicating that glutamatergic BF neurons can exert an important excitatory influence upon the LH. This influence could be exerted upon LH neurons which discharge in association with cortical activation and presumably project to the cerebral cortex (above) or upon LH neurons which discharge in association with motor activity and presumably project to the brainstem or spinal cord (Szymusiak et al., 1989; Steininger et al., 1999; Alam et al., 2002). Glutamatergic BF neurons could also act upon Orx LH neurons, which project

diffusely to all targets and could thus simultaneously promote cortical activation along with motor activity and behavioral arousal that occur during waking. Such an excitatory influence could originate from as yet chemically unidentified but possibly glutamatergic BF neurons that are maximally active during waking and minimally active during SWS and PS (Szymusiak and McGinty, 1986b; Manns et al., 2003a; Lee et al., 2004; Jones, 2005a).

Approximately 50% of BF axon terminals innervating the LH were GABAergic, indicating that a major influence of the BF in this region is inhibitory. Given that the vast majority of neurons in the LH discharge during waking (Steininger et al., 1999; Alam et al., 2002) and that inhibition of these neurons by injections of the $GABA_A$ receptor agonist muscimol into the LH suppresses waking (Lin et al., 1989), it can be concluded that the GABAergic inhibitory influence from the BF in the LH would suppress waking and promote sleep. This inhibitory influence could be upon multiple LH neurons, including Orx neurons, whose inhibition by GABAergic input would accordingly provide a very powerful impetus for sleep. We propose that this innervation originates from particular GABAergic BF neurons that are sleep-active (Modirrousta et al., 2004) and discharge during SWS or SWS and PS when muscle hypotonia and atonia occur (Szymusiak and McGinty, 1986b; Manns et al., 2000b; Lee et al., 2004; Jones, 2005a).

In conclusion, the present study reveals the presence of three phenotypically distinct BF cell groups that must according to their neurotransmitters, differentially modulate the LH. As a minor contingent, cholinergic BF neurons can act to facilitate LH neurons involved in cortical activation. As a larger

contingent, newly identified glutamatergic BF neurons can act to promote both cortical and behavioral arousal of waking. As the largest contingent, GABAergic BF neurons can act to suppress arousal and promote sleep.

Acknowledgments—We are grateful to Robert H. Edwards and Robert T. Fremeau (Departments of Neurology and Physiology, University of California San Francisco School of Medicine, San Francisco, CA 94143) for kindly supplying the antibodies for VGluT1 and 2. We thank Lynda Mainville for her excellent technical assistance.

Table 1. List of primary and secondary antibodies used for fluorescence staining of biotinylated dextran amine (BDA), vesicular transporter proteins (VTPs) and post-synaptic proteins (PSPs).

	1[17] AB (overnight)							2[17] AB (3 hours)		SA (3 hours)		
Series	**Antigen**	**Host**	**Dilution**	**Source**	**Cat. #**	**Immunogen**	**Specificity**	**IgG (Dky)[17,18]**	**Dilution**	**SA[17]**	**Dilution**	**n[19]**
Double BDA VTP	VAChT	Gt	1:5000	Chemicon[1]	AB1578	Synthetic peptide corresponding to C-terminus of cloned rat VAChT[6] (CSPP GPFDGCEDDYNYYSRS)[7]	By WB the AB recognizes a ~65-70 kD band corresponding to VAChT protein[4]	Anti-Gt-Cy3	1:800	SA-Cy2	1:800	8
	VAChT	Rb	1:1000	Sigma[2]	V5387	Synthetic peptide corresponding to AA 512-530 of C-terminus of cloned rat VAChT (K-SPPGPFDGC EDDYNYYSRS)[8]	By WB the AB recognizes a ~67-70 kD band, corresponding to VAChT protein[7]	Anti-Rb-Cy3	"	"	"	9
	VGluT1	Rb	1:1000	Gift RHE[3]	-	Synthetic peptide corresponding to 68 last AA of C-terminus of rat BNPi (VGluT1)[9]	By WB the AB recognizes a ~62 kD band from rat brain[9]	Anti-Rb-Cy3	"	"	"	4
	VGluT2	Rb	1:5000	Gift RHE	-	Synthetic peptide corresponding to 64 last AA of C-terminus of rat DNPi (VGluT2)[10]	By WB the AB recognizes a ~50-62 kD band from rat brain[10]	Anti-Rb-Cy3	"	"	"	14
	VGluT3	GP	1:1000	Chemicon	AB5421	Synthetic peptide from cloned rat VGluT3 protein[11] (AFEGEEPLSYQNEEDFSE TS)[7]	The AB labels VGluT3+ cells and fibers, in agreement with other VGluT3 antisera[11]	Anti-GP-Cy3	"	"	"	7
	VGAT	Rb	1:250	Chemicon	AB5062P	Synthetic peptide corresponding to a 17 AA peptide near C-terminus region of rat VGAT[12] (VHS LEGLIEAYRTNAED)[7]	By WB the AB recognizes a band at ~55-60 kD[12]	Anti-Rb-Cy3	"	"	"	14
Double VTP VTP	VAChT/	Gt	1:5000	Chemicon	AB1578	(above)	(above)	Anti-Gt-Cy3	1:800			4
	VGluT2	Rb	1:5000	Gift RHE	-	(above)	(above)	Anti-Rb-Cy2	1:200			
	VAChT/	Gt	1:5000	Chemicon	AB1578	(above)	(above)	Anti-Gt-Cy3	1:800			4
	VGAT	Rb	1:250	Chemicon	AB5062P	(above)	(above)	Anti-Rb-Cy2	1:200			
	VGAT/	Rb	1:250	Chemicon	AB5062P	(above)	(above)	Anti-Rb-Cy2	1:800			4
	VGluT2	GP	1:5000	Chemicon	AB5907	Synthetic peptide from cloned rat VGluT2 protein[13] (VQESAQDAYSYKDRDD YS)[7]	The AB gives labeling in agreement with other antisera to VGluT2[13]	Anti-GP-Cy3	1:200			
Triple BDA VTP PSP	VGluT2/	Rb	1:5000	Gift RHE	-	(above)	(above)	Anti-Rb-Cy5	1:800	SA-Cy2	1:800	3
	PSD-95	Ms	1:100	ABR[4]	MA1-045	Purified recombinant of rat PSD-95[14]	The AB detects post synaptic density 95kD in rat brain. By WB it recognizes a ~95 kDa band[14]	Anti-Ms-Cy3	1:800	"	"	
	VGAT/	Rb	1:250	Chemicon	AB5062P	(above)	(above)	Anti-Rb-Cy5	"	"	"	3
	Geph	Ms	1:100	SY-SY[5]	147 011	Purified rat gephyrin[15]	By WB the AB recognizes a ~93 kD band. It detects a N-terminus epitope[16]	Anti-Ms-Cy3	"	"	"	

[1] Chemicon: Chemicon International, Temecula, CA, U.S.A.
[2] Sigma: Sigma, St. Louis, Missouri, U.S.A.
[3] Gift from Edwards, R.H. and Fremeau, R.T.Jr.
[4] ABR: Affinity BioReagents, Golden, CO, U.S.A.
[5] SY-SY: Synaptic Systems, Göttingen, Germany.
[6] http://www.chemicon.com/Product/ProductDataSheet.asp?ProductItem=AB1578
[7] Supplied by Chemicon on request
[8] http://www.sigmaaldrich.com/sigma/datasheet/v5387dat.pdf
[9] Bellocchio et al., 1998
[10] Fremeau et al., 2001
[11] http://www.chemicon.com/Product/ProductDataSheet.asp?ProductItem=AB5421
[12] http://www.chemicon.com/Product/ProductDataSheet.asp?ProductItem=AB5062P
[13] http://www.chemicon.com/product/productdataSheet.asp?ProductItem=AB5907
[14] http://www.bioreagents.com/index.cfm/fuseaction/products.print/Product/MA1-045
[15] http://www.sysy.com/gephyrin/gephy_fs.html
[16] Pfeiffer et al., 1984
[17] Jackson Immuno Research Laboratories, West Grove, PA, U.S.A.
[18] For multiple labeling (ML) with minimal cross-reactivity (min X) to other species.
[19] n: number of cases (each case referring to an injection site and series from the same side of the brain, thus 1 or 2 per brain).

Abbreviations: AA, amino acid; AB, antibody; BNPi, brain specific Na^+-dependent phosphate transporter; Cat., catalog; Cy2, cyanine; Cy3, indocarbocyanine; Cy5, indodicarbocyanine; Dky, donkey; DNPi, differentiation-associated Na^+-dependent phosphate transporter; Geph, gephyrin; GP, guinea pig; Gt, goat; Ms, mouse (monoclonal); Rb, rabbit; SA, streptavidin; WB, western blot.

Table 2. Proportion of VAChT+, VGluT2+ and VGAT+ BDA-labeled BF axonal varicosities in the LH region based on stereological estimates[1].

Cases	VAChT series			VGluT2 series			VGAT series			VTP series
	BDA+ var.	BDA+/ VAChT+ var.	% VAChT+ var.	BDA+ var.	BDA+/ VGluT2+ var.	% VGluT2+ var.	BDA+ var.	BDA+/ VGAT+ var.	% VGAT+ var.	ANOVA F-ratio
BDA15-L	38,080	4,640	12.2	-	-	-	-	-	-	
BDA15-R	17,920	1,040	5.8	-	-	-	-	-	-	
BDA16-L	18,800	2,640	14.0	27,040	5,600	20.7	23,440	11,280	48.1	
BDA18-L	17,840	2,000	11.2	10,800	2,080	19.3	17,680	8,240	46.6	
BDA18-R	15,120	960	6.3	11,680	2,640	22.6	17,120	8,160	47.7	
BDA19-L	-	-	-	18,824	6,136	32.6	20,176	10,504	52.1	
BDA19-R	-	-	-	19,032	3,432	18.0	16,536	6,864	41.5	
Mean ± SEM	**21,552 ± 4,178**	**2,256 ± 673**	**9.9 ± 1.6**	**17,475 ± 2,946**	**3,978 ± 806**	**22.6 ± 2.6**	**18,990 ± 1,274**	**9,010 ± 816**	**47.2 ± 1.7**	**87.3*** **

[1]Data for individual cases (1 or 2 sides from 4 rat brains) is presented together with the mean ± SEM. Estimated numbers of varicosities were obtained by sampling from 3 sections (at levels, A 5800, A 6200 and A 6600), per series per case. The proportions of the three VTP+ varicosities differed significantly (***, $p < 0.001$ according to one-way ANOVA) across and between VTP+ varicosities (with $p < 0.05$ according to post-hoc Bonferroni-corrected multiple-comparisons). Abbreviations: Est., estimated; var., varicosities; VTP, vesicular transporter protein.

Fig. 1. BF site of BDA injection. **A**: Atlas section through the cholinergic cell area (MCPO-SI) where iontophoretic applications of BDA were placed. **B**: Composite image of typical BDA injection site (case BDA18-R, processed using ABC with DAB-Ni and counterstained with neutral red). Note the small size and restricted location of BDA-labeled cells in the MCPO. **C**: High magnification image of two BDA-labeled neurons (from B, arrowheads). Brightness and contrast was adjusted in B and C. Abbreviations: ac, anterior commissure; FS, fundus striatum; LPO, lateral preoptic area; MCPO, magnocellular preoptic nucleus; MPO, medial preoptic nucleus; oc, optic chiasm; Pir, piriform cortex; SI, substantia innominata; SO, supraoptic nucleus. Scale bars: in B, 1 mm; in C, 20 μm.

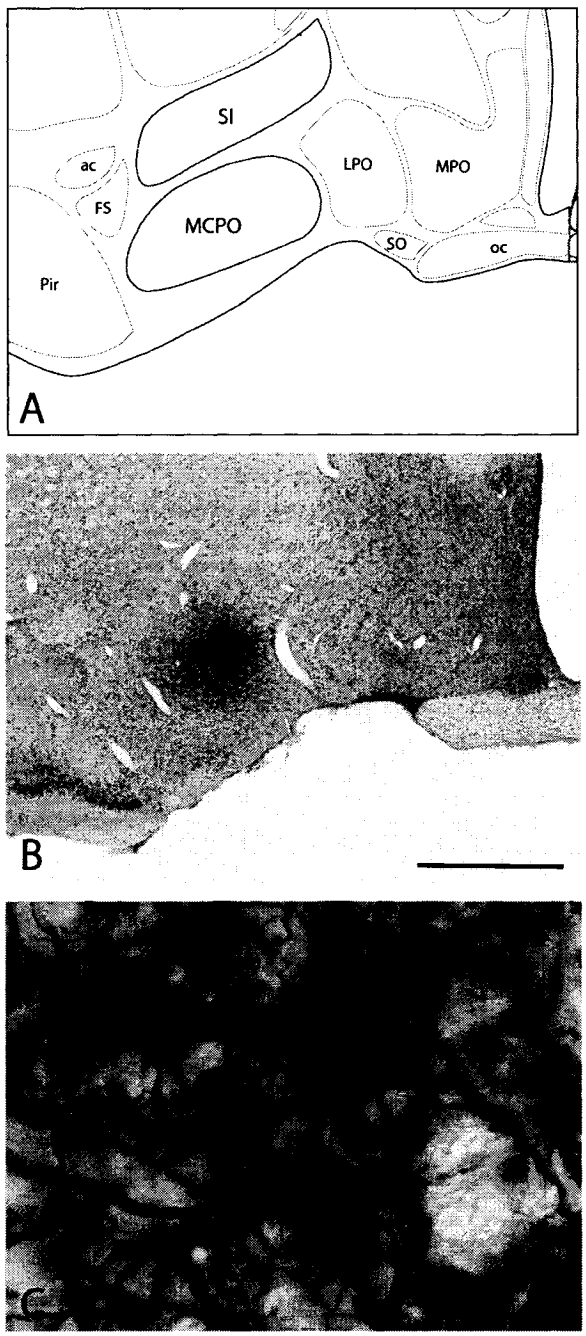

Fig. 1. BF site of BDA injection

Fig. 2. BDA-labeled fibers in the LH. **A**: Low magnification composite image of BDA+ axons (in black, DAB-Ni) and neutral red stained (NR+) cells in the LH (case BDA19-L). **B**: High magnification images showing BDA+ axons and terminals within the LH area. Varicosities appeared most commonly along axons as *boutons en passant* (solid arrowhead in B') but also at the end of axons as *boutons terminaux* (open arrowhead in B''). Many axonal varicosities (stained with DAB-Ni) were seen in the neuropil (B') or in close proximity to small (solid arrowhead in B'') or large (solid arrowhead in B''') nerve cell bodies (stained with NR, B' and B'', case BDA15-L; B''', case BDA19-L). **C**: Tracing of BDA+ axons and NR+ neurons in the LH at ~A 6200 μm (from IA0, case BDA19-L). Although concentrated more ventrally, fibers extended through the LH area and formed appositions with neurons therein (D). **D**: High magnification tracing of elements in C showing the relationship of BDA+ axons with dorsally (solid arrowheads in D'), as well as more ventrally (D'' and D''') located NR+ neurons. (The neuron in D''' corresponds to that pictured in B'''.) Tonal range for each RGB channel as well as brightness and contrast adjustment were made for pictures in A and B. Abbreviations: cp, cerebral peduncle; DMH, dorsomedial hypothalamus; f, fornix; LH, lateral hypothalamus; ot, optic tract; VMH, ventromedial hypothalamic nucleus; ZI, zona incerta. Scale bars: in A, 100 μm; in B and D, 10 μm.

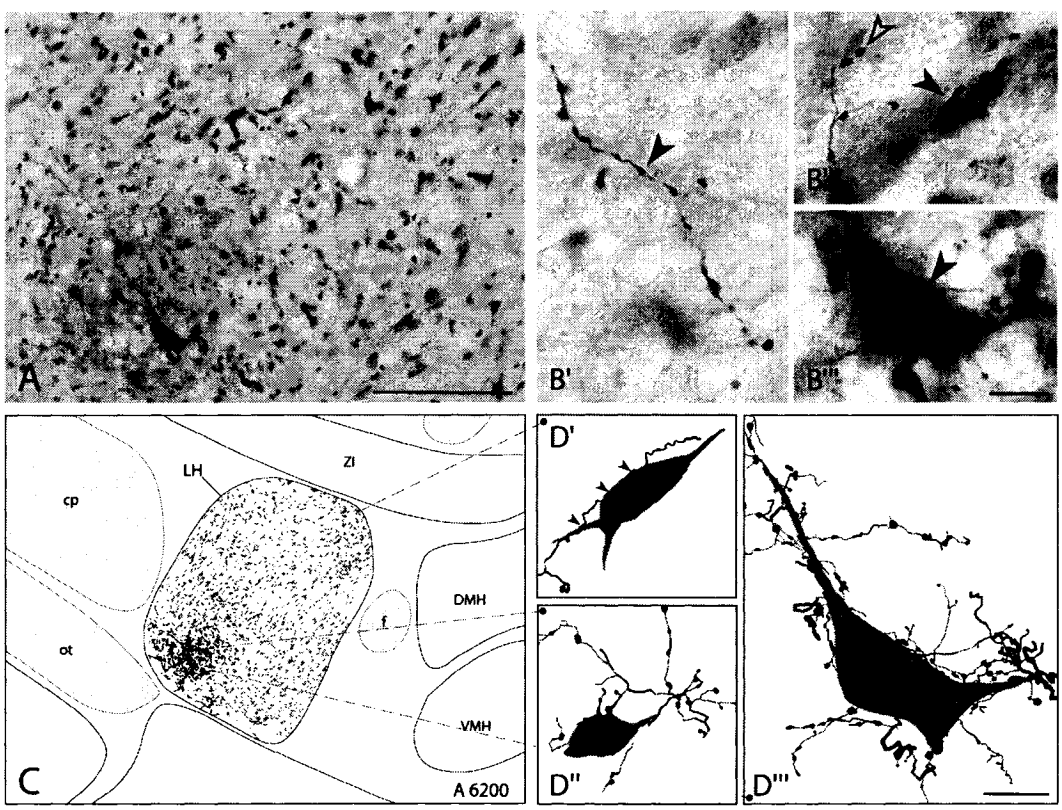

Fig. 2. BDA-labeled fibers in the LH

Fig. 3. BDA-labeled axons in LH contain VAChT, VGluT2 or VGAT. High magnification epifluorescent images illustrating anterogradely labeled BDA+ axons (left A', B' and C', green fluorescent Cy2) that are double-labeled for vesicular transporter proteins (VTPs) as shown in single (middle A'', B'' and C'', red fluorescent Cy3) and merged (right A''', B''' and C''', yellow) images and indicated by white arrowheads for those which are in focus. **A**: BDA+ varicose fiber (A') whose varicosities are positive for VAChT (A'' and A'''). **B**: BDA+ varicose axon (B') whose varicosities are positive for VGluT2 (B'' and B'''). **C**: BDA+ axon (C') whose varicosities are positive for VGAT (C'' and C'''). Tonal range in red and green channels was adjusted individually (see methods). Scale bar in C''' for all images, 10 μm.

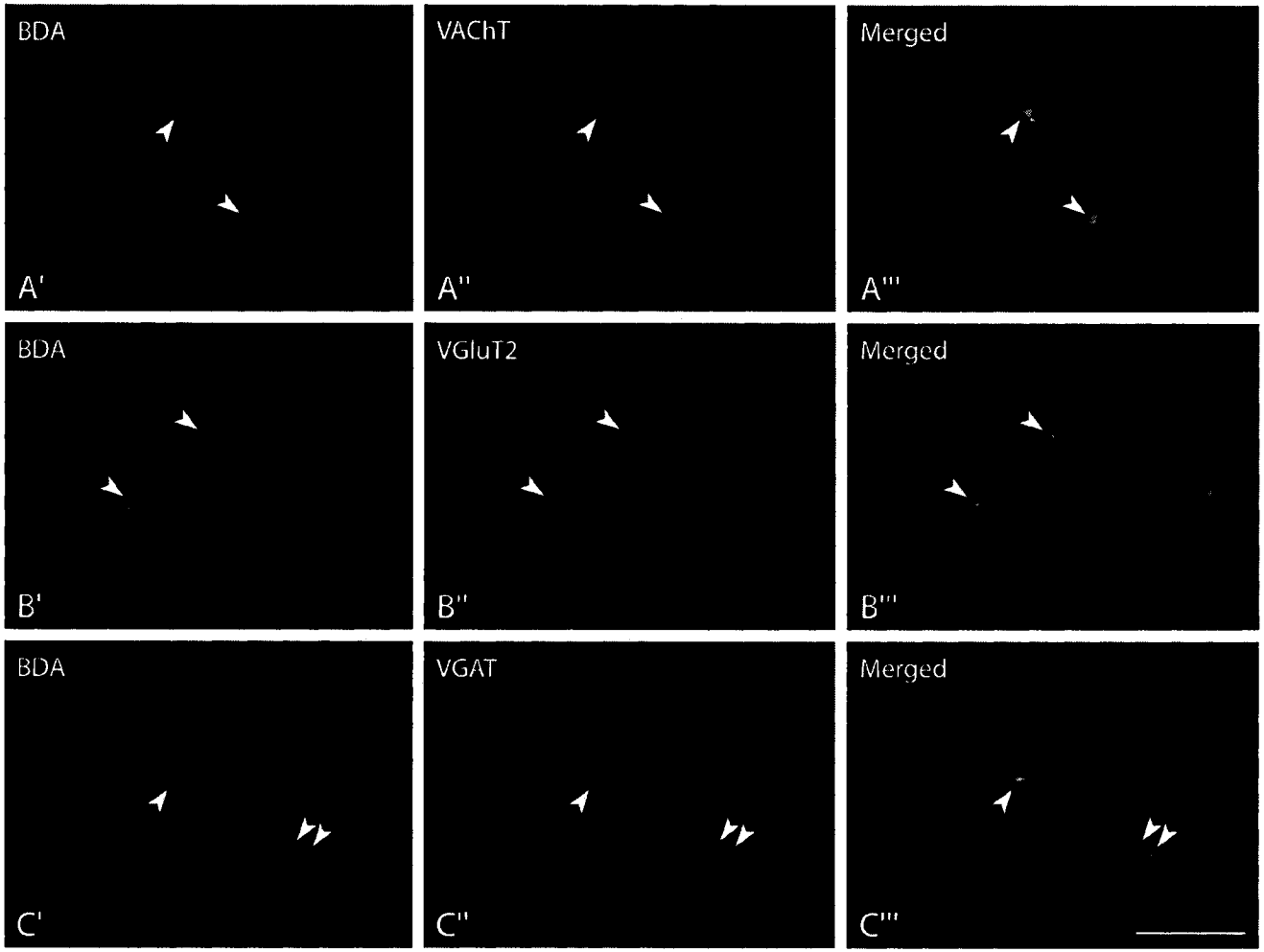

Fig. 3. BDA-labeled axons in LH contain VAChT, VGluT2 or VGAT

Fig. 4. Distribution of VAChT+, VGluT2+ and VGAT+ BDA-labeled varicosities in the LH. Plotted together are the BDA+/VAChT+ (blue circles), BDA+/VGluT2+ (green squares) and BDA+/VGAT+ (red triangles) that were marked and counted by stereological analysis from double stained fluorescent sections at the three levels through the LH (case BDA16-L). The BDA+/VTP- negative terminals, which were counted in each series, are not included. The stereological analysis was performed by sampling ¼ of the total area (using a counting frame of 90 x 90 μm within a grid of 180 x 180 μm, see Methods), and each figure thus reflects ~¼ of the total number of varicosities in a 25 μm thick section. Note the concentration of BDA+/VTP+ varicosities within the ventral and central portion of the LH, with scattered varicosities in other portions, especially at the most posterior level (A 5800). Abbreviations: f, fornix.

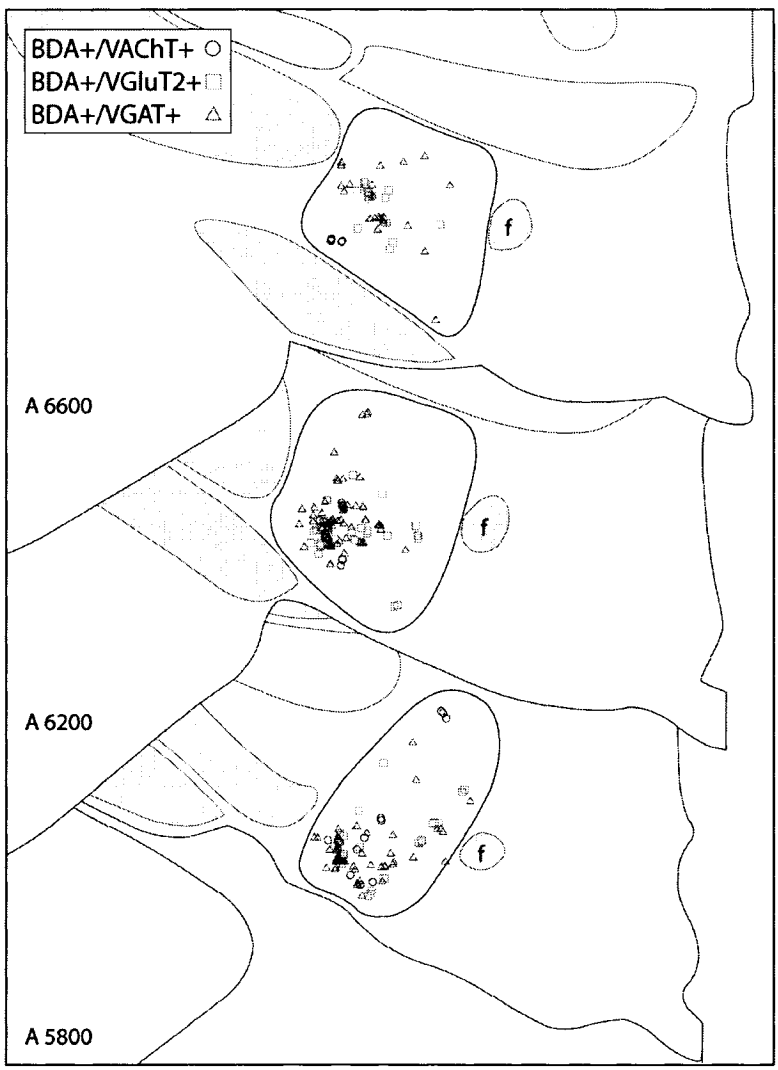

Fig. 4. Distribution of VAChT+, VGluT2+ and VGAT+ BDA-labeled varicosities in the LH

Fig. 5. Relationship of PSD-95+ puncta to VGluT2+ and Geph+ puncta to VGAT+ BDA-labeled varicosities in 3D rendered confocal images. **A and B**: Large images (8 and 12 serial 0.33 μm thick optical sections) of BDA-labeled axons and varicosities (solid arrowheads, pseudo-color green, Cy2) that are immunopositive for VGluT2 (pseudo-color blue, Cy3) and face PSD-95+ profiles (facing pointers, pseudo-color red, Cy5) and featured in the zoomed images on the right (5 and 12 serial 0.33 μm thick optical sections). Note also in the large images, the frequent association of VGluT2+ varicosities with PSD-95+ puncta (pointers). **C**: Image (8 serial sections) of a BDA+ varicosity (open arrowhead, pseudo-color green, Cy2) that is immunonegative for VGluT2 (pseudo-color blue, Cy3) and does not face a PSD-95+ profile, as also evident in the zoom images on the right (10 serial sections). Note VGluT2+ varicosities in the vicinity that are associated with PSD-95+ puncta (pointer in large image). **D and E**: Images (8 and 7 serial sections, respectively) of BDA-labeled axons and varicosities (solid arrowheads, pseudo-color green, Cy2) that are positive for VGAT (pseudo-color blue, Cy3) and face Geph+ profiles (facing pointers, pseudo-color red, Cy5), as featured in the zoomed images on right (9 and 7 serial sections). In the large image of D, VGAT+/Geph+ elements appear to surround the unlabeled soma of a neuron with the VGAT+ varicosities outside and the Geph+ puncta (pointers) inside, presumably on the cell membrane. Note in the large panels that many VGAT+ varicosities are associated with Geph+ puncta (pointers). **F**: Image (7 serial sections) of a BDA+ varicosity (open arrowhead, pseudo-color green, Cy2) that is immunonegative for VGAT (pseudo-color blue, Cy3) and is not associated

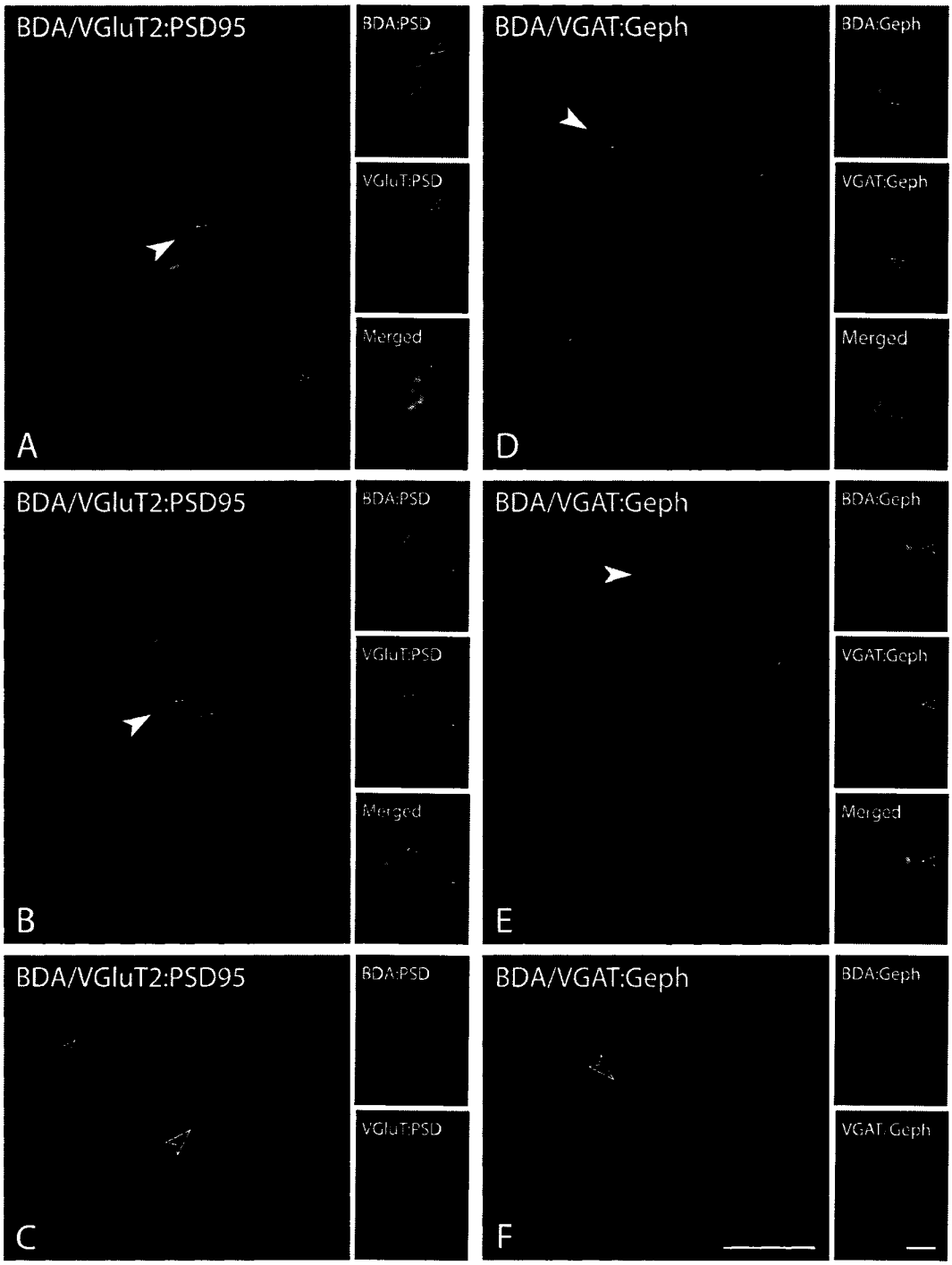

Fig. 5. Relationship of PSD-95+ puncta to VGluT2+ and Geph+ puncta to VGAT+ BDA-labeled varicosities in 3D rendered confocal images

with any Geph+ puncta, as also evident in the zoomed images on the right (5 serial sections). Note, in contrast, other VGAT+ varicosities in the vicinity are associated with Geph+ puncta (pointer). Deconvolution was applied to all images with a confidence limit of 95% (see Methods). Scale bar for large images on left (shown for all panels in F) = 5 μm; for zoom images on right (shown for all panels in F) = 1 μm.

PREFACE TO CHAPTER IV

Hypothalamic neurons which contain the peptide orexin (also called hypocretin) and distribute in the LH, the perifornical area (PF) and dorsomedial hypothalamus (DMH) have been recently described. These neurons have been shown to play a cardinal role in the maintenance of wakefulness, since their absence, or that of the Orx peptide or its receptor, leads to narcolepsy, a syndrome characterized by excessive sleepiness, sudden loss of muscle tone and intrusions of PS phenomena into W.

Given the role of the BF in the appearance of behavioral quiescence and sleep and, as described in the last chapter, the prominent projections of the BF to the LH, the possibility that these afferents may innervate, and therefore control the activity of Orx neurons, was examined.

In order to determine whether Orx neurons are innervated by BF neurons, we first mapped and quantified the Orx neurons in the hypothalamus in relation to BF afferents, using double stained material for BDA and Orx. Upon presence of significant numbers of appositions between BF axon terminals and Orx neurons, the neurochemical phenotype of those appositions and the proportions of neurons innervated by them were determined in triple stained fluorescent material for BDA, VTPs and Orx. Finally, the presence of synaptic contacts was examined by using triple stained material for BDA, PSPs and Orx.

Given the critical role of Orx neurons in the maintenance of W, the influence that GABAergic and glutamatergic BF neurons may have on Orx neuronal activity is discussed in relation to the role of the BF neurons in sleep and cortical activation.

Chapter IV

Innervation of Orexin/Hypocretin Neurons by GABAergic, Glutamatergic or Cholinergic Basal Forebrain Terminals Evidenced by Immunostaining for Presynaptic Vesicular Transporter and Postsynaptic Scaffolding Proteins

Pablo Henny and Barbara E. Jones

Montreal Neurological Institute, McGill University,

Montreal, Quebec, Canada H3A 2B4

Abbreviations:

ABC	avidin-biotin-peroxidase complex
ac	anterior commissure
AHA	anterior hypothalamic area
AMCA	aminomethylcoumarin acetate
ANPB	alpha-naphthol pyronin B
Arc	arcuate nucleus
BDA	biotinylated dextran amine
BF	basal forebrain
cp	cerebral peduncle
Cy2	cyanine
Cy3	indocarbocyanine
Cy5	indodicarbocyanine
DAB	diaminobenzidine
DAB-Ni	nickel-intensified diaminobenzidine
DMH	dorsomedial hypothalamic nucleus
f	fornix
FS	fundus striatum
Geph	gephyrin
ic	internal capsule
LH	lateral hypothalamus
LPO	lateral preoptic area
MCPO	magnocellular preoptic nucleus
MFB	medial forebrain bundle

MPO	medial preoptic nucleus
mt	mammillothalamic tract
oc	optic chiasm
Orx	orexin or hypocretin
ot	optic tract
Pe	periventricular hypothalamic nucleus
PF	perifornical area
Pir	piriform cortex
PSD-95	95-kD postsynaptic density protein
PSP	postsynaptic protein
SI	substantia innominata
SO	supraoptic nucleus
STh	subthalamic nucleus
VAChT	vesicular transporter for acetylcholine
VGAT	vesicular transporter for GABA
VGluT2	vesicular transporter for glutamate 2
VMH	ventromedial hypothalamic nucleus
VTP	vesicular transporter protein
ZI	zona incerta

ABSTRACT

Orexin/hypocretin (Orx) neurons are critical for the maintenance of waking in association with behavioral arousal and postural muscle tone, since with their loss, narcolepsy with cataplexy occurs. Given that basal forebrain (BF) neurons project to the hypothalamus and play important diverse roles in sleep-wake states, we sought to determine whether acetylcholine (ACh), glutamate (Glu) and/or GABA releasing BF neurons innervate and could thereby differentially regulate the Orx neurons. From discrete injections of biotinylated dextran amine (BDA, 10,000 MW) into the magnocellular preoptic nucleus (MCPO) and substantia innominata (SI) in the rat, BDA-labeled fibers projected to the lateral hypothalamus (LH), perifornical area (PF) and dorsomedial hypothalamus (DMH), where ~41%, ~11% and 9% of Orx-positive (+) neurons were respectively contacted in each region. Employing triple fluorescent staining for Orx, BDA and presynaptic vesicular (V) transporters (T), we found that only 4% of the innervated Orx+ neurons in the LH were contacted by BDA+[VAChT+] terminals, whereas ~31% and ~67% were respectively contacted by BDA+[VGluT2+] and BDA+[VGAT+] terminals. In 3D rendered and rotated confocal images, we confirmed the latter contacts and examined staining for postsynaptic proteins PSD-95, a marker for glutamatergic synapses, and gephyrin, a marker for GABAergic synapses, that were located on Orx+ neurons facing BDA-labeled terminals in ~20% and ~50% of contacts, respectively. With such synaptic input, BF glutamatergic neurons can excite Orx neurons and thus act to maintain behavioral arousal with muscle tone, whereas GABAergic neurons can

inhibit Orx neurons and thus promote behavioral quiescence and sleep along with muscle atonia.

INTRODUCTION

Neurons containing the peptide orexin (Orx , also called hypocretin) play a critical role in maintaining wakefulness and associated postural muscle tone, since in their absence or that of the peptide or receptor, narcolepsy with cataplexy occurs in humans and animals (Chemelli et al., 1999; Lin et al., 1999; Peyron et al., 2000; Thannickal et al., 2000; Yamanaka et al., 2003b). The Orx neurons are located within the tuberal hypothalamus where they are broadly distributed across the lateral hypothalamic area (Broberger et al., 1998; Peyron et al., 1998; Modirrousta et al., 2005; Swanson et al., 2005), a region long known to play an important role in arousal (see for review, (Jones, 2005b)). Lying there within the path of the medial forebrain bundle (MFB) (Millhouse, 1969; Veening et al., 1982), the Orx neurons have recently been shown to receive inputs from multiple forebrain and brainstem cell groups (Sakurai et al., 2005; Yoshida et al., 2006), which project through the MFB and are involved in sleep-wake state regulation (Jones, 2005b). The sources of afferent input might include the basal forebrain (BF) (Sakurai et al., 2005), which, from lesion, stimulation and recording studies is known to play diverse roles in sleep-wake state regulation through its different constituent cell groups (Szymusiak et al., 2000; Jones, 2005a; Jones, 2005b).

The BF is known particularly for the cholinergic neurons residing there within multiple nuclei and projecting to the cerebral cortex where they stimulate cortical activation during waking and paradoxical sleep (PS, also called rapid eye movement, REM, sleep) see for review (Jones, 2004). However, the BF also contains more numerous non-cholinergic neurons, including GABAergic and glutamatergic neurons which appear to play different roles in sleep-wake state

regulation, including the promotion of slow wave sleep (SWS) or conversely, waking (Lee et al., 2004; Jones, 2005a). From retrograde tracing studies, we previously found that few cholinergic neurons, but many GABAergic and other unidentified BF neurons, project caudally to the lateral hypothalamus (LH) (Gritti et al., 1994). Most recently using anterograde transport of biotinylated dextran amine (BDA) together with immunohistochemistry for the vesicular transporter proteins (VTPs), we established that a minor proportion of terminals projecting into the LH from the BF contained the VTP for acetylcholine (ACh, VAChT), whereas a major proportion contained that for GABA (VGAT) and a remaining proportion contained the VTP for glutamate (VGluT2 and not VGluT1 or VGluT3), proving an important glutamatergic in addition to GABAergic contingent of the BF inputs to the LH (Henny and Jones, 2006a). We also established in that study that the cholinergic, GABAergic and glutamatergic projecting neurons were phenotypically distinct, since the VTPs were not co-localized in the same terminals. The BF afferents would thus release ACh, GABA or glutamate. The aim of the present study was thus to examine if the Orx neurons in the hypothalamus are innervated by BF terminals and, if so, whether they might be selectively or preferentially innervated by cholinergic, glutamatergic or GABAergic terminals and thereby influenced in a particular manner by BF neurons across the sleep-waking cycle.

Using anterograde transport of 10,000 MW BDA in rats (Henny and Jones, 2006a), we examined in the present study the innervation of Orx neurons by neurons of the magnocellular preoptic nucleus (MCPO) and substantia innominata (SI) of the BF cholinergic cell area from where significant hypothalamic as well

as neocortical projections originate (Gritti et al., 1994; Gritti et al., 1997) and can influence behavioral in addition to cortical components of sleep-wake states (Szymusiak et al., 2000; Jones, 2004, 2005a; Jones, 2005b). First, using single or dual staining, we studied and estimated quantitatively with stereological analysis the distribution of Orx neurons in the hypothalamus and their contact by BDA-labeled terminals in light microscopy. Second, using triple staining for Orx, BDA and the VTPs, we examined and estimated quantitatively with stereological analysis the contacts on the Orx neurons by BDA-labeled terminals containing VAChT, VGluT2 or VGAT in fluorescence microscopy. Third, given evidence of prominent VGluT2 and VGAT containing terminals apposing the Orx neurons, we further studied their contacts by confocal laser scanning microscopy and 3D reconstruction with rotation. Lastly, to ascertain whether such varicosities might form excitatory or inhibitory synapses on the Orx neurons, we similarly examined sections triple-stained for BDA, Orx and the scaffolding postsynaptic proteins (PSPs), PSD-95 as a marker for asymmetric, glutamatergic synapses (Sheng and Pak, 2000; Sassoe-Pognetto et al., 2003) or Gephyrin (Geph) as a marker for symmetric, GABAergic synapses (Pfeiffer et al., 1984; Giustetto et al., 1998; Sassoe-Pognetto and Fritschy, 2000; Sassoe-Pognetto et al., 2000). Using 3D reconstruction with rotation of high-resolution confocal images, we document important glutamatergic and GABAergic BF inputs onto Orx neurons.

MATERIALS AND METHODS

Animals and Surgery

All procedures conformed to the guidelines of the Canadian Council on Animal Care and the U.S. NIH and were approved by the McGill University Animal Care committee.

As previously described in detail (Henny and Jones, 2006a), Long Evans rats (200-250 g, Charles River Canada, St. Constant, Quebec, Canada) were anesthetized and placed in a stereotaxic frame (David Kopf Instruments, Tujunga, CA) for surgery. Glass micropipettes (tip diameter 15 to 25 μm) were back-filled with a 0.5 M NaCl solution containing 2% 10,000 MW BDA (BDA-10,000, Molecular Probes, Eugene, OR). Since previous studies using anterograde as well as retrograde tracing methods showed no evidence for contralateral projections from BF to the posterior hypothalamus (Swanson, 1976; Gritti et al., 1994), bilateral injections of BDA were performed. The pipettes were lowered into the region of the MCPO on each side (from *Bregma*: anterior-posterior (AP), -0.5 mm; Lateral (L), +/- 2.5 mm; Vertical (V), 8.5 mm) (Paxinos and Watson, 1986) with the aid of a micropositioner (Model 660, David Kopf Instruments). Once in the targeted site, microinjection of BDA was performed by iontophoresis (using a Microiontophoresis Dual Current Generator 260, World Precision Instruments (WPI), Sarasota, FL) applying positive current pulses (5 to 10 μA) in a duty cycle of 1 sec (0.5 s on, 0.5 s off) for a period of 25 to 30 min through a stimulator (Pulsemaster A300, WPI) and stimulus isolation unit (Iso-Flex, A.M.P.I., Jerusalem, Israel).

Rats were maintained for 5 or 6 days with food and water *ad libitum* and subsequently perfused transcardially under deep sodium pentobarbital anesthesia (100 mg/kg, i.p.) with ~500 ml 4% paraformaldehyde fixative solution. The brains were removed and put in a 30% sucrose solution for 2 to 3 days, after which they were frozen at -50° C and stored at -80° C for subsequent processing.

Immunohistochemistry

Sections were cut using a freezing microtome in 25 μm thick coronal sections and collected in eight adjacent series at 200 μm intervals through the forebrain, including the magnocellular basal forebrain and the tuberal hypothalamus. To visualize BDA-labeled neurons in the BF as well anterogradely-labeled axons in the tuberal hypothalamus, the avidin-biotin-peroxidase complex (ABC) protocol was used with diaminobenzidine (DAB) intensified with Nickel (DAB-Ni). Sections were subsequently counterstained for Nissl substance using Neutral Red.

For the mapping, distribution and quantitative estimates of Orx+ cells in the hypothalamus, serial sections were incubated overnight with goat (Gt)-Anti-Orx-A (1:500, see Table 1) and stained with DAB following incubation with donkey (Dky) anti-Gt IgG and Gt peroxidase-antiperoxidase (PAP, both from Jackson Immuno Research Laboratories, West Grove, PA).

For evaluation of the injection sites, description of BDA-labeled fibers in the tuberal hypothalamus and examination of the innervation of Orx+ cells in the region, series were processed for dual-staining of BDA using the ABC procedure with DAB-Ni and Orx-A (above) using PAP with alpha-naphthol pyronin B (ANPB, Sigma, St. Louis, MI). Injection sites on one or two sides from 9 rats

were selected according to their placement in the MCPO and SI (n = 16 cases) for subsequent processing and analysis in peroxidase or fluorescent stained material.

For triple fluorescent staining of Orx with the VTPs (VAChT, VGluT2 or VGAT) and BDA (see Tables 1 and 2), free floating sections from each series were rinsed for 30 min in Trizma saline buffer (TS, 0.1 M, pH 7.4) followed by incubation for 30 min with a blocking solution of normal donkey serum (NDS, 6% in TS) containing 0.3% Triton X-100 (TX). Sections were subsequently co-incubated overnight at room temperature with VTP and Orx-A primary antibodies (in TS containing NDS 1% and TX 0.3%). Prior pilot studies determined that incubation in TX 0.3% allowed full penetration of the antibodies and streptavidin, as viewed through the z-axis under epifluorescent and confocal microscopy. The next day, sections were incubated for 3 hours in indocarbocyanine (Cy3)- and aminomethylcoumarin acetate (AMCA) or indodicarbocyanine (Cy5)-conjugated secondary antibodies, followed by three hours in cyanine (Cy2)-conjugated-streptavidin (SA) for BDA revelation. For triple fluorescent staining of BDA with the PSPs, PSD-95 or Geph, and Orx, the same protocol was used by co-incubation with the PSP and Orx antibodies overnight (see Tables 1 and 2).

All sections were mounted out of Trizma water, and the mounted sections dehydrated through alcohols, cleared in xylene and coverslipped with Permount.

Conventional microscopy, tracing and stereological analysis

Sections were examined under light and epifluorescent microscopy with a Leica DMLB or Nikon E800 microscope equipped with an x-y-z motorized stage, video or digital camera and filters appropriate for FITC or Cy2, Rhodamine or Cy3,

DAPI-AMCA and/or Cy5 fluorescence. Single as well as composite images were acquired on the Nikon or Leica microscopes using Neurolucida software from MicroBrightField (MBF, Colchester, VT), which was also used for plotting cells and tracing fibers. In light or fluorescent material, cells and varicosities were counted using the Optical Fractionator probe of StereoInvestigator software (MBF) on the Nikon microscope. For tracing or counting, a computer resident atlas of the rat brain was employed that has been developed and applied in our laboratory using standardized procedures for tissue processing. For each application, series of histology sections are matched to appropriate levels of the atlas (at 400 μm intervals) under low magnification (5 or 10x objective). At each level, the atlas image is then rotated if necessary, and the contours adjusted to optimally fit the relevant nuclei of the histology section. In the BF, the number of BDA labeled cells was counted through the injection site within the MCPO and SI (Gritti et al., 1993; Henny and Jones, 2006a). Through the hypothalamus, Orx neurons were plotted and counted through their full distribution across three AP levels (in mm from Interaural (A) zero), ~A6.6, A6.2 and A5.8 (Paxinos and Watson, 1986), and within three contours, the LH, comprising the region lateral to the fornix through which the MFB passes and present at levels ~A6.6, A6.2 and A5.8, and the perifornical area (PF), comprising the area surrounding and extending medial to the fornix, and the dorsomedial hypothalamic nucleus (DMH) and present at levels ~A6.2 and ~A5.8 (Veening et al., 1982; Modirrousta et al., 2005). BDA-labeled fibers were plotted and analyzed using the same atlas sections and contours.

For representation of the distribution of the Orx population, Orx+ neurons (stained with DAB) were plotted under brightfield illumination with a 40x objective at three levels (above) using Neurolucida. In the same material, stereological estimates of the total number of Orx+ cells across three levels in the LH, and two levels in the PF and DMH were obtained using StereoInvestigator. Within the Optical Fractionator probe, cells were counted with a 60x Oil objective (1.40 numerical aperture, NA) using a counting frame of 120 μm x 120 μm and a sampling grid size of 240 μm x 240 μm to sample 25% of the x-y area of each nucleus. Within each counting frame or block, all cells whose tops came into focus beneath the surface of the section were counted through a 10 μm dissector height in the z-axis, which corresponded to the average thickness of the mounted (dehydrated, cleared and coverslipped) sections in this series.

To examine the relationship of BF axons to the Orx neurons in the hypothalamus, BDA-labeled fibers (stained black with DAB-Ni) and Orx+ cell bodies (stained fuchsia with ANPB) were traced under brightfield illumination using the Neurolucida software (MBF). Axons and cell bodies were drawn using a 100x Oil objective within contours of the LH, PF and DMH. Unbiased estimates of the number and proportion of Orx+ neurons receiving contacts from BF varicosities were obtained in the LH, where both the Orx+ cells and BF varicosities were most numerous, as well as in PF and DMH. An Orx+ cell was considered to be contacted if a BDA+ varicosity was seen in direct apposition to the cell, with no obvious space observed between them and at a point where both were located at the approximately same focal plane. Stereological counts were

obtained of Orx+ cells that were (Orx+:BDA+) or were not (Orx+:BDA-) contacted by one or more BDA+ varicosities through the LH, PF and DMH (n = 3). Counts were performed under a 100x Oil objective (1.40 NA) at three levels (above) within the LH contour and two levels (above) within PF and DMH contours. Within the Optical Fractionator probe, a counting frame of 70 μm x 70 μm was employed with a sampling grid size of 140 μm x 140 μm so as to sample 25% of the area. Within each counting frame or block, all cells whose tops came into focus beneath the surface of the section were counted through 15 μm in the z-axis, which was the average thickness of the mounted sections in this series.

To examine the relationship of BDA+ terminals containing different VTPs [VTP+] to Orx+ cells, triple-stained sections were viewed under epifluorescent microscopy to determine if BDA+[VAChT+], BDA+[VGluT2+] or BDA+[VGAT+] varicosities appeared to come into contact with Orx+ cells stained with AMCA or Cy5 (see Table 2). Additional series were used for stereology in which Orx cells were stained with Cy5 (using the antibody from Gt in combination with anti-VTP antibodies from Rb, Table 2). Unbiased estimates were obtained of the total number and proportion of innervated Orx+ cells which were contacted by each of the BDA+[VTP+] type of varicosity by counting Orx+:BDA+[VTP+] along with Orx+:BDA+[VTP-] cells through three levels of the LH contour in each series (n = 3). In addition, estimates of the total number and proportion of contacting varicosities were computed for each of the BDA+[VTP+] type of varicosity by using counts of BDA+[VTP+]:Orx+ and BDA+[VTP-]:Orx+ varicosities (n = 3). The presence of BDA+ contacts on the

counted cells was assessed online by sequential observation of the material through the different filters at the same focal plane and multiple planes through the z axis. Counts were performed under a 100x Oil objective (with 1.40 NA) within a counting frame of 70 μm x 70 μm and using a sampling grid of 120 μm x 120 μm so as to sample ~33% of the LH area. Within each counting frame or block, all cells whose tops came into focus beneath the surface of the section were counted through 8 μm in the z-axis, which corresponded to the average thickness of the mounted sections in these series.

Confocal microscopy and image processing

Material triple-stained for BDA/VTP/Orx or BDA/PSP/Orx was examined in a Zeiss LSM 510 laser scanning confocal microscope equipped with Argon 488 nm, helium-neon 543 nm and helium-neon 633 nm lasers for Cy2, Cy3 and Cy5 excitation, respectively. Appropriate filters were used for detection of Cy2 (bandpass 500 to 530 nm, green), Cy3 (bandpass 565 to 615 nm, red) and Cy5 (bandpass 697 to 719 nm, infrared, color coded in blue). Scanning was performed through a Plan-Apochromat 100x (with 1.4 NA) objective and pinhole size of ~0.8 (0.6 to 1, Airy Units) for the three channels. Acquisition was performed with the resident LSM 510 software and consisted of stacks of images taken through the z-axis in optical slices of ~0.5 μm for VTPs, or ~0.33 μm for PSPs series. Additional high resolution stack images (optical slices of ~0.05 to 0.1 μm) were acquired for the PSP series.

Rendered 3D views of the stacks were obtained using the fluorescence rendering mode from the image software Volocity 3.7 (Improvision Inc, Lexington, MA, www.improvision.com), which provides a semi-transparent 3D view of the different elements based on the degree of intensity of each voxel (i.e., the more intense, the less transparent). The different elements could then be examined simultaneously and interactively from different angles and magnifications. Thus, varicosities could be judged to be in contact with a postsynaptic cell or process, as assessed by the absence of space between the presynaptic and postsynaptic element from any of the angles observed (Wouterlood et al., 2002b). High resolution image stacks (see above) were analyzed in the fluorescent rendering mode as well as in the isosurface rendering mode, which provides a 3D solid, non-transparent view of the element surface. Channels in which the signal was low or the noise was relatively high were restored using a deconvolution procedure (iterative restoration in Volocity).

Adjustment for brightness and contrast for all pictures, in addition to adjustment of tonal range for each individual RGB channel ("Adjust/Levels" command in Photoshop) for fluorescent images were performed with Adobe Photoshop Creative Suite edition (Adobe System, San Jose, CA, U.S.A). Figure preparation and final montage were done with Adobe Illustrator Creative Suite edition (Adobe).

RESULTS

BDA injection site and anterograde labeling in the hypothalamus

Iontophoretic application of BDA-10,000 into the region of the MCPO-SI (Fig. 1A) on 2 sides in 9 rats produced small and well restricted, spherical injection sites (Fig. 1B) of <500 μm diameter and containing (some ~1400) labeled nerve cell bodies, as previously described (Henny and Jones, 2006a). Injection sites were positioned primarily within the MCPO and SI (in n = 16 cases selected for analysis), where ~90% and ~6% of labeled cells were located, respectively. BDA-labeled fibers coursed through the MFB to reach the tuberal hypothalamus where multiple neurons, particularly in the LH, were contacted by varicosities (Fig. 1C) (Henny and Jones, 2006a).

Number and distribution of Orx+ neurons in the hypothalamus

The distribution and numbers of Orx+ neurons were examined in PAP (DAB) stained material. Orx+ cells were distributed across the tuberal hypothalamus in moderate numbers from rostral to caudal levels (~A6.6, A6.2 and A5.8, Fig. 2). Although most concentrated in the area immediately surrounding and dorsal to the fornix, cells were distributed through the LH, PF and DMH. According to stereological estimates of total numbers of cells (mean ± SEM, n = 3), ~1800 Orx+ cells were located within the LH, ~500 in the PF and ~900 in the DMH with a total of ~3200 neurons per side (Table 3). The proportions of Orx neurons were thus ~56% in the LH, ~15% in the PF and ~29% in the DMH contours as delineated here.

BDA-labeled axons in relation to Orx+ neurons

The relation of BF axon terminals to Orx cells was examined in material dual-stained using peroxidase for BDA (in black with DAB-Ni following ABC procedure) and Orx (in fuchsia with ANPB following PAP procedure) (n = 7, Fig. 3). Multiple BDA-labeled fibers were evident in the regions where Orx+ cell bodies and proximal dendrites were present, particularly in the LH (Fig. 3A). Moreover, BDA-labeled axonal *boutons en passant* (Fig. 3B') or *boutons terminaux* (Fig. 3B'' and B''') appeared to contact Orx+ cell bodies as well as dendrites. In tracings of all BDA+ fibers along with Orx+ cells at high magnification using Neurolucida, multiple fine collaterals of the coarse fibers within the MFB appeared to extend dorsally and medially to reach Orx+ neurons within the central and dorsal regions of the LH (Fig. 3C, level A 6.0, approximately intermediate to those seen in Fig. 2B and C). Here, BDA-labeled varicosities appeared to contact Orx+ soma or proximal dendrites in the LH (Fig. 3D', D'' and D'''). Some BDA-labeled fibers also extended medially to reach into the PF or DMH, although these were few in number. As determined by stereological analysis, the proportion of Orx+ neurons that were contacted by at least one BDA+ varicosity (Orx+:BDA+) within the LH, PF and DMH, was estimated to be ~41%, ~11% and ~9%, respectively (Table 3). Overall, ~28% of the total population of Orx+ neurons was contacted by BF axonal varicosities.

Given that the maximal incidence of Orx+ neurons contacted occurred in the LH and that the majority of Orx+ neurons were also contained within the LH (above), subsequent analyses of the BF innervation were focused upon the Orx+ neurons within the contour of the LH.

VAChT, VGluT2 and VGAT in BDA-labeled varicosities in relation to Orx+ neurons in the LH

To determine if BF terminals contacting Orx neurons are cholinergic, glutamatergic or GABAergic, sections which were triple-stained for BDA (with Cy2), the VTPs (VAChT, VGluT2 or VGAT with Cy3) and Orx-A (with AMCA or Cy5) were examined under epifluorescent microscopy (see number of cases, n, for each series in Table 2). In these sections, sparse VAChT+ varicosities were evident (Fig. 4A''), whereas multiple VGluT2+ (Fig. 4B'') and VGAT+ (Fig. 4C'') varicosities were present in the vicinity of the Orx+ neurons. BDA+[VAChT+] (Fig. 4A'''), BDA+[VGluT2+] (Fig. 4B''') and BDA+[VGAT+] (Fig. 4C''') BF axons were all present in the immediate surround of the Orx+ neurons as well. However, only BDA+[VGluT2+] (Fig. 4B''') and BDA+[VGAT+] varicosities (Fig. 4C''') appeared to contact the Orx+ neurons in substantial numbers.

Stereological estimates of contacts between VAChT+, VGluT2+ or VGAT+ BDA-labeled varicosities and Orx+ neurons in the LH

To determine the proportions of Orx+ neurons innervated by cholinergic, glutamatergic or GABAergic BF axon terminals, stereological analysis was used for estimation of the total numbers of Orx+ neurons contacted by each of the BDA+[VTP+] types of varicosities in the LH through the three levels studied (~A6.6, A6.2 and A5.8, n = 3 cases, Table 4). In the VAChT series, less than 4% of the Orx+:BDA+ neurons were contacted by BDA+[VAChT+] varicosities. In the VGluT2 series, ~31 % of the Orx+:BDA+ neurons were contacted by

BDA+[VGluT2+] varicosities. In the VGAT series, ~67 % of the Orx+:BDA+ neurons were contacted by BDA+[VGAT+] varicosities.

The number of BDA+[VTP+] varicosities contacting Orx+ neurons (BDA+[VTP+]:Orx+) was also determined (n = 3, Table 4). As estimated from each series, the proportions of varicosities in contact with Orx+ neurons were respectively: ~2% for BDA+[VAChT+], ~17 % for BDA+[VGluT2+] and ~58% for BDA+[VGAT+] varicosities. Across series, the numbers of terminals detected per Orx+ cell were: one for BDA+[VAChT+], one to two for BDA+[VGluT2+] and one to four for BDA+[VGAT+] varicosities. Given the minimal number of contacts by BDA+[VAChT+] varicosities and the substantial number of contacts by BDA+[VGluT2+] and BDA+[VGAT+] varicosities on the Orx+ neurons, confocal analysis was pursued for the latter terminals.

Confocal analysis of VGluT2 or VGAT inside and of PSD-95 or Gephyrin opposite BDA+ terminals on Orx+ neurons

To examine in detail the nature of the BDA+ contacts observed on Orx+ neurons, confocal microscopic analysis was performed on material triple-stained for BDA (with Cy2), Orx (with Cy5 or Cy3) and markers for the presynaptic, VTP (VGluT2 or VGAT with Cy3) or postsynaptic, PSP (PSD-95 or Geph with Cy5) (see Table 2 for number of cases processed and examined for each series). Confocal images were further viewed using 3D reconstruction and rotation with magnification to confirm that the pre- and postsynaptic elements were in contact through three spatial axes.

In series triple-stained for BDA, VGluT2 and Orx, the Orx+ neurons were seen to be surrounded by numerous VGluT2+ varicosities. In this material, many BDA-labeled VGluT2+ varicosities were apposed to Orx+ soma (Fig. 5A) or proximal dendrites (not shown). As judged from examination and rotation of 3D images from such cases, the BDA+[VGluT2+] varicosity appeared to be in contact with the Orx+ cell, since no space could be observed between the two (Fig. 5A, small images) with rotation through three axes.

In series triple-stained for BDA, PSD-95 and Orx, staining for PSD-95 appeared punctate and could be seen on the surface of Orx+ neurons (Fig. 5B). In some BDA+:Orx+ contacts (Fig. 5B), PSD-95+ puncta could be detected opposite the BDA+ varicosity and associated with the Orx+ cell (Fig. 5B, small images). From 93 acquired images of appositions (from n = 3 cases), 74 BDA+:Orx+ contacts (~80%) were confirmed in rotated and magnified 3D images, and 16 of these or 21.6 % showed staining for PSD-95 opposite the BDA+ varicosity and associated with the Orx+ cell.

To further assess the spatial relationship among the BDA+ terminals, PSD-95+ puncta and Orx+ cells, image stacks with high z-axis resolution (0.05 to 0.10 μm optical slices) were acquired of 23 appositions (from n = 3 cases) and analyzed in 3D rotations. Contacts were confirmed between BDA+ varicosities and Orx+ neurons, as shown from three different, orthogonal 3D angles of semi-transparent fluorescence images (Fig. 6A1, B1 and C1). PSD-95+ profiles were observed in apposition to BDA+ varicosities (Fig. 6A2, B2 and C2) and in association with the surface of Orx+ neurons (Fig. 6A3 and B3), being localized

between BDA+ and Orx+ elements (Fig. 6A4 and B4). Opaque isosurface rendering of the three elements further evidenced the localization of PSD-95+ puncta, which appear tucked in or hidden between the BDA+ varicosity and the Orx+ neuron (Fig. 6A5, B5 and C5).

In series triple-stained for BDA, VGAT and Orx, Orx+ neurons were also seen to be surrounded by VGAT+ varicosities. Many BDA-labeled VGAT+ varicosities were in close apposition to Orx+ soma or dendrites (Fig. 5C). As judged from the rotated and magnified 3D images of such cases, the BDA+[VGAT+] varicosity was in contact with the Orx+ cell (Fig. 5C, small images) through three axes.

In series triple-stained for BDA, Geph and Orx, Geph staining (Cy5) appeared punctate, generally in larger puncta than PSD-95 and frequently associated with Orx+ soma and dendrites (Fig. 5D). In multiple BDA+:Orx+ contacts (Fig. 5D), Geph+ puncta were seen facing the BDA+ varicosity and associated with the Orx+ cell (Fig. 5D, top small images), such that they appeared to be located between the terminal and cell in merged images (Fig. 5D lower small image). From 112 acquired images of appositions (from n = 3 cases), 93 BDA+:Orx+ contacts (>80%) were confirmed in rotated and magnified 3D images, and 44 or 47.3 % showed Geph+ puncta between the BDA+ varicosity and the Orx+ cell.

For further analysis, image stacks with high z-axis resolution (0.05 to 0.10 μm optical slices) were acquired of 19 (from n = 3 cases) BDA, Geph and Orx appositions, and examined. Contacts were seen between BDA+ varicosities and

Orx+ neurons, as evidenced from 3D orthogonal views (Fig. 6D1, E1 and F1). Geph+ profiles were observed in apposition to BDA+ varicosities (Fig. 6E2 and F2) and in association with the surface of Orx+ neurons (Fig. 6D3, E3 and F3), located between BDA+ and Orx+ elements (Fig. 6E4 and F4). Opaque isosurface rendering of the three elements evidenced the localization of Geph+ puncta between the BDA+ varicosity and the Orx+ neuron (Fig. 6D5, E5 and F5).

DISCUSSION

The present study presents qualitative and quantitative evidence that Orx neurons are innervated by afferents from the BF cholinergic cell area. Yet, from this cholinergic cell area, the afferents were predominantly comprised of noncholinergic terminals. Numerous glutamatergic and GABAergic varicosities contacted Orx neurons in the LH and could thus respectively exert excitatory and inhibitory influences on their activity during wake and sleep states.

BF projections to Orx neurons

We show here that anterogradely labeled fibers from the MCPO-SI of the BF cholinergic cell area extend into the region of the Orx cells in the tuberal hypothalamus. As shown and discussed in our previous study (Henny and Jones, 2006a), the fibers reached the caudal hypothalamus through the ventrolateral portion of the MFB, which has long been known to carry fibers from this forebrain area (Swanson, 1976; Veening et al., 1982; Grove, 1988). From this component, collaterals fan out through the LH and extend dorsomedially though less numerously through the PF and sparsely into the DMH.

We estimated here using stereology that Orx neurons are most numerous within the LH, numbering ~1800, less numerous within the PF, numbering ~500 and intermediate in the DMH numbering ~900 for a total of ~3200 neurons per side. The total number (in Long Evans rats) is similar to that previously estimated by us as ~3400 Orx+ neurons per side (in Wistar rats) (Modirrousta et al., 2005) and to one other published number estimated by stereological analysis as ~2900 Orx+ neurons per side (in Wistar rats) (Allard et al., 2004). According to

conventional delineation as the region lateral to the fornix through which the MFB fiber systems travel, >50% (or ~1800) of the Orx cells are located in the LH.

We show here that BF terminals, which would originate from a relatively small number of caudally projecting cells in the MCPO-SI labeled by the BDA injections, contact a significant proportion (~28%) of all Orx+ cells. This input was topographically arranged, as the proportions of Orx+ cells contacted were substantial (~41%) in the LH and small in the more medial PF (~11%) and DMH (~9%). Notably, from similar injection sites, BF terminals contact only ~15% of the total LH cell population (estimated at ~50,000 through the tuberal hypothalamus) (Henny and Jones, 2006a), suggesting a selective enrichment of BF terminals upon the Orx neurons relative to all other chemically unidentified neurons of the LH. According to a recent extensive survey of afferents to the Orx neurons using both anterograde and retrograde tracing (Yoshida et al., 2006), the overall proportion of Orx neurons contacted by BF afferents (~28%, from the present study) would be comparable to that originating from the adjacent ventrolateral preoptic area (31%). In the former work, the BF was not considered to be among the major afferent sources to the Orx neurons, though it contained a moderate number of afferent cells (Yoshida et al., 2006). In that study, the afferents were identified by injections of retrograde tracers into the region where the Orx+ neurons are most concentrated, immediately surrounding the fornix within the dorsal PF, the lateral DMH and the dorsomedial region of the LH, and thus highlighted major sources of input from the more medial basal telencephalic afferent systems. From our present and previous (Gritti et al., 1994; Henny and Jones, 2006a), as well as other early tracing studies (Swanson, 1976; Veening et

al., 1982; Grove, 1988), the MCPO-SI would fit within a lateral-to-medial as well as ventral-to-dorsal topographically organized system of fibers coursing within the MFB and serving as afferents to the hypothalamus and notably, as the present results indicate, the Orx neurons therein.

Predominant innervation by noncholinergic, glutamatergic and GABAergic, BF terminals of Orx neurons

In the LH, of the total number of Orx neurons contacted by BF axonal varicosities (~41%, see above), only a minimal proportion (~4%) was innervated by cholinergic varicosities, whereas the major proportion was innervated by glutamatergic or GABAergic varicosities. Similarly, only 2% of the varicosities on Orx+ cells were VAChT+ in this material. These results are in line with our previous study showing that cholinergic BF terminals in the LH comprise less than 10%, whereas glutamatergic and GABAergic terminals comprise the vast majority of the BF terminals in the LH (Henny and Jones, 2006a). They are not in agreement with the recent results of Sakurai and colleagues using a transgene for a tetanus toxin tracer (tetanus toxin C fragment fused to green fluorescent protein, TTC::GFP), which is believed to be transported transynaptically and retrogradely, linked to an *orexin* promoter together with fluorescent staining for choline acetyltransferase (ChAT) (Sakurai et al., 2005). In those studies, essentially all retrogradely labeled neurons in the cholinergic cell area of the BF were judged to be immunostained for ChAT. We recognize the possibility that the TTC::GFP tracer could be taken up by terminals on distal dendrites which were not evident in our fluorescent material. On the other hand, previous results from our lab and

from other groups utilizing retrograde transport of traditional tracers also found minimal proportions of descending projections from cholinergic BF neurons (<5%) to the brainstem or hypothalamus and the region of the Orx cell bodies and dendrites (Grove, 1988; Semba et al., 1989; Gritti et al., 1994; Bayer et al., 1999). As discussed by Sakurai and colleagues, retrograde labeling by TTC::GFP could be due to transynaptic transport along with retrograde transport that could result in labeling of a large number and proportion of cholinergic BF cells as higher order afferent neurons. Such an indirect, multisynaptic influence of cholinergic BF neurons upon Orx neurons might be expected to exist as a feedback upon the Orx neurons which project into the region of the cholinergic cells (Espana et al., 2005) and would exert an excitatory effect through Orx on the cholinergic neurons (Eggermann et al., 2001). On the other hand, from electrophysiological studies, it appears that cholinergic input can have an important influence on Orx neurons, since cholinergic agonists can depolarize and excite the Orx neurons (Bayer et al., 2005; Sakurai et al., 2005). Although the BF cholinergic cells may participate in this influence, the pontomesencephalic cholinergic neurons likely play a more dominant role given previous evidence of their more substantial projections into the region of the Orx cells (Ford et al., 1995; Bayer et al., 1999).

We found that a substantial proportion of BF-innervated Orx neurons were contacted by VGluT2 containing BDA-labeled terminals (~31%), and that a substantial proportion of the BDA-labeled terminals contacting Orx neurons were VGluT2+ (~17%). Glutamate has been shown to depolarize Orx neurons through both NMDA and AMPA receptors *in vitro* (Li et al., 2002; Yamanaka et al., 2003a). Orx neurons have been described as receiving a relatively high density of

VGluT2+ varicosities and asymmetric, presumed excitatory synapses (Horvath and Gao, 2005). From the present results, one source of these multiple glutamatergic inputs can be attributed to BF neurons.

The major proportion of BF-innervated Orx neurons were contacted by VGAT containing BDA-labeled terminals (~67%), and a major proportion of the BDA-labeled varicosities were VGAT+ (~58%), indicating that GABAergic BF neurons can have a potent influence upon Orx neurons. GABA has been shown to hyperpolarize and inhibit Orx neurons which are otherwise spontaneously active *in vitro* (Li et al., 2002; Eggermann et al., 2003; Yamanaka et al., 2003a). Interestingly, Orx neurons are considered to have a relatively sparse GABAergic input, particularly in relation to the glutamatergic input, with a ratio of inhibitory to excitatory synapses estimated as 1 to 10 (Horvath and Gao, 2005). In light of the latter results, it would appear that the BF GABAergic neurons may play a particularly important role in providing this inhibitory input and influence to the Orx cells.

BF glutamatergic and GABAergic synaptic input onto Orx neurons

We confirmed by confocal laser scanning microscopy and 3D image rendering and rotation that BDA-labeled BF varicosities appeared to contact Orx neurons in the LH. By continuous rotation through three axes, we were thus able to establish for large numbers of varicosities that there appeared to be no space between the varicosity and the Orx+ cell. Such confirmation has been considered by others to represent strong evidence for synaptic contacts (Wouterlood et al., 2002b). Yet, it

is well recognized that only the resolution of the electron microscope provides absolute proof of such contacts by presynaptic elements with postsynaptic targets.

More specific evidence is provided for the synaptic nature of glutamatergic and GABAergic terminals by the presence of the presynaptic vesicular transporters. VGluT2 and VGAT, which were demonstrated in the BDA-labeled varicosities apposed to Orx cells, confer the capacity to release glutamate and GABA and are concentrated in the presynaptic terminal at asymmetric and symmetric synapses, respectively (Gilmor et al., 1996; Chaudhry et al., 1998; Bellocchio et al., 2000; Takamori et al., 2000; Fremeau et al., 2001; Gualix et al., 2003; Fremeau et al., 2004).

Lastly, we show that in confirmed contacts of BDA-labeled varicosities with Orx cells, postsynaptic proteins of PSD-95 and Geph are situated facing the varicosity and in association with the Orx+ cell. Similar to proportions of BDA-labeled varicosities ostensibly contacting Orx+ neurons that were VGluT2+ and VGAT+ (above), the proportions of confirmed contacts by BDA-labeled varicosities upon Orx+ neurons which showed PSD-95 or Geph puncta between the terminal and cell were ~22% and ~47% respectively. Postsynaptic proteins, PSD-95 and Geph are constituent parts of the postsynaptic scaffolding of asymmetric, excitatory (Sheng and Pak, 2000) and symmetric, inhibitory synapses (Sassoe-Pognetto and Fritschy, 2000) respectively. At excitatory synapses, PSD-95 colocalizes by direct and indirect association with NMDA and AMPA receptors (Sassoe-Pognetto et al., 2003). At inhibitory synapses, Geph is colocalized with the most common synaptic subtypes of $GABA_A$ receptors and is suggested to participate in their anchoring to the postsynaptic membrane (Sassoe-

Pognetto et al., 1995; Giustetto et al., 1998). The location of postsynaptic proteins sandwiched between presynaptic and postsynaptic elements has been considered as strong evidence for synaptic contacts in 3D rendered confocal images (Wouterlood et al., 2003). We thus believe that the present results showing both pre- and postsynaptic elements for glutamatergic and GABAergic synapses in association with BDA-labeled terminals contacting Orx neurons provide compelling evidence for BF glutamatergic and GABAergic synaptic input to the Orx cells.

Functional significance of the cholinergic, glutamatergic and GABAergic BF input to Orx neurons

Orx neurons play a key role in stimulating and maintaining arousal by excitatory influences upon multiple systems, including the cerebral cortex, hypothalamic and brainstem arousal systems, as well as sympathetic and motor circuits in the spinal cord (Peyron et al., 1998; van den Pol, 1999; Saper et al., 2001; Taheri et al., 2002; Krout et al., 2003; Siegel, 2004; Jones and Muhlethaler, 2005; Sakurai, 2005). As now shown by recent studies, they are in turn influenced by afferent input from multiple forebrain and brainstem systems (Sakurai et al., 2005; Yoshida et al., 2006). Here we show that neurons of the BF cholinergic cell area, which themselves are importantly involved in regulating sleep-wake states, contribute significantly to that afferent input. The BF input was particularly dense onto the Orx neurons in the LH, which despite claims of being selectively activated with reward seeking (Harris et al., 2005), have also clearly been shown to discharge and express c-Fos in association with simple waking, arousal or

stress (Espana et al., 2003; Lee et al., 2005a; Mileykovskiy et al., 2005; Modirrousta et al., 2005).

In contrast to recent claims (above, (Sakurai et al., 2005)), the cholinergic BF cells appear to contribute minimally to the innervation of the Orx neurons in the LH. Cholinergic BF neurons discharge in a manner (Lee et al., 2005b) that differs fundamentally from that of recently identified Orx neurons across sleep-wake states (Lee et al., 2005a). Whereas cholinergic neurons discharge maximally during both waking and PS in association with cortical activation, Orx neurons discharge maximally during waking in association with movement and muscle tone and cease firing during PS sleep with muscle atonia (Jones, 2005a). It is thus not surprising that Orx neurons are not under direct control of cholinergic BF neurons. To the contrary, the silence of Orx neurons during PS sleep is the condition under which cholinergic neuronal discharge stimulates cortical activation in association with the muscle atonia of that state.

The Orx neurons receive a substantial glutamatergic input from BF neurons indicating that these glutamatergic neurons can exert a significant excitatory influence upon Orx cells. In single unit recording studies, many noncholinergic BF neurons have been identified that discharge maximally during active waking and are virtually silent during sleep including PS sleep (Szymusiak and McGinty, 1986b; Lee et al., 2004; Lee et al., 2005b). The discharge of these neurons is positively correlated with postural muscle tonus or neck electromyographic (EMG) activity (Lee et al., 2004), like that of the Orx neurons (Jones, 2005a; Lee

et al., 2005a). We propose that such noncholinergic neurons are glutamatergic and could facilitate behavioral arousal in part by exciting the Orx cells.

The major input to the Orx neurons from BF is GABAergic. Given the purportedly small inhibitory input relative to excitatory input onto Orx neurons (Horvath and Gao, 2005), this GABAergic input from BF neurons might be of critical importance in inhibiting the discharge of Orx neurons during periods of behavioral quiescence, sleep and/or muscle atonia (Lee et al., 2005a). Although we have identified GABAergic neurons which discharge in association with cortical activation (Manns et al., 2000b), we propose that the innervation of the Orx neurons originates from the particular GABAergic BF neurons that are active during sleep (Modirrousta et al., 2004) and discharge during SWS and/or PS sleep in negative correlation with muscle tonus or EMG (Szymusiak and McGinty, 1986b; Manns et al., 2000b; Lee et al., 2004; Jones, 2005a).

Orexin has been attributed a particularly important role in maintaining arousal since in its absence in knockout mice or that of its receptor in dogs or Orx neurons in humans, narcolepsy occurs (Chemelli et al., 1999; Lin et al., 1999; Peyron et al., 2000; Thannickal et al., 2000; Hara et al., 2001). In humans, narcolepsy is characterized by excessive daytime sleepiness, short onset of REM sleep and/or loss of postural muscle tone, known as cataplexy. Accordingly, the excitation of Orx neurons by presumed wake-active, glutamatergic BF neurons could normally serve to prevent sleep onset and loss of postural muscle tone, whereas the inhibition of Orx neurons by presumed sleep-active GABAergic BF neurons could promote sleep onset and the loss of postural muscle tone. It could

be due in part to withdrawal of the major BF GABAergic input to Orx neurons that neurotoxic lesions of the BF result in a severe disruption of SWS and PS (Szymusiak and McGinty, 1986a). Moreover, chemical stimulation of the BF with cholinergic agonists or agents exciting cholinergic neurons can elicit PS with atonia in cats and rats (Hernandez-Peon et al., 1963; Cape et al., 2000; Jones, 2004) and/or cataplexy in dogs (Nishino et al., 1995). Cholinergic agonists and ACh, which is released in the BF maximally during PS (Vazquez and Baghdoyan, 2001), could excite noncholinergic, presumed GABAergic BF neurons (Fort et al., 1998; Wu et al., 2000), including those which innervate the Orx neurons and thereby elicit PS and/or muscle atonia.

In conclusion, the present study reveals an important glutamatergic and GABAergic input to Orx neurons from BF neurons. Glutamatergic BF neurons can excite Orx neurons to stimulate behavioral arousal and waking. GABAergic BF neurons can inhibit Orx neurons to diminish behavioral arousal along with muscle tone and thereby promote sleep, including PS with muscle atonia.

Acknowledgments—We are grateful to Robert H. Edwards and Robert T. Fremeau (Departments of Neurology and Physiology, University of California San Francisco School of Medicine, San Francisco, CA 94143) for kindly supplying the antibody for VGluT2. We thank Lynda Mainville for her excellent technical assistance, and Mandana Modirrousta for her contribution to the study of the Orx cell population.

Table 1. Primary antibodies (AB) for immunostaining of orexin (Orx), vesicular transporter proteins (VTPs) or postsynaptic proteins (PSPs)

Antigen	Host sp	Source	Cat. #	Immunogen	Specificity
Orx					
Orx-A	Rb	Phoenix[1]	H-003-30	Full 33 AA Orx-A peptide sequence from rat (EPLPDCCRQKTCSCRLYELLH GAGNHAAGILTL)[2]	By WB the AB recognizes a ~3.5 kD band from rat brain, corresponding to the Orx-A peptide[2]
Orx-A	Gt	Santa Cruz[3]	sc-8070	Peptide mapping at the C-terminus of human Orx-A (AA 48-66 of the Orx precursor, identical to corresponding mouse sequence)[4]	AB reacts with Orx-A of mouse, rat and human by WB, immunostaining blocked with antigen peptide (sc-8070 P) and pattern of staining identical to that with Orx-A (Rb) H-003-30 (Phoenix)[5]
VTPs					
VAChT	Gt	Chemicon[6]	AB1578	Peptide corresponding to C-terminus of cloned rat VAChT[7] (CSPPGPFDGCEDDYNYYSRS)[8]	By WB the AB recognizes a ~65-70 kD band corresponding to VAChT protein[7]
VAChT	Rb	Sigma[9]	V5387	Peptide corresponding to AA 512-530 of C-terminus of cloned rat VAChT (K-SPPGPFDGCEDDYNYYSRS)[10]	By WB the AB recognizes a ~67-70 kD band, corresponding to VAChT protein[10]
VGluT2	Rb	Gift RHE[11]	-	GST fusion protein containing AA 519-582 of rat DNPi (VGluT2)[12]	By WB the AB recognizes a ~50-62 kD band from rat brain[12]
VGAT	Rb	Chemicon	AB5062P	Peptide corresponding to 17 AA near C-terminus region of rat VGAT (VHSLEGLIEAYRTNAED)[13]	By WB the AB recognizes a band at ~55-60 kD[13]
PSPs					
PSD-95	Ms	ABR[14]	MA1-045	Purified recombinant of rat PSD-95[15]	By WB the AB recognizes a ~95 kDa protein and a slightly larger species from rat brain extracts[15]
Geph	Ms	Sy-Sy[16]	147 011	Purified rat gephyrin [17]	By WB the AB recognizes a ~93 kD band. It detects a N-terminus epitope[18]

[1] Phoenix: Phoenix Pharmaceuticals Inc., Belmont, CA.
[2] http://www.phoenixpeptide.com/Catalog%20Files/Orexins%20Section/OrexinsHypocretinspage.htm
[3] Santa Cruz: Santa Cruz Biotechnology Inc., Santa Cruz, CA.
[4] Information provided by Santa Cruz data sheet and technical service.
[5] Information on WB provided by Santa Cruz data sheet and technical service, blocking experiments carried out in our lab with the Santa Cruz antigen peptide and immunostaining of Orx cell population compared for two antibodies in our lab in this and previous studies (Modirrousta et al., 2005).
[6] Chemicon: Chemicon International, Temecula, CA.
[7] http://www.chemicon.com/Product/ProductDataSheet.asp?ProductItem=AB1578
[8] Supplied by Chemicon on request.
[9] Sigma: Sigma, St. Louis, MO.
[10] http://www.sigmaaldrich.com/sigma/datasheet/v5387dat.pdf
[11] Gift from Edwards, R.H. and Fremeau, R.T.Jr.
[12] Fremeau et al., 2001.
[13] http://www.chemicon.com/Product/ProductDataSheet.asp?ProductItem=AB5062P
[14] ABR: Affinity BioReagents, Golden, CO.
[15] http://www.bioreagents.com/index.cfm/fuseaction/products.print/Product/MA1-045
[16] SY-SY: Synaptic Systems, Göttingen, Germany.
[17] http://www.sysy.com/gephyrin/gephy_fs.html
[18] Pfeiffer et al., 1984.
Abbreviations: AA, amino acid; AB, antibody; DNPi, differentiation-associated Na^+-dependent phosphate transporter; Geph, gephyrin; Gt, goat; Ms, mouse (monoclonal); Rb, rabbit; sp, species; WB, western blot.

Table 2. Combination and sequential processing of primary and secondary antibodies along with streptavidin (SA) used for triple fluorescent staining of orexin (Orx), vesicular transporter proteins (VTPs) or postsynaptic proteins (PSPs) and biotinylated dextran amine (BDA)

	1[ry] AB (overnight)[1]			2[ry] AB (3 hours)		SA (3 hours)		
Series	Antigen	Host sp	Dilution	IgG (Dky)[2,3]	Dilution	SA	Dilution	n[4]
BDA/VTP/Orx								
BDA/VAChT/Orx	VAChT	Gt	1:1000	Anti-Gt-Cy3	1:800	SA-Cy2	1:800	4
	Orx-A	Rb	1:200	Anti-Rb-AMCA	1:100			
BDA/VAChT/Orx	VAChT	Gt	1:1000	Anti-Gt-Cy3	1:800	"	"	2
	Orx-A	Rb	1:200	Anti-Rb-Cy5	1:800			
BDA/VAChT/Orx	VAChT	Rb	1:5000	Anti-Rb-Cy3	1:800	"	"	5
	Orx-A	Gt	1:200	Anti-Gt-Cy5	1:800			
BDA/VGluT2/Orx	VGluT2	Rb	1:5000	Anti-Rb-Cy3	1:800	"	"	4
	Orx-A	Gt	1:200	Anti-Gt-AMCA	1:100			
BDA/VGluT2/Orx	VGluT2	Rb	1:5000	Anti-Rb-Cy3	1:800	"	"	11
	Orx-A	Gt	1:200	Anti-Gt-Cy5	1:800			
BDA/VGAT/Orx	VGAT	Rb	1:250	Anti-Rb-Cy3	1:800	"	"	4
	Orx-A	Gt	1:200	Anti-Gt-AMCA	1:100			
BDA/VGAT/Orx	VGAT	Rb	1:250	Anti-Rb-Cy3	1:800	"	"	11
	Orx-A	Gt	1:200	Anti-Gt-Cy5	1:800			
BDA/PSP/Orx								
BDA/PSD-95/Orx	PSD-95	Ms	1:100	Anti-Ms-Cy5	1:800	SA-Cy2	1:800	3
	Orx-A	Gt	1:200	Anti-Gt-Cy3	1:800			
BDA/Geph/Orx	Geph	Ms	1:100	Anti-Ms-Cy5	1:800	"	"	3
	Orx-A	Gt	1:200	Anti-Gt-Cy3	1:800			

[1] For sources and specificity of primary antibodies from different species refer to Table 1.
[2] Jackson Immuno Research Laboratories, West Grove, PA.
[3] For multiple labeling (ML) with minimal cross-reactivity (min X) to other species.
[4] n: number of cases (each case referring to an injection site and series from the same side of the brain, thus 1 or 2 per brain from 9 rats for a total of 16 injection sites selected for their placement in the MCPO/SI).
Abbreviations: AB, antibody; AMCA, aminomethylcoumarin acetate; Cy2, cyanine; Cy3, indocarbocyanine; Cy5, indodicarbocyanine; Dky, donkey; Geph, gephyrin; Gt, goat; Ms, mouse (monoclonal); Rb, rabbit; sp, species.

Table 3. Numbers and proportions of Orx cells and Orx+ cells contacted by BDA+ varicosities estimated across hypothalamic regions[1]

Hypothalamic region	LH	PF	DMH	Total
Single-immunostained Orx series[2]				
N° Orx cells	1770.7 ± 182.3	469.3 ± 21.3	917.3 ± 149.3	3157.3 ± 259.5
% Orx cells of Total across regions	**56.0 ± 3.0 %**	**15.2 ± 2.0 %**	**28.8 ± 2.9 %**	**100 ± 0.0 %**
Dual-immunostained BDA/Orx series[3]				
N° Orx+ cells	1216.0 ± 97.8	320.0 ± 37.0	576.0 ± 97.8	2122.0 ± 97.8
N° Orx+ cells contacted by a BDA+ var. (Orx+:BDA+)	512.0 ± 110.9	42.7 ± 42.7	42.7 ± 21.3	597.3 ± 166.6
% Orx+ cells contacted by a BDA+ var. in each region	**41.4 ± 7.1 %**	**11.1 ± 11.1 %**	**8.9 ± 4.8 %**	**27.7 ± 6.6 %**

[1]Estimated numbers of cells and BDA-contacted cells were obtained by random systematic sampling of the hypothalamus at levels A6.6, A6.2 and A5.8 for LH, and levels A6.2 and A5.8 for PF and DMH using StereoInvestigator.
[2]Series from 3 different brains processed for single-immunostaining of Orx cells with DAB (see Methods).
[3]Series from 3 individual cases (injection sites) processed for dual-immunostaining of BDA (with DAB-Ni) and Orx (with ANPB, see Methods).
Data are presented as means ± SEM. Abbreviations: DMH, dorsomedial hypothalamic nucleus; LH, lateral hypothalamus; PF, perifornical area; var., varicosity.

Table 4. Numbers and proportions of Orx+ cells contacted by BDA+ varicosities positive for vesicular transporter proteins (VTP+), and numbers and proportions of BDA+[VTP+] varicosities in contact with Orx+ cells in the lateral hypothalamus (LH) [1]

Triple-immunostained BDA/VTP/Orx series	VAChT	VGluT2	VGAT
N° Orx+ cells contacted by BDA+ var. (Orx+:BDA+) in each series	548.3 ± 68.3	532.7 ± 109.7	595.3 ± 109.7
N° Orx+ cells contacted by BDA+[VTP+] var. (Orx+:BDA+[VTP+])[2]	15.7 ± 15.7	188.0 ± 81.4	376.0 ± 27.1
% Orx+ cells contacted by BDA+[VTP+] var.[2]	**3.7 ± 3.7 %**	**31.4 ± 9.4 %**	**66.7 ± 11.2 %**
N° BDA+ var. in contact with Orx+ cells (BDA+:Orx+) in each series	908.6 ± 122.4	1096.7 ± 180.7	1457.0 ± 204.9
N° BDA+[VTP+] var. in contact with an Orx+ cell (BDA+[VTP+]:Orx+)[2]	15.7 ± 15.7	203.7 ± 95.3	814.7 ± 87.2
% BDA+[VTP+] var. in contact with Orx+ cells[2]	**2.2 ± 2.2 %**	**16.6 ± 6.2 %**	**57.8 ± 8.7 %**

[1]Estimated numbers of cells were obtained by random systematic sampling of the LH area at levels A6.6, A6.2 and A5.8 using StereoInvestigator from three individual cases (injection sites).
[2]According to a non-parametric Kruskal-Wallis test, the different VTP+ varicosities differed significantly according to the numbers ($H = 6.587$, $p = 0.037$) and proportions ($H = 7.261$, $p = 0.027$) of Orx+ neurons contacted by BDA+[VTP+] and to the numbers ($H = 6.587$, $p = 0.037$) and proportions ($H = 6.938$, $p = 0.031$) of BDA+[VTP+] varicosities contacting Orx+ neurons.
Data are presented as means ± SEM. Abbreviations: var., varicosity.

Fig. 1. BDA injection site in BF and anterogradely labeled BF terminals in the LH. **A**: Atlas section through the cholinergic cell area (MCPO-SI) where iontophoretic applications of BDA were placed. **B**: Composite image of typical BDA injection site (processed using ABC with DAB-Ni and counterstained for Nissl with neutral red). Note the small size and restricted location of BDA injection site in the MCPO. **C**: High magnification images showing BDA+ axonal varicosities (arrowheads) contacting Nissl-stained cell bodies located in dorsal (C'), middle (C'') and ventral (C''') portions of the LH area. Scale bars = 1 mm in B; 10 μm in C'', also for C' and C'''.

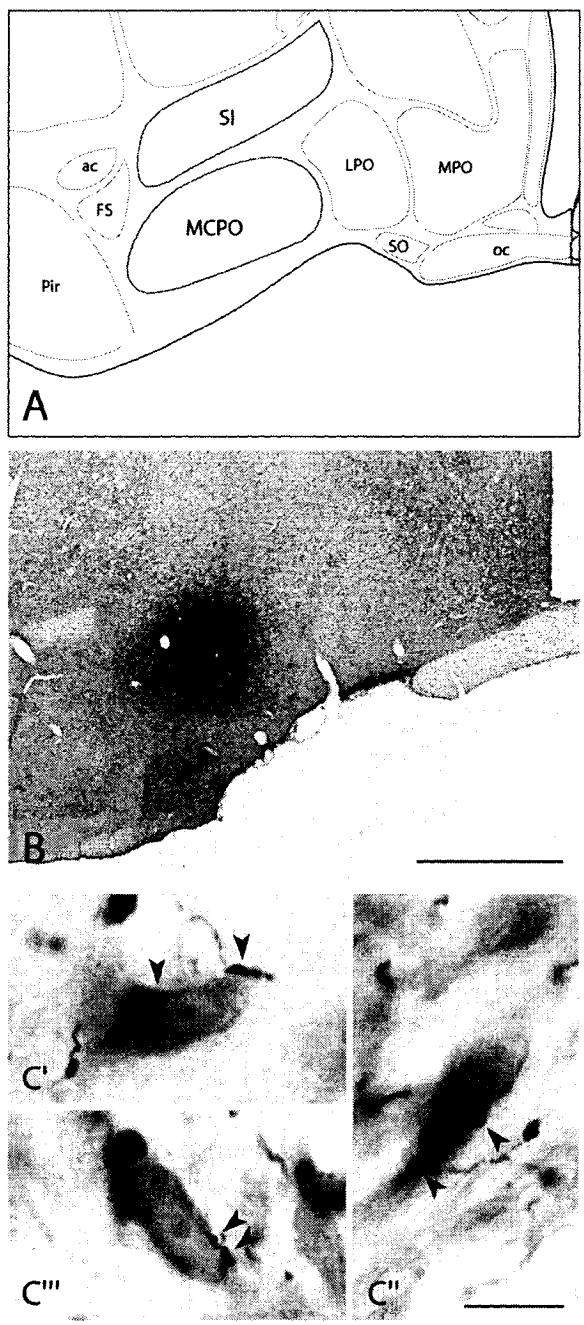

Fig. 1. BDA injection site in BF and anterogradely labeled BF terminals in the LH

Fig. 2. Distribution of Orx+ neurons at three levels through the tuberal hypothalamus. **A, B and C**: Mapping of Orx+ neurons within contours of the LH, PF and DMH at A6.6 (A), A6.2 (B) and A5.8 (C) levels, based on the material presented in *D*, *E* and *F*, respectively. Some few scattered Orx+ neurons within contours of the AHA, Pe and ZI are not shown in the mapping. **D, E and F:** Composite images of sections immunostained for Orx-A (with DAB) showing the distribution of Orx+ neurons in the hypothalamus at A6.6 (D), A6.2 (E) and A5.8 (F). Scale bar = 1 mm in F for D-F.

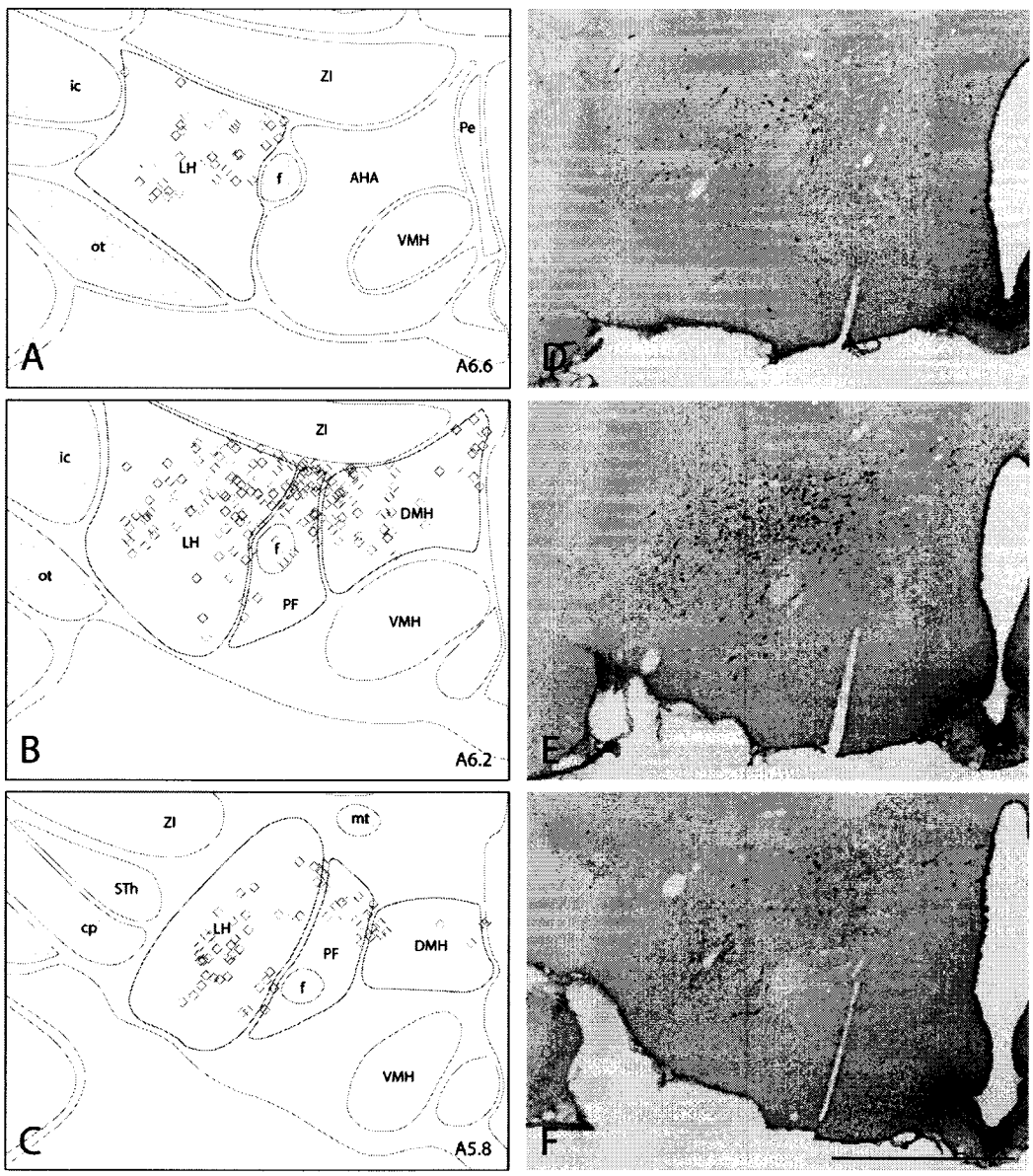

Fig. 2. Distribution of Orx+ neurons at three levels through the tuberal hypothalamus

Fig. 3. Distribution of BDA-labeled fibers in relation to Orx+ neurons. **A**: Low magnification composite image of BDA+ axons (in black, DAB-Ni) and Orx+ cells (in fuchsia, ANPB) in the LH at ~A6.0. **B**: High magnification images showing BDA+ varicosities (arrowheads) in contact with Orx+ neurons in the LH (B', B'' and B'''). **C**: Tracing and mapping of all BDA+ fibers and Orx+ neurons in the tuberal hypothalamus at ~A6.0 μm (from IA0). From coarse fibers within the ventrolateral MFB, fine varicose collaterals extended dorsally and medially to reach Orx+ cells through the LH. Some fibers also extended medially into the PF and DMH. **D**: High magnification of elements depicted in C, showing contacts of BDA+ axons by varicosities on proximal dendrites or soma of Orx+ cells located in the dorsal (D') or central (D'' and D''') region of the LH. Tonal range for each RGB channel as well as brightness and contrast adjustment were made for pictures in A and B. Scale bars = 100 μm in A; 10 μm in B and D.

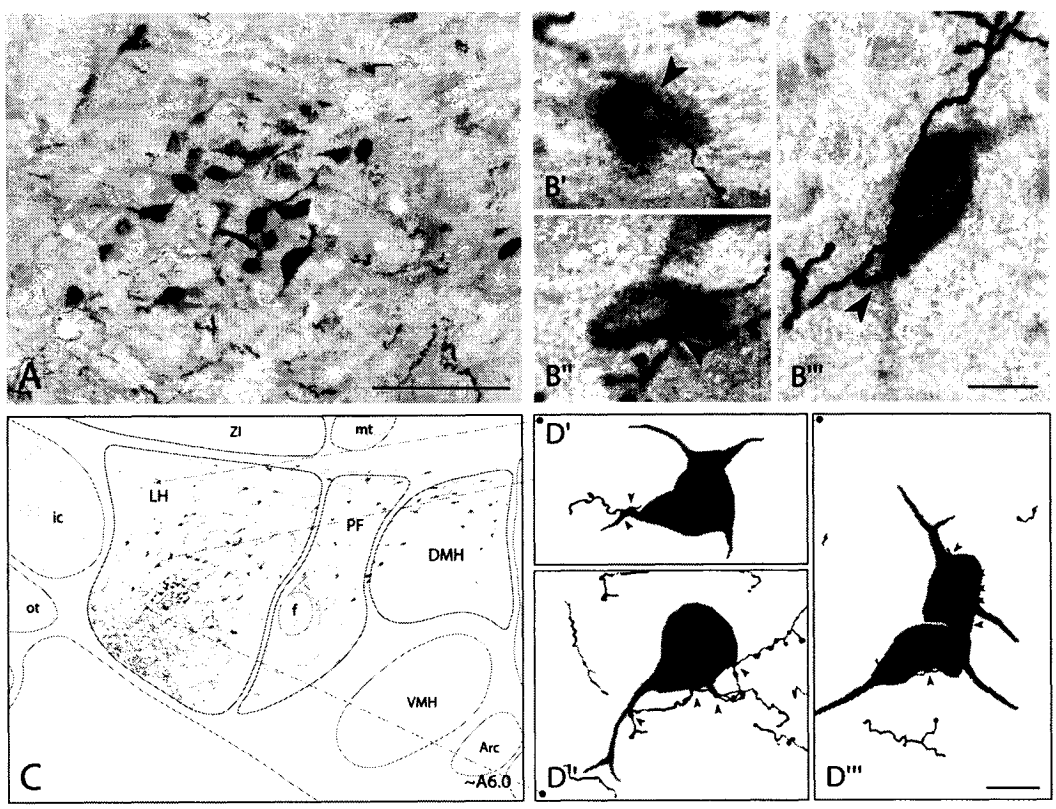

Fig. 3. Distribution of BDA-labeled fibers in relation to Orx+ neurons

Fig. 4. VAChT+, VGluT2+ or VGAT+, BDA-labeled varicosities in relation to Orx+ neurons viewed by epifluorescent microscopy. In each case, BDA is green (Cy2), the VTP red (Cy3) and Orx blue (AMCA in A or Cy5 in B and C). **A**: BDA+[VAChT+] terminals in the vicinity of an Orx+ neuron. BDA+ terminals (solid arrowheads in A') located in the vicinity yet not close to an Orx+ neuron (left) are positive for the VAChT protein (solid arrowheads in A''), as evident in the merged image (in yellow, solid arrowheads in A'''). A VAChT+ terminal that is not BDA+ (open arrowhead) is closer to the Orx+ cell body. Note also the sparse number of VAChT+ varicosities in the vicinity of Orx+ neurons. **B**: BDA+[VGluT2+] terminals in close proximity to Orx+ neurons. Two small BDA+ terminals (solid arrowheads in B') over an Orx+ cell body are positive for the VGluT2 protein (solid arrowheads in B''), as evident in the merged image (in yellow, solid arrowheads in B'''). Note also the relatively large number of VGluT2+ varicosities in close proximity to the Orx+ neurons. **C**: BDA+[VGAT+] terminals over Orx+ neurons. Two BDA+ terminals (solid arrowheads in C') in close proximity to an Orx+ neuron are positive for VGAT (solid arrowheads in C''), as evident in the merged image (in yellow, solid arrowheads in C'''). In all images, tonal range was adjusted for each RGB channel individually. Scale bar in C''' = 10 μm for A - C.

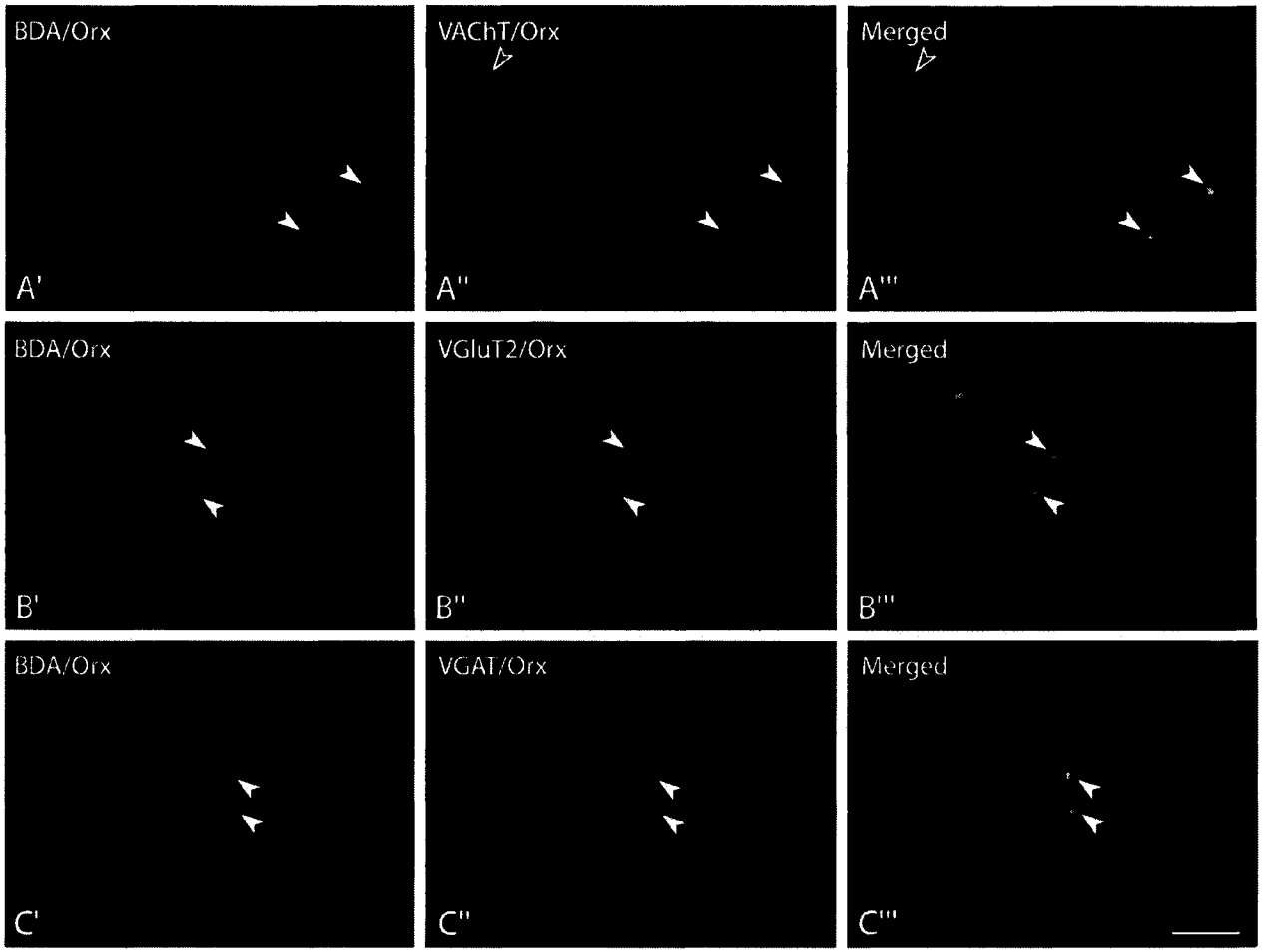

Fig. 4. VAChT+, VGluT2+ or VGAT+, BDA-labeled varicosities in relation to Orx+ neurons viewed by epifluorescent microscopy

Fig. 5. Presence of presynaptic VGluT2 or VGAT and postsynaptic PSD-95 or Gephyrin (Geph) proteins in contacts between BDA-labeled varicosities and Orx+ neurons. **A**: Rendered 3D confocal image (16 serial 0.50 μm thick optical sections) of a BDA-labeled axon (in green, Cy2), whose varicosities (in yellow) are positive for VGluT2 (in red, Cy3). One of these varicosities is in apposition (arrowhead) to an Orx+ neuron (in pseudo-color blue, Cy5), as evident in the rendered zoom images on the right (6 serial 0.5 μm thick optical sections) depicting in detail the relation between the BDA+ varicosity (top) or the contained VGluT2 (middle) with the Orx+ neuron surface and showing the three elements together in the merged image (bottom). Note also on the left, other VGluT2+ varicosities in contact with the Orx+ neuron. **B**: Rendered 3D confocal image (9 serial 0.33 μm thick optical sections) of a BDA+ varicosity (arrowhead, in green, Cy2) facing a PSD-95+ profile (opposite pointer, in pseudo-color red, Cy5) located between the varicosity and the surface of the Orx+ neuron (in pseudo-color blue, Cy3). As evident in the zoom rendered images on the right (13 serial 0.33 μm thick optical sections), the BDA+ varicosity is apposed to the Orx+ process (top image), opposite the PSD-95+ punctum which is on the surface of the Orx+ process (pointer, middle image) and between the BDA+ varicosity and the Orx+ process (pointer in the merged image, bottom). Note the presence of other PSD-95+ puncta over the Orx+ neuron (upper pointer) at the left panel. **C**: Rendered 3D confocal image (28 serial 0.5 μm thick optical sections) of a BDA-labeled axon (in green, Cy2), from which most varicosities (in yellow) are positive for VGAT (in red, Cy3) and come into contact (large arrowhead) with the

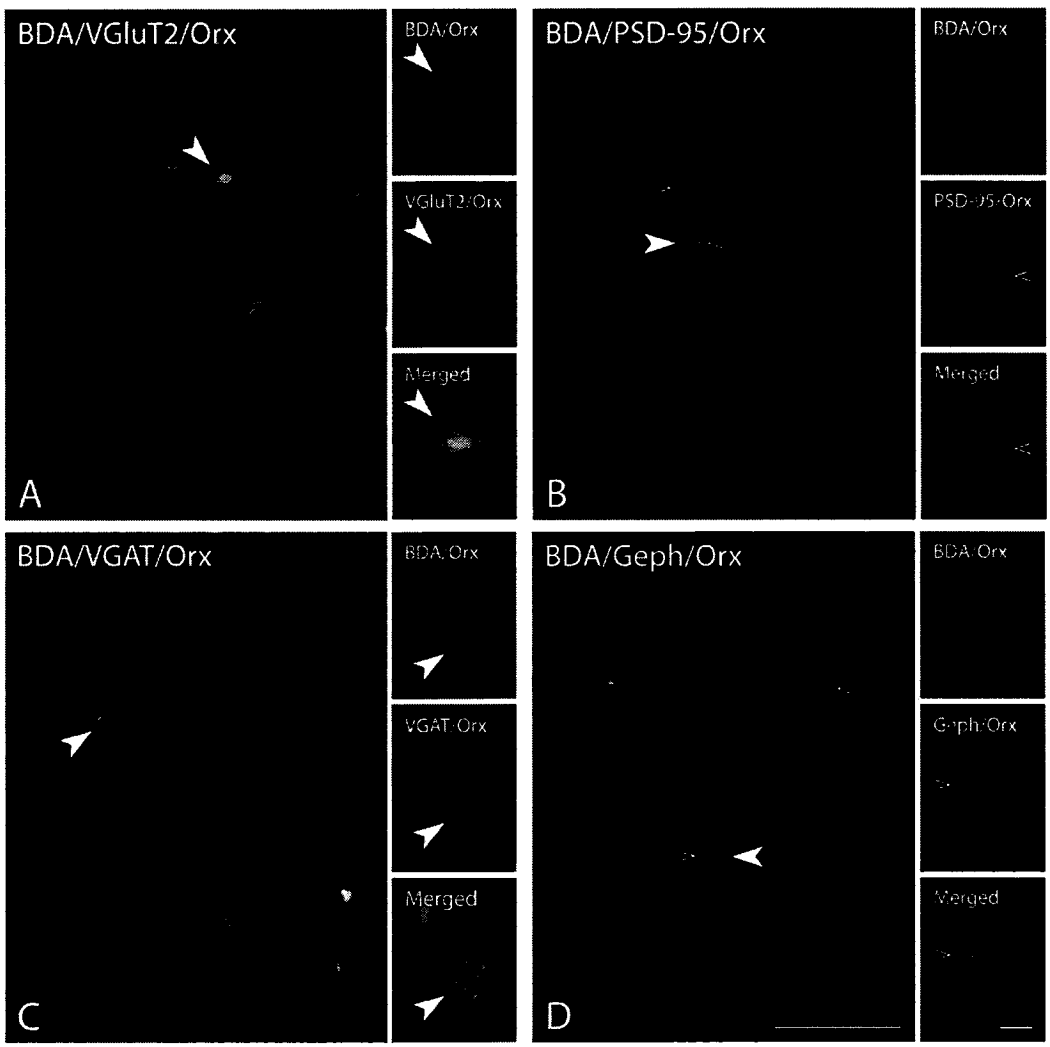

Fig. 5. Presence of presynaptic VGluT2 or VGAT and postsynaptic PSD-95 or Gephyrin (Geph) proteins in contacts between BDA-labeled varicosities and Orx+ neurons

dendrites and soma of the Orx+ neuron. As seen in the rendered zoom images on the right (8 serial 0.5 μm thick optical sections), the BDA+ varicosity (top image) containing VGAT (middle image) appears to be in contact with the surface of the Orx+ neuron (merged image, bottom). Note in the left image other VGAT+ varicosities also appear to appose the Orx+ neuron. **D**: Rendered 3D confocal image (14 serial 0.33 μm thick optical sections) of BDA-labeled axonal varicosities (arrowhead, green, Cy2) facing Geph+ puncta (facing pointer, pseudo-color red, Cy5) over an Orx+ neuron (pseudo-color blue, Cy3). As evident in the zoom rendered images at the right (12 serial 0.33 μm thick optical sections), the apposition of the BDA+ varicosity with the Orx+ neuron (top image) is associated with a Geph+ punctum on the surface of the Orx+ neuron (pointer, middle image) and between the BDA+ varicosity and the Orx+ neuron (merged image, pointer, bottom). Note the presence of other Geph+ puncta over the Orx+ neuron (upper pointers) in the left panel. Deconvolution iterative restoration (see Methods) was applied to the Cy5 channel (in B and C left panels and in A, B, C and D right panels), the Cy3 channel (in C left panel and in C and D right panels) and the Cy2 channel (in B, C and D). Tonal range adjustments for each individual RGB channel were made for all pictures. Scale bars = 10 μm in left large panel in D, also for large left panels in A, B and C; 1 μm in D zoom bottom image, also for zoom images in A, B and C.

Fig. 6. Three-dimensional localization of postsynaptic proteins PSD-95 or Gephyrin (Geph) between BDA+ terminals and Orx+ neurons. A-C: Orthogonal views (see below) of a high resolution rendered confocal 3D image (40 serial ~0.06 μm thick optical sections) in semi-transparent fluorescence rendering (columns 1-4) or opaque isosurface (column 5) views of a single contact between a BDA+ varicosity (in green, Cy2) and an Orx+ proximal dendrite (in blue, Cy3), with presence of PSD-95+ puncta (in red, Cy5) between the varicosity and dendrite. The BDA+ varicosity is in contact with the Orx+ process (A1-C1), and in clear apposition to a PSD-95+ profile (solid arrowheads in A2-C2,), which is in turn located on the surface of the Orx+ neuron (solid arrowheads in A3 and B3). The localization of the PSD-95+ profile between the two structures is evident in the triple merged fluorescent image (solid arrowheads in A4 and B4) as well as in the triple merged isosurface rendering image, where the punctum appears almost completely occluded (dotted arrowheads in A5-C5). The PSD-95+ punctum is completely occluded in certain of the orthogonal views (dotted arrowheads in C3, C4 and C5). (A6-C6): Representation of the three orthogonal views with orientation markers showing the X, Y, Z axes. D-F: Orthogonal views of a high resolution rendered confocal 3D image (38 serial ~0.08 μm thick optical sections) in semi-transparent fluorescence rendering (columns 1-4) or opaque isosurface rendering (column 5) views of a single contact between a BDA+ varicosity (in green, Cy2) and an Orx+ soma (in blue, Cy3), with the presence of Geph+ puncta (in red, Cy5) between the terminal and soma. The BDA+ varicosity is in contact with an Orx+ soma (D1-F1) and in clear apposition to a Geph+ profile (solid

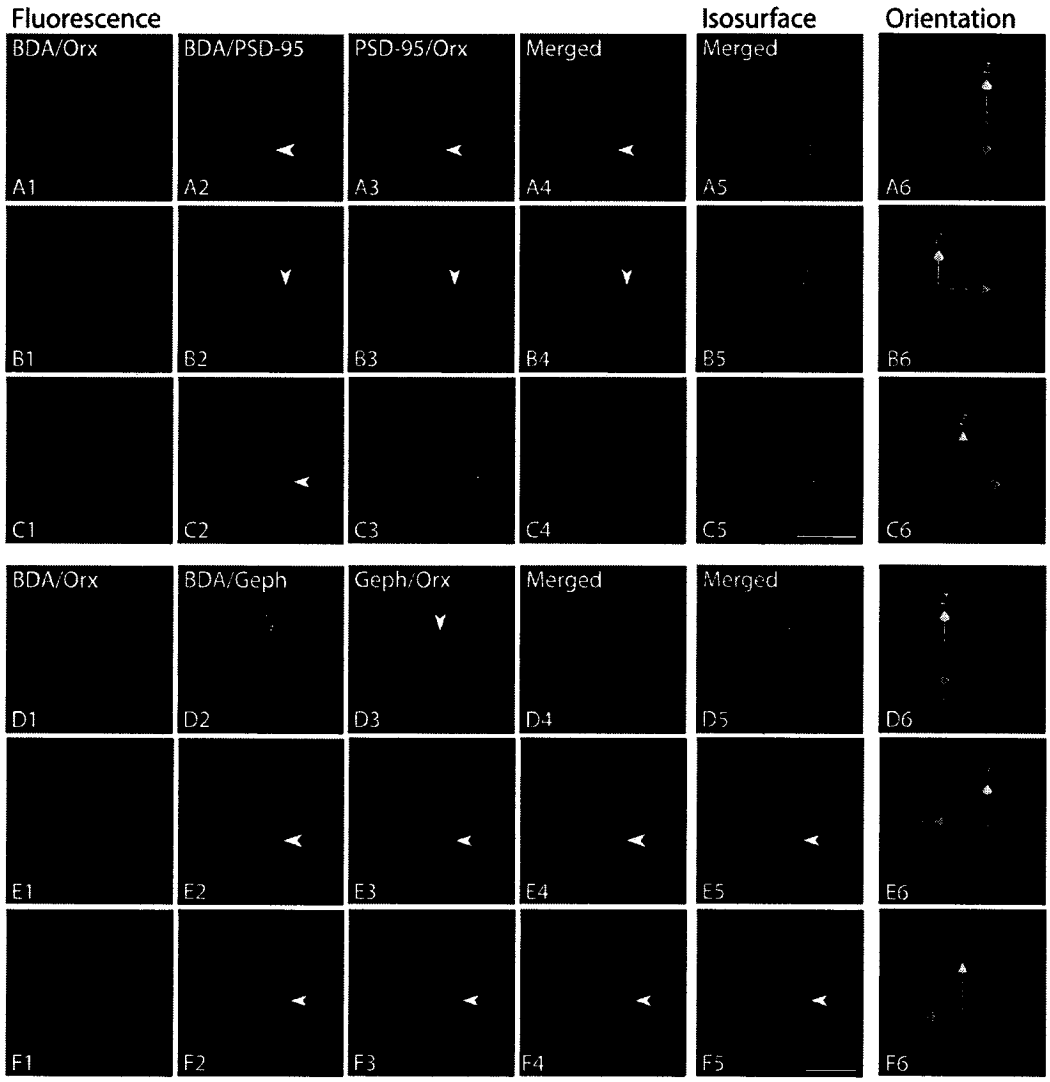

Fig. 6. Three-dimensional localization of postsynaptic proteins PSD-95 or Gephyrin (Geph) between BDA+ terminals and Orx+ neurons

arrowheads in E2-F2,), which is in turn located on the surface of the Orx+ neuron (solid arrowheads in D3-F3). The localization of the Geph+ profile between the two structures is evident in the triple merged fluorescent image (solid arrowheads in E4-F4) as well as in the triple merged isosurface image (solid arrowheads in E5 and F5). Note the relative occlusion of the Geph+ profile in the rendered isosurface images, evidencing its location between the two structures. Due to the orthogonal views, the Geph+ puncta are completely occluded in some of them (dotted arrowheads in D2, D4 and D5). (D6-F6): Representation of the three orthogonal views with orientation markers showing the X, Y, Z axes. Deconvolution iterative restoration (see Methods) was applied to Cy5, Cy3 and Cy2 channels. Scale bars: 1 μm in C5 for A, B and C, and in F5 for D, E and F.

GENERAL DISCUSSION

The present thesis work provides evidence for the existence of neurons in the BF that have the capacity to synthesize and release glutamate. By the presence of VGluT3 in the cell bodies of ChAT+, GAD+ or PAG+ neurons, it appears that a pool of synthesized glutamate may be released from the soma or dendrites of BF neurons to regulate, as proposed, synaptic inputs and neuronal excitability. By the presence of VGluT2, another pool of synthesized glutamate may be used by neurons to release glutamate from axon terminals. By projections to cerebral cortex, these as well as other prominent cholinergic and GABAergic contingents may influence cortical neurons to modulate cortical activity in association with different states. By descending projections to the LH, predominant glutamatergic and GABAergic neurons innervate LH and Orx neurons to provide reciprocal influences to promote either behavioral arousal or behavioral quiescence and sleep.

Cholinergic, GABAergic and glutamatergic phenotypes of basal forebrain neurons

Along with previous results (Manns et al., 2001), the results of this thesis allow the parceling of the BF into groups of neurons according to synthetic enzymes and VTPs. A hypothetical, although reasonable sketch of this parcelation is depicted in Figure 4. The main group of neurons is constituted by those able to synthesize glutamate (PAG+) (Chapter I). This group also includes neurons that synthesize ACh (ChAT+/PAG+), as well as an important proportion of those that synthesize GABA (GAD+/PAG+) (Manns et al., 2001). As evident from the absence of

PAG in some GAD neurons, a proportion of GABA-synthesizing neurons would fall out of this category (GAD+/PAG-). A majority of the neurons that contain PAG also contains VGluT3 (VGluT3+) (Chapter I). This group would include neurons that synthesize ACh (ChAT+/PAG+/VGluT3+), as well as those that synthesize GABA and contain PAG (GAD+/PAG+/VGluT3+), but not those that do not contain PAG (GAD+/PAG-/VGluT3-) (Chapter I). Based on the absence of co-localization of VTPs (Chapters II and III), it is assumed that only VAChT would be contained in axon terminals of neurons that synthesize ACh (ChAT+/PAG+/VGluT3+). Similarly, only VGAT would be contained in axons of neurons that synthesize GABA, irrespective of whether they express or not PAG or VGluT3 (GAD+/PAG+/VGluT3+ or GAD+/PAG-/VGluT3-). Finally, it is assumed that VGluT2 would only be contained in the axon terminals of neurons that contain PAG and only in those that do not synthesize ACh or GABA (PAG+/ChAT-/GAD-). Whether this group may or may not have VGluT3 in their cell bodies is uncertain. Finally, a group of neurons of unknown axon terminal phenotype, and therefore unidentifiable somatic phenotype, is assumed to exist based on the proportion of axon terminals not accountable for VAChT+, VGAT+ or VGluT2+ BF terminals (Chapters II and III).

This division reveals the dual role that glutamate may have in the organization of BF circuits. As shown in the cortex, the dendritic release of glutamate via VGluT3 by pyramidal cells is involved in the depression of inhibitory input from interneourns via activation of glutamate metabotropic receptors located presynaptically (Zilberter, 2000; Harkany et al., 2004). As proposed, this depression could maintain pyramidal cell excitability and temporal

pattern of discharge. It is likely that the release of glutamate from the somato-dendritic domain of BF neurons may serve a similar role (Harkany et al., 2003), as BF neurons, like pyramidal neurons, are strongly innervated by GABAergic terminals and thus provide a prominent inhibitory influence (Ingham et al., 1988; Khateb et al., 1992; Gritti et al., 1993), which as explained may be attenuated by somato-dendritic release of glutamate. This regulation may help BF neurons to maintain their intrinsic discharge pattern (Khateb et al., 1992; Fort et al., 1998), which as discussed previously may play a critical role in the modulation of cortical activity (Manns et al., 2000a, b, 2003a; Lee et al., 2005b). On the other hand, the VGluT2-mediated release of glutamate from the axon terminal domain of BF glutamatergic neurons, may act to modulate the activity of post-synaptic cells in a more classical manner, by direct depolarization through postysynaptically located AMPA and NMDA receptors (Fremeau et al., 2004).

The basal forebrain as a region involved in the coordination of cortical activity and behavioral states

The BF projection to cortex is comprised by three neurochemically differentiated neuronal contingents that, as discussed extensively, may have different influences over cortical activity. Similarly, the descending projections to LH may be involved in reciprocal promotion and attenuation of behavioral arousal. Given the concurrent changes in cortical activity that occur in association with different behavioral states, it is possible to conceive the BF as a region involved in the coordination of both processes.

As discussed previously, cholinergic neurons innervating PFC appear to have a critical role in attention (Sarter et al., 2003), which in turn may be associated with a relative attenuation of behavioral arousal as shown by the increase in parasympathetic activity during attention to conditioned stimuli (Hunt and Campbell, 1997). Interestingly, selective activation of BF cholinergic neurons by injections of neurotensin in the BF provoke bursting of cholinergic neurons, prominent cortical theta and gamma activity and yet no increase in motor activity but instead the appearance of a quiescent waking state, shortly followed by PS (Cape et al., 2000). As cholinergic neurons with projections to frontal cortex have been found to provide extensive local collateralization and innervation to PV+, likely GABAergic BF neurons (Zaborszky and Duque, 2000), it is plausible to hypothesize that activation of cholinergic neurons, while promoting cortical theta activity in association with attention, may lead to excitation of BF GABAergic neurons involved in the attenuation of behavioral arousal, such as those seen here to provide innervation to the LH.

Sleep active neurons in the BF may participate in the cortical correlates of sleep, such as SWA during SWS (Sterman and Clemente, 1962a; Manns et al., 2000b). Concurrently, sleep active neurons may inhibit arousal regions such as the LH (Sterman and Clemente, 1962b; Manns et al., 2003; Modirrousta et al., 2004). Given that cortically projecting neurons form a different group than those projecting caudally (Semba et al., 1989), it is unlikely that the simultaneous promotion of SWA and behavioral quiescence originate from the same population of neurons. Thus, their simultaneous activation may be mediated through other mechanisms. As also discussed previously, SWA-active GABAergic neurons,

which discharge phasically and project to PFC may promote the appearance of cortical SWA (Manns et al., 2000b) through direct innervation of pyramidal cells (Chapter II). Interestingly, it has been shown that the output of PFC to BF, carried out by layer V pyramidal cells, is also directed to PV+ neurons (Zaborszky et al., 1997), which as pointed out in the previous paragraph likely correspond to GABAergic neurons. Again, it is possible to hypothesize that these BF GABAergic neurons with descending projections to LH and Orx neurons and involved in the attenuation of behavioral arousal, may act under these circumstances in synergism with cortically projecting GABAergic neurons to promote and maintain sleep.

Finally, neurons in the BF have been recorded that discharge maximally during W and decrease their activity as sleep appears and progresses (Lee et al., 2004). Given the positive correlation of their discharge rate with the amplitude of muscle tone, these neurons are hypothesized to be involved in promotion of behavioral arousal along with facilitation of motor activity (Jones, 2005a) and, as proposed in Chapter IV, to correspond to those neurons that provide an excitatory input to Orx neurons. It is conceivable that neurons with similar characteristics may provide innervation to PFC, as proposed in Chapter II. Indeed, it has been shown that glutamate in PFC promotes increases in sympathetic activity (Resstel and Correa, 2005, 2006), supporting a role in behavioral arousal. Consonantly, acute stress elicited either by a restraint procedure or forced swimming are associated with increases in the release of glutamate in PFC, again suggesting a role in mediating arousal (Moghaddam, 1993). Mechanisms through which both populations may be co-activated during behavioral arousal may involve reciprocal

innervation through local axon collaterals, or alternatively, glutamatergic interneurons suggested to populate the BF (Hur et al., 2002).

The major output of the basal forebrain is GABAergic

The majority of BF terminals in the cortex and hypothalamus presented a GABAergic phenotype, outnumbering cholinergic terminals by a factor of two and five, respectively (Chapters II and III). Overall, these results agree with previous reports indicating that in both cortical as well as subcortical projections, BF GABAergic neurons represent a larger contingent than those with a cholinergic phenotype (Gritti et al., 1994; Gritti et al., 1997). They also agree with the quantitative estimations provided in Chapter I, where the GABAergic population outnumbers by several folds that comprised by cholinergic neurons.

In relation to the functional role of GABAergic terminals in the cortex, these results also suggest a prominent role of this projection in neuropathologies associated with dysfunction of the basalo-cortical system, such as Alzheimer's disease (Rossor et al., 1982). Indeed, this disease is associated with the degeneration of both cholinergic and non-cholinergic cells in the BF (Rasool et al., 1986) as well as decreases in the activity of both cholinergic and GABAergic markers in the cortex (Rossor et al., 1982). The involvement of the GABAergic system may be particularly relevant in the decrease of cortical high frequency activity observed in Alzheimer's patients (Jeong, 2004), which may be due to the dysfunction of tonically discharging GABAergic neurons that discharge at high frequencies and may promote gamma activity in the cortex (Manns et al., 2000b, 2003a).

Regarding the descending projections to the LH, the predominant influence of the BF could be considered inhibitory. Thus, it is likely that the activation of caudally projecting neurons may be responsible for the generation of behavioral quiescence, decreases in sympathetic activity and promotion of sleep seen after BF stimulation (Hess, 1957; Sterman and Clemente, 1962b). Conversely, the chemical inactivation of neurons involved in these projections may be responsible for increases in W and insomnia (Satoh et al., 2003). It is thus plausible to conceive and hypothesize that treatments involving specific stimulation of caudally projecting BF neurons (by as yet unknown mechanism) may be beneficial in ameliorating excessive arousal and hyperactivity that are observed in cases of severe insomnia (Lugaresi et al., 1998). Equally, inactivation of the BF descending projecting system may be relevant in the treatment of those symptoms such as excessive somnolence or incapacity to maintain appropriate muscle activity seen in the disorder narcolepsy (Nishino et al., 1995; Nishino and Mignot, 1997).

Final conclusion (Figure 5)

In conclusion, the BF comprises populations of neurons that have the capacity to synthesize and release ACh, GABA or glutamate. The three types of neurons project and innervate the PFC and yet in different proportions, the LH. Contingent upon the their discharge profile across sleep-wake states, as well as upon the function of ACh, GABA and glutamate in these regions, it is concluded that: 1) BF cholinergic neurons may promote theta activity in PFC during certain waking states and PS. This influence would contribute synergistically to aspects

of PFC cognitive and autonomic function, such as attention and working memory, along with attenuation of motor and sympathetic output; 2) Cortically projecting GABAergic neurons may have a dual influence on PFC activity. Whereas some GABAergic neurons may facilitate cortical activation through promotion of high frequency activity during wakefulness and PS, others may promote the appearance of rhythmic SWA during SWS. Akin sleep-active neurons would provide an innervation of the LH and particularly Orx neurons to dampen behavioral arousal and promote behavioral quiescence and sleep; 3) By direct innervation of PFC, BF glutamatergic neurons may contribute to cortical activation and function, though their influence would be more related to those aspects mediating behavioral arousal. This would also be the case for the prominent innervation they provide to the LH and Orx neurons. Through this influence, glutamatergic BF neurons may support behavioral arousal of waking by promoting motor and sympathetic activation (Figure 5).

Figure 4: Proposed division of basal forebrain neuronal groups. A hypothetical partition of basal forebrain neurons according to the presence of synthetic enzymes and vesicular transporter proteins is provided. The major contingent of BF neurons is constituted by those neurons that synthesize glutamate (in green) as containing phosphate activated glutaminase (PAG). The vast majority of the neurons that synthesize ACh (in blue) as containing choline acetyltransferase (ChAT), and a large proportion of those that synthesize GABA (in red) as containing glutamic acid decarboxylase (GAD) are part of this group (ChAT+/PAG+ and GAD+/PAG+). A large proportion of neurons that contain PAG also contain VGluT3 (PAG+/VGluT3+). This population would also include most of ChAT+ (ChAT+/PAG+/VGluT3+) and a majority of GAD+ (GAD+/PAG+/VGluT3+) cells. GAD+ neurons that do not contain PAG would correspond to those that do not contain VGluT3 either (GAD+/PAG-/VGluT3-). ChAT+ neurons would only be able to release ACh, as only containing the vesicular ACh transporter (VAChT) in their axon terminals (VAChT+). GAD+ neurons, irrespective of their PAG or VGluT3 content, would contain and only contain the vesicular GABA transporter (VGAT) in their axonal terminals (VGAT) to release GABA. Accordingly, glutamate would be only released by those PAG+ neurons that do not contain ChAT nor GAD (PAG+/ChAT-/GAD-) and would express the vesicular glutamate transporter 2 (VGluT2) in their axon terminals (VGluT2+). Axon terminals that do not contain VAChT, VGAT or VGluT2 would comprise a still unidentified population of (aspartergic?) neurons (in violet). As a result, while displaying complex neurochemical phenotypes in their cell bodies, which may underlie complex mechanisms for regulation of cell

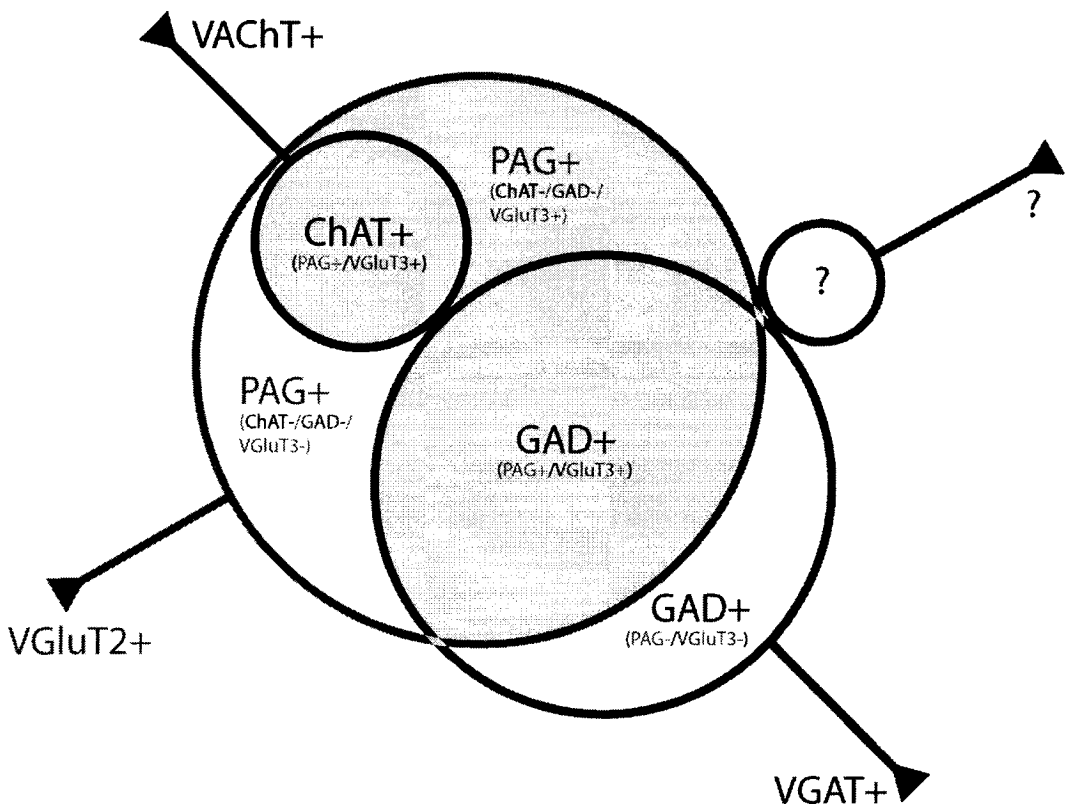

Figure 4. Proposed division of basal forebrain neuronal groups

excitability, BF neurons display simpler phenotype in their axon terminals to regulate through independent mechanisms postsynaptic neurons.

Figure 5: Ascending and descending projections of the basal forebrain. The basal forebrain innervates cortical and hypothalamic regions through axonal efferents that, as indicated by the presence of vesicular transporter proteins (VTPs) would not only contain, but have the mechanisms to release ACh, GABA or glutamate. In the prefrontal cortex (PFC), these contingents may independently promote cortical activity in association with different waking and sleep states through innervation of cortical populations. In the lateral hypothalamus (LH) and through direct innervation of LH and Orx neurons, BF glutamatergic neurons may provide excitatory influences to promote wakefulness (W) together with behavioral arousal and muscle tone. Reciprocally, BF GABAergic may promote behavioral quiescence and sleep along with disfacilitation and suppression of muscle tone. By modulation and control of cortical activity and behavioral states, the BF may be seen as a key piece in the complex neuronal machinery that coordinates concurrent changes in cortical, somatomotor and autonomic function through sleep-wake states. Other abbreviations: ac, anterior commissure; ChAT, choline acetyltransferase; CPu, caudate putamen; EMG, electromyographic activity; GAD, glutamic acid decarboxylase; Gi, gigantocellular reticular formation; GiA, gigantocellular reticular formation, alpha part; GiV, gigantocellular reticular formation, ventral part; GP, globus pallidus; Hi, hippocampus; LC, locus coeruleus; LDTg, laterodorsal tegmental nucleus; LH, lateral hypothalamus; Mes RF, mesencephalic reticular formation; opt, optic tract; PAG, phosphate activated glutaminase PnC, pontine reticular formation, caudal part; PnO, pontine reticular formation, oral part; POA, preoptic area; PPTg, pedunculopontine tegmental nucleus; PS, paradoxical sleep; Rt, reticular thalamic nucleus; SWS, slow wave

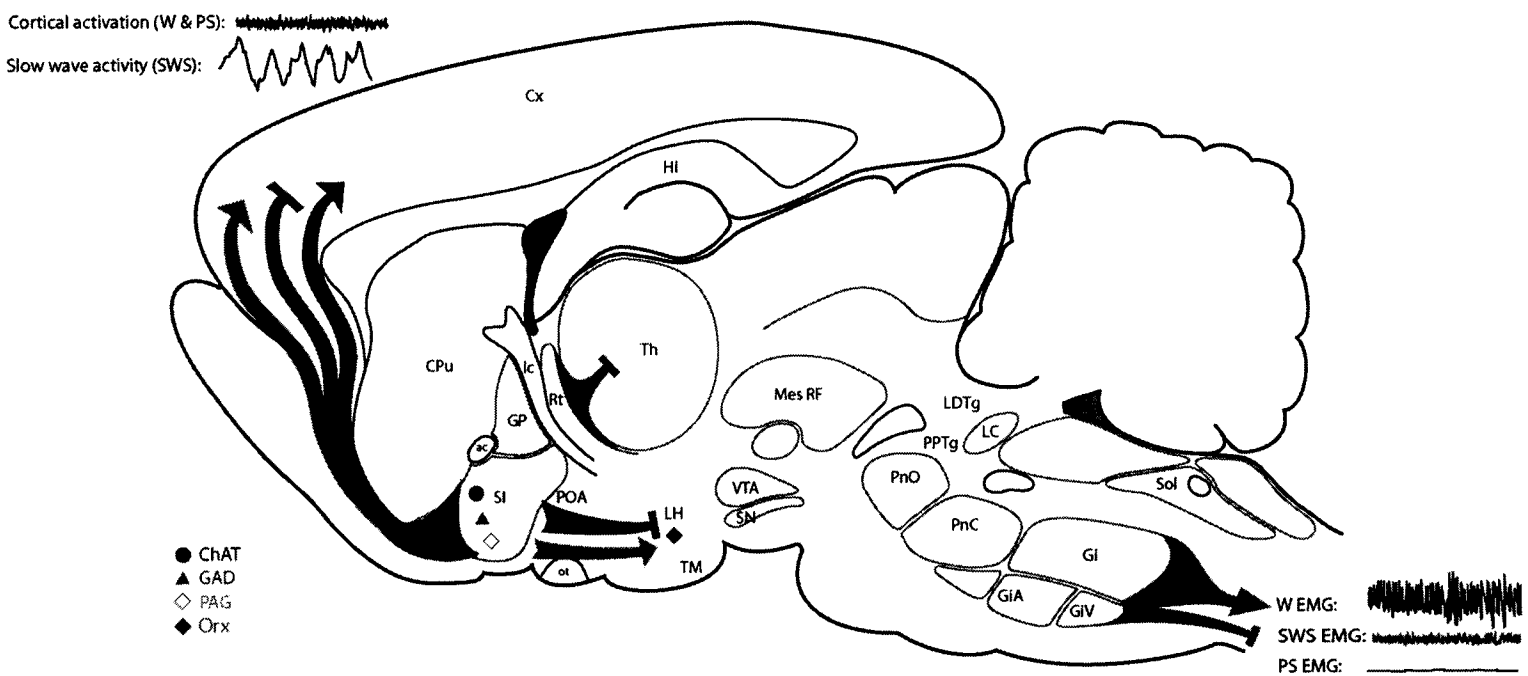

Figure 5. Ascending and descending projections of the basal forebrain

sleep; SN, substantia nigra; Sol, solitary tract nucleus; Th, thalamus; TM, tuberomammillary nucleus; VTA, ventral tegmental area; W, wakefulness. Modified with permission from Jones BE (2005a), Figure 1.

SUMMARY

Wakefulness (W), slow wave sleep (SWS) and paradoxical sleep (PS) are the three main behavioral states that occur in mammals. The generation and maintenance of these states, as well as the physiological changes that concur with them, are controlled by different regions in the central nervous system (CNS). Among those, the basal forebrain (BF) has been shown to play an important role in promoting the appearance of cortical activation, a phenomenon characterized by the presence of high frequency activity and associated with cortical processing, which occurs during W and PS. Yet, the BF has also been shown to play a role in the generation of cortical slow wave activity (SWA) that occurs during SWS, as well as on the direct promotion of behavioral quiescence and sleep.

In order to understand the mechanisms by which the BF participates in these processes, a project was carried out to identify and study the neuronal groups that populate the BF and participate in the projections that the BF sends to the cortex, and through which it controls cortical activity, and those that participate in the projections to the lateral hypothalamus (LH), a region involved in the promotion of arousal and W, and through whose inhibition BF sleep active neurons may promote sleep.

We found that, in addition to neurons that synthesize ACh or GABA, which are known to populate the BF, a large number of neurons in the BF have the capacity to synthesize glutamate. In the BF, these three groups represented ~6% (~22,000 neurons), ~35% (~120,000 neurons) and ~90% (~310,000 neurons) of the total number of neurons in the BF, respectively. We also found that most of glutamate-synthesizing neurons had also the mechanisms to release glutamate

from their somato-dendritic compartments, which may represent a mechanism to regulate the strength of inhibitory inputs that they receive from other neurons and thus maintain their excitability.

By labeling BF neurons and their axonal processes with anterograde tracers, we were also able to identify BF axons innervating cortical regions and examine whether they had the capacity to release ACh, GABA or glutamate, by detecting the presence of presynaptic markers specific for each neurotransmitter. In the prefrontal cortex (PFC) we found that different contingents of BF axons have the capacity to release ACh, GABA or glutamate, and they respectively accounted for ~19%, ~52% and ~15% of the total number of BF terminals in this cortical region. These axonal contingents innervated deep layers of the PFC and appeared to provide innervation to pyramidal or interneuronal cell types. By these means, the BF could modulate cortical activity through cholinergic, GABAergic and glutamatergic mechanisms and thus promotes changes in cortical activity and in association with different behavioral states. In addition, by innervating deep layers of PFC, the BF may also influence the corticofugal output to thalamus and other subcortical regions known to be involved in the regulation of behavioral states, such as the LH.

In the LH we also found BF axons which presented cholinergic, GABAergic and glutamatergic phenotypes, representing ~10%, ~25% and ~50% of the total BF axonal terminals in the LH, respectively. As providing the major proportions, glutamatergic and GABAergic axon terminals were found to provide synaptic innervation to hypothalamic neurons, including those that express the peptide orexin (Orx, or hypocretin), neurons that have been shown to be critical for the

maintenance of W, as their absence is cause of narcolepsy. Of those Orx neurons innervated by BF axons, ~30% received glutamatergic inputs and ~65% received GABAergic ones. Thus, through a prominent inhibitory projection to the LH and to wake-active Orx neurons, the BF may suppress wakefulness and promote sleep. Reciprocally, glutamatergic BF neurons may participate in the maintenance of W through excitation of Orx neurons.

By providing multiple influences to cortex and LH, the BF may not only fulfill its multiple roles in modulation of cortical activity and behavioral states, but also to play a key role in the coordination of the concurrent changes at cortical and behavioral levels that occur across sleep-wake states.

LIST OF REFERENCES

Abercrombie M (1946) Estimation of nuclear population from microtome sections. Anat Rec 94:239-247.

Adams CE, Cepeda C, Boylan MK, Fisher RS, Hull CD, Buchwald NA, Wainer BH, Levine MS (1986) Basal forebrain neurons have axon collaterals that project to widely divergent cortical areas in the cat. Brain Res 397:365-371.

Aihara Y, Mashima H, Onda H, Hisano S, Kasuya H, Hori T, Yamada S, Tomura H, Yamada Y, Inoue I, Kojima I, Takeda J (2000) Molecular cloning of a novel brain-type Na(+)-dependent inorganic phosphate cotransporter. J Neurochem 74:2622-2625.

Akiyama H, Kaneko T, Mizuno N, McGeer PL (1990) Distribution of phosphate-activated glutaminase in the human cerebral cortex. J Comp Neurol 297:239-252.

Alam MN, Gong H, Alam T, Jaganath R, McGinty D, Szymusiak R (2002) Sleep-waking discharge patterns of neurons recorded in the rat perifornical lateral hypothalamic area. J Physiol 538:619-631.

Alfonso A, Grundahl K, Duerr JS, Han HP, Rand JB (1993) The Caenorhabditis elegans unc-17 gene: a putative vesicular acetylcholine transporter. Science 261:617-619.

Alheid GF, Heimer L (1988) New perspectives in basal forebrain organization of special relevance for neuropsychiatric disorders: the striatopallidal, amygdaloid, and corticopetal components of substantia innominata. Neuroscience 27:1-39.

Allaire P, Ikonomov O, Garrett MK, Jacob MH (2000) Synaptic interactions regulate gephyrin expression in avian cholinergic neurons in vivo. Neuropharmacology 39:2691-2698.

Allard JS, Tizabi Y, Shaffery JP, Trouth CO, Manaye K (2004) Stereological analysis of the hypothalamic hypocretin/orexin neurons in an animal model of depression. Neuropeptides 38:311-315.

Arvidsson U, Riedl M, Elde R, Meister B (1997) Vesicular acetylcholine transporter (VAChT) protein: a novel and unique marker for cholinergic neurons in the central and peripheral nervous systems. J Comp Neurol 378:454-467.

Baxter MG, Bucci DJ, Gorman LK, Wiley RG, Gallagher M (1995) Selective immunotoxic lesions of basal forebrain cholinergic cells: effects on learning and memory in rats. Behav Neurosci 109:714-722.

Bayer L, Risold PY, Griffond B, Fellmann D (1999) Rat diencephalic neurons producing melanin-concentrating hormone are influenced by ascending cholinergic projections. Neuroscience 91:1087-1101.

Bayer L, Eggermann E, Serafin M, Grivel J, Machard D, Muhlethaler M, Jones BE (2005) Opposite effects of noradrenaline and acetylcholine upon hypocretin/orexin versus melanin concentrating hormone neurons in rat hypothalamic slices. Neuroscience 130:807-811.

Bayraktar T, Staiger JF, Acsady L, Cozzari C, Freund TF, Zilles K (1997) Co-localization of vasoactive intestinal polypeptide, gamma-aminobutyric acid and choline acetyltransferase in neocortical interneurons of the adult rat. Brain Res 757:209-217.

Beaulieu C, Somogyi P (1991) Enrichment of cholinergic synaptic terminals on GABAergic neurons and coexistence of immunoreactive GABA and choline acetyltransferase in the same synaptic terminals in the striate cortex of the cat. J Comp Neurol 304:666-680.

Bellocchio EE, Reimer RJ, Fremeau RT, Jr., Edwards RH (2000) Uptake of glutamate into synaptic vesicles by an inorganic phosphate transporter. Science 289:957-960.

Bellocchio EE, Hu H, Pohorille A, Chan J, Pickel VM, Edwards RH (1998) The localization of the brain-specific inorganic phosphate transporter suggests a specific presynaptic role in glutamatergic transmission. J Neurosci 18:8648-8659.

Berntson GG, Shafi R, Sarter M (2002) Specific contributions of the basal forebrain corticopetal cholinergic system to electroencephalographic activity and sleep/waking behaviour. Eur J Neurosci 16:2453-2461.

Berthoud HR (2002) Multiple neural systems controlling food intake and body weight. Neurosci Biobehav Rev 26:393-428.

Bradford HF, Ward HK, Thomas AJ (1978) Glutamine--a major substrate for nerve endings. J Neurochem 30:1453-1459.

Brashear HR, Zaborszky L, Heimer L (1986) Distribution of GABAergic and cholinergic neurons in the rat diagonal band. Neuroscience 17:439-451.

Bremer F (1929) Cerveau "isolé" et physiologie du sommeil. C R Soc Biol (Paris) 102:1235.

Broberger C, De Lecea L, Sutcliffe JG, Hokfelt T (1998) Hypocretin/orexin- and melanin-concentrating hormone-expressing cells form distinct populations

in the rodent lateral hypothalamus: relationship to the neuropeptide Y and agouti gene-related protein systems. J Comp Neurol 402:460-474.

Butcher LL (1995) Cholinergic neurons and networks. In: The rat nervous system, Second Edition (Paxinos G, ed), pp 1003-1015. Sydney: Academic Press Australia.

Butcher LL, Semba K (1989) Reassessing the cholinergic basal forebrain: nomenclature schemata and concepts. Trends Neurosci 12:483-485.

Buzsaki G, Chrobak JJ (1995) Temporal structure in spatially organized neuronal ensembles: a role for interneuronal networks. Curr Opin Neurobiol 5:504-510.

Buzsaki G, Bickford RG, Ponomareff G, Thal LJ, Mandel R, Gage FH (1988) Nucleus basalis and thalamic control of neocortical activity in the freely moving rat. J Neurosci 8:4007-4026.

Campbell MJ, Morrison JH (1989) Monoclonal antibody to neurofilament protein (SMI-32) labels a subpopulation of pyramidal neurons in the human and monkey neocortex. J Comp Neurol 282:191-205.

Cape EG, Jones BE (1998) Differential modulation of high-frequency gamma-electroencephalogram activity and sleep-wake state by noradrenaline and serotonin microinjections into the region of cholinergic basalis neurons. J Neurosci 18:2653-2666.

Cape EG, Jones BE (2000) Effects of glutamate agonist versus procaine microinjections into the basal forebrain cholinergic cell area upon gamma and theta EEG activity and sleep-wake state. Eur J Neurosci 12:2166-2184.

Cape EG, Manns ID, Alonso A, Beaudet A, Jones BE (2000) Neurotensin-induced bursting of cholinergic basal forebrain neurons promotes gamma and theta cortical activity together with waking and paradoxical sleep. J Neurosci 20:8452-8461.

Celio MR (1986) Parvalbumin in most gamma-aminobutyric acid-containing neurons of the rat cerebral cortex. Science 231:995-997.

Celio MR (1990) Calbindin D-28k and parvalbumin in the rat nervous system. Neuroscience 35:375-475.

Chaudhry FA, Reimer RJ, Bellocchio EE, Danbolt NC, Osen KK, Edwards RH, Storm-Mathisen J (1998) The vesicular GABA transporter, VGAT, localizes to synaptic vesicles in sets of glycinergic as well as GABAergic neurons. J Neurosci 18:9733-9750.

Chemelli RM, Willie JT, Sinton CM, Elmquist JK, Scammell T, Lee C, Richardson JA, Williams SC, Xiong Y, Kisanuki Y, Fitch TE, Nakazato M, Hammer RE, Saper CB, Yanagisawa M (1999) Narcolepsy in orexin knockout mice: molecular genetics of sleep regulation. Cell 98:437-451.

Chen L, Chetkovich DM, Petralia RS, Sweeney NT, Kawasaki Y, Wenthold RJ, Bredt DS, Nicoll RA (2000) Stargazin regulates synaptic targeting of AMPA receptors by two distinct mechanisms. Nature 408:936-943.

Coggan JS, Bartol TM, Esquenazi E, Stiles JR, Lamont S, Martone ME, Berg DK, Ellisman MH, Sejnowski TJ (2005) Evidence for ectopic neurotransmission at a neuronal synapse. Science 309:446-451.

Colom LV, Castaneda MT, Reyna T, Hernandez S, Garrido-Sanabria E (2005) Characterization of medial septal glutamatergic neurons and their projection to the hippocampus. Synapse 58:151-164.

Conroy WG, Liu Z, Nai Q, Coggan JS, Berg DK (2003) PDZ-containing proteins provide a functional postsynaptic scaffold for nicotinic receptors in neurons. Neuron 38:759-771.

Cortes R, Ceccatelli S, Schalling M, Hokfelt T (1990) Differential effects of intracerebroventricular colchicine administration on the expression of mRNAs for neuropeptides and neurotransmitter enzymes, with special emphasis on galanin: an in situ hybridization study. Synapse 6:369-391.

Crippa GE, Peres-Polon VL, Kuboyama RH, Correa FM (1999) Cardiovascular response to the injection of acetylcholine into the anterior cingulate region of the medial prefrontal cortex of unanesthetized rats. Cereb Cortex 9:362-365.

Damasio AR, Graff-Radford NR, Eslinger PJ, Damasio H, Kassell N (1985) Amnesia following basal forebrain lesions. Arch Neurol 42:263-271.

Danik M, Cassoly E, Manseau F, Sotty F, Mouginot D, Williams S (2005) Frequent coexpression of the vesicular glutamate transporter 1 and 2 genes, as well as coexpression with genes for choline acetyltransferase or glutamic acid decarboxylase in neurons of rat brain. J Neurosci Res 81:506-521.

Davies P, Maloney AJ (1976) Selective loss of central cholinergic neurons in Alzheimer's disease. Lancet 2:1403.

de Lecea L, Kilduff TS, Peyron C, Gao X, Foye PE, Danielson PE, Fukuhara C, Battenberg EL, Gautvik VT, Bartlett FS, 2nd, Frankel WN, van den Pol AN, Bloom FE, Gautvik KM, Sutcliffe JG (1998) The hypocretins: hypothalamus-specific peptides with neuroexcitatory activity. Proc Natl Acad Sci U S A 95:322-327.

De Lima AD, Singer W (1986) Cholinergic innervation of the cat striate cortex: a choline acetyltransferase immunocytochemical analysis. J Comp Neurol 250:324-338.

DeFelipe J (1997) Types of neurons, synaptic connections and chemical characteristics of cells immunoreactive for calbindin-D28K, parvalbumin and calretinin in the neocortex. J Chem Neuroanat 14:1-19.

Dement WC (1958) The occurrence of low voltage, fast, electroencephalogram patterns during behavioral sleep in the cat. Electroencephalogr Clin Neurophysiol Suppl 10:291-296.

Descarries L, Gisiger V, Steriade M (1997) Diffuse transmission by acetylcholine in the CNS. Prog Neurobiol 53:603-625.

Descarries L, Mechawar N, Aznavour N, Watkins KC (2004) Structural determinants of the roles of acetylcholine in cerebral cortex. Prog Brain Res 145:45-58.

DiLeone RJ, Georgescu D, Nestler EJ (2003) Lateral hypothalamic neuropeptides in reward and drug addiction. Life Sci 73:759-768.

Domino EF, Yamamoto K, Dren AT (1968) Role of cholinergic mechanisms in states of wakefulness and sleep. Prog Brain Res 28:113-133.

Donoghue JP, Wenthold RJ, Altschuler RA (1985) Localization of glutaminase-like and aspartate aminotransferase-like immunoreactivity in neurons of cerebral neocortex. J Neurosci 5:2597-2608.

Dunnett SB, Everitt BJ, Robbins TW (1991) The basal forebrain-cortical cholinergic system: interpreting the functional consequences of excitotoxic lesions. Trends Neurosci 14:494-501.

Duque A, Balatoni B, Detari L, Zaborszky L (2000) EEG correlation of the discharge properties of identified neurons in the basal forebrain. J Neurophysiol 84:1627-1635.

Eckenstein FP, Baughman RW, Quinn J (1988) An anatomical study of cholinergic innervation in rat cerebral cortex. Neuroscience 25:457-474.

Edwards FA (1995) Anatomy and electrophysiology of fast central synapses lead to a structural model for long-term potentiation. Physiol Rev 75:759-787.

Eggermann E, Serafin M, Bayer L, Machard D, Saint-Mleux B, Jones BE, Muhlethaler M (2001) Orexins/hypocretins excite basal forebrain cholinergic neurones. Neuroscience 108:177-181.

Eggermann E, Bayer L, Serafin M, Saint-Mleux B, Bernheim L, Machard D, Jones BE, Muhlethaler M (2003) The wake-promoting hypocretin-orexin neurons are in an intrinsic state of membrane depolarization. J Neurosci 23:1557-1562.

Espana RA, Valentino RJ, Berridge CW (2003) Fos immunoreactivity in hypocretin-synthesizing and hypocretin-1 receptor-expressing neurons: effects of diurnal and nocturnal spontaneous waking, stress and hypocretin-1 administration. Neuroscience 121:201-217.

Espana RA, Reis KM, Valentino RJ, Berridge CW (2005) Organization of hypocretin/orexin efferents to locus coeruleus and basal forebrain arousal-related structures. J Comp Neurol 481:160-178.

Everitt BJ, Robbins TW (1997) Central cholinergic systems and cognition. Annu Rev Psychol 48:649-684.

Fisher RS, Buchwald NA, Hull CD, Levine MS (1988) GABAergic basal forebrain neurons project to the neocortex: the localization of glutamic acid decarboxylase and choline acetyltransferase in feline corticopetal neurons. J Comp Neurol 272:489-502.

Ford B, Holmes C, Mainville L, Jones BE (1995) GABAergic neurons in the rat pontomesencephalic tegmentum: codistribution with cholinergic and other tegmental neurons projecting to the posterior lateral hypothalamus. J Comp Neurol 363:177-196.

Fort P, Khateb A, Serafin M, Muhlethaler M, Jones BE (1998) Pharmacological characterization and differentiation of non-cholinergic nucleus basalis neurons *in vitro*. NeuroReport 9:1-5.

Fremeau RT, Jr., Voglmaier S, Seal RP, Edwards RH (2004) VGLUTs define subsets of excitatory neurons and suggest novel roles for glutamate. Trends Neurosci 27:98-103.

Fremeau RT, Jr., Troyer MD, Pahner I, Nygaard GO, Tran CH, Reimer RJ, Bellocchio EE, Fortin D, Storm-Mathisen J, Edwards RH (2001) The expression of vesicular glutamate transporters defines two classes of excitatory synapse. Neuron 31:247-260.

Fremeau RT, Jr., Burman J, Qureshi T, Tran CH, Proctor J, Johnson J, Zhang H, Sulzer D, Copenhagen DR, Storm-Mathisen J, Reimer RJ, Chaudhry FA, Edwards RH (2002) The identification of vesicular glutamate transporter 3 suggests novel modes of signaling by glutamate. Proc Natl Acad Sci U S A 99:14488-14493.

Freund TF, Antal M (1988) GABA-containing neurons in the septum control inhibitory interneurons in the hippocampus. Nature 336:170-173.

Freund TF, Gulyas AI (1991) GABAergic interneurons containing calbindin D28K or somatostatin are major targets of GABAergic basal forebrain afferents in the rat neocortex. J Comp Neurol 314:187-199.

Freund TF, Meskenaite V (1992) gamma-Aminobutyric acid-containing basal forebrain neurons innervate inhibitory interneurons in the neocortex. Proc Natl Acad Sci U S A 89:738-742.

Fujiyama F, Furuta T, Kaneko T (2001) Immunocytochemical localization of candidates for vesicular glutamate transporters in the rat cerebral cortex. J Comp Neurol 435:379-387.

Gabbott PL, Warner TA, Jays PR, Salway P, Busby SJ (2005) Prefrontal cortex in the rat: projections to subcortical autonomic, motor, and limbic centers. J Comp Neurol 492:145-177.

Garzon M, Pickel VM (2000) Dendritic and axonal targeting of the vesicular acetylcholine transporter to membranous cytoplasmic organelles in laterodorsal and pedunculopontine tegmental nuclei. J Comp Neurol 419:32-48.

Gaykema RP, Luiten PG, Nyakas C, Traber J (1990) Cortical projection patterns of the medial septum-diagonal band complex. J Comp Neurol 293:103-124.

Gaykema RP, van Weeghel R, Hersh LB, Luiten PG (1991) Prefrontal cortical projections to the cholinergic neurons in the basal forebrain. J Comp Neurol 303:563-583.

Geeraedts LM, Nieuwenhuys R, Veening JG (1990) Medial forebrain bundle of the rat: III. Cytoarchitecture of the rostral (telencephalic) part of the medial forebrain bundle bed nucleus. J Comp Neurol 294:507-536.

Gerashchenko D, Salin-Pascual R, Shiromani PJ (2001a) Effects of hypocretin-saporin injections into the medial septum on sleep and hippocampal theta. Brain Res 913:106-115.

Gerashchenko D, Kohls MD, Greco M, Waleh NS, Salin-Pascual R, Kilduff TS, Lappi DA, Shiromani PJ (2001b) Hypocretin-2-saporin lesions of the lateral hypothalamus produce narcoleptic-like sleep behavior in the rat. J Neurosci 21:7273-7283.

Gilmor ML, Nash NR, Roghani A, Edwards RH, Yi H, Hersch SM, Levey AI (1996) Expression of the putative vesicular acetylcholine transporter in rat brain and localization in cholinergic synaptic vesicles. J Neurosci 16:2179-2190.

Giustetto M, Kirsch J, Fritschy JM, Cantino D, Sassoe-Pognetto M (1998) Localization of the clustering protein gephyrin at GABAergic synapses in the main olfactory bulb of the rat. J Comp Neurol 395:231-244.

Gomez-Lira G, Lamas M, Romo-Parra H, Gutierrez R (2005) Programmed and induced phenotype of the hippocampal granule cells. J Neurosci 25:6939-6946.

Gras C, Herzog E, Bellenchi GC, Bernard V, Ravassard P, Pohl M, Gasnier B, Giros B, El Mestikawy S (2002) A third vesicular glutamate transporter expressed by cholinergic and serotoninergic neurons. J Neurosci 22:5442-5451.

Gritti I, Mainville L, Jones BE (1993) Codistribution of GABA- with acetylcholine-synthesizing neurons in the basal forebrain of the rat. J Comp Neurol 329:438-457.

Gritti I, Mainville L, Jones BE (1994) Projections of GABAergic and cholinergic basal forebrain and GABAergic preoptic-anterior hypothalamic neurons to the posterior lateral hypothalamus of the rat. J Comp Neurol 339:251-268.

Gritti I, Mainville L, Mancia M, Jones BE (1997) GABAergic and other noncholinergic basal forebrain neurons, together with cholinergic neurons, project to the mesocortex and isocortex in the rat. J Comp Neurol 383:163-177.

Gritti I, Manns ID, Mainville L, Jones BE (2003) Parvalbumin, calbindin, or calretinin in cortically projecting and GABAergic, cholinergic, or glutamatergic basal forebrain neurons of the rat. J Comp Neurol 458:11-31.

Groenewegen HJ, Uylings HB (2000) The prefrontal cortex and the integration of sensory, limbic and autonomic information. Prog Brain Res 126:3-28.

Grove EA (1988) Efferent connections of the substantia innominata in the rat. J Comp Neurol 277:347-364.

Gualix J, Gomez-Villafuertes R, Diaz-Hernandez M, Miras-Portugal MT (2003) Presence of functional ATP and dinucleotide receptors in glutamatergic synaptic terminals from rat midbrain. J Neurochem 87:160-171.

Guillery RW, Herrup K (1997) Quantification without pontification: choosing a method for counting objects in sectioned tissues. J Comp Neurol 386:2-7.

Hajszan T, Alreja M, Leranth C (2004) Intrinsic vesicular glutamate transporter 2-immunoreactive input to septohippocampal parvalbumin-containing neurons: novel glutamatergic local circuit cells. Hippocampus 14:499-509.

Hara J, Beuckmann CT, Nambu T, Willie JT, Chemelli RM, Sinton CM, Sugiyama F, Yagami K, Goto K, Yanagisawa M, Sakurai T (2001) Genetic ablation of orexin neurons in mice results in narcolepsy, hypophagia, and obesity. Neuron 30:345-354.

Harkany T, Hartig W, Berghuis P, Dobszay MB, Zilberter Y, Edwards RH, Mackie K, Ernfors P (2003) Complementary distribution of type 1 cannabinoid receptors and vesicular glutamate transporter 3 in basal forebrain suggests input-specific retrograde signalling by cholinergic neurons. Eur J Neurosci 18:1979-1992.

Harkany T, Holmgren C, Hartig W, Qureshi T, Chaudhry FA, Storm-Mathisen J, Dobszay MB, Berghuis P, Schulte G, Sousa KM, Fremeau RT, Jr., Edwards RH, Mackie K, Ernfors P, Zilberter Y (2004) Endocannabinoid-independent retrograde signaling at inhibitory synapses in layer 2/3 of

neocortex: involvement of vesicular glutamate transporter 3. J Neurosci 24:4978-4988.

Harris GC, Wimmer M, Aston-Jones G (2005) A role for lateral hypothalamic orexin neurons in reward seeking. Nature 437:556-559.

Hendry SH, Jones EG, Emson PC, Lawson DE, Heizmann CW, Streit P (1989) Two classes of cortical GABA neurons defined by differential calcium binding protein immunoreactivities. Exp Brain Res 76:467-472.

Henny P, Jones BE (2006a) Vesicular glutamate (VGluT), GABA (VGAT), and acetylcholine (VAChT) transporters in basal forebrain axon terminals innervating the lateral hypothalamus. J Comp Neurol 496:453-467.

Henny P, Jones BE (2006b) Innervation of orexin/hypocretin neurons by GABAergic, glutamatergic or cholinergic basal forebrain terminals evidenced by immunostaining for presynaptic vesicular transporter and postsynaptic scaffolding proteins. J Comp Neurol 499:645-661.

Hernandez Peon R, Chavez Ibarra G (1963) Sleep induced by electrical or chemical stimulation of the forebrain. Electroencephalogr Clin Neurophysiol:Suppl 24:188+.

Hernandez-Peon R, Chavez-Ibarra G, Morgane PJ, Timo-Iaria C (1963) Limbic cholinergic pathways involved in sleep and emotional behavior. Exptl Neurol 8:93-111.

Herzog E, Gilchrist J, Gras C, Muzerelle A, Ravassard P, Giros B, Gaspar P, El Mestikawy S (2004) Localization of VGLUT3, the vesicular glutamate transporter type 3, in the rat brain. Neuroscience 123:983-1002.

Herzog E, Bellenchi GC, Gras C, Bernard V, Ravassard P, Bedet C, Gasnier B, Giros B, El Mestikawy S (2001) The existence of a second vesicular glutamate transporter specifies subpopulations of glutamatergic neurons. J Neurosci 21:RC181.

Hess WR (1957) The functional organization of the diencephalon. New York: Grune & Stratton.

Hisano S, Hoshi K, Ikeda Y, Maruyama D, Kanemoto M, Ichijo H, Kojima I, Takeda J, Nogami H (2000) Regional expression of a gene encoding a neuron-specific Na(+)-dependent inorganic phosphate cotransporter (DNPI) in the rat forebrain. Brain Res Mol Brain Res 83:34-43.

Holstege G (1987) Some anatomical observations on the projections from the hypothalamus to brainstem and spinal cord: An HRP and autoradiographic tracing study in the cat. J Comp Neurol 260:98-126.

Horvath TL, Gao XB (2005) Input organization and plasticity of hypocretin neurons: possible clues to obesity's association with insomnia. Cell Metab 1:279-286.

Houser CR, Crawford GD, Salvaterra PM, Vaughn JE (1985) Immunocytochemical localization of choline acetyltransferase in rat cerebral cortex: a study of cholinergic neurons and synapses. J Comp Neurol 234:17-34.

Houser CR, Crawford GD, Barber RP, Salvaterra PM, Vaughn JE (1983) Organization and morphological characteristics of cholinergic neurons: an immunocytochemical study with a monoclonal antibody to choline acetyltransferase. Brain Res 266:97-119.

Hunt PS, Campbell BA (1997) Autonomic and behavioral correlates of appetitive conditioning in rats. Behav Neurosci 111:494-502.

Hur EE, Zaborszky L (2005) Vglut2 afferents to the medial prefrontal and primary somatosensory cortices: a combined retrograde tracing in situ hybridization. J Comp Neurol 483:351-373.

Hur EE, Stornetta RL, Guyenet PG, Zaborszky L (2002) Distribution of Glutamate Neurons in the Basal Forebrain as Revealed by the Presence of Vesicular Glutamate Transporter (VGLUT2). In: Society for Neuroscience, 2002. Orlando, FL, U.S.A.

Hurley KM, Herbert H, Moga MM, Saper CB (1991) Efferent projections of the infralimbic cortex of the rat. J Comp Neurol 308:249-276.

Ingham CA, Bolam JP, Smith AD (1988) GABA-immunoreactive synaptic boutons in the rat basal forebrain: comparison of neurons that project to the neocortex with pallidosubthalamic neurons. J Comp Neurol 273:263-282.

Jasper HH, Tessier J (1971) Acetylcholine liberation from cerebral cortex during paradoxical (REM) sleep. Science 172:601-602.

Jefferys JG, Traub RD, Whittington MA (1996) Neuronal networks for induced '40 Hz' rhythms. Trends Neurosci 19:202-208.

Jeong J (2004) EEG dynamics in patients with Alzheimer's disease. Clin Neurophysiol 115:1490-1505.

Johnston MV, McKinney M, Coyle JT (1979) Evidence for a cholinergic projection to neocortex from neurons in basal forebrain. Proc Natl Acad Sci U S A 76:5392-5396.

Jones BE (1991) Noradrenergic locus coeruleus neurons: their distant connections and their relationship to neighboring (including cholinergic and GABAergic) neurons of the central gray and reticular formation. Prog Brain Res 88:15-30.

Jones BE (1995) Reticular formation: cytoarchitecture, transmitters, and projections. In: The rat nervous system, Second Edition (Paxinos G, ed), pp 155-171. Sydney: Academic Press Australia.

Jones BE (2003) Arousal systems. Front Biosci 8:s438-451.

Jones BE (2004) Activity, modulation and role of basal forebrain cholinergic neurons innervating the cerebral cortex. Prog Brain Res 145:157-169.

Jones BE (2005a) From waking to sleeping: neuronal and chemical substrates. Trends Pharmacol Sci 26:578-586.

Jones BE (2005b) Basic mechanisms of sleep-wake states. In: Principles and Practice of Sleep Medicine, 4th Edition (Kryger MH, Roth T, Dement WC, eds), pp 136-153. Philadelphia: Elsevier Saunders.

Jones BE (2005c) Sleep-Wake Mechanisms: Neurophysiology and Chemical Neuroanatomy. In: SRS Basics of Sleep Guide (Opp MR, ed), pp 57-64. Westchester, IL: Sleep Research Society.

Jones BE, Cuello AC (1989) Afferents to the basal forebrain cholinergic cell area from pontomesencephalic--catecholamine, serotonin, and acetylcholine--neurons. Neuroscience 31:37-61.

Jones BE, Muhlethaler M (2005) Modulation of cortical activity and sleep-wake state by hypocretin/orexin. In: The Hypocretins: Integrators of

Physiological Systems (de Lecea L, Sutcliffe JG, eds), pp 289-301. New York: Springer.

Jouvet M (1965) Paradoxical Sleep--a Study of Its Nature and Mechanisms. Prog Brain Res 18:20-62.

Kaneko T, Mizuno N (1988) Immunohistochemical study of glutaminase-containing neurons in the cerebral cortex and thalamus of the rat. J Comp Neurol 267:590-602.

Kaneko T, Mizuno N (1994) Glutamate-synthesizing enzymes in GABAergic neurons of the neocortex: a double immunofluorescence study in the rat. Neuroscience 61:839-849.

Kaneko T, Fujiyama F (2002) Complementary distribution of vesicular glutamate transporters in the central nervous system. Neurosci Res 42:243-250.

Kaneko T, Nakaya Y, Mizuno N (1992) Paucity of glutaminase-immunoreactive nonpyramidal neurons in the rat cerebral cortex. J Comp Neurol 322:181-190.

Kaneko T, Itoh K, Shigemoto R, Mizuno N (1989) Glutaminase-like immunoreactivity in the lower brainstem and cerebellum of the adult rat. Neuroscience 32:79-98.

Kawaguchi Y, Kubota Y (1993) Correlation of physiological subgroupings of nonpyramidal cells with parvalbumin- and calbindinD28k-immunoreactive neurons in layer V of rat frontal cortex. J Neurophysiol 70:387-396.

Kayaba Y, Nakamura A, Kasuya Y, Ohuchi T, Yanagisawa M, Komuro I, Fukuda Y, Kuwaki T (2003) Attenuated defense response and low basal blood

pressure in orexin knockout mice. Am J Physiol Regul Integr Comp Physiol 285:R581-593.

Khateb A, Muhlethaler M, Alonso A, Serafin M, Mainville L, Jones BE (1992) Cholinergic nucleus basalis neurons display the capacity for rhythmic bursting activity mediated by low-threshold calcium spikes. Neuroscience 51:489-494.

Kievit J, Kuypers HG (1975) Basal forebrain and hypothalamic connection to frontal and parietal cortex in the Rhesus monkey. Science 187:660-662.

Kimura H, McGeer PL, Peng F, McGeer EG (1980) Choline acetyltransferase-containing neurons in rodent brain demonstrated by immunohistochemistry. Science 208:1057-1059.

Kimura H, McGeer PL, Peng JH, McGeer EG (1981) The central cholinergic system studied by choline acetyltransferase immunohistochemistry in the cat. J Comp Neurol 200:151-201.

Kirkcaldie MT, Dickson TC, King CE, Grasby D, Riederer BM, Vickers JC (2002) Neurofilament triplet proteins are restricted to a subset of neurons in the rat neocortex. J Chem Neuroanat 24:163-171.

Kohler C, Chan-Palay V, Wu J-Y (1984) Septal neurons containing glutamic acid decarboxylase immunoreactivity project to the hippocampal region in the rat brain. Anat Embryol 169:41-44.

Kornau HC, Schenker LT, Kennedy MB, Seeburg PH (1995) Domain interaction between NMDA receptor subunits and the postsynaptic density protein PSD-95. Science 269:1737-1740.

Koyama Y, Takahashi K, Kodama T, Kayama Y (2003) State-dependent activity of neurons in the perifornical hypothalamic area during sleep and waking. Neuroscience 119:1209-1219.

Krettek JE, Price JL (1977) The cortical projections of the mediodorsal nucleus and adjacent thalamic nuclei in the rat. J Comp Neurol 171:157-191.

Krnjevic K (1967) Chemical transmission and cortical arousal. Anesthesiology 28:100-105.

Krout KE, Mettenleiter TC, Loewy AD (2003) Single CNS neurons link both central motor and cardiosympathetic systems: a double-virus tracing study. Neuroscience 118:853-866.

Kubota Y, Hattori R, Yui Y (1994) Three distinct subpopulations of GABAergic neurons in rat frontal agranular cortex. Brain Res 649:159-173.

Lamour Y, Dutar P, Jobert A (1982) Topographic organization of basal forebrain neurons projecting to the rat cerebral cortex. Neurosci Lett 34:117-122.

Lanciego JL, Wouterlood FG, Erro E, Arribas J, Gonzalo N, Urra X, Cervantes S, Gimenez-Amaya JM (2000) Complex brain circuits studied via simultaneous and permanent detection of three transported neuroanatomical tracers in the same histological section. J Neurosci Methods 103:127-135.

Lee MG, Hassani OK, Jones BE (2005a) Discharge of identified orexin/hypocretin neurons across the sleep-waking cycle. J Neurosci 25:6716-6720.

Lee MG, Manns ID, Alonso A, Jones BE (2004) Sleep-wake related discharge properties of basal forebrain neurons recorded while applying juxtacellular labeling in head-fixed rats. Under revision in Journal of Neurophysiology.

Lee MG, Hassani OK, Alonso A, Jones BE (2005b) Cholinergic basal forebrain neurons burst with theta during waking and paradoxical sleep. J Neurosci 25:4365-4369.

Lee MG, Chrobak JJ, Sik A, Wiley RG, Buzsaki G (1994) Hippocampal theta activity following selective lesion of the septal cholinergic system. Neuroscience 62:1033-1047.

Lehmann J, Nagy JI, Atmadia S, Fibiger HC (1980) The nucleus basalis magnocellularis: the origin of a cholinergic projection to the neocortex of the rat. Neuroscience 5:1161-1174.

Levey AI, Edmunds SM, Hersch SM, Wiley RG, Heilman CJ (1995) Light and electron microscopic study of m2 muscarinic acetylcholine receptor in the basal forebrain of the rat. J Comp Neurol 351:339-356.

Lewis PR, Shute CC (1967) The cholinergic limbic system: projections to hippocampal formation, medial cortex, nuclei of the ascending cholinergic reticular system, and the subfornical organ and supra-optic crest. Brain 90:521-540.

Li Y, Gao XB, Sakurai T, van den Pol AN (2002) Hypocretin/Orexin excites hypocretin neurons via a local glutamate neuron-A potential mechanism for orchestrating the hypothalamic arousal system. Neuron 36:1169-1181.

Lin JS, Sakai K, Vanni-Mercier G, Jouvet M (1989) A critical role of the posterior hypothalamus in the mechanisms of wakefulness determined by microinjection of muscimol in freely moving cats. Brain Res 479:225-240.

Lin L, Faraco J, Li R, Kadotani H, Rogers W, Lin X, Qiu X, de Jong PJ, Nishino S, Mignot E (1999) The sleep disorder canine narcolepsy is caused by a mutation in the hypocretin (orexin) receptor 2 gene. Cell 98:365-376.

Lin W, McKinney K, Liu L, Lakhlani S, Jennes L (2003) Distribution of vesicular glutamate transporter-2 messenger ribonucleic Acid and protein in the septum-hypothalamus of the rat. Endocrinology 144:662-670.

Liu Y, Krantz DE, Waites C, Edwards RH (1999) Membrane trafficking of neurotransmitter transporters in the regulation of synaptic transmission. Trends Cell Biol 9:356-363.

Llinas R, Ribary U (1993) Coherent 40-Hz oscillation characterizes dream state in humans. Proc Natl Acad Sci U S A 90:2078-2081.

Lo Conte G, Casamenti F, Bigl V, Milaneschi E, Pepeu G (1982) Effect of magnocellular forebrain nuclei lesions on acetylcholine output from the cerebral cortex, electrocorticogram and behaviour. Arch Ital Biol 120:176-188.

Lugaresi E, Tobler I, Gambetti P, Montagna P (1998) The pathophysiology of fatal familial insomnia. Brain Pathol 8:521-526.

Luiten PG, Gaykema RP, Traber J, Spencer DG, Jr. (1987) Cortical projection patterns of magnocellular basal nucleus subdivisions as revealed by anterogradely transported Phaseolus vulgaris leucoagglutinin. Brain Res 413:229-250.

Lysakowski A, Wainer BH, Bruce G, Hersh LB (1989) An atlas of the regional and laminar distribution of choline acetyltransferase immunoreactivity in rat cerebral cortex. Neuroscience 28:291-336.

Lysakowski A, Wainer BH, Rye DB, Bruce G, Hersh LB (1986) Cholinergic innervation displays strikingly different laminar preferences in several cortical areas. Neurosci Lett 64:102-108.

Manns ID, Alonso A, Jones BE (2000a) Discharge properties of juxtacellularly labeled and immunohistochemically identified cholinergic basal forebrain neurons recorded in association with the electroencephalogram in anesthetized rats. J Neurosci 20:1505-1518.

Manns ID, Alonso A, Jones BE (2000b) Discharge profiles of juxtacellularly labeled and immunohistochemically identified GABAergic basal forebrain neurons recorded in association with the electroencephalogram in anesthetized rats. J Neurosci 20:9252-9263.

Manns ID, Mainville L, Jones BE (2001) Evidence for glutamate, in addition to acetylcholine and GABA, neurotransmitter synthesis in basal forebrain neurons projecting to the entorhinal cortex. Neuroscience 107:249-263.

Manns ID, Alonso A, Jones BE (2003a) Rhythmically discharging basal forebrain units comprise cholinergic, GABAergic, and putative glutamatergic cells. J Neurophysiol 89:1057-1066.

Manns ID, Lee MG, Modirrousta M, Hou YP, Jones BE (2003b) Alpha 2 adrenergic receptors on GABAergic, putative sleep-promoting basal forebrain neurons. Eur J Neurosci 18:723-727.

Markram H, Toledo-Rodriguez M, Wang Y, Gupta A, Silberberg G, Wu C (2004) Interneurons of the neocortical inhibitory system. Nat Rev Neurosci 5:793-807.

Massimini M, Huber R, Ferrarelli F, Hill S, Tononi G (2004) The sleep slow oscillation as a traveling wave. J Neurosci 24:6862-6870.

McCormick DA (1993) Actions of acetylcholine in the cerebral cortex and thalamus and implications for function. Prog Brain Res 98:303-308.

McCormick DA, Prince DA (1985) Two types of muscarinic response to acetylcholine in mammalian cortical neurons. Proc Natl Acad Sci U S A 82:6344-6348.

McGinty DJ, Sterman MB (1968) Sleep suppression after basal forebrain lesions in the cat. Science 160:1253-1255.

McIntire SL, Reimer RJ, Schuske K, Edwards RH, Jorgensen EM (1997) Identification and characterization of the vesicular GABA transporter. Nature 389:870-876.

McLaughlin BJ, Wood JG, Saito K, Barber R, Vaughn JE, Roberts E, Wu JY (1974) The fine structural localization of glutamate decarboxylase in synaptic terminals of rodent cerebellum. Brain Res 76:377-391.

Mechawar N, Cozzari C, Descarries L (2000) Cholinergic innervation in adult rat cerebral cortex: a quantitative immunocytochemical description. J Comp Neurol 428:305-318.

Mesulam MM, Mufson EJ, Wainer BH, Levey AI (1983a) Central cholinergic pathways in the rat: an overview based on an alternative nomenclature (Ch1-Ch6). Neuroscience 10:1185-1201.

Mesulam MM, Mufson EJ, Levey AI, Wainer BH (1983b) Cholinergic innervation of cortex by the basal forebrain: cytochemistry and cortical connections of the septal area, diagonal band nuclei, nucleus basalis (substantia innominata), and hypothalamus in the rhesus monkey. J Comp Neurol 214:170-197.

Metherate R, Cox CL, Ashe JH (1992) Cellular bases of neocortical activation: modulation of neural oscillations by the nucleus basalis and endogenous acetylcholine. J Neurosci 12:4701-4711.

Miettinen RA, Kalesnykas G, Koivisto EH (2002) Estimation of the total number of cholinergic neurons containing estrogen receptor-alpha in the rat basal forebrain. J Histochem Cytochem 50:891-902.

Mignot E, Taheri S, Nishino S (2002) Sleeping with the hypothalamus: emerging therapeutic targets for sleep disorders. Nat Neurosci 5 Suppl:1071-1075.

Mileykovskiy BY, Kiyashchenko LI, Siegel JM (2005) Behavioral correlates of activity in identified hypocretin/orexin neurons. Neuron 46:787-798.

Millhouse OE (1969) A golgi study of the descending medial forebrain bundle. Brain Res 15:341-363.

Modirrousta M, Mainville L, Jones BE (2004) Gabaergic neurons with alpha2-adrenergic receptors in basal forebrain and preoptic area express c-Fos during sleep. Neuroscience 129:803-810.

Modirrousta M, Mainville L, Jones BE (2005) Orexin and MCH neurons express c-Fos differently after sleep deprivation vs. recovery and bear different adrenergic receptors. Eur J Neurosci 21:2807-2816.

Moghaddam B (1993) Stress preferentially increases extraneuronal levels of excitatory amino acids in the prefrontal cortex: comparison to hippocampus and basal ganglia. J Neurochem 60:1650-1657.

Moruzzi G, Magoun HW (1949) Brainstem reticular formation and activation of the EEG. Electroencephalogr Clin Neurophysiol 1:455-473.

Muller GJ, Moller A, Johansen FF (2001) Stereological cell counts of GABAergic neurons in rat dentate hilus following transient cerebral ischemia. Exp Brain Res 141:380-388.

Nauta WJH (1946) Hypothalamic regulation of sleep in rats. An experimental study. J Neurophysiol 9:285-316.

Ni B, Rosteck PR, Jr., Nadi NS, Paul SM (1994) Cloning and expression of a cDNA encoding a brain-specific Na(+)-dependent inorganic phosphate cotransporter. Proc Natl Acad Sci U S A 91:5607-5611.

Ni B, Wu X, Yan GM, Wang J, Paul SM (1995) Regional expression and cellular localization of the Na(+)-dependent inorganic phosphate cotransporter of rat brain. J Neurosci 15:5789-5799.

Nieuwenhuys R, Geeraedts LM, Veening JG (1982) The medial forebrain bundle of the rat. I. General introduction. J Comp Neurol 206:49-81.

Nishino S, Mignot E (1997) Pharmacological aspects of human and canine narcolepsy. Prog Neurobiol 52:27-78.

Nishino S, Tafti M, Reid MS, Shelton J, Siegel JM, Dement WC, Mignot E (1995) Muscle atonia is triggered by cholinergic stimulation of the basal forebrain: implication for the pathophysiology of canine narcolepsy. J Neurosci 15:4806-4814.

Nyakas C, Luiten PG, Spencer DG, Traber J (1987) Detailed projection patterns of septal and diagonal band efferents to the hippocampus in the rat with emphasis on innervation of CA1 and dentate gyrus. Brain Res Bull 18:533-545.

O'Brien RJ, Xu D, Petralia RS, Steward O, Huganir RL, Worley P (1999) Synaptic clustering of AMPA receptors by the extracellular immediate-early gene product Narp. Neuron 23:309-323.

Oertel WH, Schmechel DE, Mugnaini E, Tappaz ML, Kopin IJ (1981) Immunocytochemical localization of glutamate decarboxylase in rat cerebellum with a new antiserum. Neuroscience 6:2715-2735.

Olds J, Milner P (1954) Positive reinforcement produced by electrical stimulation of septal area and other regions of rat brain. J Comp Physiol Psychol 47:419-427.

Ortells MO, Lunt GG (1995) Evolutionary history of the ligand-gated ion-channel superfamily of receptors. Trends Neurosci 18:121-127.

Parker MJ, Zhao S, Bredt DS, Sanes JR, Feng G (2004) PSD93 regulates synaptic stability at neuronal cholinergic synapses. J Neurosci 24:378-388.

Paxinos G, Watson C (1986) The Rat Brain in Stereotaxic Coordinates. Sydney: Academic Press.

Peter D, Liu Y, Sternini C, de Giorgio R, Brecha N, Edwards RH (1995) Differential expression of two vesicular monoamine transporters. J Neurosci 15:6179-6188.

Peyron C, Tighe DK, van den Pol AN, de Lecea L, Heller HC, Sutcliffe JG, Kilduff TS (1998) Neurons containing hypocretin (orexin) project to multiple neuronal systems. J Neurosci 18:9996-10015.

Peyron C, Faraco J, Rogers W, Ripley B, Overeem S, Charnay Y, Nevsimalova S, Aldrich M, Reynolds D, Albin R, Li R, Hungs M, Pedrazzoli M, Padigaru M, Kucherlapati M, Fan J, Maki R, Lammers GJ, Bouras C, Kucherlapati R, Nishino S, Mignot E (2000) A mutation in a case of early onset narcolepsy and a generalized absence of hypocretin peptides in human narcoleptic brains. Nat Med 6:991-997.

Pfeiffer F, Simler R, Grenningloh G, Betz H (1984) Monoclonal antibodies and peptide mapping reveal structural similarities between the subunits of the glycine receptor of rat spinal cord. Proc Natl Acad Sci U S A 81:7224-7227.

Pow DV, Robinson SR (1994) Glutamate in some retinal neurons is derived solely from glia. Neuroscience 60:355-366.

Price JL, Stern R (1983) Individual cells in the nucleus basalis--diagonal band complex have restricted axonal projections to the cerebral cortex in the rat. Brain Res 269:352-356.

Rasool CG, Svendsen CN, Selkoe DJ (1986) Neurofibrillary degeneration of cholinergic and noncholinergic neurons of the basal forebrain in Alzheimer's disease. Ann Neurol 20:482-488.

Reimer RJ, Fon EA, Edwards RH (1998) Vesicular neurotransmitter transport and the presynaptic regulation of quantal size. Curr Opin Neurobiol 8:405-412.

Reiner A, Veenman CL, Medina L, Jiao Y, Del Mar N, Honig MG (2000) Pathway tracing using biotinylated dextran amines. J Neurosci Methods 103:23-37.

Resstel LB, Correa FM (2005) Pressor and tachycardic responses evoked by microinjections of L-glutamate into the medial prefrontal cortex of unanaesthetized rats. Eur J Neurosci 21:2513-2520.

Resstel LB, Correa FM (2006) Involvement of the medial prefrontal cortex in central cardiovascular modulation in the rat. Auton Neurosci 126-127:130-138.

Roghani A, Feldman J, Kohan SA, Shirzadi A, Gundersen CB, Brecha N, Edwards RH (1994) Molecular cloning of a putative vesicular transporter for acetylcholine. Proc Natl Acad Sci U S A 91:10620-10624.

Rolls ET, Inoue K, Browning A (2003) Activity of primate subgenual cingulate cortex neurons is related to sleep. J Neurophysiol 90:134-142.

Rossor MN, Garrett NJ, Johnson AL, Mountjoy CQ, Roth M, Iversen LL (1982) A post-mortem study of the cholinergic and GABA systems in senile dementia. Brain 105:313-330.

Rye DB, Wainer BH, Mesulam MM, Mufson EJ, Saper CB (1984) Cortical projections arising from the basal forebrain: a study of cholinergic and noncholinergic components employing combined retrograde tracing and immunohistochemical localization of choline acetyltransferase. Neuroscience 13:627-643.

Sagne C, El Mestikawy S, Isambert MF, Hamon M, Henry JP, Giros B, Gasnier B (1997) Cloning of a functional vesicular GABA and glycine transporter by screening of genome databases. FEBS Lett 417:177-183.

Sakai K, El Mansari M, S. LJ, Zhang G, Vanni-Mercier G (1990) The posterior hypothalamus in the regulation of wakefulness and paradoxical sleep. In: The Diencephalon and Sleep (Mancia M, Marini, G., ed), pp 171-198. New York: Raven Press, Ltd.

Sakurai T (2005) Roles of orexin/hypocretin in regulation of sleep/wakefulness and energy homeostasis. Sleep Med Rev 9:231-241.

Sakurai T, Nagata R, Yamanaka A, Kawamura H, Tsujino N, Muraki Y, Kageyama H, Kunita S, Takahashi S, Goto K, Koyama Y, Shioda S, Yanagisawa M (2005) Input of orexin/hypocretin neurons revealed by a genetically encoded tracer in mice. Neuron 46:297-308.

Sakurai T, Amemiya A, Ishii M, Matsuzaki I, Chemelli RM, Tanaka H, Williams SC, Richardson JA, Kozlowski GP, Wilson S, Arch JR, Buckingham RE, Haynes AC, Carr SA, Annan RS, McNulty DE, Liu WS, Terrett JA, Elshourbagy NA, Bergsma DJ, Yanagisawa M (1998) Orexins and orexin receptors: a family of hypothalamic neuropeptides and G protein-coupled receptors that regulate feeding behavior. Cell 92:573-585.

Saper CB (1984) Organization of cerebral cortical afferent systems in the rat. I. Magnocellular basal nucleus. J Comp Neurol 222:313-342.

Saper CB (1985) Organization of cerebral cortical afferent systems in the rat. II. Hypothalamocortical projections. J Comp Neurol 237:21-46.

Saper CB, Swanson LW, Cowan WM (1979) An autoradiographic study of the efferent connections of the lateral hypothalamic area in the rat. J Comp Neurol 183:689-706.

Saper CB, Chou TC, Scammell TE (2001) The sleep switch: hypothalamic control of sleep and wakefulness. Trends Neurosci 24:726-731.

Sarter M, Givens B, Bruno JP (2001) The cognitive neuroscience of sustained attention: where top-down meets bottom-up. Brain Res Brain Res Rev 35:146-160.

Sarter M, Bruno JP, Givens B (2003) Attentional functions of cortical cholinergic inputs: what does it mean for learning and memory? Neurobiol Learn Mem 80:245-256.

Sassoe-Pognetto M, Fritschy JM (2000) Mini-review: gephyrin, a major postsynaptic protein of GABAergic synapses. Eur J Neurosci 12:2205-2210.

Sassoe-Pognetto M, Panzanelli P, Sieghart W, Fritschy JM (2000) Colocalization of multiple GABA(A) receptor subtypes with gephyrin at postsynaptic sites. J Comp Neurol 420:481-498.

Sassoe-Pognetto M, Utvik JK, Camoletto P, Watanabe M, Stephenson FA, Bredt DS, Ottersen OP (2003) Organization of postsynaptic density proteins and glutamate receptors in axodendritic and dendrodendritic synapses of the rat olfactory bulb. J Comp Neurol 463:237-248.

Sassoe-Pognetto M, Kirsch J, Grunert U, Greferath U, Fritschy JM, Mohler H, Betz H, Wassle H (1995) Colocalization of gephyrin and GABAA-receptor subunits in the rat retina. J Comp Neurol 357:1-14.

Satoh S, Matsumura H, Nakajima T, Nakahama K, Kanbayashi T, Nishino S, Yoneda H, Shigeyoshi Y (2003) Inhibition of rostral basal forebrain neurons promotes wakefulness and induces FOS in orexin neurons. Eur J Neurosci 17:1635-1645.

Schafer MK, Varoqui H, Defamie N, Weihe E, Erickson JD (2002) Molecular cloning and functional identification of mouse vesicular glutamate transporter 3 and its expression in subsets of novel excitatory neurons. J Biol Chem 277:50734-50748.

Schwierin B, Achermann P, Deboer T, Oleksenko A, Borbely AA, Tobler I (1999) Regional differences in the dynamics of the cortical EEG in the rat after sleep deprivation. Clin Neurophysiol 110:869-875.

Semba K (2004) Phylogenetic and ontogenetic aspects of the basal forebrain cholinergic neurons and their innervation of the cerebral cortex. Prog Brain Res 145:3-43.

Semba K, Reiner PB, McGeer EG, Fibiger HC (1989) Brainstem projecting neurons in the rat basal forebrain: neurochemical, topographical, and physiological distinctions from cortically projecting cholinergic neurons. Brain Res Bull 22:501-509.

Sheng M, Pak DT (2000) Ligand-gated ion channel interactions with cytoskeletal and signaling proteins. Annu Rev Physiol 62:755-778.

Shute CC, Lewis PR (1967) The ascending cholinergic reticular system: neocortical, olfactory and subcortical projections. Brain 90:497-520.

Siegel JM (1999) Narcolepsy: a key role for hypocretins (orexins). Cell 98:409-412.

Siegel JM (2004) Hypocretin (orexin): role in normal behavior and neuropathology. Annu Rev Psychol 55:125-148.

Sloviter RS, Dichter MA, Rachinsky TL, Dean E, Goodman JH, Sollas AL, Martin DL (1996) Basal expression and induction of glutamate decarboxylase and GABA in excitatory granule cells of the rat and monkey hippocampal dentate gyrus. J Comp Neurol 373:593-618.

Smith DE, Rapp PR, McKay HM, Roberts JA, Tuszynski MH (2004) Memory impairment in aged primates is associated with focal death of cortical neurons and atrophy of subcortical neurons. J Neurosci 24:4373-4381.

Sotty F, Danik M, Manseau F, Laplante F, Quirion R, Williams S (2003) Distinct electrophysiological properties of glutamatergic, cholinergic and GABAergic rat septohippocampal neurons: novel implications for hippocampal rhythmicity. J Physiol 551:927-943.

Starzl TE, W. TC, Magoun HW (1951) Ascending conduction in reticular activating system, with special reference to the diencephalon. J Neurophysiol 14:461-477.

Steininger TL, Alam MN, Gong H, Szymusiak R, McGinty D (1999) Sleep-waking discharge of neurons in the posterior lateral hypothalamus of the albino rat. Brain Res 840:138-147.

Steriade M (2005) Brain Electrical Activity and Sensory Processing During Waking and Sleep States. In: Principles and Practice of Sleep Medicine, 4th Edition (Kryger MH, Roth T, Dement WC, eds). Philadelphia: Elsevier Saunders.

Sterman MB, Clemente CD (1962a) Forebrain inhibitory mechanisms: cortical synchronization induced by basal forebrain stimulation. Exp Neurol 6:91-102.

Sterman MB, Clemente CD (1962b) Forebrain inhibitory mechanisms: sleep patterns induced by basal forebrain stimulation in the behaving cat. Exp Neurol 6:103-117.

Sternberger LA, Sternberger NH (1983) Monoclonal antibodies distinguish phosphorylated and nonphosphorylated forms of neurofilaments in situ. Proc Natl Acad Sci U S A 80:6126-6130.

Stewart DJ, MacFabe DF, Vanderwolf CH (1984) Cholinergic activation of the electrocorticogram: role of the substantia innominata and effects of atropine and quinuclidinyl benzilate. Brain Res 322:219-232.

Stichel CC, Singer W (1985) Organization and morphological characteristics of choline acetyltransferase-containing fibers in the visual thalamus and striate cortex of the cat. Neurosci Lett 53:155-160.

Swanson LW (1976) An autoradiographic study of the efferent connections of the preoptic region in the rat. J Comp Neurol 167:227-256.

Swanson LW (1992) Brain Maps: Structure of the Rat Brain: Elsevier.

Swanson LW, Sanchez-Watts G, Watts AG (2005) Comparison of melanin-concentrating hormone and hypocretin/orexin mRNA expression patterns in a new parceling scheme of the lateral hypothalamic zone. Neurosci Lett 387:80-84.

Swett CP, Hobson JA (1968) The effects of posterior hypothalamic lesions on behavioral and electrographic manifestations of sleep and waking in cats. Arch Ital Biol 106:283-293.

Szymusiak R, McGinty D (1986a) Sleep suppression following kainic acid-induced lesions of the basal forebrain. Exp Neurol 94:598-614.

Szymusiak R, McGinty D (1986b) Sleep-related neuronal discharge in the basal forebrain of cats. Brain Res 370:82-92.

Szymusiak R, McGinty D (1989) Sleep-waking discharge of basal forebrain projection neurons in cats. Brain Res Bull 22:423-430.

Szymusiak R, Iriye T, McGinty D (1989) Sleep-waking discharge of neurons in the posterior lateral hypothalamic area of cats. Brain Res Bull 23:111-120.

Szymusiak R, Alam N, McGinty D (2000) Discharge patterns of neurons in cholinergic regions of the basal forebrain during waking and sleep. Behav Brain Res 115:171-182.

Taheri S, Zeitzer JM, Mignot E (2002) The role of hypocretins (orexins) in sleep regulation and narcolepsy. Annu Rev Neurosci 25:283-313.

Takamori S, Riedel D, Jahn R (2000) Immunoisolation of GABA-specific synaptic vesicles defines a functionally distinct subset of synaptic vesicles. J Neurosci 20:4904-4911.

Thannickal TC, Moore RY, Nienhuis R, Ramanathan L, Gulyani S, Aldrich M, Cornford M, Siegel JM (2000) Reduced number of hypocretin neurons in human narcolepsy. Neuron 27:469-474.

Turrini P, Casu MA, Wong TP, De Koninck Y, Ribeiro-da-Silva A, Cuello AC (2001) Cholinergic nerve terminals establish classical synapses in the rat

cerebral cortex: synaptic pattern and age-related atrophy. Neuroscience 105:277-285.

van den Pol AN (1991) Glutamate and aspartate immunoreactivity in hypothalamic presynaptic axons. J Neurosci 11:2087-2101.

van den Pol AN (1999) Hypothalamic hypocretin (orexin): robust innervation of the spinal cord. J Neurosci 19:3171-3182.

Van der Gucht E, Jacobs S, Kaneko T, Vandesande F, Arckens L (2003) Distribution and morphological characterization of phosphate-activated glutaminase-immunoreactive neurons in cat visual cortex. Brain Res 988:29-42.

Van Eden CG, Buijs RM (2000) Functional neuroanatomy of the prefrontal cortex: autonomic interactions. Prog Brain Res 126:49-62.

Vazquez J, Baghdoyan HA (2001) Basal forebrain acetylcholine release during REM sleep is significantly greater than during waking. Am J Physiol Regul Integr Comp Physiol 280:R598-601.

Veening JG, Swanson LW, Cowan WM, Nieuwenhuys R, Geeraedts LM (1982) The medial forebrain bundle of the rat. II. An autoradiographic study of the topography of the major descending and ascending components. J Comp Neurol 206:82-108.

Veenman CL, Reiner A, Honig MG (1992) Biotinylated dextran amine as an anterograde tracer for single- and double-labeling studies. J Neurosci Methods 41:239-254.

Verberne AJ, Owens NC (1998) Cortical modulation of the cardiovascular system. Prog Neurobiol 54:149-168.

Vertes RP (2004) Differential projections of the infralimbic and prelimbic cortex in the rat. Synapse 51:32-58.

Villablanca J, Salinas-Zeballos ME (1972) Sleep-wakefulness, EEG and behavioral studies of chronic cats without the thalamus: the 'athalamic' cat. Arch Ital Biol 110:383-411.

von Economo C (1930) Sleep as a problem of localization. The Journal of Nervous and Mental disorders 71.

von Economo C (1931) Encephalitis Lethargica. Its Sequelae and Treatment. London: Oxford University Press.

Wainer BH, Rye DB (1984) Retrograde horseradish peroxidase tracing combined with localization of choline acetyltransferase immunoreactivity. J Histochem Cytochem 32:439-443.

Wainer BH, Bolam JP, Freund TF, Henderson Z, Totterdell S, Smith AD (1984) Cholinergic synapses in the rat brain: a correlated light and electron microscopic immunohistochemical study employing a monoclonal antibody against choline acetyltransferase. Brain Res 308:69-76.

Wang XJ, Tegner J, Constantinidis C, Goldman-Rakic PS (2004) Division of labor among distinct subtypes of inhibitory neurons in a cortical microcircuit of working memory. Proc Natl Acad Sci U S A 101:1368-1373.

Wenk GL (1997) The nucleus basalis magnocellularis cholinergic system: one hundred years of progress. Neurobiol Learn Mem 67:85-95.

West MJ (1993) New stereological methods for counting neurons. Neurobiol Aging 14:275-285.

Winsky-Sommerer R, Boutrel B, de Lecea L (2005) Stress and arousal: the corticotrophin-releasing factor/hypocretin circuitry. Mol Neurobiol 32:285-294.

Wouterlood FG, Jorritsma-Byham B (1993) The anterograde neuroanatomical tracer biotinylated dextran-amine: comparison with the tracer Phaseolus vulgaris-leucoagglutinin in preparations for electron microscopy. J Neurosci Methods 48:75-87.

Wouterlood FG, Vinkenoog M, van den Oever M (2002a) Tracing tools to resolve neural circuits. Network 13:327-342.

Wouterlood FG, Bockers T, Witter MP (2003) Synaptic contacts between identified neurons visualized in the confocal laser scanning microscope. Neuroanatomical tracing combined with immunofluorescence detection of post-synaptic density proteins and target neuron-markers. J Neurosci Methods 128:129-142.

Wouterlood FG, van Haeften T, Blijleven N, Perez-Templado P, Perez-Templado H (2002b) Double-label confocal laser-scanning microscopy, image restoration, and real-time three-dimensional reconstruction to study axons in the central nervous system and their contacts with target neurons. Appl Immunohistochem Mol Morphol 10:85-95.

Wu M, Shanabrough M, Leranth C, Alreja M (2000) Cholinergic excitation of septohippocampal GABA but not cholinergic neurons: implications for learning and memory. J Neurosci 20:3900-3908.

Yamanaka A, Muraki Y, Tsujino N, Goto K, Sakurai T (2003a) Regulation of orexin neurons by the monoaminergic and cholinergic systems. Biochem Biophys Res Commun 303:120-129.

Yamanaka A, Beuckmann CT, Willie JT, Hara J, Tsujino N, Mieda M, Tominaga M, Yagami K, Sugiyama F, Goto K, Yanagisawa M, Sakurai T (2003b) Hypothalamic orexin neurons regulate arousal according to energy balance in mice. Neuron 38:701-713.

Yamuy J, Fung SJ, Xi M, Chase MH (2004) Hypocretinergic control of spinal cord motoneurons. J Neurosci 24:5336-5345.

Yoshida K, McCormack S, Espana RA, Crocker A, Scammell TE (2006) Afferents to the orexin neurons of the rat brain. J Comp Neurol 494:845-861.

Young WS, 3rd, Alheid GF, Heimer L (1984) The ventral pallidal projection to the mediodorsal thalamus: a study with fluorescent retrograde tracers and immunohistofluorescence. J Neurosci 4:1626-1638.

Zaborszky L, Duque A (2000) Local synaptic connections of basal forebrain neurons. Behav Brain Res 115:143-158.

Zaborszky L, Carlsen J, Brashear HR, Heimer L (1986) Cholinergic and GABAergic afferents to the olfactory bulb in the rat with special emphasis on the projection neurons in the nucleus of the horizontal limb of the diagonal band. J Comp Neurol 243:488-509.

Zaborszky L, Gaykema RP, Swanson DJ, Cullinan WE (1997) Cortical input to the basal forebrain. Neuroscience 79:1051-1078.

Zhang W, Sakurai T, Fukuda Y, Kuwaki T (2006) Orexin neuron-mediated skeletal muscle vasodilation and shift of baroreflex during defense response in mice. Am J Physiol Regul Integr Comp Physiol 290:R1654-1663.

Zilberter Y (2000) Dendritic release of glutamate suppresses synaptic inhibition of pyramidal neurons in rat neocortex. J Physiol 528:489-496.

In addition to the manuscript specified above, I want permission to reproduce another JCN accepted paper, of which I am also the first author, but it is still in press.

The title of that work is:
"Innervation of Orexin/Hypocretin Neurons by GABAergic, Glutamatergic or Cholinergic Basal Forebrain Terminals Evidenced by Immunostaining for Presynaptic Vesicular Transporter and Postsynaptic Scaffolding Proteins"; Pablo Henny & Barbara E. Jones

The Copyright Transfer Agreement was received and sent back to John Wiley & Sons, at the beginning of July 2006.

While considering this a vacation period, I would appreciate enormously if you can process this requirement as fast as possible, since the deadline for thesis submission is August 31 2006.

Thank you very much,

Pablo

THE JOURNAL OF COMPARATIVE NEUROLOGY 496:453–467 (2006)

Vesicular Glutamate (VGluT), GABA (VGAT), and Acetylcholine (VAChT) Transporters in Basal Forebrain Axon Terminals Innervating the Lateral Hypothalamus

PABLO HENNY AND BARBARA E. JONES*
Montreal Neurological Institute, McGill University, Montreal, Quebec H3A 2B4, Canada

ABSTRACT

The basal forebrain (BF) is known to play important roles in cortical activation and sleep, which are likely mediated by chemically differentiated cell groups including cholinergic, γ-aminobutyric acid (GABA)ergic and other unidentified neurons. One important target of these cells is the lateral hypothalamus (LH), which is critical for arousal and the maintenance of wakefulness. To determine whether chemically specific BF neurons provide an innervation to the LH, we employed anterograde transport of 10,000 MW biotinylated dextran amine (BDA) together with immunohistochemical staining of the vesicular transporter proteins (VTPs) for glutamate (VGluT1, -2, and -3), GABA (VGAT), or acetylcholine (ACh, VAChT). In addition, we applied triple staining for the postsynaptic proteins (PSPs), PSD-95 with VGluT or Gephyrin (Geph) with VGAT, to examine whether the BDA-labeled varicosities may form excitatory or inhibitory synapses in the LH. Axons originating from BDA-labeled neurons in the magnocellular preoptic nucleus (MCPO) and substantia innominata (SI) descended within the medial forebrain bundle and extended collateral varicose fibers to contact LH neurons. In the LH, the BDA-labeled varicosities were immunopositive (+) for VAChT (~10%), VGluT2 (~25%), or VGAT (~50%), revealing an important influence of newly identified glutamatergic together with GABAergic BF inputs. Moreover, in confocal microscopy, VGluT2+ and VGAT+ terminals were apposed to PSD-95+ and Geph+ profiles respectively, indicating that they formed synaptic contacts with LH neurons. The important inputs from glutamatergic and GABAergic BF cells could thus regulate LH neurons in an opposing manner to stimulate vs. suppress cortical activation and behavioral arousal reciprocally. J. Comp. Neurol. 496:453–467, 2006.

Indexing terms: glutamatergic; GABAergic; cholinergic; BDA; PSD-95; Gephyrin; rat; sleep-wake states

The basal forebrain (BF) plays an important role in the modulation of cortical activity and regulation of sleep-wake states. As known from early studies, it serves as the ventral extrathalamic relay to the cerebral cortex from the brainstem reticular activating and arousal systems (Starzl et al., 1951; Jones, 2005a). Yet, it is also importantly involved in sleep, because lesions of the BF are associated with insomnia (von Economo, 1931; Nauta, 1946; McGinty and Sterman, 1968; Jones, 2005a). These opposing roles could be mediated by chemically differentiated cell groups in the BF that include cholinergic, γ-aminobutyric acid (GABA)ergic, and non-cholinergic/non-GABAergic, presumed glutamatergic, neurons (Gritti et al., 1993, 1994, 1997; Manns et al., 2001). According to multiple lines of evidence, cholinergic neurons actively

Grant sponsor: Canadian Institutes of Health Research; Grant number: CIHR 13458; Grant sponsor: U.S. National Institutes of Health; Grant number: NIH RO1 MH-60119-01A.

*Correspondence to: Barbara E. Jones, Montreal Neurological Institute, McGill University, Montreal, Quebec H3A 2B4, Canada.
E-mail: barbara.jones@mcgill.ca

Received 12 November 2004;Revised 24 March 2005; 8 December 2005
DOI 10.1002/cne.20928
Published online in Wiley InterScience (www.interscience.wiley.com).

stimulate cortical activation during waking and paradoxical sleep (PS, also called rapid eye movement [REM] sleep; Buzsaki et al., 1988; Metherate et al., 1992; Duque et al., 2000; Manns et al., 2000b; Jones, 2004; Lee et al., 2005b). Some putative glutamatergic neurons can act in parallel with the cholinergic neurons in this process (Manns et al., 2003). In contrast, most GABAergic BF neurons are minimally active during cortical activation (Manns et al., 2000a), and, as reflected by c-Fos expression, many are maximally active during sleep (Modirrousta et al., 2004), indicating that they can promote sleep, including slow wave sleep (SWS).

In addition to projections to the cerebral cortex (Gritti et al., 1997), BF neurons give rise to projections to the posterior lateral hypothalamus (LH; Gritti et al., 1994), a region long known to be crucial for waking (von Economo, 1931; Nauta, 1946; Hess, 1957; Swett and Hobson, 1968; Jones, 2005c). Recently, neurons have been localized in the LH that contain the peptide orexin (Orx, also called hypocretin), which is critical for sustaining waking, because absence of the peptide, its receptor, or the Orx neurons results in narcolepsy (Chemelli et al., 1999; Lin et al., 1999; Peyron et al., 2000; Thannickal et al., 2000).

Although previous studies combining retrograde transport with immunohistochemical staining for neurotransmitter enzymes indicated that cholinergic, GABAergic, and other BF neurons project to the LH (Gritti et al., 1994), they did not reveal the efferent BF fibers projecting into the LH nor did they prove the use of acetylcholine (ACh), GABA, or, as proposed, glutamate as neurotransmitters by the projection neurons. Recently, proof of the uptake, storage, and release of specific neurotransmitters has become possible by immunohistochemical staining for specific vesicular transporter proteins (VTPs), including those for ACh (VAChT; Gilmor et al., 1996), GABA (VGAT; Chaudhry et al., 1998) and glutamate (VGluT1, -2, and -3; Fremeau et al., 2001, 2002; Fujiyama et al., 2001). We thus combined anterograde transport of 10,000 MW biotinylated dextran amine (BDA) with immunohistochemical staining for VAChT, VGluT (1, 2, and 3), and VGAT to determine whether cholinergic, glutamatergic, or GABAergic neurons located in the magnocellular preoptic nucleus (MCPO) and substantia innominata (SI) project to the LH. To assess whether the VGluT+ and VGAT+ varicosities form synapses in the LH, we employed triple immunostaining for the postsynaptic proteins (PSPs) PSD-95, a marker for excitatory synapses (Sheng and Pak, 2000), or Gephryin (Geph), a marker for inhibitory synapses (Sassoe-Pognetto and Fritschy, 2000; Sassoe-Pognetto et al., 2000).

Abbreviations

ac	anterior commissure
BDA	biotinylated dextran amine
BF	basal forebrain
cp	cerebral peduncle
DMH	dorsomedial hypothalamus
f	fornix
FS	fundus striatum
Geph	Gephyrin
LH	lateral hypothalamus
LPO	lateral preoptic area
MCPO	magnocellular preoptic nucleus
MPO	medial preoptic nucleus
oc	optic chiasm
ot	optic tract
Pir	piriform cortex
PSD-95	< postsynaptic density
SI	substantia innominata
SO	supraoptic nucleus
VAChT	vesicular acetylcholine transporter
VGAT	vesicular γ-aminobutyric acid transporter
VGluT2	vesicular glutamate transporter 2
VMH	ventromedial hypothalamic nucleus
ZI	zona incerta

MATERIALS AND METHODS

Animals and Surgery

All procedures conformed to the guidelines of the Canadian Council on Animal Care and the U.S. National Institutes of Health and were approved by the McGill University Animal Care Committee.

Long-Evans rats (200–250 g, Charles River Canada, St. Constant, Quebec, Canada) were anesthetized with ketamine/xylazine/acepromazine (65/5/1 mg/kg, i.p.) and placed in a stereotaxic frame (David Kopf Instruments, Tujunga, CA) for surgery. Anesthesia level was monitored during the experiment and augmented by boosters if necessary. Because previous studies based on retrograde as well as anterograde tracing showed no evidence of contralateral projections from the BF to the LH (Swanson, 1976; Gritti et al., 1994), injections of BDA were done on left and right sides of each brain. Holes were drilled in the skull, and the *dura mater* was removed on each side over the BF. Glass micropipettes (tip diameter 15–25 μm) were back-filled with a 0.5 M NaCl solution containing 2% 10,000 MW BDA (BDA-10,000, Molecular Probes, Eugene, OR). With the aid of a micropositioner (model 660, David Kopf Instruments), a BDA-filled pipette was lowered into the BF on each side aimed at the magnocellular preoptic nucleus (MCPO; from Bregma: anterior-posterior [AP], −0.5 lateral [L], ±2.5 mm; vertical [V], 8.5 mm). A holding current of −300 nA was maintained (using a Microiontophoresis Dual Current Generator 260, World Precision Instruments [WPI], Sarasota, FL) during the descent to avoid leakage of the solution. Once the pipette was in the targeted site, microinjection of BDA was performed by iontophoresis applying positive current pulses (5–10 μA) in a duty cycle of 1 second (0.5 seconds on, 0.5 seconds off) for a period of 25–30 minutes through a stimulator (Pulsemaster A300, WPI) and stimulus isolation unit (Iso-Flex, A.M.P.I., Jerusalem, Israel). After the injection, the micropipette was held in place for 10 minutes and removed during renewed application of the holding current.

Rats were maintained for 5 or 6 days with food and water ad libitum to allow anterograde transport of the tracer. They were subsequently perfused transcardially under deep sodium pentobarbital anesthesia (100 mg/kg, i.p.) with ~500 ml 4% paraformaldehyde fixative solution. The brains were removed and put in a 30% sucrose solution for 2–3 days or until they sank, after which they were frozen at −50°C and stored at −80°C for subsequent processing.

Immunohistochemistry

Sections were cut by using a freezing microtome in 25-μm-thick coronal sections and collected in eight adjacent series at 200-μm intervals through the forebrain, including the magnocellular BF area and the tuberal-posterior hypothalamus. Series were processed for evalu-

ation of the BDA injection site in the BF and BDA-labeled fibers in the LH by light microscopy. For this purpose, the avidin-biotin complex (ABC) procedure was performed by using the Vectastain ABC Elite kit (Vector, Burlingame, CA) with nickel-intensified diaminobenzidine (DAB-Ni) and combined with a Nissl counterstain using neutral red (NR).

Adjacent series containing the tuberal-posterior LH region were processed for double or triple fluorescent staining (Table 1). Prior pilot studies were performed to determine the conditions necessary for antibody as well as streptavidin penetration through the full depth of the sections. As viewed through the z-axis under epifluorescent and confocal microscopy, we established that 0.1 or 0.3% Triton X-100 (TX) allowed full penetration of antibodies and streptavidin through 25-μm-thick sections in double- or triple-stained series, respectively. Free-floating sections from each series were rinsed for 30 minutes in Trizma saline buffer (TS; 0.1 M, pH 7.4) followed by incubation for 30 minutes with a blocking solution of normal donkey serum (NDS; 6% in TS) containing TX (0.1 or 0.3%). Subsequent incubations and rinses (30 minutes between incubations) were done by using TS containing NDS (1%) and TX (0.1 or 0.3%). Incubations were performed at room temperature overnight with primary antibodies and for 3 hours with secondary antibodies or streptavidin.

For double labeling of BDA and one of the VTPs, sections were incubated (by using 0.1% TX) first with primary antibodies against VAChT, VGluT1, -2, or -3, or VGAT (from various species) and then with appropriate Cy3-conjugated secondary antibodies (from donkey [Dky]) followed by Cy2-conjugated streptavidin for revelation of BDA (see Table 1, Double BDA/VTP).

For double labeling of two VTPs, sections were incubated (by using 0.1% TX) with two primary antibodies against VAChT, VGluT2, and/or VGAT (from different species) and then with appropriate Cy2- and Cy3-conjugated secondary antibodies (from Dky) (see Table 1, Double VTP/VTP).

For triple labeling of BDA, the VTPs, and the PSPs, sections were incubated (by using 0.3% TX) with two primary antibodies against VGluT2 or VGAT and PSD-95 or Geph, respectively (from different species) and then with appropriate Cy3 or Cy5 secondary antibodies (from Dky). They were subsequently incubated with Cy2-conjugated streptavidin for revelation of BDA (see Table 1, Triple BDA/VTP:PSP).

All sections were mounted out of Trizma water, and the mounted sections were dehydrated through alcohols, cleared in xylene, and coverslipped with Permount.

Conventional microscopy, tracing, and stereological analysis

Sections were examined under light and epifluorescent microscopy with a Leica DMLB microscope or Nikon Eclipse E800 equipped with x-y-z motorized stages, a video or digital camera, and filters appropriate for fluorescein isothiocyanate (FITC) (or Cy2), Rhodamine (or Cy3), and (on the Nikon) Cy5 fluorescence. Single as well as composite images were acquired, and drawings were made by using Neurolucida software (MicroBrightField [MBF], Colchester, VT). Cells and varicosities were counted by using the Optical Fractionator probe of Stereo Investigator software (MBF). For tracing or counting, a computer resident atlas of the rat brain was employed that was developed and applied in our laboratory by using standardized procedures for tissue processing (Gritti et al., 1993, 1994). For each application, series of histology sections are matched to appropriate levels of the atlas (at 400-μm intervals) under low magnification (5 or 10× objective). At each level, the atlas image is then rotated if necessary, and the contours are adjusted to fit the relevant nuclei of the histology section optimally.

Injection sites from eight rats (BDA 14, 15, 16, 18, 19, 20, 21, and 22) were examined under brightfield illumination in DAB-Ni-stained material. In 14 cases, the labeled cells were centered in the MCPO-SI (on the left and/or right sides). From these, five injection sites ("cases" on the left and/or right sides) from three rats (BDA 16, 18, and 19) were selected for quantitative estimate of the cells in the injection sites. From the 14 cases, innervation of the LH was studied qualitatively and quantitatively in DAB-Ni and fluorescent stained material (see text and Table 1).

Under brightfield illumination, unbiased estimates of the total number of DAB-Ni-stained, BDA-labeled nerve cell bodies were performed by using the Optical Fractionator probe of Stereo Investigator. Cells were counted within contours of the BF and surrounding nuclei, including the MCPO, SI, nucleus of the diagonal band of Broca (DBB), olfactory tubercle (OTu), lateral preoptic area (LPO), fundus of the striatum (FS), piriform cortex (Pir), nucleus of the lateral olfactory tract (LOT), and anterior amygdaloid area (AA). Counts were made under a 60× oil objective (with 1.40 numerical aperture [NA]) through six or seven BF levels (at 200-μm intervals) by using an x-y sampling grid size (of 120 × 120 μm) that was equal to the counting frame size, so as to sample 100% of each area. Counting was performed through 10 μm in the z-axis (starting 1 μm from the surface in mounted sections having an average of ~12-μm thickness following dehydration). Following the stereological procedures imposed in Stereo Investigator, cells were counted if their tops were contained within the defined counting block.

Projections of the DAB-Ni-stained, BDA-labeled axons were examined through the tuberal-posterior LH and in relation to NR stained neurons viewed under brightfield illumination. The axons and neurons were drawn by using a 100× oil objective within a contour of the LH using Neurolucida software (MBF).

Given evidence for contacts of BF fibers on LH neurons, the total number of NR stained neurons that were or were not contacted by one or more DAB-Ni-stained, BDA+ varicosities (NR+:BDA+ or NR+:BDA−) was estimated by using the Optical Fractionator probe through the LH (n = 3 cases). Counts were performed under a 100× oil objective (1.4 NA) on the Nikon microscope. The cells were sampled in the LH, as defined in the computer resident atlas, through three levels separated by 400-μm intervals (5,800, 6,200, and 6,600 μm anterior [A] to interaural zero [IA0]). The sampling grid size (210 × 210 μm) was set to be larger than the counting frame (70 × 70 μm) so as to sample ~11% of the LH area. Counting was performed through 16 μm of the section thickness (starting 1 μm from the surface of the mounted sections, which had an average thickness of ~19 μm following their minimal dehydration and differentiation for NR). As above, cells were counted if their tops were contained within the defined counting block.

TABLE 1. List of Primary and Secondary Antibodies Used for Fluorescence Staining of Biotinylated Dextran Amine (BDA), Vesicular Transporter Proteins (VTPs) and Postsynaptic Proteins (PSPs)

	1ry AB (overnight)							2ry AB (3 hours)		SA (3 hours)		
Series	Antigen	Host	Dilution	Source	Cat. #	Immunogen	Specificity	IgG (Dky)[17,18]	Dilution	SA[17]	Dilution	n[19]
Double BDA VTP	VAChT	Gt	1:5000	Chemicon[1]	AB1578	Synthetic peptide corresponding to C-terminus of cloned rat VAChT[6] (CSPP GPFDGCEDDYNYYSRS)[7]	By WB the AB recognizes a ≈65–70 kD band corresponding to VAChT protein[4]	Anti-Gt-Cy3	1:800	SA-Cy2	1:800	8
	VAChT	Rb	1:1000	Sigma[2]	V5387	Synthetic peptide corresponding to AA 512–530 of C-terminus of cloned rat VAChT (K-SPPGPFDGCEDDYNYYSRS)[8]	By WB the AB recognizes a ≈67–70 kD band, corresponding to VAChT protein[7]	Anti-Rb-Cy3	1:800	SA-Cy2	1:800	9
	VGluT1	Rb	1:1000	Gift RHE[3]	–	Synthetic peptide corresponding to 68 last AA of C-terminus of rat BNPi (VGluT1)[9]	By WB the AB recognizes a ≈62 kD band from rat brain[9]	Anti-Rb-Cy3	1:800	SA-Cy2	1:800	4
	VGluT2	Rb	1:5000	Gift RHE	–	Synthetic peptide corresponding to 64 last AA of C-terminus of rat DNPi (VGluT2)[10]	By WB the AB recognizes a ≈50–62 kD band from rat brain[10]	Anti-Rb-Cy3	1:800	SA-Cy2	1:800	14
	VGluT3	GP	1:1000	Chemicon	AB5421	Synthetic peptide from cloned rat VGluT3 protein[11] (AFEGEEPLSYQNEEDFSETS)[7]	The AB labels VGluT3 + cells and fibers, in agreement with other VGluT3 antisera[11]	Anti-GP-Cy3	1:800	SA-Cy2	1:800	7
	VGAT	Rb	1:250	Chemicon	AB5062P	Synthetic peptide corresponding to a 17 AA peptide near C-terminus region of rat VGAT[12] (VHSLEGLIEAYRTNAED)[7]	By WB the AB recognizes a band at ≈55–60 kD[12]	Anti-Rb-Cy3	1:800	SA-Cy2	1:800	14
Double VTP	VAChT/	Gt	1:5000	Chemicon	AB1578	(above)	(above)	Anti-Gt-Cy3	1:800			4
VTP	VGluT2	Rb	1:5000	Gift RHE	-	(above)	(above)	Anti-Rb-Cy2	1:200			
	VAChT/	Gt	1:5000	Chemicon	AB1578	(above)	(above)	Anti-Gt-Cy3	1:800			4
	VGAT	Rb	1:250	Chemicon	AB5062P	(above)	(above)	Anti-Rb-Cy2	1:200			
	VGAT/	Rb	1:250	Chemicon	AB5062P	(above)	(above)	Anti-Rb-Cy2	1:200			4
	VGluT2	GP	1:5000	Chemicon	AB5907	Synthetic peptide from cloned rat VGluT2 protein[13] (VQESAQDAYSYKDRDDYS)[7]	The AB gives labeling in agreement with other antisera to VGluT2[13]	Anti-GP-Cy3	1:800			
Triple BDA VTP PSP	VGluT2/	Rb	1:5000	Gift RHE	-	(above)	(above)	Anti-Rb-Cy5	1:800	SA-Cy2	1:800	3
	PSD-95	Ms	1:100	ABR[4]	MA1-045	Purified recombinant of rat PSD-95[14]	The AB detects post synaptic density 95kD in rat brain. By WB it recognizes a ≈95 kDa band[14]	Anti-Ms-Cy3	1:800	SA-Cy2	1:800	
	VGAT/	Rb	1:250	Chemicon	AB5062P	(above)	(above)	Anti-Rb-Cy5	1:800	SA-Cy2	1:800	3
	Geph	Ms	1:100	SY-SY[5]	147 011	Purified rat gephyrin[15]	By WB the AB recognizes a ≈93 kD band. It detects a N-terminus epitope[16]	Anti-Ms-Cy3	1:800	SA-Cy2	1:800	

[1]Chemicon: Chemicon International, Temecula, CA
[2]Sigma: Sigma, St. Louis, MO
[3]Gift from Edwards, R.H. and Fremeau, R.T. Jr.
[4]ABR: Affinity BioReagents, Golden, CO.
[5]SY-SY: Synaptic Systems, Göttingen, Germany.
[6]http://www.chemicon.com/Product/ProductDataSheet.asp?ProductItem=AB1578
[7]Supplied by Chemicon on request
[8]http://www.sigmaaldrich.com/sigma/datasheet/v5387dat.pdf
[9]Bellocchio et al., 1998
[10]Fremeau et al., 2001
[11]http://www.chemicon.com/Product/ProductDataSheet.asp?ProductItem=AB5421
[12]http://www.chemicon.com/Product/ProductDataSheet.asp?ProductItem=AB5062P
[13]http://www.chemicon.com/product/productdataSheet.asp?ProductItem=AB5907
[14]http://www.bioreagents.com/index.cfm/fuseaction/products.print/Product/MA1-045
[15]http://www.sysy.com/gephyrin/gephy_fs.html
[16]Pfeiffer et al., 1984
[17]Jackson Immuno Research Laboratories, West Grove, PA.
[18]For multiple labeling (ML) with minimal cross-reactivity (min X) to other species.
[19]n, number of cases (each case referring to an injection site and series from the same side of the brain, thus 1 or 2 per brain).

AA, amino acid; AB, antibody; BNPi, brain specific Na^+-dependent phosphate transporter; Cat., catalog; Cy2, cyanine; Cy3, indocarbocyanine; Cy5, indodicarbocyanine; Dky, donkey; DNPi, differentiation-associated Na^+-dependent phosphate transporter; Geph, gephyrin; GP, guinea pig; Gt, goat; Ms, mouse (monoclonal); Rb, rabbit; SA, streptavidin; WB, western blot.

Under epifluorescent illumination, fluorescent stained BDA-positive (+) varicosities were examined for double labeling with the VTPs in the LH. After double labeling with VAChT, VGluT2, and VGAT was found, unbiased estimates of the total numbers of single BDA+ and double-labeled BDA+/VAChT+, BDA+/VGluT2+, or BDA+/VGAT+ varicosities were estimated in the LH for each series by using the Optical Fractionator probe of Stereo Investigator. In five cases analyzed per series in stereology, all VTPs were stained by using antibodies raised in rabbit (Rb; VAChT, VGluT2, and VGAT; see Table 1). Counts were performed under a 100× oil objective (with 1.40 NA) on the Leica microscope. The varicosities were sampled in the LH, as defined in the computer resident atlas, through three levels separated by 400-μm intervals (A 5,800, A 6,200, and A 6,600) of the tuberal-posterior LH (in four cases per series; Table 2). The sampling grid size (180 × 180 μm) was set to be larger than the counting frame (90 × 90 μm) so as to sample 25% of the LH area. Counting was performed through 8 μm of the section thickness (starting 1 μm from the surface of the mounted sections having an average thickness of ~12 μm following dehydration). In each counting block and frame, all BDA+ varicosities (in green, Cy2) were counted, including those that were and were not double-labeled for the VTP (in red, Cy3) to obtain an estimate of the proportion of double-labeled varicosities for each VTP.

Double labeling for VAChT, VGluT2, and/or VGAT was assessed under epifluorescent illumination on the Leica microscope (in four cases per series; Table 1). In the absence of any double labeling, no quantification was undertaken.

Confocal microscopy and image processing

To examine the presence of PSPs in association with BDA+/VTP+ varicosities, triple-stained sections were analyzed by confocal microscopy with a Zeiss LSM 510 laser scanning microscope equipped with Argon 488 nm, helium-neon 543 nm, and helium-neon 633 nm lasers for Cy2, Cy3, and Cy5 excitation as well as with appropriate filters for detection of Cy2 (bandpass 500–530 nm, green), Cy3 (bandpass 565–615 nm, red), and Cy5 (bandpass 697–719 nm, infrared). Scanning was performed through a Plan-Apochromat 100× (with 1.40 NA) objective and pinhole size of 1 (Airy Units) for each of the three channels. Images were acquired for the three chromogens by using the resident LSM 510 software and consisted of stacks taken through the z-axis in optical slices of ~0.33 μm. Rendered 3D views of the image stacks were obtained by using the image software Volocity 3.5.1 (Improvision, Lexington, MA, www.improvision.com), which allowed interactive visualization, magnification, and rotation of the 3D images in order to determine the relative location of each of the elements from the three channels.

In some images, a deconvolution procedure or iterative restoration in Volocity was applied by using a 95% confidence level in order to maximize the signal-to-noise ratio and assess relationships among elements better in the triple-stained material. As assessed in three cases per series (Table 1), contacts between VTP+/BDA+ varicosities and PSP+ profiles were evaluated in the rotated images and validated by lack of separation between the pre- and postsynaptic elements.

Adjustments for brightness and contrast in brightfield images and tonal range for each individual RGB channel

TABLE 2. Proportion of VAChT+, VGluT2+ and VGAT+ BDA-labeled BF Axonal Varicosities in the LH Region Based on Stereological Estimates[1]

	VAChT series			VGluT2 series			VGAT series			VTP series
Cases	BDA + var.	BDA+/VAChT+ var.	% VAChT+ var.	BDA + var.	BDA+/VGluT2+ var.	% VGluT2+ var.	BDA + var.	BDA+/VGAT+ var.	% VGAT + var.	ANOVA F-ratio
BDA15-L	38,080	4,640	12.2	-	-	-	-	-	-	
BDA15-R	17,920	1,040	5.8	-	-	-	-	-	-	
BDA16-L	18,800	2,640	14.0	27,040	5,600	20.7	23,440	11,280	48.1	
BDA18-L	17,840	2,000	11.2	10,800	2,080	19.3	17,680	8,240	46.6	
BDA18-R	15,120	960	6.3	11,680	2,640	22.6	17,120	8,160	47.7	
BDA19-L	-	-	-	18,824	6,136	32.6	20,176	10,504	52.1	
BDA19-R	-	-	-	19,032	3,432	18.0	16,536	6,864	41.5	
Mean ± SEM	**21,552 ± 4,178**	**2,256 ± 673**	**9.9 ± 1.6**	**17,475 ± 2,946**	**3,978 ± 806**	**22.6 ± 2.6**	**18,990 ± 1,274**	**9,010 ± 816**	**47.2 ± 1.7**	**87.3*****

[1]Data for individual cases (1 or 2 sides from 4 rat brains) is presented together with the mean ± SEM. Estimated numbers of varicosities were obtained by sampling from 3 sections (at levels, A 5800, A 6200 and A 6600), per series per case. The proportions of the three VTP+ varicosities differed significantly (***, $P < 0.001$ according to one-way ANOVA) across and between VTP+ varicosities (with $P < 0.05$ according to post-hoc Bonferroni-corrected multiple-comparisons). var., varicosities; VTP, vesicular transporter protein.

("Adjust/levels" command in Photoshop) in fluorescent images were performed with Adobe Photoshop Creative Suite edition (Adobe Systems, San Jose, CA).

RESULTS

BDA injection site and cellular labeling

Iontophoretic application of BDA-10,000 into the region of the magnocellular preoptic area and substantia innominata (MCPO-SI, Fig. 1A) produced a small and well-restricted, spherical injection site (Fig. 1B) containing labeled cell bodies and dendrites (Fig. 1C). The injection sites ranged in size from 300 to 500 μm in diameter and were consistently located primarily within the MCPO and secondarily in the overlying SI (n = 11 injection sites).

To appraise the number of cells labeled and their precise location in BF nuclei, stereological estimates were obtained through the BF. The average number of BDA-labeled neurons per injection was ~1,400 (mean ± SEM, 1,430.6 ± 315, n = 5 injection sites). The labeled cells were almost exclusively (96.2 ± 1.7%; range, 90–100%) located within the MCPO (90.2%) and SI (6.0%). A few scattered cells were variably found in immediately adjacent regions including the olfactory tubercle, lateral olfactory tract nucleus, or anterior amygdaloid area (3.5 ± 1.8%). Isolated cells were found in the nearby fundus of the striatum or piriform cortex in some cases. No labeled cells were seen in the more rostral DBB. No labeled cells were seen in distant regions known to project to the MCPO-SI, including the prefrontal cortex or, importantly, the LH, indicating a lack of retrograde transport of the BDA-10,000 in these afferent systems.

BDA was found within axons in the diencephalon (n = 14 cases) and in cortical and subcortical telencephalic regions where different MCPO-SI neurons are known to project from retrograde (Gritti et al., 1994, 1997) and other anterograde tracing studies (Luiten et al., 1987; Grove, 1988).

BDA-labeled fibers and varicosities in the LH

In the diencephalon, thick fascicles of fibers were evident in the ventrolateral posterior LH (Fig. 2A). From these coarse fibers, collateral fine fibers extended out through the LH. Some fibers continued sparsely into the perifornical area, but most remained within the LH. The fine fibers bore varicosities along their axons (boutons en passant, Fig. 2B′) or occasionally at the end of their axons (boutons terminaux, Fig. 2B″). Although many varicose axons did not appear to contact nerve cell bodies in the region (Fig. 2B′), a significant number did appear to do so, innervating either small (Fig. 2B″) or large (Fig. 2B‴) neurons by varicose processes that could entirely envelop the soma. To visualize the fiber distribution and innervation of nerve cell bodies better within the LH, high-magnification tracing of the DAB-Ni-stained axons and neutral red (NR+) stained cells was performed. As seen in Figure 2C, the major axon fascicles were seen to course within the ventrolateral part of the medial forebrain bundle (MFB) from which they extended fine varicose fibers to contact and sometimes entirely surround cells in ventral, central, and dorsal portions of the LH (Fig. 2D′,D″,D‴).

To appraise the extent of the innervation of neurons in the LH, stereological estimates were obtained of the num-

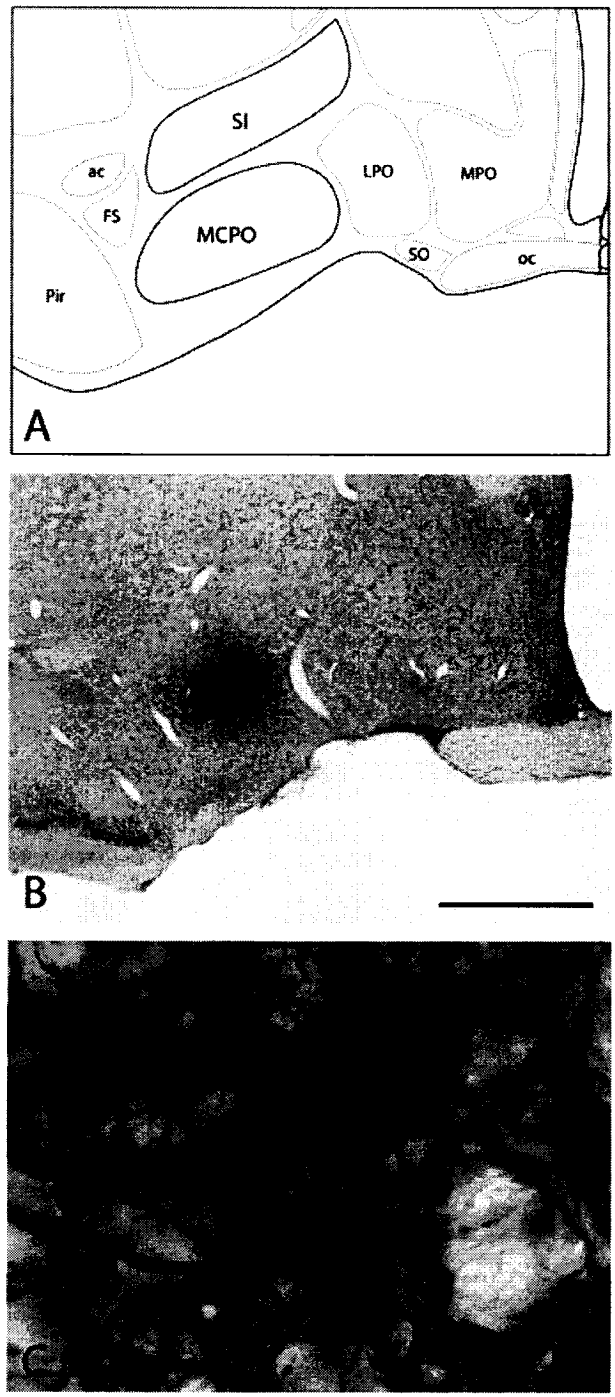

Fig. 1. BF site of BDA injection. **A:** Atlas section through the cholinergic cell area (MCPO-SI) where iontophoretic applications of BDA were placed. **B:** Composite image of typical BDA injection site (case BDA18-R, processed by using ABC with DAB-Ni and counterstained with neutral red). Note the small size and restricted location of BDA-labeled cells in the MCPO. **C:** High-magnification image of two BDA-labeled neurons (from B, arrowheads). Brightness and contrast were adjusted in B and C. For abbreviations, see list. Scale bar = 1 mm in B; 20 μm in C.

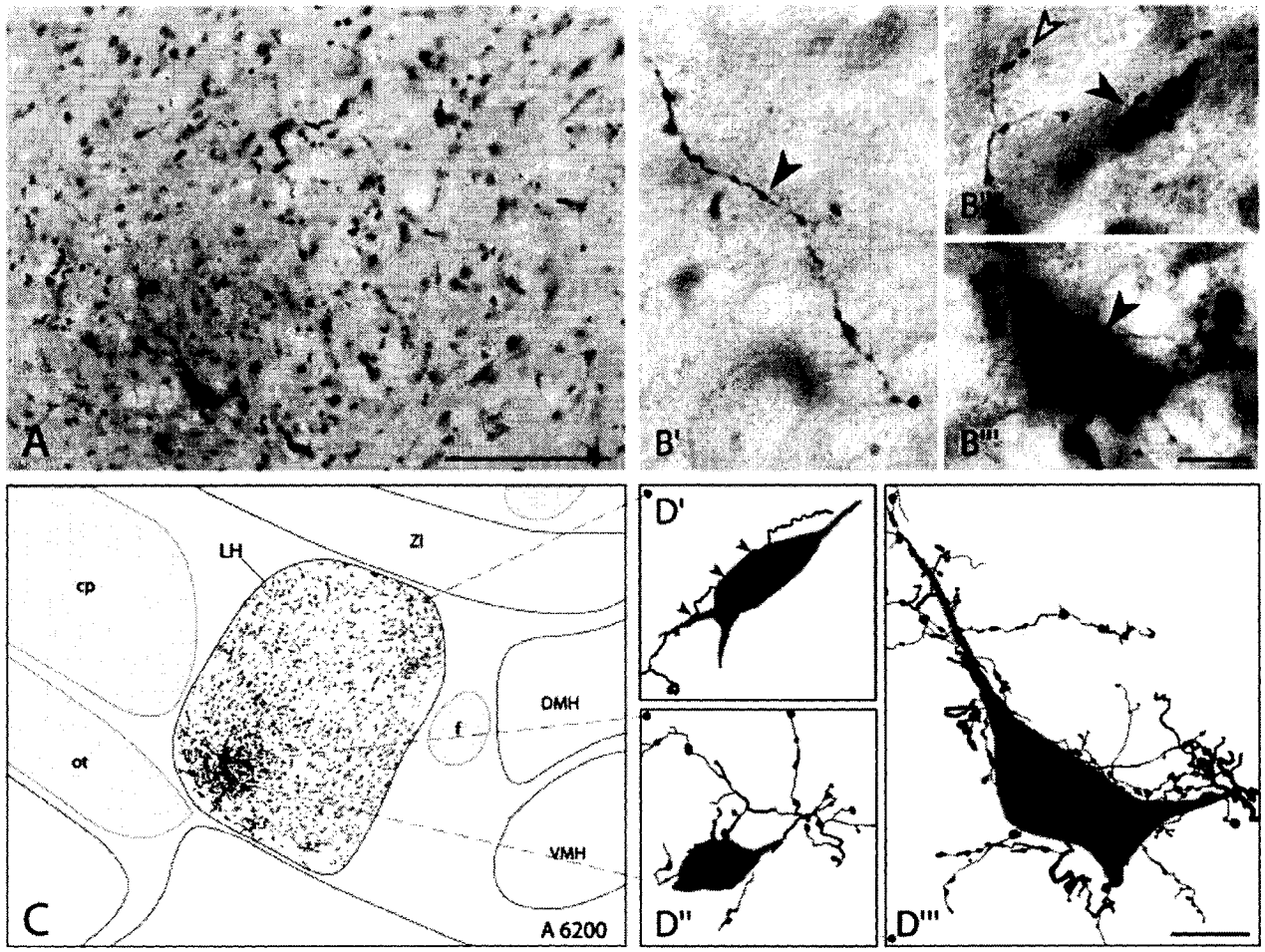

Fig. 2. BDA-labeled fibers in the LH. **A:** Low-magnification composite image of BDA+ axons (in black, DAB-Ni) and neutral red stained (NR+) cells in the LH (case BDA19-L). **B:** High-magnification images showing BDA+ axons and terminals within the LH area. Varicosities appeared most commonly along axons as boutons en passant (solid arrowhead in B') but also at the end of axons as boutons terminaux (open arrowhead in B''). Many axonal varicosities (stained with DAB-Ni) were seen in the neuropil (B') or in close proximity to small (solid arrowhead in B'') or large (solid arrowhead in B''') nerve cell bodies (stained with NR, B' and B'', case BDA15-L; B''', case BDA19-L). **C:** Tracing of BDA+ axons and NR+ neurons in the LH at ~6,200 μm (from IA0, case BDA19-L). Although concentrated more ventrally, fibers extended through the LH area and formed appositions with neurons therein (D). **D:** High-magnification tracing of elements in C showing the relationship of BDA+ axons with dorsally (solid arrowheads in D'), as well as more ventrally (D'' and D''') located NR+ neurons. (The neuron in D''' corresponds to that pictured in B'''.) Tonal ranges for each RGB channel as well as brightness and contrast adjustments were made for pictures in A and B. For abbreviations, see list. Scale bar = 100 μm in A; 10 μm in B,D.

ber and proportion of LH cells ostensibly contacted by BDA-labeled varicosities in the light microscope images. In three cases, the NR+ cells that were contacted (NR+:BDA+) together with those that were not contacted (NR+:BDA−) were counted in random sampling through three levels of the LH (~A 5,800, A 6,200, and A 6,600). The number of contacted cells (NR+:BDA+ = 8,027 ± 3,639 neurons) corresponded to ~14% (14.4 ± 5.3%) of the total number of NR+ cells (NR+:BDA+ plus NR+:BDA− = 52,495 ± 5,611 neurons) estimated in the LH.

VAChT, VGluT, and VGAT within BDA-labeled varicosities in the LH

Series that were double stained for BDA and the VTPs were examined to determine whether BF axonal varicosities in the LH were immunopositive (+) for VAChT, VGluT, or VGAT.

VAChT+ varicosities were relatively sparse in the LH. Nonetheless, some BDA-labeled terminals were double-labeled for VAChT (Fig. 3A). The BDA+/VAChT+ varicosities were most often located along axons (Fig. 3A',A'',A''').

Both VGluT1+ (not shown) and VGluT2+ varicosities were densely distributed through the LH, although the VGluT2 most densely so. VGluT3+ varicosities were also present although sparse (not shown). In adjacent series processed for BDA and VGluT1, -2, or -3, only VGluT2 was found to be present in BDA-labeled varicosities (Fig. 3B). The BDA+/VGluT2+ varicosities most frequently appeared to be boutons en passant (Fig. 3B',B'',B'''), although some appeared to be boutons terminaux.

Varicosities that were VGAT+ were densely distributed within the LH area. Many of the BDA-labeled axonal varicosities were VGAT+ (Fig. 3C). The BDA+/VGAT+ varicosities were most commonly boutons en passant (Fig.

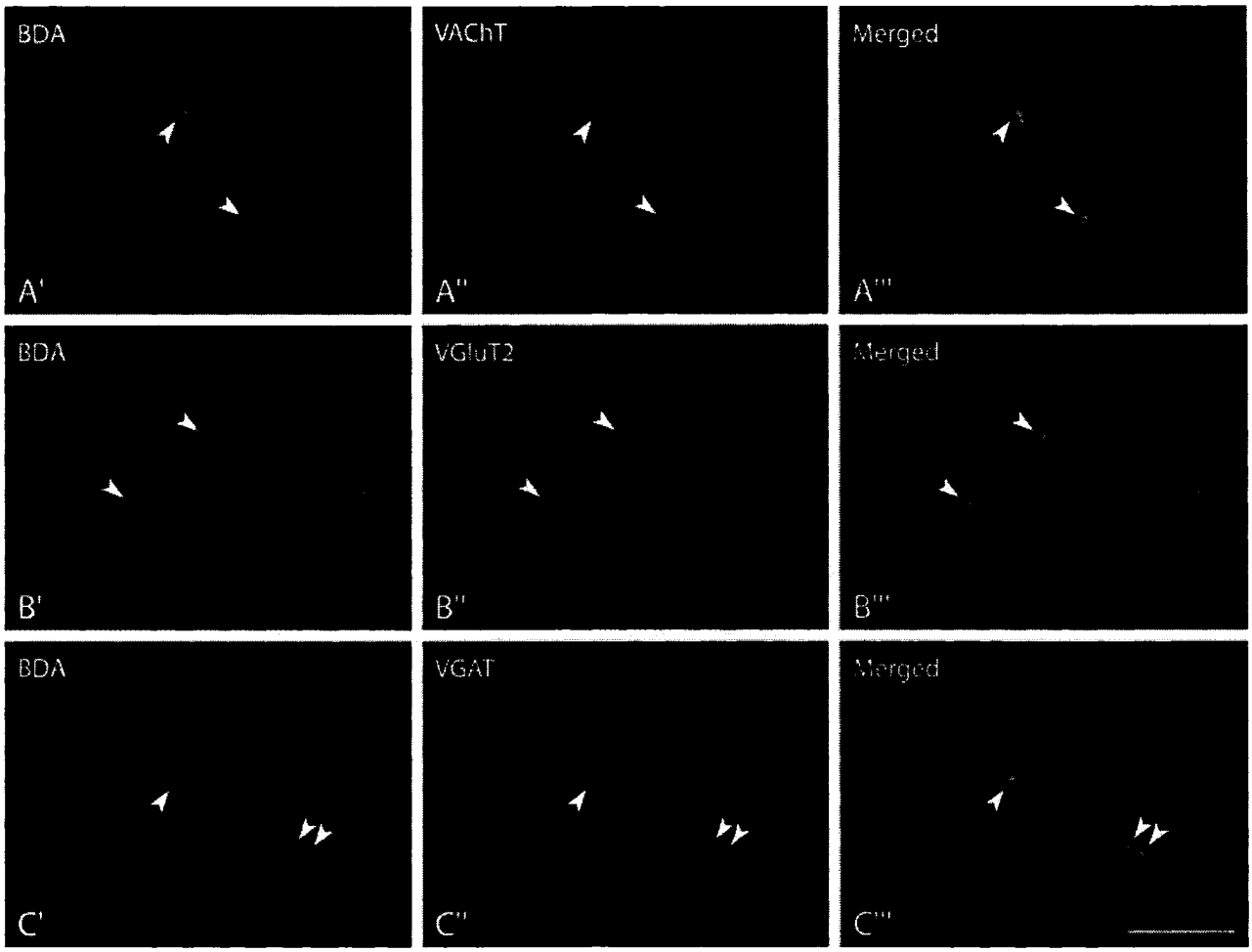

Fig. 3. BDA-labeled axons in LH contain VAChT, VGluT2, or VGAT. High-magnification epifluorescent images illustrating anterogradely labeled BDA+ axons (A', B', and C', green fluorescent Cy2) that are double-labeled for vesicular transporter proteins (VTPs) as shown in single (A'', B'', and C'', red fluorescent Cy3) and merged (right A''', B''', and C''', yellow) images and indicated by white arrowheads for those that are in focus. **A:** BDA+ varicose fiber (A') whose varicosities are positive for VAChT (A'' and A'''). **B:** BDA+ varicose axon (B') whose varicosities are positive for VGluT2 (B'' and B'''). **C:** BDA+ axon (C') whose varicosities are positive for VGAT (C'' and C'''). Tonal range in red and green channels was adjusted individually (see Materials and Methods). For abbreviations, see list. Scale bar = 10 μm in C''' (applies to A'–C''').

3C',C'',C'''), although some appeared to be boutons terminaux.

Double staining for different VTPs was subsequently examined (n = 4 cases per series) to determine whether they might be colocalized in the BF terminals. Double labeling for VAChT/VGluT2, VAChT/VGAT, or VGluT2/VGAT was not detected in varicosities of the LH (not shown). These negative results indicated that multiple VTPs are not colocalized in the same BF axonal varicosities innervating the LH.

Proportion and distribution of VAChT+, VGluT2+, and VGAT+ BDA-labeled varicosities

To determine the proportions of cholinergic, glutamatergic, and GABAergic BF axon terminals, stereological analysis was used for estimation of the total numbers of BDA+ and BDA+/VTP+ varicosities in the tuberal-posterior LH (~A 5,800, A 6,200, and A 6,600; Table 2). In the double-stained VAChT series, ~10% of the BDA+ varicosities were BDA+/VAChT+. In the VGluT2 series, ~23% of BDA+ varicosities were BDA+/VGluT2+. In the VGAT series, ~47% of the BDA+ varicosities were BDA+/VGAT+.

As evident in plots of the sampled BDA+/VAChT+, BDA+/VGluT2+, and BDA+/VGAT+ (Fig. 4, representing ~25% of the estimated total number of varicosities), the three types of terminals were codistributed across the LH. The three were commonly most dense within the ventral and central portions of the LH, although they were also scattered through more dorsal portions of the LH.

PSD-95 or Geph in relation to BDA+/VGluT2+ or BDA+/VGAT+ terminals

To assess whether PSPs were present in association with the numerous BDA+/VGluT2+ or BDA+/VGAT+

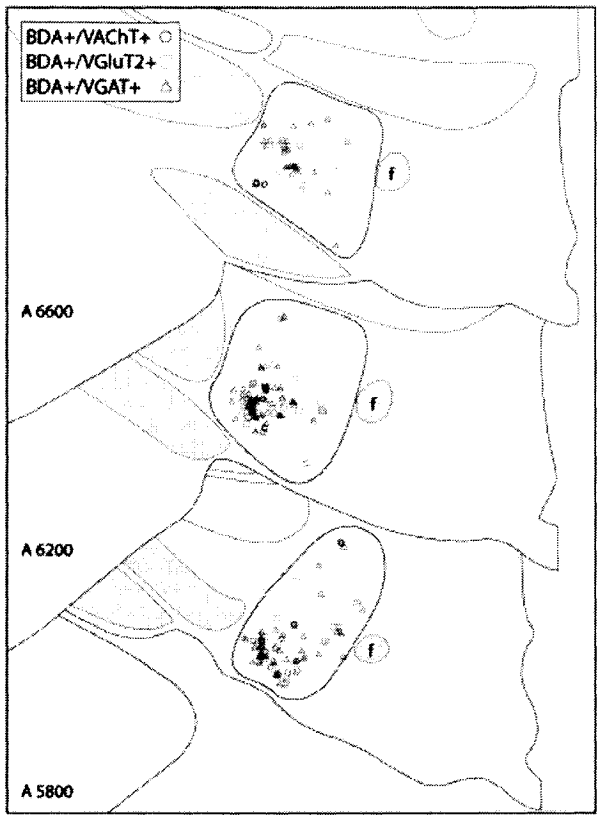

Fig. 4. Distribution of VAChT+, VGluT2+, and VGAT+ BDA-labeled varicosities in the LH. Plotted together are the BDA+/VAChT+ (blue circles), BDA+/VGluT2+ (green squares), and BDA+/VGAT+ (red triangles) that were marked and counted by stereological analysis from double-stained fluorescent sections at the three levels through the LH (case BDA16-L). The BDA+/VTP-negative terminals, which were counted in each series, are not included. The stereological analysis was performed by sampling one-fourth of the total area (using a counting frame of 90 × 90 μm within a grid of 180 × 180 μm; see Materials and Methods), and each figure thus reflects about one-fourth of the total number of varicosities in a 25-μm-thick section. Note the concentration of BDA+/VTP+ varicosities within the ventral and central portion of the LH, with scattered varicosities in other portions, especially at the most posterior level (A 5800). For abbreviations, see list.

varicosities, triple fluorescent staining for BDA (Cy2), VGluT2 or VGAT (Cy3), and PSD-95 or Geph (Cy5) was performed in LH sections and analyzed by confocal microscopy by using 3D reconstruction and rotation of the images (in three cases per series).

In the series stained for BDA, VGluT2, and PSD-95, the PSD-95 staining appeared to be punctate and smaller in size than VGluT2+ varicosities. As judged from magnified and rotated 3D images, PSD-95+ puncta were often seen closely associated with VGluT2+ varicosities (Fig. 5A–C, pointers). BDA+/VGluT2+ varicosities were commonly seen in close association with one or more PSD-95+ puncta (BDA+/VGluT2+:PSD-95+, Fig. 5A,B, pointers opposite filled arrowheads). As confirmed in 3D rotations, the BDA+/VGluT2+ varicosities were apposed to the PSD-95+ profiles (Fig. 5A,B, insets). BDA+/VGluT2− varicosities were generally seen unassociated with PSD-95+ puncta (Fig. 5C), although some BDA+/VGluT2−: PSD-95+ profiles were seen (not shown).

In series stained for BDA, VGAT, and Geph, Geph staining appeared to be punctate. The Geph+ puncta were generally larger that the PSD-95+ puncta. As judged from magnified and rotated 3D images, Geph+ puncta were frequently seen in close association with VGAT+ varicosities, and conversely VGAT varicosities were frequently seen in close association with Geph+ puncta (Fig. 5D–F, pointers). BDA+/VGAT+ axonal varicosities were apposed to Geph+ puncta (BDA+/VGAT+:Geph+), usually with one Geph+ profile per BDA+/VGAT+ varicosity (Fig. 5D,E). Occasionally, unlabeled LH cells appeared to be surrounded by VGAT+ varicosities, including BDA+/VGAT+ ones that were apposed to Geph+ puncta, located on the inner side of the varicosities and thus presumably in the cell membrane of the innervated cell body (Fig. 5D). BDA+/VGAT− varicosities were not seen in apposition to Geph+ profiles (Fig. 5F).

DISCUSSION

The present study provides evidence that cholinergic, glutamatergic, and GABAergic BF neurons project to the LH. The quantitatively most important, glutamatergic and GABAergic, fibers also appear to form excitatory and inhibitory synapses, respectively, on LH neurons. Through this projection, BF neurons can thus have a dual influence in the LH to excite or inhibit neurons involved in promoting cortical activation and behavioral arousal.

Technical considerations

Confirming its documented utility as an anterograde tracer (Veenman et al., 1992; Wouterlood and Jorritsma-Byham, 1993; Lanciego et al., 2000; Reiner et al., 2000), we found that BDA-10,000 provided discrete labeling of BF cell bodies and reliable anterograde labeling of BF fibers and varicosities. Although we noticed some labeled cells in areas surrounding the injection site in the MCPO-SI, which might have been retrogradely labeled, we did not find cells retrogradely labeled at a distance in the prefrontal cortex or LH, confirming that BDA-10,000, in contrast to BDA-3000 MW, results in neglible retrograde labeling (Wouterlood and Jorritsma-Byham, 1993; Reiner et al., 2000). Here, from the labeled cells located predominantly (>90% on average) in the MCPO of the BF, the BDA-labeled axons were seen to course within the ventrolateral, a, subdivision of the MFB, which has been known to carry descending fibers from the MCPO (Veening et al., 1982). In the posterior LH, the axons sent collateral branches through the LH region in a manner also previously described from the MCPO by application of other anterograde tracers, including *Phaseolus vulgaris* leucoagglutinin (PHA-L; Grove, 1988) and proteins synthesized from tritiated amino acids (Swanson, 1976).

This distribution of efferent fibers to the LH from MCPO-SI fits within a lateral to medial topographic organization of projections to the tuberal-posterior hypothalamus from forebrain structures (Veening et al., 1982). Moreover, the BDA-labeled varicose fibers extended through a region in the LH from which neurons in the MCPO and SI had previously been retrogradely labeled with cholera toxin in large numbers in our laboratory (Gritti et al., 1994). Here, we labeled only a small propor-

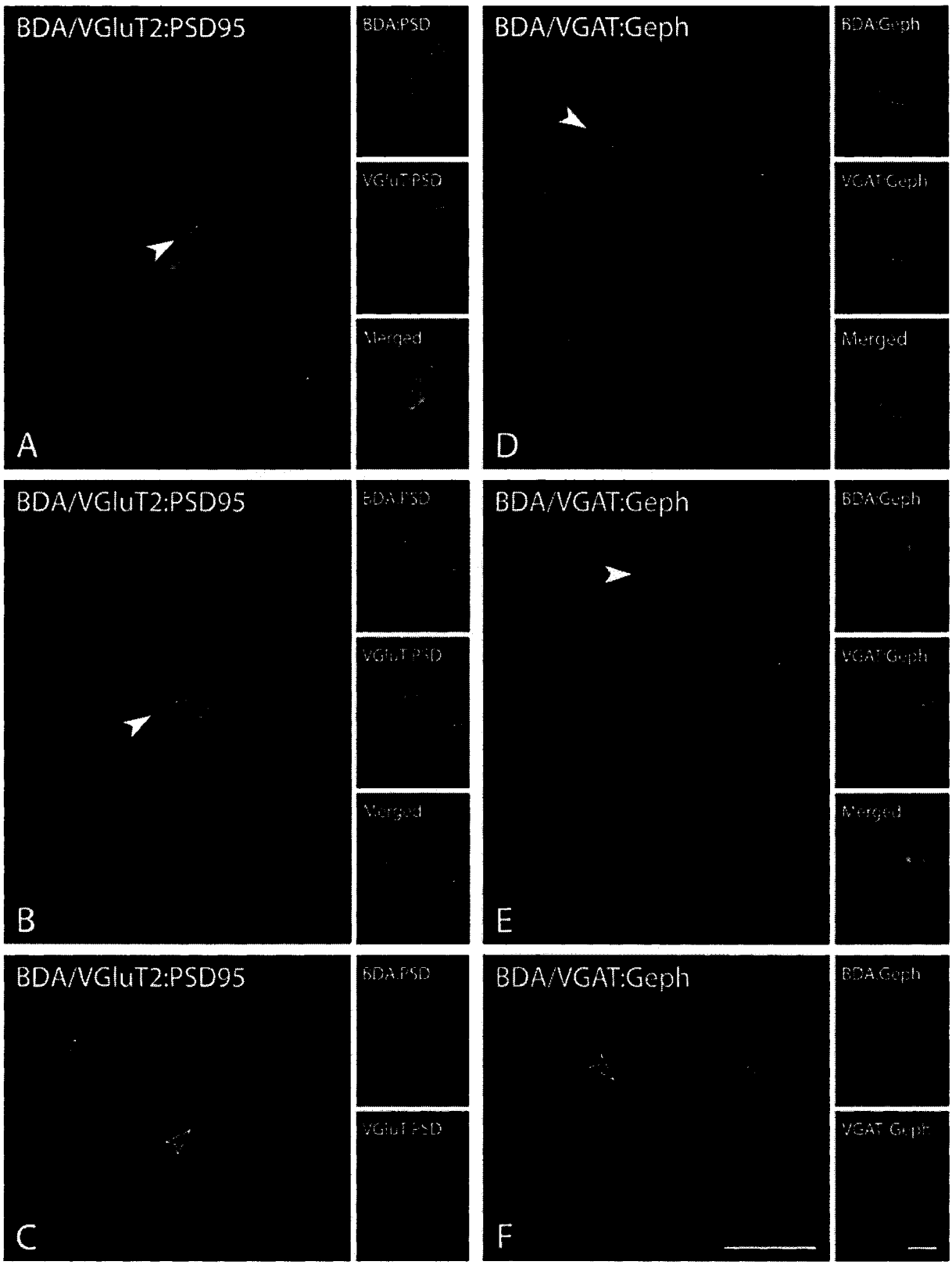
BDA/VGluT2:PSD95
BDA:PSD
VGluT:PSD
Merged
A
BDA/VGAT:Geph
BDA:Geph
VGAT:Geph
Merged
D
BDA/VGluT2:PSD95
BDA:PSD
VGluT:PSD
Merged
B
BDA/VGAT:Geph
BDA:Geph
VGAT:Geph
Merged
E
BDA/VGluT2:PSD95
BDA:PSD
VGluT:PSD
C
BDA/VGAT:Geph
BDA:Geph
VGAT:Geph
F

Figure 5

tion of these afferent neurons, according to their numbers and distribution (Gritti et al., 1993, 1994, 2003), because our injection site was intentionally discrete so as to be maximally restricted to the MCPO and overlying SI. With this relatively small proportion of projection neurons labeled, we found nonetheless that an estimated ~22,000 terminals were labeled with BDA in the LH and ~8,000 cells (~15% of the estimated total LH cell population) were contacted by BDA+ terminals, thus providing a good sample of the basalo-hypothalamic projection to the LH.

Confirming the utility of BDA as an anterograde tracer that can be readily used along with immunostaining for elucidating complex neural circuits (Lanciego et al., 2000), we were able to apply double staining for BDA and the VTPs in order to identify the neurotransmitters utilized by the BF neurons projecting to the LH. We found that with the use of Triton (0.1%), we obtained complete penetration in material double stained for VTP antibodies and streptavidin (through 25-μm-thick sections). Such reliable, homogeneous staining thus permitted the application of stereological analysis to assess the proportions of the different VTP+ terminals in the LH. We were also able to apply triple staining for BDA, the VTPs, and PSPs (by using 0.3% TX).

Double staining with the VTPs allowed unequivocal identification of the neurotransmitter utilized by the projecting neurons (Chaudhry et al., 1998; Bellocchio et al., 2000). Together with other elements necessary for recycling, VTPs form docking and fusion of synaptic vesicles, a critical component of the machinery for neurotransmitter release at presynaptic sites (Liu et al., 1999; Fremeau et al., 2004). Particularly in the case of VGAT and VGluT2, they have been found to be concentrated at symmetrical and asymmetrical synapses, respectively, to co-purify with other synaptic proteins and to colocalize with synaptophysin and/or synaptobrevin in synaptic terminals (Chaudhry et al., 1998; Takamori et al., 2000; Gualix et al., 2003; Fremeau et al., 2004).

Triple staining with PSPs here confirmed that the BDA-labeled VGluT+ and VGAT+ terminals abutted excitatory and inhibitory postsynaptic elements, respectively. The PSPs, PSD-95 and Geph, form part of the postsynaptic scaffolding of excitatory (Kornau et al., 1995; O'Brien et al., 1999; Sheng and Pak, 2000) and inhibitory (Pfeiffer et al., 1984; Sassoe-Pognetto et al., 1995, 2000; Sassoe-Pognetto and Fritschy, 2000) synapses, respectively. Indeed, PSD-95 colocalizes with glutamate receptors by interacting directly with the C-terminus of synaptic NMDA receptor subunits (Kornau et al., 1995) and indirectly through the protein stargazin with AMPA receptors (Chen et al., 2000). Although not binding $GABA_A$ receptors directly, Geph colocalizes with the most common and synaptically located $GABA_A$ receptor subunits as well as the glycine receptor (Pfeiffer et al., 1984; Sassoe-Pognetto et al., 2000).

We employed laser scanning confocal microscopy and state-of-the-art 3D rendering technology to visualize appositions between BDA+/VTP+ terminals and PSP+ profiles, an approach that has been proposed to be suitable for judging the existence of synaptic contacts by confocal microscopy (Wouterlood et al., 2002, 2003), while recognizing that absolute proof of such contacts necessitates electron microscopy. Thus, we believe that the presynaptic enrichment of VTPs for glutamate and GABA in BDA+ terminals and their apposition with PSPs associated with excitatory and inhibitory synapses respectively, represents strong evidence for the synaptic contacts of glutamatergic and GABAergic BF terminals on LH neurons.

BF cholinergic, glutamatergic, and GABAergic fibers in the LH

The immunohistochemical localization of VAChT, VGluT2, and VGAT in anterogradely labeled BF varicosities demonstrates that BF neurons have the capacity, endowed by the VTPs, to release ACh, glutamate, or GABA, respectively (Gilmor et al., 1996; Chaudhry et al., 1998; Bellocchio et al., 2000; Fremeau et al., 2001). Their neurotransmitter phenotypes would appear to be unambiguous, because, in contrast to previous evidence for the presence of multiple mRNAs or proteins for synthetic enzymes of ACh, glutamate, or GABA in BF cell bodies (Manns et al., 2001; Sotty et al., 2003), no evidence for colocalization of the VTP proteins was found here in terminals within the LH. BF neurons innervating the LH can thus be phenotypically identified as cholinergic, glutamatergic, or GABAergic.

By demonstrating the presence of VGluT2 proteins in BF terminals, the present results provide the first proof for the existence of BF neurons that utilize glutamate as a neurotransmitter and can thus be considered glutamatergic. Another recent report showed by in situ hybridization that cortically projecting BF neurons contain mRNA for VGluT2 and accordingly have the capacity to synthesize the VGluT2 protein (Hur and Zaborszky, 2005). Previous results had also suggested the existence of glutamatergic BF neurons based on the presence of phosphate-activated-glutaminase (PAG; Manns et al., 2001), the enzyme uti-

Fig. 5. Relationship of PSD-95+ puncta to VGluT2+ and Geph+ puncta to VGAT+ BDA-labeled varicosities in 3D rendered confocal images. **A,B:** Large images (8 and 12 serial 0.33-μm-thick optical sections) of BDA-labeled axons and varicosities (solid arrowheads, pseudo-color green, Cy2) that are immunopositive for VGluT2 (pseudo-color blue, Cy3), face PSD-95+ profiles (facing pointers, pseudo-color red, Cy5) and featured in the zoomed images on the right (5 and 12 serial 0.33-μm-thick optical sections). Note also, in the large images, the frequent association of VGluT2+ varicosities with PSD-95+ puncta (pointers). **C:** Image (eight serial sections) of a BDA+ varicosity (open arrowhead, pseudo-color green, Cy2) that is immunonegative for VGluT2 (pseudo-color blue, Cy3) and does not face a PSD-95+ profile, as is also evident in the zoom images on the right (10 serial sections). Note VGluT2+ varicosities in the vicinity that are associated with PSD-95+ puncta (pointer in large image). **D,E:** Images (eight and seven serial sections, respectively) of BDA-labeled axons and varicosities (solid arrowheads, pseudo-color green, Cy2) that are positive for VGAT (pseudo-color blue, Cy3) and face Geph+ profiles (facing pointers, pseudo-color red, Cy5), as featured in the zoomed images on the right (nine and seven serial sections). In the large image of D, VGAT+/Geph+ elements appear to surround the unlabeled soma of a neuron with the VGAT+ varicosities outside and the Geph+ puncta (pointers) inside, presumably on the cell membrane. Note in the large panels that many VGAT+ varicosities are associated with Geph+ puncta (pointers). **F:** Image (seven serial sections) of a BDA+ varicosity (open arrowhead, pseudo-color green, Cy2) that is immunonegative for VGAT (pseudo-color blue, Cy3) and is not associated with any Geph+ puncta, as is also evident in the zoomed images on the right (five serial sections). Note, in contrast, that other VGAT+ varicosities in the vicinity are associated with Geph+ puncta (pointer). Deconvolution was applied to all images with a confidence limit of 95% (see Materials and Methods). For abbreviations, see list. Scale bar = 5 μm in F (applies to A–F, large images; 1 μm in F, lower right corner (applies to A–F, small images).

lized for the synthesis of glutamate from glutamine, yet possibly also used for the synthesis of GABA from the same substrate in some cells (Fujiyama et al., 2001). The presence of glutamatergic BF neurons that utilize VGluT2 follows the principle that in the forebrain, VGluT2 neurons are localized predominantly in subcortical structures, whereas VGluT1 neurons are localized predominantly in the cortex (Fremeau et al., 2001). A third type of vesicular transporter for glutamate (VGluT3) has more recently been visualized in cell bodies within some cortical and subcortical neurons, notably including BF neurons (Fremeau et al., 2002; Schafer et al., 2002; Harkany et al., 2003; Herzog et al., 2004). In the present analysis, we did not find evidence for concentration of VGluT3 in BF varicosities within the LH. It would thus appear that BF neurons might contain VGluT3 in their cell bodies but not transport it to their terminals or, alternatively, that BF neurons that do transport VGluT3 to their terminals do not project caudally to the LH.

Of the total number of BF axonal varicosities in the LH, the smallest proportion was VAChT+ (~10%), a medium proportion was VGluT2+ (~25%), and the largest proportion was VGAT+ (~50%). Previous studies employing retrograde transport with immunostaining for the synthetic enzymes of ACh (choline acetyltransferase [ChAT]) and GABA (glutamic acid decarboxylase [GAD]) found that of the BF cells within the MCPO projecting to the LH, <5% were ChAT+, ~20% were GAD+ and up to ~75% were neither and thus presumed to be glutamatergic (Gritti et al., 1994). The higher proportions of anterogradely labeled VAChT+ and VGAT+ varicosities relative to retrogradely labeled ChAT+ and GAD+ cell bodies might be due to more axonal collateralization per neuron or more varicosities per axon length in GABAergic and cholinergic than non-GABAergic/non-cholinergic neurons, which would include the glutamatergic neurons.

Irrespective of these possible differences, only 25% of the varicosities were found to be glutamatergic, and another ~15% of varicosities could not be accounted for as glutamatergic, cholinergic, or GABAergic. It is possible that this contingent might use another type of excitatory neurotransmitter, such as aspartate, which is not recognized as a substrate by the vesicular glutamate transporters (Bellocchio et al., 2000; Fremeau et al., 2001, 2002). Indeed, aspartate has been found in axon terminals forming asymmetric synapses in the hypothalamus (van den Pol, 1991). Another possibility is that this proportion might simply reflect negative immunohistochemical staining due to insufficient amounts of some or all of the VTPs in terminals.

By showing the presence of PSD-95 and Geph in apposition to BF identified glutamatergic and GABAergic terminals, respectively, in the LH, the results substantiate the synaptic nature of this projection and also corroborate the principle that glutamate and GABA terminals generally form synapses with postsynaptic target neurons (Edwards, 1995). Given the small number and proportion of BDA+/VAChT+ varicosities in the LH and the less well-known association of cholinergic terminals with specific PSPs (Parker et al., 2004) or synaptic specializations (Descarries et al., 1997), we did not examine the relationship of the BDA+/VAChT+ boutons to PSPs. ACh might act predominantly by diffuse transmission through ectopic release and extrasynaptic receptors (Levey et al., 1995; Coggan et al., 2005).

Functional significance of the cholinergic, glutamatergic, and GABAergic BF projections to LH

Neurons in the LH project to brainstem arousal systems and/or spinal cord sympathetic and motor systems as well as forebrain limbic areas and the cerebral cortex (Saper et al., 1979; Saper, 1985; Holstege, 1987). By means of these multiple projections, the LH is well suited to play a central role in arousal. Indeed, the LH has been shown to influence positively several arousal-related processes such as sympathetic tone, locomotion, and exploratory behavior, including food seeking, reward, and cortical activation (Olds and Milner, 1954; Hess, 1957; Berthoud, 2002; DiLeone et al., 2003; Jones, 2005a). Recently, diffusely projecting neurons have been identified in the LH that contain the peptide Orx (de Lecea et al., 1998; Peyron et al., 1998; Sakurai et al., 1998), which appears to be critical for arousal and postural muscle tone because in absence of the peptide or its receptor, narcolepsy with cataplexy occurs (Chemelli et al., 1999; Lin et al., 1999; Peyron et al., 2000; Thannickal et al., 2000; Gerashchenko et al., 2001; Hara et al., 2001). Physiologically as well as anatomically and chemically, the LH is comprised of different cell types, the vast majority of which discharge at high rates during active waking with behavioral arousal (Szymusiak et al., 1989; Sakai et al., 1990; Steininger et al., 1999; Koyama et al., 2003). Some discharge in association with cortical activation during both waking and PS. Identified Orx neurons have recently been found to discharge maximally during active wakefulness and to virtually cease firing during SWS and PS (Lee et al., 2005a; Mileykovskiy et al., 2005).

In the present study, we found that the LH received input from cholinergic BF terminals, which represented ~10% of all BF varicosities. Because cholinergic BF neurons have been found to discharge in association with cortical activation during both waking and PS (Manns et al., 2000b; Lee et al., 2005b), they could possibly influence similar neurons in the LH that project selectively to the cerebral cortex and discharge with cortical activation during both waking and PS (Szymusiak et al., 1989; Sakai et al., 1990; Steininger et al., 1999; Koyama et al., 2003).

Glutamatergic terminals accounted for up to 25% of the total BF innervation of the LH, indicating that glutamatergic BF neurons can exert an important excitatory influence on the LH. This influence could be exerted on LH neurons that discharge in association with cortical activation and presumably project to the cerebral cortex (see above) or on LH neurons that discharge in association with motor activity and presumably project to the brainstem or spinal cord (Szymusiak et al., 1989; Steininger et al., 1999; Alam et al., 2002). Glutamatergic BF neurons could also act on Orx LH neurons, which project diffusely to all targets and could thus simultaneously promote cortical activation along with motor activity and behavioral arousal that occur during waking. Such an excitatory influence could originate from as yet chemically unidentified but possibly glutamatergic BF neurons that are maximally active during waking and minimally active during SWS and PS (Szymusiak and McGinty, 1986; Manns et al., 2003; Lee et al., 2004; Jones, 2005b).

Approximately 50% of BF axon terminals innervating the LH were GABAergic, indicating that a major influence of the BF in this region is inhibitory. Given that the vast

majority of neurons in the LH discharge during waking (Steininger et al., 1999; Alam et al., 2002) and that inhibition of these neurons by injections of the $GABA_A$ receptor agonist muscimol into the LH suppresses waking (Lin et al., 1989), it can be concluded that the GABAergic inhibitory influence from the BF in the LH would suppress waking and promote sleep. This inhibitory influence could be on multiple LH neurons, including Orx neurons, whose inhibition by GABAergic input would accordingly provide a very powerful impetus for sleep. We propose that this innervation originates from particular GABAergic BF neurons that are sleep-active (Modirrousta et al., 2004) and discharge during SWS or SWS and PS when muscle hypotonia and atonia occur (Szymusiak and McGinty, 1986; Manns et al., 2000a; Lee et al., 2004; Jones, 2005b).

In conclusion, the present study reveals the presence of three phenotypically distinct BF cell groups that, according to their neurotransmitters, differentially modulate the LH. As a minor contingent, cholinergic BF neurons can act to facilitate LH neurons involved in cortical activation. As a larger contingent, newly identified glutamatergic BF neurons can act to promote both cortical and behavioral arousal of waking. As the largest contingent, GABAergic BF neurons can act to suppress arousal and promote sleep.

ACKNOWLEDGMENTS

We are grateful to Robert H. Edwards and Robert T. Fremeau (Departments of Neurology and Physiology, University of California San Francisco School of Medicine, San Francisco, CA 94143) for kindly supplying the antibodies for VGluT1 and 2. We thank Lynda Mainville for her excellent technical assistance.

LITERATURE CITED

Alam MN, Gong H, Alam T, Jaganath R, McGinty D, Szymusiak R. 2002. Sleep-waking discharge patterns of neurons recorded in the rat perifornical lateral hypothalamic area. J Physiol 538:619–631.

Bellocchio EE, Reimer RJ, Fremeau RT, Jr., Edwards RH. 2000. Uptake of glutamate into synaptic vesicles by an inorganic phosphate transporter. Science 289:957–960.

Berthoud HR. 2002. Multiple neural systems controlling food intake and body weight. Neurosci Biobehav Rev 26:393–428.

Buzsaki G, Bickford RG, Ponomareff G, Thal LJ, Mandel R, Gage FH. 1988. Nucleus basalis and thalamic control of neocortical activity in the freely moving rat. J Neurosci 8:4007–4026.

Chaudhry FA, Reimer RJ, Bellocchio EE, Danbolt NC, Osen KK, Edwards RH, Storm-Mathisen J. 1998. The vesicular GABA transporter, VGAT, localizes to synaptic vesicles in sets of glycinergic as well as GABAergic neurons. J Neurosci 18:9733–9750.

Chemelli RM, Willie JT, Sinton CM, Elmquist JK, Scammell T, Lee C, Richardson JA, Williams SC, Xiong Y, Kisanuki Y, Fitch TE, Nakazato M, Hammer RE, Saper CB, Yanagisawa M. 1999. Narcolepsy in orexin knockout mice: molecular genetics of sleep regulation. Cell 98:437–451.

Chen L, Chetkovich DM, Petralia RS, Sweeney NT, Kawasaki Y, Wenthold RJ, Bredt DS, Nicoll RA. 2000. Stargazin regulates synaptic targeting of AMPA receptors by two distinct mechanisms. Nature 408:936–943.

Coggan JS, Bartol TM, Esquenazi E, Stiles JR, Lamont S, Martone ME, Berg DK, Ellisman MH, Sejnowski TJ. 2005. Evidence for ectopic neurotransmission at a neuronal synapse. Science 309:446–451.

de Lecea L, Kilduff TS, Peyron C, Gao X, Foye PE, Danielson PE, Fukuhara C, Battenberg EL, Gautvik VT, Bartlett FS, 2nd, Frankel WN, van den Pol AN, Bloom FE, Gautvik KM, Sutcliffe JG. 1998. The hypocretins: hypothalamus-specific peptides with neuroexcitatory activity. Proc Natl Acad Sci U S A 95:322–327.

Descarries L, Gisiger V, Steriade M. 1997. Diffuse transmission by acetylcholine in the CNS. Prog Neurobiol 53:603–625.

DiLeone RJ, Georgescu D, Nestler EJ. 2003. Lateral hypothalamic neuropeptides in reward and drug addiction. Life Sci 73:759–768.

Duque A, Balatoni B, Detari L, Zaborszky L. 2000. EEG correlation of the discharge properties of identified neurons in the basal forebrain. J Neurophysiol 84:1627–1635.

Edwards FA. 1995. Anatomy and electrophysiology of fast central synapses lead to a structural model for long-term potentiation. Physiol Rev 75:759–787.

Fremeau RT Jr, Troyer MD, Pahner I, Nygaard GO, Tran CH, Reimer RJ, Bellocchio EE, Fortin D, Storm-Mathisen J, Edwards RH. 2001. The expression of vesicular glutamate transporters defines two classes of excitatory synapse. Neuron 31:247–260.

Fremeau RT Jr, Burman J, Qureshi T, Tran CH, Proctor J, Johnson J, Zhang H, Sulzer D, Copenhagen DR, Storm-Mathisen J, Reimer RJ, Chaudhry FA, Edwards RH. 2002. The identification of vesicular glutamate transporter 3 suggests novel modes of signaling by glutamate. Proc Natl Acad Sci U S A 99:14488–14493.

Fremeau RT Jr, Voglmaier S, Seal RP, Edwards RH. 2004. VGLUTs define subsets of excitatory neurons and suggest novel roles for glutamate. Trends Neurosci 27:98–103.

Fujiyama F, Furuta T, Kaneko T. 2001. Immunocytochemical localization of candidates for vesicular glutamate transporters in the rat cerebral cortex. J Comp Neurol 435:379–387.

Gerashchenko D, Kohls MD, Greco M, Waleh NS, Salin-Pascual R, Kilduff TS, Lappi DA, Shiromani PJ. 2001. Hypocretin-2-saporin lesions of the lateral hypothalamus produce narcoleptic-like sleep behavior in the rat. J Neurosci 21:7273–7283.

Gilmor ML, Nash NR, Roghani A, Edwards RH, Yi H, Hersch SM, Levey AI. 1996. Expression of the putative vesicular acetylcholine transporter in rat brain and localization in cholinergic synaptic vesicles. J Neurosci 16:2179–2190.

Gritti I, Mainville L, Jones BE. 1993. Codistribution of GABA- with acetylcholine-synthesizing neurons in the basal forebrain of the rat. J Comp Neurol 329:438–457.

Gritti I, Mainville L, Jones BE. 1994. Projections of GABAergic and cholinergic basal forebrain and GABAergic preoptic-anterior hypothalamic neurons to the posterior lateral hypothalamus of the rat. J Comp Neurol 339:251–268.

Gritti I, Mainville L, Mancia M, Jones BE. 1997. GABAergic and other non-cholinergic basal forebrain neurons project together with cholinergic neurons to meso- and iso-cortex in the rat. J Comp Neurol 383: 163–177.

Gritti I, Manns ID, Mainville L, Jones BE. 2003. Parvalbumin, calbindin, or calretinin in cortically projecting and GABAergic, cholinergic, or glutamatergic basal forebrain neurons of the rat. J Comp Neurol 458: 11–31.

Grove EA. 1988. Efferent connections of the substantia innominata in the rat. J Comp Neurol 277:347–364.

Gualix J, Gomez-Villafuertes R, Diaz-Hernandez M, Miras-Portugal MT. 2003. Presence of functional ATP and dinucleotide receptors in glutamatergic synaptic terminals from rat midbrain. J Neurochem 87:160–171.

Hara J, Beuckmann CT, Nambu T, Willie JT, Chemelli RM, Sinton CM, Sugiyama F, Yagami K, Goto K, Yanagisawa M, Sakurai T. 2001. Genetic ablation of orexin neurons in mice results in narcolepsy, hypophagia, and obesity. Neuron 30:345–354.

Harkany T, Hartig W, Berghuis P, Dobszay MB, Zilberter Y, Edwards RH, Mackie K, Ernfors P. 2003. Complementary distribution of type 1 cannabinoid receptors and vesicular glutamate transporter 3 in basal forebrain suggests input-specific retrograde signalling by cholinergic neurons. Eur J Neurosci 18:1979–1992.

Herzog E, Gilchrist J, Gras C, Muzerelle A, Ravassard P, Giros B, Gaspar P, El Mestikawy S. 2004. Localization of VGLUT3, the vesicular glutamate transporter type 3, in the rat brain. Neuroscience 123:983–1002.

Hess WR. 1957. The functional organization of the diencephalon. New York: Grune & Stratton.

Holstege G. 1987. Some anatomical observations on the projections from the hypothalamus to brainstem and spinal cord: An HRP and autoradiographic tracing study in the cat. J Comp Neurol 260:98–126.

Hur EE, Zaborszky L. 2005. Vglut2 afferents to the medial prefrontal and primary somatosensory cortices: a combined retrograde tracing in situ hybridization. J Comp Neurol 483:351–373.

Jones BE. 2004. Activity, modulation and role of basal forebrain cholin-

ergic neurons innervating the cerebral cortex. Progr Brain Res 145: 157–169.

Jones BE. 2005a. Basic mechanisms of sleep-wake states. In: Kryger MH, Roth T, Dement WC, editors. Principles and practice of sleep medicine, 4th ed. Philadelphia: Elsevier Saunders. p 136–153.

Jones BE. 2005b. From waking to sleeping: neuronal and chemical substrates. Trends Pharmacol Sci 26:578–586.

Jones BE. 2005c. Sleep-wake mechanisms: neurophysiology and chemical neuroanatomy. In: Opp MR, editor. SRS basics of sleep guide. Westchester, IL: Sleep Research Society. p 57–64.

Kornau HC, Schenker LT, Kennedy MB, Seeburg PH. 1995. Domain interaction between NMDA receptor subunits and the postsynaptic density protein PSD-95. Science 269:1737–1740.

Koyama Y, Takahashi K, Kodama T, Kayama Y. 2003. State-dependent activity of neurons in the perifornical hypothalamic area during sleep and waking. Neuroscience 119:1209–1219.

Lanciego JL, Wouterlood FG, Erro E, Arribas J, Gonzalo N, Urra X, Cervantes S, Gimenez-Amaya JM. 2000. Complex brain circuits studied via simultaneous and permanent detection of three transported neuroanatomical tracers in the same histological section. J Neurosci Methods 103:127–135.

Lee MG, Hassani O, Jones BE. 2005a. Discharge of identified orexin/hypocretin neurons across the sleep-waking cycle. J Neurosci 25:6716–6720.

Lee MG, Hassani OK, Alonso A, Jones BE. 2005b. Cholinergic basal forebrain neurons burst with theta during waking and paradoxical sleep. J Neurosci 25:4365–4369.

Lee MG, Manns ID, Alonso A, Jones BE. 2004. Sleep-wake related discharge properties of basal forebrain neurons recorded with micropipettes in head-fixed rats. J Neurophysiol 92:1182–1198.

Levey AI, Edmunds SM, Hersch SM, Wiley RG, Heilman CJ. 1995. Light and electron microscopic study of m2 muscarinic acetylcholine receptor in the basal forebrain of the rat. J Comp Neurol 351:339–356.

Lin JS, Sakai K, Vanni-Mercier G, Jouvet M. 1989. A critical role of the posterior hypothalamus in the mechanisms of wakefulness determined by microinjection of muscimol in freely moving cats. Brain Res 479: 225–240.

Lin L, Faraco J, Li R, Kadotani H, Rogers W, Lin X, Qiu X, de Jong PJ, Nishino S, Mignot E. 1999. The sleep disorder canine narcolepsy is caused by a mutation in the hypocretin (orexin) receptor 2 gene. Cell 98:365–376.

Liu Y, Krantz DE, Waites C, Edwards RH. 1999. Membrane trafficking of neurotransmitter transporters in the regulation of synaptic transmission. Trends Cell Biol 9:356–363.

Luiten PGM, Gaykema RPA, Traber J, Spencer DG. 1987. Cortical projection patterns of magnocellular basal nucleus subdivisions as revealed by anterogradely transported *Phaseolus vulgaris* leucoagglutinin. Brain Res 413:229–250.

Manns ID, Alonso A, Jones BE. 2000a. Discharge profiles of juxtacellularly labeled and immunohistochemically identified GABAergic basal forebrain neurons recorded in association with the electroencephalogram in anesthetized rats. J Neurosci 20:9252–9263.

Manns ID, Alonso A, Jones BE. 2000b. Discharge properties of juxtacellularly labeled and immunohistochemically identified cholinergic basal forebrain neurons recorded in association with the electroencephalogram in anesthetized rats. J Neurosci 20:1505–1518.

Manns ID, Mainville L, Jones BE. 2001. Evidence for glutamate, in addition to acetylcholine and GABA, neurotransmitter synthesis in basal forebrain neurons projecting to the entorhinal cortex. Neuroscience 107:249–263.

Manns ID, Alonso A, Jones BE. 2003. Rhythmically discharging basal forebrain units comprise cholinergic, GABAergic, and putative glutamatergic cells. J Neurophysiol 89:1057–1066.

McGinty DJ, Sterman MB. 1968. Sleep suppression after basal forebrain lesions in the cat. Science 160:1253–1255.

Metherate R, Cox CL, Ashe JH. 1992. Cellular bases of neocortical activation: modulation of neural oscillations by the nucleus basalis and endogenous acetylcholine. J Neurosci 12:4701–4711.

Mileykovskiy BY, Kiyashchenko LI, Siegel JM. 2005. Behavioral correlates of activity in identified hypocretin/orexin neurons. Neuron 46:787–798.

Modirrousta M, Mainville L, Jones BE. 2004. GABAergic neurons with alpha2-adrenergic receptors in basal forebrain and preoptic area express c-Fos during sleep. Neuroscience 129:803–810.

Nauta WJH. 1946. Hypothalamic regulation of sleep in rats. An experimental study. J Neurophysiol 9:285–316.

O'Brien RJ, Xu D, Petralia RS, Steward O, Huganir RL, Worley P. 1999. Synaptic clustering of AMPA receptors by the extracellular immediate-early gene product Narp. Neuron 23:309–323.

Olds J, Milner P. 1954. Positive reinforcement produced by electrical stimulation of septal area and other regions of rat brain. J Comp Physiol Psychol 47:419–427.

Parker MJ, Zhao S, Bredt DS, Sanes JR, Feng G. 2004. PSD93 regulates synaptic stability at neuronal cholinergic synapses. J Neurosci 24:378–388.

Peyron C, Tighe DK, van den Pol AN, de Lecea L, Heller HC, Sutcliffe JG, Kilduff TS. 1998. Neurons containing hypocretin (orexin) project to multiple neuronal systems. J Neurosci 18:9996–10015.

Peyron C, Faraco J, Rogers W, Ripley B, Overeem S, Charnay Y, Nevsimalova S, Aldrich M, Reynolds D, Albin R, Li R, Hungs M, Pedrazzoli M, Padigaru M, Kucherlapati M, Fan J, Maki R, Lammers GJ, Bouras C, Kucherlapati R, Nishino S, Mignot E. 2000. A mutation in a case of early onset narcolepsy and a generalized absence of hypocretin peptides in human narcoleptic brains. Nat Med 6:991–997.

Pfeiffer F, Simler R, Grenningloh G, Betz H. 1984. Monoclonal antibodies and peptide mapping reveal structural similarities between the subunits of the glycine receptor of rat spinal cord. Proc Natl Acad Sci U S A 81:7224–7227.

Reiner A, Veenman CL, Medina L, Jiao Y, Del Mar N, Honig MG. 2000. Pathway tracing using biotinylated dextran amines. J Neurosci Methods 103:23–37.

Sakai K, El Mansari M, Lin J-S, Zhang G, Vanni-Mercier G. 1990. The posterior hypothalamus in the regulation of wakefulness and paradoxical sleep. In: Mancia M, Marini G, editors. The diencephalon and sleep. New York: Raven Press. p 171–198.

Sakurai T, Amemiya A, Ishii M, Matsuzaki I, Chemelli RM, Tanaka H, Williams SC, Richardson JA, Kozlowski GP, Wilson S, Arch JR, Buckingham RE, Haynes AC, Carr SA, Annan RS, McNulty DE, Liu WS, Terrett JA, Elshourbagy NA, Bergsma DJ, Yanagisawa M. 1998. Orexins and orexin receptors: a family of hypothalamic neuropeptides and G protein-coupled receptors that regulate feeding behavior. Cell 92:573–585.

Saper CB. 1985. Organization of cerebral cortical afferent systems in the rat. II. Hypothalamocortical projections. J Comp Neurol 237:21–46.

Saper CB, Swanson LW, Cowan WM. 1979. An autoradiographic study of the efferent connections of the lateral hypothalamic area in the rat. J Comp Neurol 183:689–706.

Sassoe-Pognetto M, Fritschy JM. 2000. Mini-review: gephyrin, a major postsynaptic protein of GABAergic synapses. Eur J Neurosci 12:2205–2210.

Sassoe-Pognetto M, Kirsch J, Grunert U, Greferath U, Fritschy JM, Mohler H, Betz H, Wassle H. 1995. Colocalization of gephyrin and GABAA-receptor subunits in the rat retina. J Comp Neurol 357:1–14.

Sassoe-Pognetto M, Panzanelli P, Sieghart W, Fritschy JM. 2000. Colocalization of multiple GABA(A) receptor subtypes with gephyrin at postsynaptic sites. J Comp Neurol 420:481–498.

Schafer MK, Varoqui H, Defamie N, Weihe E, Erickson JD. 2002. Molecular cloning and functional identification of mouse vesicular glutamate transporter 3 and its expression in subsets of novel excitatory neurons. J Biol Chem 277:50734–50748.

Sheng M, Pak DT. 2000. Ligand-gated ion channel interactions with cytoskeletal and signaling proteins. Annu Rev Physiol 62:755–778.

Sotty F, Danik M, Manseau F, Laplante F, Quirion R, Williams S. 2003. Distinct electrophysiological properties of glutamatergic, cholinergic and GABAergic rat septohippocampal neurons: novel implications for hippocampal rhythmicity. J Physiol 551:927–943.

Starzl TE, Taylor CW, Magoun HW. 1951. Ascending conduction in reticular activating system, with special reference to the diencephalon. J Neurophysiol 14:461–477.

Steininger TL, Alam MN, Gong H, Szymusiak R, McGinty D. 1999. Sleep-waking discharge of neurons in the posterior lateral hypothalamus of the albino rat. Brain Res 840:138–147.

Swanson LW. 1976. An autoradiographic study of the efferent connections of the preoptic region in the rat. J Comp Neurol 167:227–256.

Swett CP, Hobson JA. 1968. The effects of posterior hypothalamic lesions on behavioral and electrographic manifestations of sleep and waking in cats. Arch Ital Biol 106:283–293.

Szymusiak R, McGinty D. 1986. Sleep-related neuronal discharge in the basal forebrain of cats. Brain Res 370:82–92.

Szymusiak R, Iriye T, McGinty D. 1989. Sleep-waking discharge of neurons

in the posterior lateral hypothalamic area of cats. Brain Res Bull 23:111–120.

Takamori S, Riedel D, Jahn R. 2000. Immunoisolation of GABA-specific synaptic vesicles defines a functionally distinct subset of synaptic vesicles. J Neurosci 20:4904–4911.

Thannickal TC, Moore RY, Nienhuis R, Ramanathan L, Gulyani S, Aldrich M, Cornford M, Siegel JM. 2000. Reduced number of hypocretin neurons in human narcolepsy. Neuron 27:469–474.

van den Pol AN. 1991. Glutamate and aspartate immunoreactivity in hypothalamic presynaptic axons. J Neurosci 11:2087–2101.

Veening JG, Swanson LW, Cowan WM, Nieuwenhuys R, Geeraedts LMG. 1982. The medial forebrain bundle of the rat. II. An autoradiographic study of the topography of the major descending and ascending components. J Comp Neurol 206:82–108.

Veenman CL, Reiner A, Honig MG. 1992. Biotinylated dextran amine as an anterograde tracer for single- and double-labeling studies. J Neurosci Methods 41:239–254.

von Economo C. 1931. Encephalitis lethargica. Its sequelae and treatment. London: Oxford University Press.

Wouterlood FG, Jorritsma-Byham B. 1993. The anterograde neuroanatomical tracer biotinylated dextran-amine: comparison with the tracer *Phaseolus vulgaris*-leucoagglutinin in preparations for electron microscopy. J Neurosci Methods 48:75–87.

Wouterlood FG, van Haeften T, Blijleven N, Perez-Templado P, Perez-Templado H. 2002. Double-label confocal laser-scanning microscopy, image restoration, and real-time three-dimensional reconstruction to study axons in the central nervous system and their contacts with target neurons. Appl Immunohistochem Mol Morphol 10:85–95.

Wouterlood FG, Bockers T, Witter MP. 2003. Synaptic contacts between identified neurons visualized in the confocal laser scanning microscope. Neuroanatomical tracing combined with immunofluorescence detection of post-synaptic density proteins and target neuron-markers. J Neurosci Methods 128:129–142.

THE JOURNAL OF COMPARATIVE NEUROLOGY 499:645–661 (2006)

Innervation of Orexin/Hypocretin Neurons by GABAergic, Glutamatergic or Cholinergic Basal Forebrain Terminals Evidenced by Immunostaining for Presynaptic Vesicular Transporter and Postsynaptic Scaffolding Proteins

PABLO HENNY AND BARBARA E. JONES*
Montreal Neurological Institute, McGill University, Montreal, Quebec H3A 2B4, Canada

ABSTRACT

Orexin/hypocretin (Orx) neurons are critical for the maintenance of waking in association with behavioral arousal and postural muscle tone, since with their loss narcolepsy with cataplexy occurs. Given that basal forebrain (BF) neurons project to the hypothalamus and play important diverse roles in sleep/wake states, we sought to determine whether acetylcholine (ACh), glutamate (Glu), and/or GABA-releasing BF neurons innervate and could thereby differentially regulate the Orx neurons. From discrete injections of biotinylated dextran amine (BDA, 10,000 MW) into the magnocellular preoptic nucleus (MCPO) and substantia innominata (SI) in the rat, BDA-labeled fibers projected to the lateral hypothalamus (LH), perifornical area (PF), and dorsomedial hypothalamus (DMH), where ~41%, ~11%, and 9% of Orx-positive (+) neurons were respectively contacted in each region. Employing triple fluorescent staining for Orx, BDA, and presynaptic vesicular (V) transporters (T), we found that only 4% of the innervated Orx+ neurons in the LH were contacted by BDA+[VAChT+] terminals, whereas ~31% and ~67% were respectively contacted by BDA+[VGluT2+] and BDA+[VGAT+] terminals. In 3D-rendered and rotated confocal images, we confirmed the latter contacts and examined staining for postsynaptic proteins PSD-95, a marker for glutamatergic synapses, and gephyrin, a marker for GABAergic synapses, that were located on Orx+ neurons facing BDA-labeled terminals in ~20% and ~50% of contacts, respectively. With such synaptic input, BF glutamatergic neurons can excite Orx neurons and thus act to maintain behavioral arousal with muscle tone, whereas GABAergic neurons can inhibit Orx neurons and thus promote behavioral quiescence and sleep along with muscle atonia. J. Comp. Neurol. 499:645–661, 2006.

Indexing terms: BDA; gephyrin; narcolepsy; PSD-95; rat; paradoxical sleep; REM sleep; sleep/wake states; stereology; VAChT; VGAT; VGluT2

Neurons containing the peptide orexin (Orx, also called hypocretin) play a critical role in maintaining wakefulness and associated postural muscle tone, since in their absence or that of the peptide or receptor, narcolepsy with cataplexy occurs in humans and animals (Chemelli et al., 1999; Lin et al., 1999; Peyron et al., 2000; Thannickal et al., 2000; Yamanaka et al., 2003a). The Orx neurons are located within the tuberal hypothalamus, where they are broadly distributed across the lateral hypothalamic area (Broberger et al., 1998; Peyron et al., 1998; Modirrousta et al., 2005; Swanson et al., 2005), a region long known to play an important role in arousal (see, for review, Jones, 2005a). Lying there within the path of the medial forebrain bundle (MFB) (Millhouse, 1969; Veening et al., 1982), the Orx neurons have recently been shown to re-

Grant sponsors: Canadian Institutes of Health Research; Grant number: CIHR 13458; Grant sponsor: U.S. National Institutes of Health (NIH); Grant number: RO1 MH-60119-01A.

*Correspondence to: Dr. Barbara E. Jones, Montreal Neurological Institute, McGill University, 3801 University St., Montreal, Quebec, Canada H3A 2B4. E-mail: barbara.jones@mcgill.ca

Received 24 January 2006; Revised 7 March 2006; Accepted 5 July 2006
DOI 10.1002/cne.21131
Published online in Wiley InterScience (www.interscience.wiley.com).

ceive inputs from multiple forebrain and brainstem cell groups (Sakurai et al., 2005; Yoshida et al., 2006), which project through the MFB and are involved in sleep/wake state regulation (Jones, 2005a). The sources of afferent input might include the basal forebrain (BF) (Sakurai et al., 2005), which, from lesion, stimulation, and recording studies is known to play diverse roles in sleep/wake state regulation through its different constituent cell groups (Szymusiak et al., 2000; Jones, 2005a,b).

The BF is known particularly for the cholinergic neurons residing there within multiple nuclei and projecting to the cerebral cortex, where they stimulate cortical activation during waking and paradoxical sleep (PS, also called rapid eye movement, REM, sleep; see, for review, Jones, 2004). However, the BF also contains more numerous noncholinergic neurons, including GABAergic and glutamatergic neurons that appear to play different roles in sleep/wake state regulation, including the promotion of slow wave sleep (SWS) or, conversely, waking (Lee et al., 2004; Jones, 2005b). From retrograde tracing studies, we previously found that few cholinergic neurons, but many GABAergic and other unidentified BF neurons, project caudally to the lateral hypothalamus (LH) (Gritti et al., 1994). Most recently, using anterograde transport of biotinylated dextran amine (BDA) together with immunohistochemistry for the vesicular transporter proteins (VTPs), we established that a minor proportion of terminals projecting into the LH from the BF contained the VTP for acetylcholine (ACh, VAChT), whereas a major proportion contained that for GABA (VGAT) and a remaining proportion contained the VTP for glutamate (VGluT2 and not VGluT1 or VGluT3), proving an important glutamatergic in addition to GABAergic contingent of the BF inputs to the LH (Henny and Jones, 2006). We also established in that study that the cholinergic, GABAergic, and glutamatergic projecting neurons were phenotypically distinct, since the VTPs were not colocalized in the same terminals. The BF afferents would thus release ACh, GABA, or glutamate. The aim of the present study was thus to examine if the Orx neurons in the hypothalamus are innervated by BF terminals and, if so, whether they might be selectively or preferentially innervated by cholinergic, glutamatergic, or GABAergic terminals and thereby influenced in a particular manner by BF neurons across the sleep/waking cycle.

Using anterograde transport of 10,000 MW BDA in rats (Henny and Jones, 2006), we examined in the present study the innervation of Orx neurons by neurons of the magnocellular preoptic nucleus (MCPO) and substantia innominata (SI) of the BF cholinergic cell area from where significant hypothalamic as well as neocortical projections originate (Gritti et al., 1994, 1997) and can influence behavioral in addition to cortical components of sleep/wake states (Szymusiak et al., 2000; Jones, 2004, 2005a,b). First, using single or dual-staining, we quantitatively studied and estimated with stereological analysis the distribution of Orx neurons in the hypothalamus and their contact by BDA-labeled terminals in light microscopy. Second, using triple-staining for Orx, BDA, and the VTPs, we quantitatively examined and estimated with stereological analysis the contacts on the Orx neurons by BDA-labeled terminals containing VAChT, VGluT2, or VGAT in fluorescence microscopy. Third, given evidence of prominent VGluT2 and VGAT-containing terminals apposing the Orx neurons, we further studied their contacts by confocal laser scanning microscopy and 3D reconstruction with rotation. Lastly, to ascertain whether such varicosities might form excitatory or inhibitory synapses on the Orx neurons, we similarly examined sections triple-stained for BDA, Orx, and the scaffolding postsynaptic proteins (PSPs), PSD-95 as a marker for asymmetric, glutamatergic synapses (Sheng and Pak, 2000; Sassoe-Pognetto et al., 2003) or gephyrin (Geph) as a marker for symmetric, GABAergic synapses (Pfeiffer et al., 1984; Giustetto et al., 1998; Sassoe-Pognetto and Fritschy, 2000; Sassoe-Pognetto et al., 2000). Using 3D reconstruction with rotation of high-resolution confocal images, we document important glutamatergic and GABAergic BF inputs onto Orx neurons.

MATERIALS AND METHODS

Animals and surgery

All procedures conformed to the guidelines of the Canadian Council on Animal Care and the US NIH and were

Abbreviations

ABC	Avidin-biotin-peroxidase complex	MCPO	Magnocellular preoptic nucleus
ac	Anterior commissure	MFB	Medial forebrain bundle
AHA	Anterior hypothalamic area	MPO	Medial preoptic nucleus
AMCA	Aminomethylcoumarin acetate	mt	Mammillothalamic tract
ANPB	Alpha-naphthol pyronin B	oc	Optic chiasm
Arc	Arcuate nucleus	Orx	Orexin or hypocretin
BDA	Biotinylated dextran amine	ot	Optic tract
BF	Basal forebrain	Pe	Periventricular hypothalamic nucleus
cp	Cerebral peduncle	PF	Perifornical area
Cy2	Cyanine	Pir	Piriform cortex
Cy3	Indocarbocyanine	PSD-95	95-kD postsynaptic density protein
Cy5	Indodicarbocyanine	PSP	Postsynaptic protein
DAB	Diaminobenzidine	SI	Substantia innominata
DAB-Ni	Nickel-intensified diaminobenzidine	SO	Supraoptic nucleus
DMH	Dorsomedial hypothalamic nucleus	STh	Subthalamic nucleus
f	Fornix	VAChT	Vesicular transporter for acetylcholine
FS	Fundus striatum	VGAT	Vesicular transporter for GABA
Geph	Gephyrin	VGluT2	Vesicular transporter for glutamate 2
ic	Internal capsule	VMH	Ventromedial hypothalamic nucleus
LH	Lateral hypothalamus	VTP	Vesicular transporter protein
LPO	Lateral preoptic area	ZI	Zona incerta

TABLE 1. Primary Antibodies (AB) for Immunostaining of Orexin (Orx), Vesicular Transporter Proteins (VTPs) or Postsynaptic Proteins (PSPs)

Antigen	Host sp	Source	Cat. #	Immunogen	Specificity
Orx					
Orx-A	Rb	Phoenix[1]	H-003-30	Full 33 AA Orx-A peptide sequence from rat (EPLPDCCRQKTCSCRLYELLHGAGNHAAGILTL)[2]	By WB the AB recognizes a ≈3.5 kD band from rat brain, corresponding to the Orx-A peptide[2]
Orx-A	Gt	Santa Cruz[3]	sc-8070	Peptide mapping at the C-terminus of human Orx-A (AA 48–66 of the Orx precursor, identical to corresponding mouse sequence)[4]	AB reacts with Orx-A of mouse, rat and human by WB, immunostaining blocked with antigen peptide (sc-8070 P) and pattern of staining identical to that with Orx-A (Rb) H-003-30 (Phoenix)[5]
VTPs					
VAChT	Gt	Chemicon[6]	AB1578	Peptide corresponding to C-terminus of cloned rat VAChT[7] (CSPPGPFDGCEDDYNYYSRS)[8]	By WB the AB recognizes a ≈65–70 kD band corresponding to VAChT protein[7]
VAChT	Rb	Sigma[9]	V5387	Peptide corresponding to AA 512–530 of C-terminus of cloned rat VAChT (K-SPPGPFDGCEDDYNYYSRS)[10]	By WB the AB recognizes a ≈67–70 kD band, corresponding to VAChT protein[10]
VGluT2	Rb	Gift RHE[11]	-	GST fusion protein containing AA 519–582 of rat DNPi (VGluT2)[12]	By WB the AB recognizes a ≈50–62 kD band from rat brain[12]
VGAT	Rb	Chemicon	AB5062P	Peptide corresponding to 17 AA near C-terminus region of rat VGAT (VHSLEGLIEAYRTNAED)[13]	By WB the AB recognizes a band at ≈55–60 kD[13]
PSPs					
PSD-95	Ms	ABR[14]	MA1-045	Purified recombinant of rat PSD-95[15]	By WB the AB recognizes a ≈95 kDa protein and a slightly larger species from rat brain extracts[15]
Geph	Ms	Sy-Sy[16]	147011	Purified rat gephyrin[17]	By WB the AB recognizes a ≈93 kD band. It detects a N-terminus epitope[18]

AA, amino acid; AB, antibody; DNPi, differentiation-associated Na^+-dependent phosphate transporter; Geph, gephyrin; Gt, goat; Ms, mouse (monoclonal); Rb, rabbit; sp, species; WB, western blot.
[1]Phoenix Pharmaceuticals, Belmont, CA.
[2]http://www.phoenixpeptide.com/Catalog%20Files/Orexins%20Section/OrexinsHypocretinspage.htm
[3]Santa Cruz Biotechnology, Santa Cruz, CA.
[4]Information provided by Santa Cruz data sheet and technical service.
[5]Information on WB provided by Santa Cruz data sheet and technical service, blocking experiments carried out in our lab with the Santa Cruz antigen peptide and immunostaining of Orx cell population compared for two antibodies in our lab in this and previous studies (Modirrousta et al., 2005).
[6]Chemicon International, Temecula, CA.
[7]http://www.chemicon.com/Product/ProductDataSheet.asp?ProductItem=AB1578
[8]Supplied by Chemicon on request.
[9]Sigma, St. Louis, MO.
[10]http://www.sigmaaldrich.com/sigma/datasheet/v5387dat.pdf
[11]Gift from R.H. Edwards and R.T. Fremeau Jr.
[12]Fremeau et al., 2001.
[13]http://www.chemicon.com/Product/ProductDataSheet.asp?ProductItem=AB5062P
[14]ABR: Affinity BioReagents, Golden, CO.
[15]http://www.bioreagents.com/index.cfm/fuseaction/products.print/Product/MA1-045
[16]SY-SY: Synaptic Systems, Goettingen, Germany.
[17]http://www.sysy.com/gephyrin/gephy_fs.html
[18]Pfeiffer et al., 1984.

approved by the McGill University Animal Care Committee.

As previously described in detail (Henny and Jones, 2006), Long Evans rats (200–250 g, Charles River Canada, St. Constant, Quebec, Canada) were anesthetized and placed in a stereotaxic frame (David Kopf Instruments, Tujunga, CA) for surgery. Glass micropipettes (tip diameter 15–25 μm) were back-filled with a 0.5 M NaCl solution containing 2% 10,000 MW BDA (BDA-10,000, Molecular Probes, Eugene, OR). Since previous studies using anterograde as well as retrograde tracing methods showed no evidence for contralateral projections from BF to the posterior hypothalamus (Swanson, 1976; Gritti et al., 1994), bilateral injections of BDA were performed. The pipettes were lowered into the region of the MCPO on each side (from bregma: anterior-posterior (AP), −0.5 mm; lateral (L), ± 2.5 mm; vertical (V), 8.5 mm) (Paxinos and Watson, 1986) with the aid of a micropositioner (Model 660, David Kopf Instruments). Once in the targeted site, microinjection of BDA was performed by iontophoresis (using a Microiontophoresis Dual Current Generator 260, World Precision Instruments (WPI), Sarasota, FL) applying positive current pulses (5–10 μA) in a duty cycle of 1 second (0.5 seconds on, 0.5 seconds off) for a period of 25–30 minutes through a stimulator (Pulsemaster A300, WPI) and stimulus isolation unit (Iso-Flex, A.M.P.I., Jerusalem, Israel).

Rats were maintained for 5 or 6 days with food and water ad libitum and subsequently perfused transcardially under deep sodium pentobarbital anesthesia (100 mg/kg, intraperitoneally, i.p.) with ~500 mL 4% paraformaldehyde fixative solution. The brains were removed and put in a 30% sucrose solution for 2–3 days, after which they were frozen at −50°C and stored at −80°C for subsequent processing.

Immunohistochemistry

Sections were cut using a freezing microtome in 25 μm-thick coronal sections and collected in eight adjacent series at 200-μm intervals through the forebrain, including the magnocellular basal forebrain and the tuberal hypothalamus. To visualize BDA-labeled neurons in the BF as well anterogradely labeled axons in the tuberal hypothalamus, the avidin-biotin-peroxidase complex (ABC) protocol was used with diaminobenzidine (DAB) intensified with Nickel (DAB-Ni). Sections were subsequently counterstained for Nissl substance using Neutral Red.

For the mapping, distribution, and quantitative estimates of Orx+ cells in the hypothalamus, serial sections were incubated overnight with goat (Gt)-Anti-Orx-A (1:500, see Table 1) and stained with DAB following incubation with donkey (Dky) anti-Gt IgG and Gt peroxidase-antiperoxidase

TABLE 2. Combination and Sequential Processing of Primary and Secondary Antibodies along with Streptavidin (SA) Used for Triple Fluorescent Staining of Orexin (Orx), Vesicular Transporter Proteins (VTPs), or Postsynaptic Proteins (PSPs) and Biotinylated Dextran Amine (BDA)

	1ry AB (overnight)[1]			2ry AB (3 hours)		SA (3 hours)		
Series	Antigen	Hostsp	Dilution	IgG (Dky)[2,3]	Dilution	SA	Dilution	n[4]
BDA/VTP/Orx								
BDA/VAChT/Orx	VAChT Orx-A	Gt Rb	1:1000 1:200	Anti-Gt-Cy3 Anti-Rb-AMCA	1:800 1:100	SA-Cy2	1:800	4
BDA/VAChT/Orx	VAChT Orx-A	Gt Rb	1:1000 1:200	Anti-Gt-Cy3 Anti-Rb-Cy5	1:800 1:800	"	"	2
BDA/VAChT/Orx	VAChT Orx-A	Rb Gt	1:5000 1:200	Anti-Rb-Cy3 Anti-Gt-Cy5	1:800 1:800	"	"	5
BDA/VGluT2/Orx	VGluT2 Orx-A	Rb Gt	1:5000 1:200	Anti-Rb-Cy3 Anti-Gt-AMCA	1:800 1:100	"	"	4
BDA/VGluT2/Orx	VGluT2 Orx-A	Rb Gt	1:5000 1:200	Anti-Rb-Cy3 Anti-Gt-Cy5	1:800 1:800	"	"	11
BDA/VGA T/Orx	VGA T Orx-A	Rb Gt	1:250 1:200	Anti-Rb-Cy3 Anti-Gt-AMCA	1:800 1:100	"	"	4
BDA/VGA T/Orx	VGA T Orx-A	Rb Gt	1:250 1:200	Anti-Rb-Cy3 Anti-Gt-Cy5	1:800 1:800	"	"	11
BDA/PSP/Orx								
BDA/PSD-95/Orx	PSD-95 Orx-A	Ms Gt	1:100 1:200	Anti-Ms-Cy5 Anti-Gt-Cy3	1:800 1:800	SA-Cy2	1:800	3
BDA/Geph/Orx	Geph Orx-A	Ms Gt	1:100 1:200	Anti-Ms-Cy5 Anti-Gt-Cy3	1:800 1:800	"	"	3

AB, antibody; AMCA, aminomethylcoumarin acetate; Cy2, cyanine; Cy3, indocarbocyanine; Cy5, indodicarbocyanine; Dky, donkey; Geph, gephyrin; Gt, goat; Ms, mouse (monoclonal); Rb, rabbit; sp, species.
[1]For sources and specificity of primary antibodies from different species, refer to Table 1.
[2]Jackson ImmunoResearch Laboratories, West Grove, PA.
[3]For multiple labeling (ML) with minimal crossreactivity (min X) to other species.
[4]n: number of cases (each case referring to an injection site and series from the same side of the brain, thus 1 or 2 per brain from 9 rats for a total of 16 injection sites selected for their placement in the MCPO/SI).

(PAP, both from Jackson ImmunoResearch Laboratories, West Grove, PA).

For evaluation of the injection sites, description of BDA-labeled fibers in the tuberal hypothalamus, and examination of the innervation of Orx+ cells in the region, series were processed for dual-staining of BDA using the ABC procedure with DAB-Ni and Orx-A (above) using PAP with alpha-naphthol pyronin B (ANPB, Sigma, St. Louis, MO). Injection sites on one or two sides from nine rats were selected according to their placement in the MCPO and SI (n = 16 cases) for subsequent processing and analysis in peroxidase or fluorescent stained material.

For triple fluorescent staining of Orx with the VTPs (VAChT, VGluT2, or VGAT) and BDA (see Tables 1 and 2), free-floating sections from each series were rinsed for 30 minutes in Trizma saline buffer (TS, 0.1 M, pH 7.4) followed by incubation for 30 minutes with a blocking solution of normal donkey serum (NDS, 6% in TS) containing 0.3% Triton X-100 (TX). Sections were subsequently coincubated overnight at room temperature with VTP and Orx-A primary antibodies (in TS containing NDS 1% and TX 0.3%). Prior pilot studies determined that incubation in TX 0.3% allowed full penetration of the antibodies and streptavidin, as viewed through the z-axis under epifluorescent and confocal microscopy. The next day sections were incubated for 3 hours in indocarbocyanine (Cy3)- and aminomethylcoumarin acetate (AMCA) or indodicarbocyanine (Cy5)-conjugated secondary antibodies, followed by 3 hours in cyanine (Cy2)-conjugated-streptavidin (SA) for BDA revelation. For triple fluorescent staining of BDA with the PSPs, PSD-95 or Geph, and Orx, the same protocol was used by coincubation with the PSP and Orx antibodies overnight (see Tables 1 and 2).

All sections were mounted out of Trizma water and the mounted sections dehydrated through alcohols, cleared in xylene, and coverslipped with Permount.

Conventional microscopy, tracing, and stereological analysis

Sections were examined under light and epifluorescent microscopy with a Leica DMLB or Nikon E800 microscope equipped with an x-y-z motorized stage, video or digital camera, and filters appropriate for FITC or Cy2, Rhodamine or Cy3, DAPI-AMCA, and/or Cy5 fluorescence. Single as well as composite images were acquired on the Nikon or Leica microscopes using Neurolucida software from MicroBrightField (MBF, Colchester, VT), which was also used for plotting cells and tracing fibers. In light or fluorescent material, cells and varicosities were counted using the Optical Fractionator probe of StereoInvestigator software (MBF) on the Nikon microscope. For tracing or counting, a computer-resident atlas of the rat brain was employed that was developed and applied in our laboratory using standardized procedures for tissue processing. For each application, series of histology sections are matched to appropriate levels of the atlas (at 400-μm intervals) under low magnification (5 or 10× objective). At each level the atlas image is then rotated, if necessary, and the contours adjusted to optimally fit the relevant nuclei of the histology section. In the BF, the number of BDA-labeled cells was counted through the injection site within the MCPO and SI (Gritti et al., 1993; Henny and Jones, 2006). Through the hypothalamus, Orx neurons were plotted and counted through their full distribution across three AP levels (in mm from Interaural (A) zero): ~A6.6, A6.2, and A5.8 (Paxinos and Watson, 1986), and

within three contours, the LH, comprising the region lateral to the fornix through which the MFB passes and present at levels ~A6.6, A6.2, and A5.8; the perifornical area (PF), comprising the area surrounding and extending medial to the fornix; and the dorsomedial hypothalamic nucleus (DMH) and present at levels ~A6.2 and ~A5.8 (Veening et al., 1982; Modirrousta et al., 2005). BDA-labeled fibers were plotted and analyzed using the same atlas sections and contours.

For representation of the distribution of the Orx population, Orx+ neurons (stained with DAB) were plotted under brightfield illumination with a 40× objective at three levels (above) using Neurolucida. In the same material, stereological estimates of the total number of Orx+ cells across three levels in the LH, and two levels in the PF and DMH, were obtained using StereoInvestigator. Within the optical fractionator probe, cells were counted with a 60× oil objective (1.40 numerical aperture, NA) using a counting frame of 120 × 120 μm and a sampling grid size of 240 × 240 μm to sample 25% of the x-y area of each nucleus. Within each counting frame or block, all cells whose tops came into focus beneath the surface of the section were counted through a 10-μm dissector height in the z-axis, which corresponded to the average thickness of the mounted (dehydrated, cleared, and coverslipped) sections in this series.

To examine the relationship of BF axons to the Orx neurons in the hypothalamus, BDA-labeled fibers (stained black with DAB-Ni) and Orx+ cell bodies (stained fuchsia with ANPB) were traced under brightfield illumination using the Neurolucida software (MBF). Axons and cell bodies were drawn using a 100× oil objective within contours of the LH, PF, and DMH. Unbiased estimates of the number and proportion of Orx+ neurons receiving contacts from BF varicosities were obtained in the LH, where both the Orx+ cells and BF varicosities were most numerous, as well as in PF and DMH. An Orx+ cell was considered to be contacted if a BDA+ varicosity was seen in direct apposition to the cell, with no obvious space observed between them and at a point where both were located at the approximately same focal plane. Stereological counts were obtained of Orx+ cells that were (Orx+:BDA+) or were not (Orx+:BDA−) contacted by one or more BDA+ varicosities through the LH, PF, and DMH (n = 3). Counts were performed under a 100× oil objective (1.40 NA) at three levels (above) within the LH contour and two levels (above) within PF and DMH contours. Within the optical fractionator probe, a counting frame of 70 × 70 μm was employed with a sampling grid size of 140 × 140 μm so as to sample 25% of the area. Within each counting frame or block, all cells whose tops came into focus beneath the surface of the section were counted through 15 μm in the z-axis, which was the average thickness of the mounted sections in this series.

To examine the relationship of BDA+ terminals containing different VTPs [VTP+] to Orx+ cells, triple-stained sections were viewed under epifluorescent microscopy to determine if BDA+[VAChT+], BDA+[VGluT2+], or BDA+[VGAT+] varicosities appeared to come into contact with Orx+ cells stained with AMCA or Cy5 (see Table 2). Additional series were used for stereology in which Orx cells were stained with Cy5 (using the antibody from Gt in combination with anti-VTP antibodies from Rb; Table 2). Unbiased estimates were obtained of the total number and proportion of innervated Orx+ cells that were contacted by each of the BDA+[VTP+] type of varicosity by counting Orx+:BDA+[VTP+] along with Orx+:BDA+[VTP−] cells through three levels of the LH contour in each series (n = 3). In addition, estimates of the total number and proportion of contacting varicosities were computed for each of the BDA+[VTP+] type of varicosity by using counts of BDA+[VTP+]:Orx+ and BDA+[VTP−]:Orx+ varicosities (n = 3). The presence of BDA+ contacts on the counted cells was assessed online by sequential observation of the material through the different filters at the same focal plane and multiple planes through the z-axis. Counts were performed under a 100× oil objective (with 1.40 NA) within a counting frame of 70 × 70 μm and using a sampling grid of 120 × 120 μm so as to sample ~33% of the LH area. Within each counting frame or block, all cells whose tops came into focus beneath the surface of the section were counted through 8 μm in the z-axis, which corresponded to the average thickness of the mounted sections in these series.

Confocal microscopy and image processing

Material triple-stained for BDA/VTP/Orx or BDA/PSP/Orx was examined in a Zeiss LSM 510 laser scanning confocal microscope equipped with Argon 488 nm, helium-neon 543 nm, and helium-neon 633 nm lasers for Cy2, Cy3, and Cy5 excitation, respectively. Appropriate filters were used for detection of Cy2 (bandpass 500–530 nm, green), Cy3 (bandpass 565–615 nm, red), and Cy5 (bandpass 697–719 nm, infrared, color-coded in blue). Scanning was performed through a Plan-Apochromat 100× (with 1.4 NA) objective and pinhole size of ~0.8 (0.6–1, Airy Units) for the three channels. Acquisition was performed with the resident LSM 510 software and consisted of stacks of images taken through the z-axis in optical slices of ~0.5 μm for VTPs, or ~0.33 μm for PSPs series. Additional high-resolution stack images (optical slices of ~0.05–0.1 μm) were acquired for the PSP series.

Rendered 3D views of the stacks were obtained using the fluorescence rendering mode from the image software Volocity 3.7 (Improvision, Lexington, MA, www.improvision.com), which provides a semitransparent 3D view of the different elements based on the degree of intensity of each voxel (i.e., the more intense, the less transparent). The different elements could then be examined simultaneously and interactively from different angles and magnifications. Thus, varicosities could be judged to be in contact with a postsynaptic cell or process, as assessed by the absence of space between the presynaptic and postsynaptic element from any of the angles observed (Wouterlood et al., 2002). High-resolution image stacks (see above) were analyzed in the fluorescent rendering mode as well as in the isosurface rendering mode, which provides a 3D solid, nontransparent view of the element surface. Channels in which the signal was low or the noise was relatively high were restored using a deconvolution procedure (iterative restoration in Volocity).

Adjustment for brightness and contrast for all pictures, in addition to adjustment of tonal range for each individual RGB channel ("Adjust/Levels" command in Photoshop) for fluorescent images were performed with Adobe Photoshop Creative Suite edition (Adobe System, San Jose, CA). Figure preparation and final montage were done with Adobe Illustrator Creative Suite edition.

RESULTS

BDA injection site and anterograde labeling in the hypothalamus

Iontophoretic application of BDA-10,000 into the region of the MCPO-SI (Fig. 1A) on two sides in nine rats produced small and well-restricted, spherical injection sites (Fig. 1B) of <500 μm diameter and containing (some ~1,400) labeled nerve cell bodies, as previously described (Henny and Jones, 2006). Injection sites were positioned primarily within the MCPO and SI (in n = 16 cases selected for analysis), where ~90% and ~6% of labeled cells were located, respectively. BDA-labeled fibers coursed through the MFB to reach the tuberal hypothalamus, where multiple neurons, particularly in the LH, were contacted by varicosities (Fig. 1C) (Henny and Jones, 2006).

Number and distribution of Orx+ neurons in the hypothalamus

The distribution and numbers of Orx+ neurons were examined in PAP (DAB)-stained material. Orx+ cells were distributed across the tuberal hypothalamus in moderate numbers from rostral to caudal levels (~A6.6, A6.2, and A5.8, Fig. 2). Although most concentrated in the area immediately surrounding and dorsal to the fornix, cells were distributed through the LH, PF, and DMH. According to stereological estimates of total numbers of cells (mean ± SEM, n = 3), ~1,800 Orx+ cells were located within the LH, ~500 in the PF, and ~900 in the DMH with a total of ~3,200 neurons per side (Table 3). The proportions of Orx neurons were thus ~56% in the LH, ~15% in the PF, and ~29% in the DMH contours as delineated here.

BDA-labeled axons in relation to Orx+ neurons

The relation of BF axon terminals to Orx cells was examined in material dual-stained using peroxidase for BDA (in black with DAB-Ni following ABC procedure) and Orx (in fuchsia with ANPB following PAP procedure) (n = 7, Fig. 3). Multiple BDA-labeled fibers were evident in the regions where Orx+ cell bodies and proximal dendrites were present, particularly in the LH (Fig. 3A). Moreover, BDA-labeled axonal boutons en passant (Fig. 3B′) or boutons terminaux (Fig. 3B″,B‴) appeared to contact Orx+ cell bodies as well as dendrites. In tracings of all BDA+ fibers along with Orx+ cells at high magnification using Neurolucida, multiple fine collaterals of the coarse fibers within the MFB appeared to extend dorsally and medially to reach Orx+ neurons within the central and dorsal regions of the LH (Fig. 3C, level A6.0, approximately intermediate to those seen in Fig. 2B,C). Here, BDA-labeled varicosities appeared to contact Orx+ soma or proximal dendrites in the LH (Fig. 3D′,D″,D‴). Some BDA-labeled fibers also extended medially to reach into the PF or DMH, although these were few in number. As determined by stereological analysis, the proportion of Orx+ neurons that were contacted by at least one BDA+ varicosity (Orx+:BDA+) within the LH, PF, and DMH, was estimated to be ~41%, ~11%, and ~9%, respectively (Table 3). Overall, ~28% of the total population of Orx+ neurons was contacted by BF axonal varicosities.

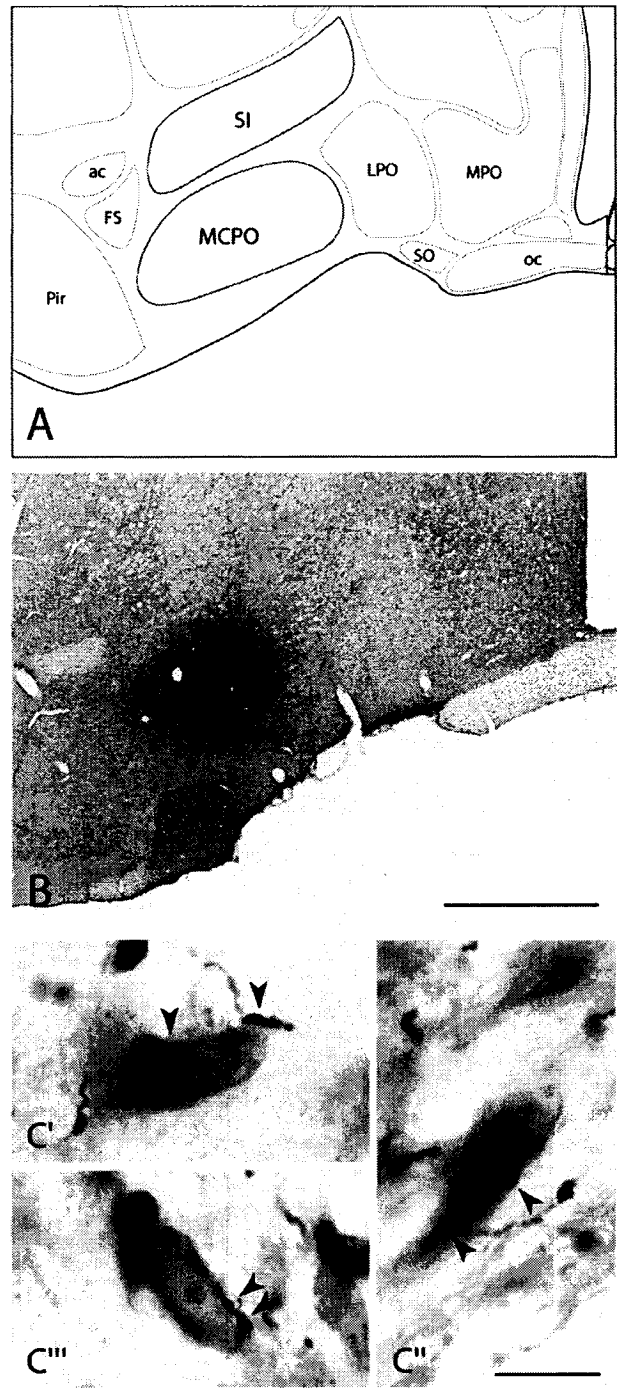

Fig. 1. BDA injection site in BF and anterogradely labeled BF terminals in the LH. **A:** Atlas section through the cholinergic cell area (MCPO-SI) where iontophoretic applications of BDA were placed. **B:** Composite image of typical BDA injection site (processed using ABC with DAB-Ni and counterstained for Nissl with neutral red). Note the small size and restricted location of BDA injection site in the MCPO. **C:** High-magnification images showing BDA+ axonal varicosities (arrowheads) contacting Nissl-stained cell bodies located in dorsal (C′), middle (C″), and ventral (C‴) portions of the LH area. Scale bars = 1 mm in B; 10 μm in all C.

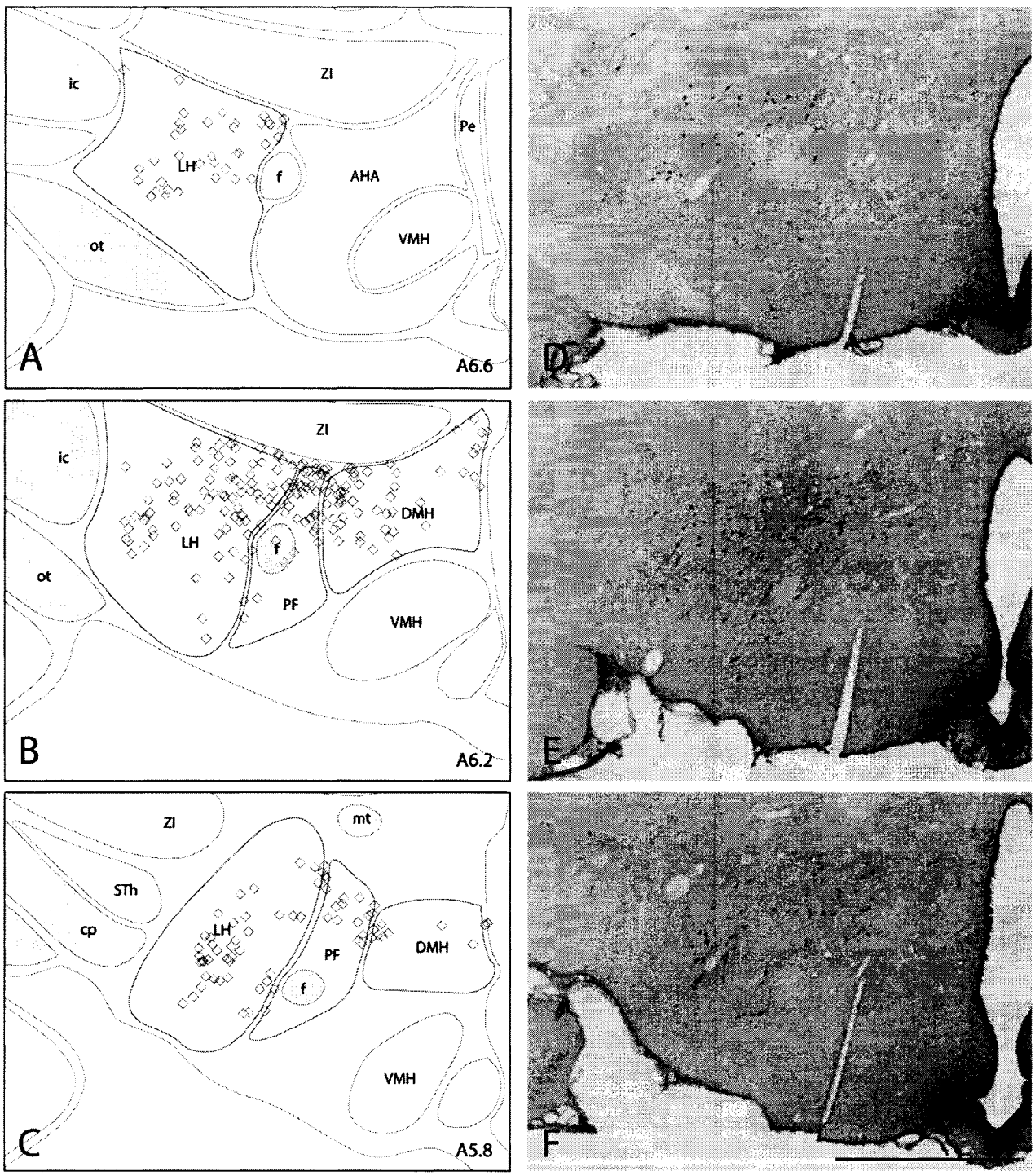

Fig. 2. Distribution of Orx+ neurons at three levels through the tuberal hypothalamus. **A–C:** Mapping of Orx+ neurons within contours of the LH, PF, and DMH at A6.6 (A), A6.2 (B), and A5.8 (C) levels, based on the material presented in D–F, respectively. Some few scattered Orx+ neurons within contours of the AHA, Pe and ZI are not shown in the mapping. **D–F:** Composite images of sections immunostained for Orx-A (with DAB) showing the distribution of Orx+ neurons in the hypothalamus at A6.6 (D), A6.2 (E), and A5.8 (F). Scale bar = 1 mm in F (applies to D–F).

TABLE 3. Numbers and Proportions of Orx Cells and Orx+ Cells Contacted by BDA+ Varicosities Estimated across Hypothalamic Regions[1]

Hypothalamic region	LH	PF	DMH	Total
Single-immunostained Orx series[2]				
N° Orx cells	1770.7 ± 182.3	469.3 ± 21.3	917.3 ± 149.3	3157.3 ± 259.5
% Orx cells of Total across regions	**56.0 ± 3.0 %**	**15.2 ± 2.0 %**	**28.8 ± 2.9 %**	**100 ± 0.0 %**
Dual-immunostained BDA/Orx series[3]				
N° Orx+ cells	1216.0 ± 97.8	320.0 ± 37.0	576.0 ± 97.8	2122.0 ± 97.8
N° Orx+ cells contacted by a BDA + var. (Orx+:BDA+)	512.0 ± 110.9	42.7 ± 42.7	42.7 ± 21.3	597.3 ± 166.6
% Orx+ cells contacted by a BDA+ var. in each region	**41.4 ± 7.1 %**	**11.1 ± 11.1 %**	**8.9 ± 4.8 %**	**27.7 ± 6.6 %**

Data are presented as means ± SEM. DMH, dorsomedial hypothalamic nucleus; LH, lateral hypothalamus; PF, perifornical area; var., varicosity.
[1]Estimated numbers of cells and BDA-contacted cells were obtained by random systematic sampling of the hypothalamus at levels A6.6, A6.2 and A5.8 for LH, and levels A6.2 and A5.8 for PF and DMH using StereoInvestigator.
[2]Series from 3 different brains processed for single-immunostaining of Orx cells with DAB (see Methods).
[3]Series from 3 individual cases (injection sites) processed for dual-immunostaining of BDA (with DAB-Ni) and Orx (with ANPB, see Materials and Methods).

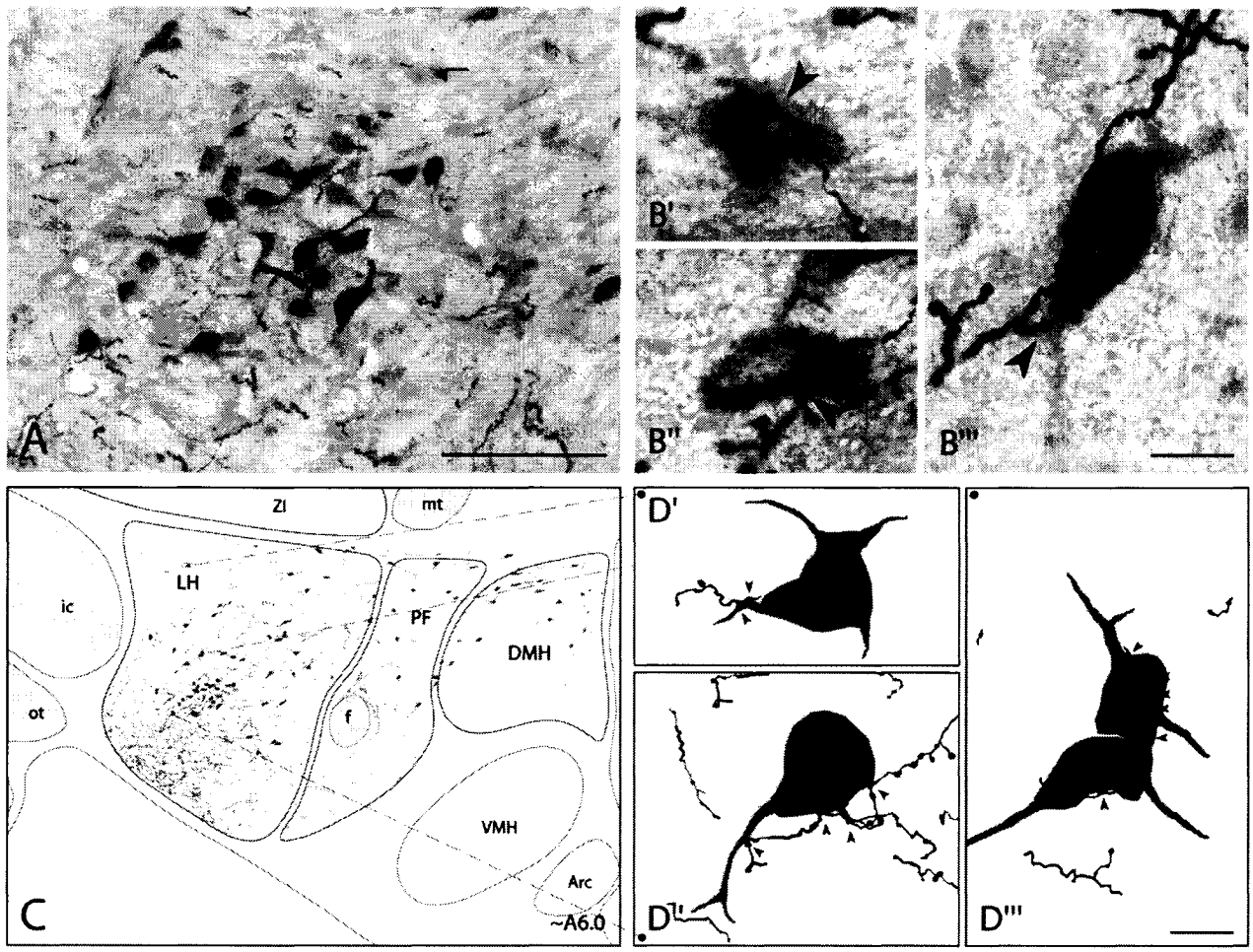

Fig. 3. Distribution of BDA-labeled fibers in relation to Orx+ neurons. **A:** Low-magnification composite image of BDA+ axons (in black, DAB-Ni) and Orx+ cells (in fuchsia, ANPB) in the LH at ~A6.0. **B:** High-magnification images showing BDA+ varicosities (arrowheads) in contact with Orx+ neurons in the LH (B', B'', and B'''). **C:** Tracing and mapping of all BDA+ fibers and Orx+ neurons in the tuberal hypothalamus at ~A6.0 μm (from IA0). From coarse fibers within the ventrolateral MFB, fine varicose collaterals extended dorsally and medially to reach Orx+ cells through the LH. Some fibers also extended medially into the PF and DMH. **D:** High magnification of elements depicted in C, showing contacts of BDA+ axons by varicosities on proximal dendrites or soma of Orx+ cells located in the dorsal (D') or central (D'' and D''') region of the LH. Tonal range for each RGB channel as well as brightness and contrast adjustment were made for pictures in A and B. Scale bars = 100 μm in A; 10 μm in B,D.

Given that the maximal incidence of Orx+ neurons contacted occurred in the LH and that the majority of Orx+ neurons were also contained within the LH (above), subsequent analyses of the BF innervation were focused on the Orx+ neurons within the contour of the LH.

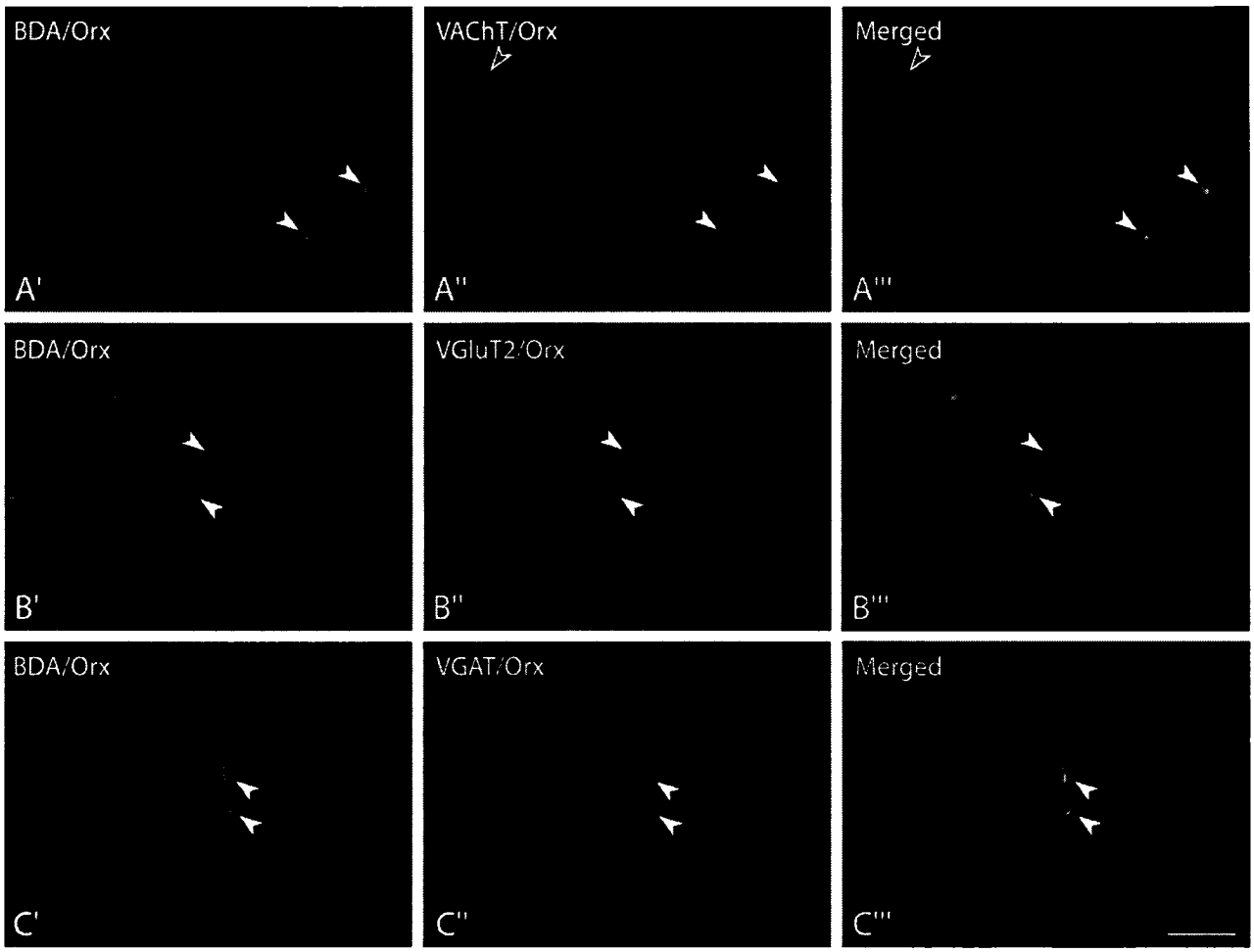

Fig. 4. VAChT+, VGluT2+ or VGAT+, BDA-labeled varicosities in relation to Orx+ neurons viewed by epifluorescent microscopy. In each case, BDA is green (Cy2), VTP red (Cy3), and Orx blue (AMCA in A or Cy5 in B and C). **A:** BDA+[VAChT+] terminals in the vicinity of an Orx+ neuron. BDA+ terminals (solid arrowheads in A') located in the vicinity, yet not close to an Orx+ neuron (left), are positive for the VAChT protein (solid arrowheads in A''), as evident in the merged image (in yellow, solid arrowheads in A'''). A VAChT+ terminal that is not BDA+ (open arrowhead) is closer to the Orx+ cell body. Note also the sparse number of VAChT+ varicosities in the vicinity of Orx+ neurons. **B:** BDA+[VGluT2+] terminals in close proximity to Orx+ neurons. Two small BDA+ terminals (solid arrowheads in B') over an Orx+ cell body are positive for the VGluT2 protein (solid arrowheads in B''), as evident in the merged image (in yellow, solid arrowheads in B'''). Note also the relatively large number of VGluT2+ varicosities in close proximity to the Orx+ neurons. **C:** BDA+[VGAT+] terminals over Orx+ neurons. Two BDA+ terminals (solid arrowheads in C') in close proximity to an Orx+ neuron are positive for VGAT (solid arrowheads in C''), as evident in the merged image (in yellow, solid arrowheads in C'''). In all images, tonal range was adjusted for each RGB channel individually. Scale bar = 10 μm in C''' (applies to A–C).

VAChT, VGluT2, and VGAT in BDA-labeled varicosities in relation to Orx+ neurons in the LH

To determine if BF terminals contacting Orx neurons are cholinergic, glutamatergic, or GABAergic, sections that were triple-stained for BDA (with Cy2), the VTPs (VAChT, VGluT2, or VGAT with Cy3), and Orx-A (with AMCA or Cy5) were examined under epifluorescent microscopy (see number of cases, n, for each series in Table 2). In these sections, sparse VAChT+ varicosities were evident (Fig. 4A''), whereas multiple VGluT2+ (Fig. 4B'') and VGAT+ (Fig. 4C'') varicosities were present in the vicinity of the Orx+ neurons. BDA+[VAChT+] (Fig. 4A'''), BDA+[VGluT2+] (Fig. 4B'''), and BDA+[VGAT+] (Fig. 4C''') BF axons were all present in the immediate surround of the Orx+ neurons as well. However, only BDA+[VGluT2+] (Fig. 4B''') and BDA+[VGAT+] varicosities (Fig. 4C''') appeared to contact the Orx+ neurons in substantial numbers.

Stereological estimates of contacts between VAChT+, VGluT2+, or VGAT+ BDA-labeled varicosities and Orx+ neurons in the LH

To determine the proportions of Orx+ neurons innervated by cholinergic, glutamatergic, or GABAergic BF axon terminals, stereological analysis was used for estimation of the total numbers of Orx+ neurons contacted by each of the BDA+[VTP+] types of varicosities in the LH through the three levels studied (~A6.6, A6.2, and A5.8,

TABLE 4. Numbers and Proportions of Orx+ Cells Contacted by BDA+ Varicosities Positive for Vesicular Transporter Proteins (VTP+), and Numbers and Proportions of BDA+[VTP+] Varicosities in Contact with Orx+ Cells in the Lateral Hypothalamus (LH)[1]

Triple-immunostained BDA/VTP/Orx series	VAChT	VGluT2	VGAT
N° Orx+ cells contacted by BDA+ var. (Orx+:BDA+) in each series	548.3 ± 68.3	532.7 ± 109.7	595.3 ± 109.7
N° Orx+ cells contacted by BDA+[VTP+] var. (Orx+:BDA+[VTP+])[2]	15.7 ± 15.7	188.0 ± 81.4	376.0 ± 27.1
% Orx+ cells contacted by BDA+[VTP+] var.[2]	**3.7 ± 3.7 %**	**31.4 ± 9.4 %**	**66.7 ± 11.2 %**
N° BDA+ var. in contact with Orx+ cells (BDA+:Orx+) in each series	908.6 ± 122.4	1096.7 ± 180.7	1457.0 ± 204.9
N° BDA+[VTP+] var. in contact with an Orx+ cells (BDA+[VTP+]:Orx+)[2]	15.7 ± 15.7	203.7 ± 95.3	814.7 ± 87.2
% BDA+[VTP+] var. in contact with Orx+ cells[2]	**2.2 ± 2.2 %**	**16.6 ± 6.2 %**	**57.8 ± 8.7 %**

Data are presented as means ± SEM. var., varicosity.
[1]Estimated numbers of cells were obtained by random systematic sampling of the LH area at levels A6.6, A6.2 and A5.8 using StereoInvestigator from three individual cases (injection sites).
[2]According to a non-parametric Kruskal-Wallis test, the different VTP+ varicosities differed significantly according to the numbers ($H = 6.587$, $P = 0.037$) and proportions ($H = 7.261$, $P = 0.027$) of Orx+ neurons contacted by BDA+[VTP+] and to the numbers ($H = 6.587$, $P = 0.037$) and proportions ($H = 6.938$, $P = 0.031$) of BDA+[VTP+] varicosities contacting Orx+ neurons.

n = 3 cases, Table 4). In the VAChT series, less than 4% of the Orx+:BDA+ neurons were contacted by BDA+[VAChT+] varicosities. In the VGluT2 series, ~31% of the Orx+:BDA+ neurons were contacted by BDA+[VGluT2+] varicosities. In the VGAT series, ~67% of the Orx+:BDA+ neurons were contacted by BDA+[VGAT+] varicosities.

The number of BDA+[VTP+] varicosities contacting Orx+ neurons (BDA+[VTP+]:Orx+) was also determined (n = 3, Table 4). As estimated from each series, the proportions of varicosities in contact with Orx+ neurons were, respectively: ~2% for BDA+[VAChT+], ~17% for BDA+[VGluT2+], and ~58% for BDA+[VGAT+] varicosities. Across series, the numbers of terminals detected per Orx+ cell were: one for BDA+[VAChT+], one to two for BDA+[VGluT2+], and one to four for BDA+[VGAT+] varicosities. Given the minimal number of contacts by BDA+[VAChT+] varicosities and the substantial number of contacts by BDA+[VGluT2+] and BDA+[VGAT+] varicosities on the Orx+ neurons, confocal analysis was pursued for the latter terminals.

Confocal analysis of VGluT2 or VGAT inside and of PSD-95 or gephyrin opposite BDA+ terminals on Orx+ neurons

To examine in detail the nature of the BDA+ contacts observed on Orx+ neurons, confocal microscopic analysis was performed on material triple-stained for BDA (with Cy2), Orx (with Cy5 or Cy3) and markers for the presynaptic, VTP (VGluT2 or VGAT with Cy3) or postsynaptic, PSP (PSD-95 or Geph with Cy5) (see Table 2 for number of cases processed and examined for each series). Confocal images were further viewed using 3D reconstruction and rotation with magnification to confirm that the pre- and postsynaptic elements were in contact through three spatial axes.

In series triple-stained for BDA, VGluT2, and Orx, the Orx+ neurons were seen to be surrounded by numerous VGluT2+ varicosities. In this material, many BDA-labeled VGluT2+ varicosities were apposed to Orx+ soma (Fig. 5A) or proximal dendrites (not shown). As judged from examination and rotation of 3D images from such cases, the BDA+[VGluT2+] varicosity appeared to be in contact with the Orx+ cell, since no space could be observed between the two (Fig. 5A, small images) with rotation through three axes.

In series triple-stained for BDA, PSD-95, and Orx, staining for PSD-95 appeared punctate and could be seen on the surface of Orx+ neurons (Fig. 5B). In some BDA+:Orx+ contacts (Fig. 5B), PSD-95+ puncta could be detected opposite the BDA+ varicosity and associated with the Orx+ cell (Fig. 5B, small images). From 93 acquired images of appositions (from n = 3 cases), 74 BDA+:Orx+ contacts (~80%) were confirmed in rotated and magnified 3D images, and 16 of these, 21.6%, showed staining for PSD-95 opposite the BDA+ varicosity and associated with the Orx+ cell.

To further assess the spatial relationship among the BDA+ terminals, PSD-95+ puncta, and Orx+ cells, image stacks with high z-axis resolution (0.05–0.10 μm optical slices) were acquired of 23 appositions (from n = 3 cases) and analyzed in 3D rotations. Contacts were confirmed between BDA+ varicosities and Orx+ neurons, as shown from three different, orthogonal 3D angles of semitransparent fluorescence images (Fig. 6A1,B1,C1). PSD-95+ profiles were observed in apposition to BDA+ varicosities (Fig. 6A2,B2,C2) and in association with the surface of Orx+ neurons (Fig. 6A3,B3), being localized between BDA+ and Orx+ elements (Fig. 6A4,B4). Opaque isosurface rendering of the three elements further evidenced the localization of PSD-95+ puncta, which appear tucked in or hidden between the BDA+ varicosity and the Orx+ neuron (Fig. 6A5,B5,C5).

In series triple-stained for BDA, VGAT, and Orx, Orx+ neurons were also seen to be surrounded by VGAT+ varicosities. Many BDA-labeled VGAT+ varicosities were in close apposition to Orx+ soma or dendrites (Fig. 5C). As judged from the rotated and magnified 3D images of such cases, the BDA+[VGAT+] varicosity was in contact with the Orx+ cell (Fig. 5C, small images) through three axes.

In series triple-stained for BDA, Geph, and Orx, Geph staining (Cy5) appeared punctate, generally in larger puncta than PSD-95 and frequently associated with Orx+ soma and dendrites (Fig. 5D). In multiple BDA+:Orx+ contacts (Fig. 5D), Geph+ puncta were seen facing the BDA+ varicosity and associated with the Orx+ cell (Fig. 5D, top small images), such that they appeared to be located between the terminal and cell in merged images (Fig. 5D, lower small image). From 112 acquired images of appositions (from n = 3 cases), 93 BDA+:Orx+ contacts (>80%) were confirmed in rotated and magnified 3D images, and 44 or 47.3% showed Geph+ puncta between the BDA+ varicosity and the Orx+ cell.

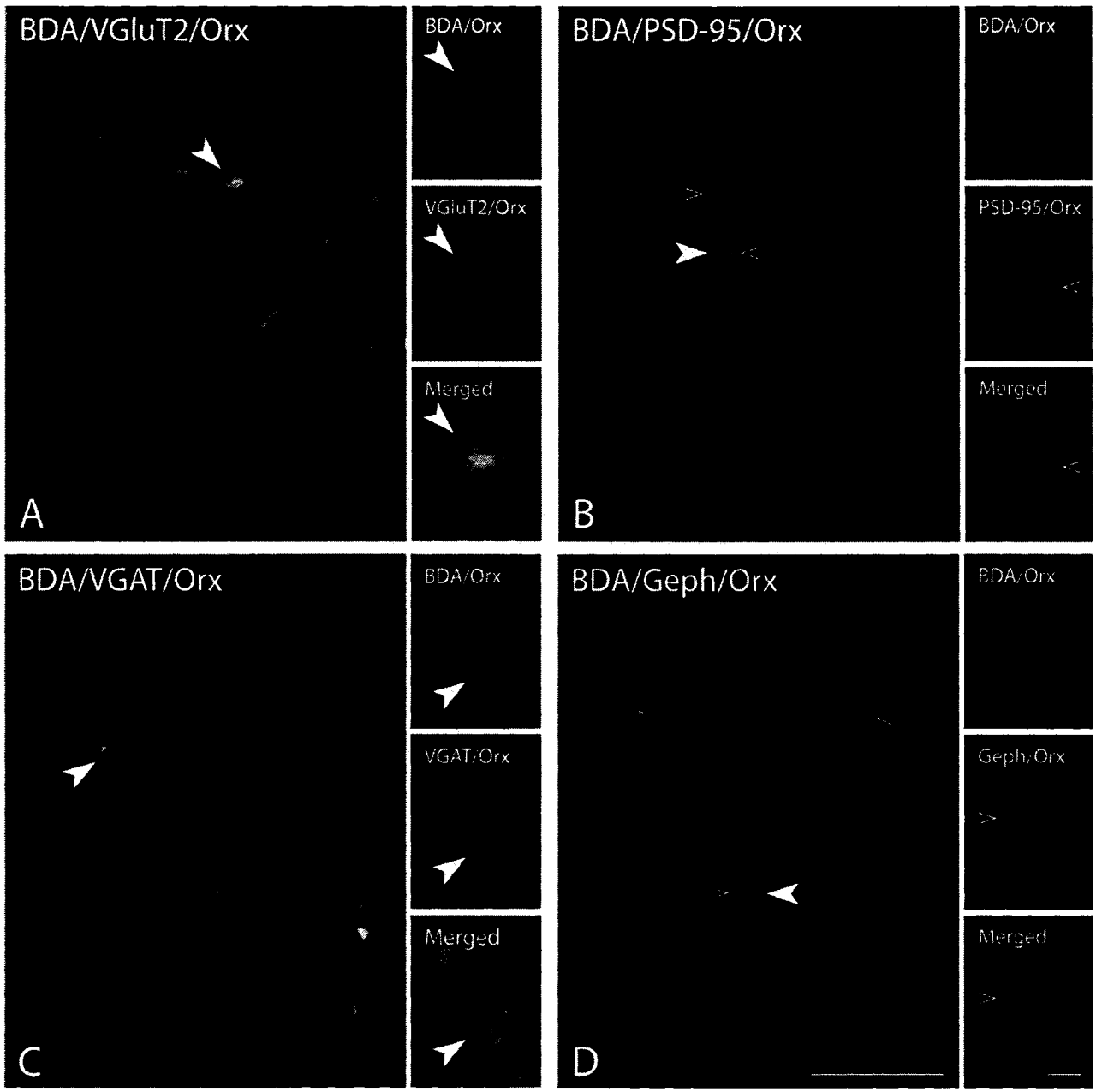

Fig. 5. The presence of presynaptic VGluT2 or VGAT and postsynaptic PSD-95 or Gephyrin (Geph) proteins in contacts between BDA-labeled varicosities and Orx+ neurons. **A:** Rendered 3D confocal image (16 serial 0.50-μm thick optical sections) of a BDA-labeled axon (in green, Cy2), whose varicosities (in yellow) are positive for VGluT2 (in red, Cy3). One of these varicosities is in apposition (arrowhead) to an Orx+ neuron (in pseudocolor blue, Cy5), as evident in the rendered zoom images on the right (6 serial 0.5-μm thick optical sections) depicting in detail the relation between the BDA+ varicosity (top) or the contained VGluT2 (middle) with the Orx+ neuron surface and showing the three elements together in the merged image (bottom). Note also on the left other VGluT2+ varicosities in contact with the Orx+ neuron. **B:** Rendered 3D confocal image (9 serial 0.33-μm thick optical sections) of a BDA+ varicosity (arrowhead, in green, Cy2) facing a PSD-95+ profile (opposite pointer, in pseudocolor red, Cy5) located between the varicosity and the surface of the Orx+ neuron (in pseudocolor blue, Cy3). As evident in the zoom rendered images on the right (13 serial 0.33-μm thick optical sections), the BDA+ varicosity is apposed to the Orx+ process (top image), opposite the PSD-95+ punctum, which is on the surface of the Orx+ process (pointer, middle image) and between the BDA+ varicosity and the Orx+ process (pointer in the merged image, bottom). Note the presence of other PSD-95+ puncta over the Orx+ neuron (upper pointer) at the left panel. **C:** Rendered 3D confocal image (28 serial 0.5-μm thick optical sections) of a BDA-labeled axon (in green, Cy2), from which most varicosities (in yellow) are positive for VGAT (in red, Cy3) and come into contact (large arrowhead) with the dendrites and soma of the Orx+ neuron. As seen in the rendered zoom images on the right (8 serial 0.5-μm thick optical sections), the BDA+ varicosity (top image) containing VGAT (middle image) appears to be in contact with the surface of the Orx+ neuron (merged image, bottom). Note in the left image other VGAT+ varicosities also appear to appose the Orx+ neuron. **D:** Rendered 3D confocal image (14 serial 0.33-μm thick optical sections) of BDA-labeled axonal varicosities (arrowhead, green, Cy2) facing Geph+ puncta (facing pointer, pseudocolor red, Cy5) over an Orx+ neuron (pseudocolor blue, Cy3). As evident in the zoom rendered images at the right (12 serial 0.33-μm thick optical sections), the apposition of the BDA+ varicosity with the Orx+ neuron (top image) is associated with a Geph+ punctum on the surface of the Orx+ neuron (pointer, middle image) and between the BDA+ varicosity and the Orx+ neuron (merged image, pointer, bottom). Note the presence of other Geph+ puncta over the Orx+ neuron (upper pointers) in the left panel. Deconvolution iterative restoration (see Materials and Methods) was applied to the Cy5 channel (in B and C, left panels, and in A–D, right panels), the Cy3 channel (in C, left panel, and in C,D, right panels) and the Cy2 channel (in B–D). Tonal range adjustments for each individual RGB channel were made for all pictures. Scale bars = 10 μm in left large panel in D (applies to large left panels in A–C); 1 μm in D, zoom bottom image (applies to zoom images in A–C).

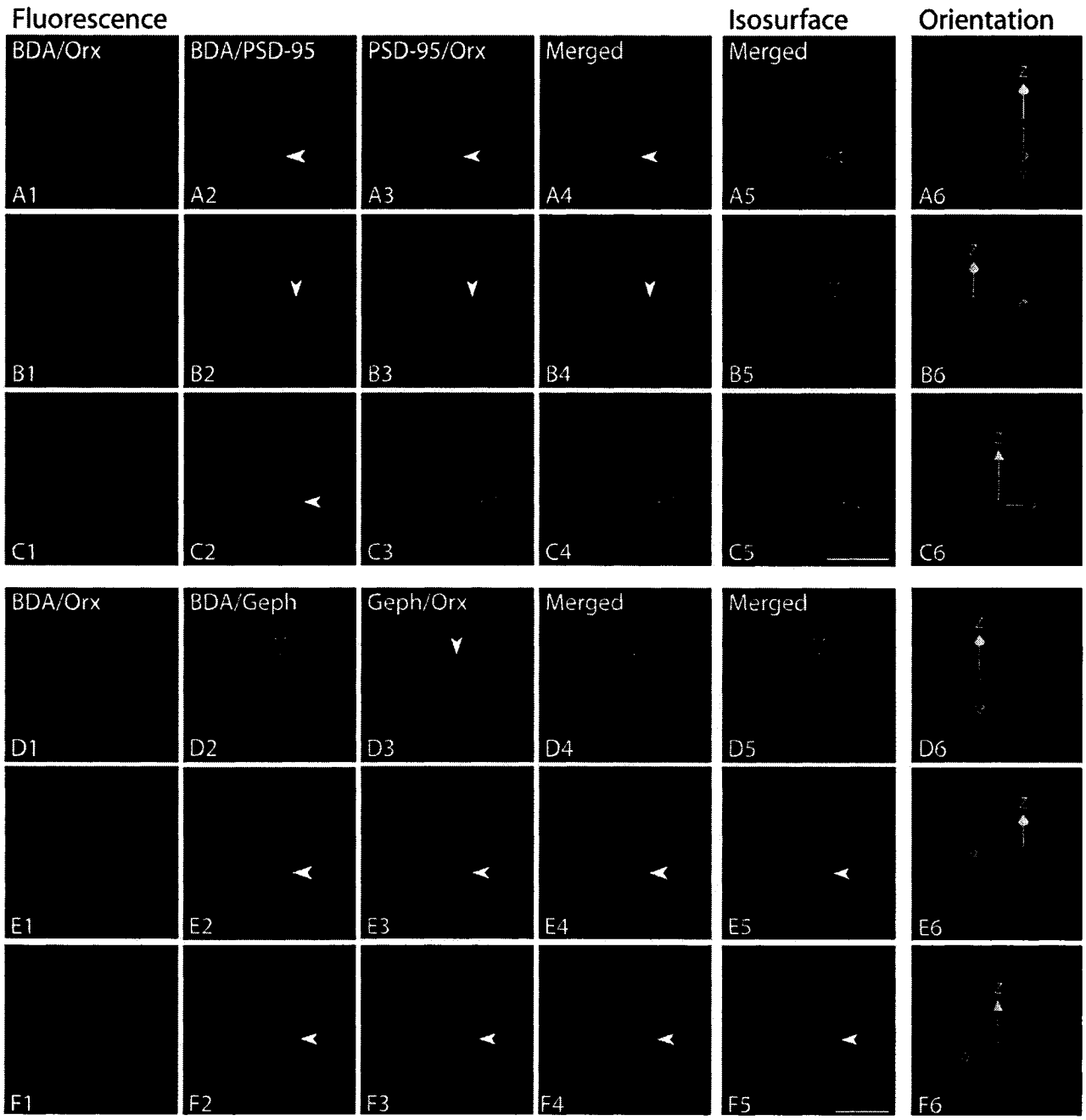

Fig. 6. 3D localization of postsynaptic proteins PSD-95 or gephyrin (Geph) between BDA+ terminals and Orx+ neurons. **A–C:** Orthogonal views (see below) of a high-resolution rendered confocal 3D image (40 serial ~0.06-μm thick optical sections) in semitransparent fluorescence rendering (columns 1–4) or opaque isosurface (column 5) views of a single contact between a BDA+ varicosity (in green, Cy2) and an Orx+ proximal dendrite (in blue, Cy3), with the presence of PSD-95+ puncta (in red, Cy5) between the varicosity and dendrite. The BDA+ varicosity is in contact with the Orx+ process (A1–C1), and in clear apposition to a PSD-95+ profile (solid arrowheads in A2–C2,), which is in turn located on the surface of the Orx+ neuron (solid arrowheads in A3,B3). The localization of the PSD-95+ profile between the two structures is evident in the triple merged fluorescent image (solid arrowheads in A4,B4) as well as in the triple merged isosurface rendering image, where the punctum appears almost completely occluded (dotted arrowheads in A5–C5). The PSD-95+ punctum is completely occluded in certain of the orthogonal views (dotted arrowheads in C3–C5). A6–C6: Representation of the three orthogonal views with orientation markers showing the X, Y, Z axes. **D–F:** Orthogonal views of a high-resolution rendered confocal 3D image (38 serial ~0.08-μm thick optical sections) in semitransparent fluorescence rendering (columns 1–4) or opaque isosurface rendering (column 5) views of a single contact between a BDA+ varicosity (in green, Cy2) and an Orx+ soma (in blue, Cy3), with the presence of Geph+ puncta (in red, Cy5) between the terminal and soma. The BDA+ varicosity is in contact with an Orx+ soma (D1–F1) and in clear apposition to a Geph+ profile (solid arrowheads in E2,F2), which is in turn located on the surface of the Orx+ neuron (solid arrowheads in D3–F3). The localization of the Geph+ profile between the two structures is evident in the triple merged fluorescent image (solid arrowheads in E4,F4) as well as in the triple merged isosurface image (solid arrowheads in E5,F5). Note the relative occlusion of the Geph+ profile in the rendered isosurface images, evidencing its location between the two structures. Due to the orthogonal views, the Geph+ puncta are completely occluded in some of them (dotted arrowheads in D2,D4,D5). D6–F6: Representation of the three orthogonal views with orientation markers showing the X, Y, Z axes. Deconvolution iterative restoration (see Materials and Methods) was applied to the Cy5, Cy3, and Cy2 channels. Scale bars = 1 μm in C5 (applies to A–C), and in F5 (applies to D–F).

For further analysis, image stacks with high z-axis resolution (0.05–0.10 μm optical slices) were acquired of 19 (from n = 3 cases) BDA, Geph, and Orx appositions and examined. Contacts were seen between BDA+ varicosities and Orx+ neurons, as evidenced from 3D orthogonal views (Fig. 6D1,E1,F1). Geph+ profiles were observed in apposition to BDA+ varicosities (Fig. 6E2,F2) and in association with the surface of Orx+ neurons (Fig. 6D3,E3,F3), located between BDA+ and Orx+ elements (Fig. 6E4,F4). Opaque isosurface rendering of the three elements evidenced the localization of Geph+ puncta between the BDA+ varicosity and the Orx+ neuron (Fig. 6D5,E5,F5).

DISCUSSION

The present study presents qualitative and quantitative evidence that Orx neurons are innervated by afferents from the BF cholinergic cell area. Yet from this cholinergic cell area the afferents were predominantly comprised of noncholinergic terminals. Numerous glutamatergic and GABAergic varicosities contacted Orx neurons in the LH and could thus respectively exert excitatory and inhibitory influences on their activity during wake and sleep states.

BF projections to Orx neurons

We show here that anterogradely labeled fibers from the MCPO-SI of the BF cholinergic cell area extend into the region of the Orx cells in the tuberal hypothalamus. As shown and discussed in our previous study (Henny and Jones, 2006), the fibers reached the caudal hypothalamus through the ventrolateral portion of the MFB, which has long been known to carry fibers from this forebrain area (Swanson, 1976; Veening et al., 1982; Grove, 1988). From this component, collaterals fan out through the LH and extend dorsomedially, although less numerously, through the PF and sparsely into the DMH.

We estimated here using stereology that Orx neurons are most numerous within the LH, numbering ~1,800, less numerous within the PF, numbering ~500, and intermediate in the DMH numbering ~900 for a total of ~3,200 neurons per side. The total number (in Long Evans rats) is similar to that previously estimated by us as ~3,400 Orx+ neurons per side (in Wistar rats) (Modirrousta et al., 2005) and to one other published number estimated by stereological analysis as ~2900 Orx+ neurons per side (in Wistar rats) (Allard et al., 2004). According to conventional delineation as the region lateral to the fornix through which the MFB fiber systems travel, >50% (or ~1,800) of the Orx cells are located in the LH.

We show here that BF terminals, which would originate from a relatively small number of caudally projecting cells in the MCPO-SI labeled by the BDA injections, contact a significant proportion (~28%) of all Orx+ cells. This input was topographically arranged, as the proportions of Orx+ cells contacted were substantial (~41%) in the LH and small in the more medial PF (~11%) and DMH (~9%). Notably, from similar injection sites, BF terminals contact only ~15% of the total LH cell population (estimated at ~50,000 through the tuberal hypothalamus) (Henny and Jones, 2006), suggesting a selective enrichment of BF terminals upon the Orx neurons relative to all other chemically unidentified neurons of the LH. According to a recent extensive survey of afferents to the Orx neurons using both anterograde and retrograde tracing (Yoshida et al., 2006), the overall proportion of Orx neurons contacted by BF afferents (~28%, from the present study) would be comparable to that originating from the adjacent ventrolateral preoptic area (31%). In the former work, the BF was not considered to be among the major afferent sources to the Orx neurons, although it contained a moderate number of afferent cells (Yoshida et al., 2006). In that study the afferents were identified by injections of retrograde tracers into the region where the Orx+ neurons are most concentrated, immediately surrounding the fornix within the dorsal PF, the lateral DMH, and the dorsomedial region of the LH, and thus highlighted major sources of input from the more medial basal telencephalic afferent systems. From our present and previous (Gritti et al., 1994; Henny and Jones, 2006), as well as other early tracing studies (Swanson, 1976; Veening et al., 1982; Grove, 1988), the MCPO-SI would fit within a lateral-to-medial as well as ventral-to-dorsal topographically organized system of fibers coursing within the MFB and serving as afferents to the hypothalamus and, notably, as the present results indicate, the Orx neurons therein.

Predominant innervation by noncholinergic, glutamatergic, and GABAergic BF terminals of Orx neurons

In the LH, of the total number of Orx neurons contacted by BF axonal varicosities (~41%, see above), only a minimal proportion (~4%) was innervated by cholinergic varicosities, whereas the major proportion was innervated by glutamatergic or GABAergic varicosities. Similarly, only 2% of the varicosities on Orx+ cells were VAChT+ in this material. These results are in line with our previous study showing that cholinergic BF terminals in the LH comprise less than 10%, whereas glutamatergic and GABAergic terminals comprise the vast majority of the BF terminals in the LH (Henny and Jones, 2006). These are not in agreement with the recent results of Sakurai et al. (2005) using a transgene for a tetanus toxin tracer (tetanus toxin C fragment fused to green fluorescent protein, TTC::GFP), which is believed to be transported transynaptically and retrogradely, linked to an *orexin* promoter together with fluorescent staining for choline acetyltransferase (ChAT). In those studies, essentially all retrogradely labeled neurons in the cholinergic cell area of the BF were judged to be immunostained for ChAT. We recognize the possibility that the TTC::GFP tracer could be taken up by terminals on distal dendrites that were not evident in our fluorescent material. On the other hand, previous results from our lab and from other groups utilizing retrograde transport of traditional tracers also found minimal proportions of descending projections from cholinergic BF neurons (<5%) to the brainstem or hypothalamus and the region of the Orx cell bodies and dendrites (Grove, 1988; Semba et al., 1989; Gritti et al., 1994; Bayer et al., 1999). As discussed by Sakurai et al. (2005), retrograde labeling by TTC::GFP could be due to transynaptic transport along with retrograde transport that could result in labeling of a large number and proportion of cholinergic BF cells as higher-order afferent neurons. Such an indirect, multisynaptic influence of cholinergic BF neurons upon Orx neurons might be expected to exist as a feedback on the Orx neurons that project into the region of the cholinergic cells (Espana et al., 2005) and would exert an excitatory effect through Orx on the cholinergic neurons (Eggermann et al.,

2001). On the other hand, from electrophysiological studies it appears that cholinergic input can have an important influence on Orx neurons, since cholinergic agonists can depolarize and excite the Orx neurons (Bayer et al., 2005; Sakurai et al., 2005). Although the BF cholinergic cells may participate in this influence, the pontomesencephalic cholinergic neurons likely play a more dominant role, given previous evidence of their more substantial projections into the region of the Orx cells (Ford et al., 1995; Bayer et al., 1999).

We found that a substantial proportion of BF-innervated Orx neurons were contacted by VGluT2 containing BDA-labeled terminals (~31%), and that a substantial proportion of the BDA-labeled terminals contacting Orx neurons were VGluT2+ (~17%). Glutamate has been shown to depolarize Orx neurons through both NMDA and AMPA receptors in vitro (Li et al., 2002; Yamanaka et al., 2003b). Orx neurons have been described as receiving a relatively high density of VGluT2+ varicosities and asymmetric, presumed excitatory synapses (Horvath and Gao, 2005). From the present results, one source of these multiple glutamatergic inputs can be attributed to BF neurons.

The major proportion of BF-innervated Orx neurons were contacted by VGAT containing BDA-labeled terminals (~67%), and a major proportion of the BDA-labeled varicosities were VGAT+ (~58%), indicating that GABAergic BF neurons can have a potent influence on Orx neurons. GABA has been shown to hyperpolarize and inhibit Orx neurons that are otherwise spontaneously active in vitro (Li et al., 2002; Eggermann et al., 2003; Yamanaka et al., 2003b). Interestingly, Orx neurons are considered to have a relatively sparse GABAergic input, particularly in relation to the glutamatergic input, with a ratio of inhibitory to excitatory synapses estimated as 1 to 10 (Horvath and Gao, 2005). In light of the latter results, it would appear that the BF GABAergic neurons may play a particularly important role in providing this inhibitory input and influence to the Orx cells.

BF glutamatergic and GABAergic synaptic input onto Orx neurons

We confirmed by confocal laser scanning microscopy and 3D image rendering and rotation that BDA-labeled BF varicosities appeared to contact Orx neurons in the LH. By continuous rotation through three axes, we were thus able to establish for large numbers of varicosities that there appeared to be no space between the varicosity and the Orx+ cell. Such confirmation has been considered by others to represent strong evidence for synaptic contacts (Wouterlood et al., 2002). Yet it is well recognized that only the resolution of the electron microscope provides absolute proof of such contacts by presynaptic elements with postsynaptic targets.

More specific evidence is provided for the synaptic nature of glutamatergic and GABAergic terminals by the presence of the presynaptic vesicular transporters. VGluT2 and VGAT, which were demonstrated in the BDA-labeled varicosities apposed to Orx cells, confer the capacity to release glutamate and GABA and are concentrated in the presynaptic terminal at asymmetric and symmetric synapses, respectively (Gilmor et al., 1996; Chaudhry et al., 1998; Bellocchio et al., 2000; Takamori et al., 2000; Fremeau et al., 2001, 2004; Gualix et al., 2003).

Lastly, we show that in confirmed contacts of BDA-labeled varicosities with Orx cells, postsynaptic proteins of PSD-95 and Geph are situated facing the varicosity and in association with the Orx+ cell. Similar to proportions of BDA-labeled varicosities ostensibly contacting Orx+ neurons that were VGluT2+ and VGAT+ (above), the proportions of confirmed contacts by BDA-labeled varicosities on Orx+ neurons that showed PSD-95 or Geph puncta between the terminal and cell were ~22% and ~47%, respectively. Postsynaptic proteins, PSD-95, and Geph are constituent parts of the postsynaptic scaffolding of asymmetric, excitatory (Sheng and Pak, 2000), and symmetric inhibitory synapses (Sassoe-Pognetto and Fritschy, 2000), respectively. At excitatory synapses, PSD-95 colocalizes by direct and indirect association with NMDA and AMPA receptors (Sassoe-Pognetto et al., 2003). At inhibitory synapses, Geph is colocalized with the most common synaptic subtypes of $GABA_A$ receptors and is suggested to participate in their anchoring to the postsynaptic membrane (Sassoe-Pognetto et al., 1995; Giustetto et al., 1998). The location of postsynaptic proteins sandwiched between presynaptic and postsynaptic elements has been considered strong evidence for synaptic contacts in 3D rendered confocal images (Wouterlood et al., 2003). We thus believe that the present results showing both pre- and postsynaptic elements for glutamatergic and GABAergic synapses in association with BDA-labeled terminals contacting Orx neurons provide compelling evidence for BF glutamatergic and GABAergic synaptic input to the Orx cells.

Functional significance of the cholinergic, glutamatergic, and GABAergic BF input to Orx neurons

Orx neurons play a key role in stimulating and maintaining arousal by excitatory influences on multiple systems, including the cerebral cortex, hypothalamic, and brainstem arousal systems, as well as sympathetic and motor circuits in the spinal cord (Peyron et al., 1998; van den Pol, 1999; Saper et al., 2001; Taheri et al., 2002; Krout et al., 2003; Siegel, 2004; Jones and Muhlethaler, 2005; Sakurai, 2005). As now shown by recent studies, they are in turn influenced by afferent input from multiple forebrain and brainstem systems (Sakurai et al., 2005; Yoshida et al., 2006). Here we show that neurons of the BF cholinergic cell area, which themselves are importantly involved in regulating sleep/wake states, contribute significantly to that afferent input. The BF input was particularly dense onto the Orx neurons in the LH, which despite claims of being selectively activated with reward seeking (Harris et al., 2005), have also clearly been shown to discharge and express c-Fos in association with simple waking, arousal, or stress (Espana et al., 2003; Lee et al., 2005a; Mileykovskiy et al., 2005; Modirrousta et al., 2005).

In contrast to recent claims (above, Sakurai et al., 2005), the cholinergic BF cells appear to contribute minimally to the innervation of the Orx neurons in the LH. Cholinergic BF neurons discharge in a manner (Lee et al., 2005b) that differs fundamentally from that of recently identified Orx neurons across sleep/wake states (Lee et al., 2005a). Whereas cholinergic neurons discharge maximally during both waking and PS in association with cortical activation, Orx neurons discharge maximally during waking in association with movement and muscle tone and cease firing during PS sleep with muscle atonia (Jones, 2005b). It is

thus not surprising that Orx neurons are not under the direct control of cholinergic BF neurons. To the contrary, the silence of Orx neurons during PS sleep is the condition under which cholinergic neuronal discharge stimulates cortical activation in association with the muscle atonia of that state.

The Orx neurons receive a substantial glutamatergic input from BF neurons, indicating that these glutamatergic neurons can exert a significant excitatory influence on Orx cells. In single unit recording studies, many noncholinergic BF neurons have been identified that discharge maximally during active waking and are virtually silent during sleep, including PS sleep (Szymusiak and McGinty, 1986b; Lee et al., 2004, 2005b). The discharge of these neurons is positively correlated with postural muscle tonus or neck electromyographic (EMG) activity (Lee et al., 2004), like that of the Orx neurons (Jones, 2005b; Lee et al., 2005b). We propose that such noncholinergic neurons are glutamatergic and could facilitate behavioral arousal in part by exciting the Orx cells.

The major input to the Orx neurons from BF is GABAergic. Given the purportedly small inhibitory input relative to excitatory input onto Orx neurons (Horvath and Gao, 2005), this GABAergic input from BF neurons might be of critical importance in inhibiting the discharge of Orx neurons during periods of behavioral quiescence, sleep, and/or muscle atonia (Lee et al., 2005a). Although we have identified GABAergic neurons that discharge in association with cortical activation (Manns et al., 2000), we propose that the innervation of the Orx neurons originates from the particular GABAergic BF neurons that are active during sleep (Modirrousta et al., 2004) and discharge during SWS and/or PS sleep in negative correlation with muscle tonus or EMG (Szymusiak and McGinty, 1986b; Manns et al., 2000; Lee et al., 2004; Jones, 2005b).

Orexin has been attributed a particularly important role in maintaining arousal, since in its absence in knockout mice or that of its receptor in dogs or Orx neurons in humans, narcolepsy occurs (Chemelli et al., 1999; Lin et al., 1999; Peyron et al., 2000; Thannickal et al., 2000; Hara et al., 2001). In humans, narcolepsy is characterized by excessive daytime sleepiness, short onset of REM sleep, and/or loss of postural muscle tone, known as cataplexy. Accordingly, the excitation of Orx neurons by presumed wake-active, glutamatergic BF neurons could normally serve to prevent sleep onset and loss of postural muscle tone, whereas the inhibition of Orx neurons by presumed sleep-active GABAergic BF neurons could promote sleep onset and the loss of postural muscle tone. It could be due in part to withdrawal of the major BF GABAergic input to Orx neurons that neurotoxic lesions of the BF result in a severe disruption of SWS and PS (Szymusiak and McGinty, 1986a). Moreover, chemical stimulation of the BF with cholinergic agonists or agents exciting cholinergic neurons can elicit PS with atonia in cats and rats (Hernandez-Peon et al., 1963; Cape et al., 2000; Jones, 2004) and/or cataplexy in dogs (Nishino et al., 1995). Cholinergic agonists and ACh, which is released in the BF maximally during PS (Vazquez and Baghdoyan, 2001), could excite noncholinergic, presumed GABAergic BF neurons (Fort et al., 1998; Wu et al., 2000), including those that innervate the Orx neurons and thereby elicit PS and/or muscle atonia.

In conclusion, the present study reveals an important glutamatergic and GABAergic input to Orx neurons from BF neurons. Glutamatergic BF neurons can excite Orx neurons to stimulate behavioral arousal and waking. GABAergic BF neurons can inhibit Orx neurons to diminish behavioral arousal along with muscle tone and thereby promote sleep, including PS with muscle atonia.

ACKNOWLEDGMENTS

We thank Robert H. Edwards and Robert T. Fremeau (Departments of Neurology and Physiology, University of California San Francisco School of Medicine, San Francisco, CA) for kindly supplying the antibody for VGluT2. We thank Lynda Mainville for excellent technical assistance, and Mandana Modirrousta for contributions to the study of the Orx cell population.

LITERATURE CITED

Allard JS, Tizabi Y, Shaffery JP, Trouth CO, Manaye K. 2004. Stereological analysis of the hypothalamic hypocretin/orexin neurons in an animal model of depression. Neuropeptides 38:311–315.

Bayer L, Risold PY, Griffond B, Fellmann D. 1999. Rat diencephalic neurons producing melanin-concentrating hormone are influenced by ascending cholinergic projections. Neuroscience 91:1087–1101.

Bayer L, Eggermann E, Serafin M, Grivel J, Machard D, Muhlethaler M, Jones BE. 2005. Opposite effects of noradrenaline and acetylcholine upon hypocretin/orexin versus melanin concentrating hormone neurons in rat hypothalamic slices. Neuroscience 130:807–811.

Bellocchio EE, Reimer RJ, Fremeau RT Jr, Edwards RH. 2000. Uptake of glutamate into synaptic vesicles by an inorganic phosphate transporter. Science 289:957–960.

Broberger C, De Lecea L, Sutcliffe JG, Hokfelt T. 1998. Hypocretin/orexin- and melanin-concentrating hormone-expressing cells form distinct populations in the rodent lateral hypothalamus: relationship to the neuropeptide Y and agouti gene-related protein systems. J Comp Neurol 402:460–474.

Cape EG, Manns ID, Alonso A, Beaudet A, Jones BE. 2000. Neurotensin-induced bursting of cholinergic basal forebrain neurons promotes gamma and theta cortical activity together with waking and paradoxical sleep. J Neurosci 20:8452–8461.

Chaudhry FA, Reimer RJ, Bellocchio EE, Danbolt NC, Osen KK, Edwards RH, Storm-Mathisen J. 1998. The vesicular GABA transporter, VGAT, localizes to synaptic vesicles in sets of glycinergic as well as GABAergic neurons. J Neurosci 18:9733–9750.

Chemelli RM, Willie JT, Sinton CM, Elmquist JK, Scammell T, Lee C, Richardson JA, Williams SC, Xiong Y, Kisanuki Y, Fitch TE, Nakazato M, Hammer RE, Saper CB, Yanagisawa M. 1999. Narcolepsy in orexin knockout mice: molecular genetics of sleep regulation. Cell 98:437–451.

Eggermann E, Serafin M, Bayer L, Machard D, Saint-Mleux B, Jones BE, Muhlethaler M. 2001. Orexins/hypocretins excite basal forebrain cholinergic neurones. Neuroscience 108:177–181.

Eggermann E, Bayer L, Serafin M, Saint-Mleux B, Bernheim L, Machard D, Jones BE, Muhlethaler M. 2003. The wake-promoting hypocretin-orexin neurons are in an intrinsic state of membrane depolarization. J Neurosci 23:1557–1562.

Espana RA, Valentino RJ, Berridge CW. 2003. Fos immunoreactivity in hypocretin-synthesizing and hypocretin-1 receptor-expressing neurons: effects of diurnal and nocturnal spontaneous waking, stress and hypocretin-1 administration. Neuroscience 121:201–217.

Espana RA, Reis KM, Valentino RJ, Berridge CW. 2005. Organization of hypocretin/orexin efferents to locus coeruleus and basal forebrain arousal-related structures. J Comp Neurol 481:160–178.

Ford B, Holmes C, Mainville L, Jones BE. 1995. GABAergic neurons in the rat pontomesencephalic tegmentum: codistribution with cholinergic and other tegmental neurons projecting to the posterior lateral hypothalamus. J Comp Neurol 363:177–196.

Fort P, Khateb A, Serafin M, Muhlethaler M, Jones BE. 1998. Pharmacological characterization and differentiation of non-cholinergic nucleus basalis neurons in vitro. Neuroreport 9:1–5.

Fremeau RT Jr, Troyer MD, Pahner I, Nygaard GO, Tran CH, Reimer RJ, Bellocchio EE, Fortin D, Storm-Mathisen J, Edwards RH. 2001. The expression of vesicular glutamate transporters defines two classes of excitatory synapse. Neuron 31:247–260.

Fremeau RT Jr, Voglmaier S, Seal RP, Edwards RH. 2004. VGLUTs define subsets of excitatory neurons and suggest novel roles for glutamate. Trends Neurosci 27:98–103.

Gilmor ML, Nash NR, Roghani A, Edwards RH, Yi H, Hersch SM, Levey AI. 1996. Expression of the putative vesicular acetylcholine transporter in rat brain and localization in cholinergic synaptic vesicles. J Neurosci 16:2179–2190.

Giustetto M, Kirsch J, Fritschy JM, Cantino D, Sassoe-Pognetto M. 1998. Localization of the clustering protein gephyrin at GABAergic synapses in the main olfactory bulb of the rat. J Comp Neurol 395:231–244.

Gritti I, Mainville L, Jones BE. 1993. Codistribution of GABA- with acetylcholine-synthesizing neurons in the basal forebrain of the rat. J Comp Neurol 329:438–457.

Gritti I, Mainville L, Jones BE. 1994. Projections of GABAergic and cholinergic basal forebrain and GABAergic preoptic-anterior hypothalamic neurons to the posterior lateral hypothalamus of the rat. J Comp Neurol 339:251–268.

Gritti I, Mainville L, Mancia M, Jones BE. 1997. GABAergic and other non-cholinergic basal forebrain neurons project together with cholinergic neurons to meso- and iso-cortex in the rat. J Comp Neurol 383: 163–177.

Grove EA. 1988. Efferent connections of the substantia innominata in the rat. J Comp Neurol 277:347–364.

Gualix J, Gomez-Villafuertes R, Diaz-Hernandez M, Miras-Portugal MT. 2003. Presence of functional ATP and dinucleotide receptors in glutamatergic synaptic terminals from rat midbrain. J Neurochem 87:160–171.

Hara J, Beuckmann CT, Nambu T, Willie JT, Chemelli RM, Sinton CM, Sugiyama F, Yagami K, Goto K, Yanagisawa M, Sakurai T. 2001. Genetic ablation of orexin neurons in mice results in narcolepsy, hypophagia, and obesity. Neuron 30:345–354.

Harris GC, Wimmer M, Aston-Jones G. 2005. A role for lateral hypothalamic orexin neurons in reward seeking. Nature 437:556–559.

Henny P, Jones BE. 2006. Vesicular glutamate (VGluT), GABA (VGAT), and acetylcholine (VAChT) transporters in basal forebrain axon terminals innervating the lateral hypothalamus. J Comp Neurol 496:453–467.

Hernandez-Peon R, Chavez-Ibarra G, Morgane PJ, Timo-Iaria C. 1963. Limbic cholinergic pathways involved in sleep and emotional behavior. Exp Neurol 8:93–111.

Horvath TL, Gao XB. 2005. Input organization and plasticity of hypocretin neurons: possible clues to obesity's association with insomnia. Cell Metab 1:279–286.

Jones BE. 2004. Activity, modulation and role of basal forebrain cholinergic neurons innervating the cerebral cortex. Prog Brain Res 145:157–169.

Jones BE. 2005a. Basic mechanisms of sleep-wake states. In: Kryger MH, Roth T, Dement WC, editors. Principles and practice of sleep medicine, 4th ed. Philadelphia: Elsevier Saunders. p 136–153.

Jones BE. 2005b. From waking to sleeping: neuronal and chemical substrates. Trends Pharmacol Sci 26:578–586.

Jones BE, Muhlethaler M. 2005. Modulation of cortical activity and sleep-wake state by hypocretin/orexin. In: de Lecea L, Sutcliffe JG, editors. The hypocretins: integrators of physiological systems. New York: Springer. p 289–301.

Krout KE, Mettenleiter TC, Loewy AD. 2003. Single CNS neurons link both central motor and cardiosympathetic systems: a double-virus tracing study. Neuroscience 118:853–866.

Lee MG, Manns ID, Alonso A, Jones BE. 2004. Sleep-wake related discharge properties of basal forebrain neurons recorded with micropipettes in head-fixed rats. J Neurophysiol 92:1182–1198.

Lee MG, Hassani O, Jones BE. 2005a. Discharge of identified orexin/hypocretin neurons across the sleep-waking cycle. J Neurosci 25:6716–6720.

Lee MG, Hassani OK, Alonso A, Jones BE. 2005b. Cholinergic basal forebrain neurons burst with theta during waking and paradoxical sleep. J Neurosci 25:4365–4369.

Li Y, Gao XB, Sakurai T, van den Pol AN. 2002. Hypocretin/orexin excites hypocretin neurons via a local glutamate neuron—a potential mechanism for orchestrating the hypothalamic arousal system. Neuron 36: 1169–1181.

Lin L, Faraco J, Li R, Kadotani H, Rogers W, Lin X, Qiu X, de Jong PJ, Nishino S, Mignot E. 1999. The sleep disorder canine narcolepsy is caused by a mutation in the hypocretin (orexin) receptor 2 gene. Cell 98:365–376.

Manns ID, Alonso A, Jones BE. 2000. Discharge profiles of juxtacellularly labeled and immunohistochemically identified GABAergic basal forebrain neurons recorded in association with the electroencephalogram in anesthetized rats. J Neurosci 20:9252–9263.

Mileykovskiy BY, Kiyashchenko LI, Siegel JM. 2005. Behavioral correlates of activity in identified hypocretin/orexin neurons. Neuron 46:787–798.

Millhouse OE. 1969. A Golgi study of the descending medial forebrain bundle. Brain Res 15:341–363.

Modirrousta M, Mainville L, Jones BE. 2004. GABAergic neurons with alpha2-adrenergic receptors in basal forebrain and preoptic area express c-Fos during sleep. Neuroscience 129:803–810.

Modirrousta M, Mainville L, Jones BE. 2005. Orexin and MCH neurons express c-Fos differently after sleep deprivation vs. recovery and bear different adrenergic receptors. Eur J Neurosci 21:2807–2816.

Nishino S, Tafti M, Reid MS, Shelton J, Siegel JM, Dement WC, Mignot E. 1995. Muscle atonia is triggered by cholinergic stimulation of the basal forebrain: implication for the pathophysiology of canine narcolepsy. J Neurosci 15:4806–4814.

Paxinos G, Watson C. 1986. The rat brain in stereotaxic coordinates. Sydney: Academic Press.

Peyron C, Tighe DK, van den Pol AN, de Lecea L, Heller HC, Sutcliffe JG, Kilduff TS. 1998. Neurons containing hypocretin (orexin) project to multiple neuronal systems. J Neurosci 18:9996–10015.

Peyron C, Faraco J, Rogers W, Ripley B, Overeem S, Charnay Y, Nevsimalova S, Aldrich M, Reynolds D, Albin R, Li R, Hungs M, Pedrazzoli M, Padigaru M, Kucherlapati M, Fan J, Maki R, Lammers GJ, Bouras C, Kucherlapati R, Nishino S, Mignot E. 2000. A mutation in a case of early onset narcolepsy and a generalized absence of hypocretin peptides in human narcoleptic brains. Nat Med 6:991–997.

Pfeiffer F, Simler R, Grenningloh G, Betz H. 1984. Monoclonal antibodies and peptide mapping reveal structural similarities between the subunits of the glycine receptor of rat spinal cord. Proc Natl Acad Sci U S A 81:7224–7227.

Sakurai T. 2005. Roles of orexin/hypocretin in regulation of sleep/wakefulness and energy homeostasis. Sleep Med Rev 9:231–241.

Sakurai T, Nagata R, Yamanaka A, Kawamura H, Tsujino N, Muraki Y, Kageyama H, Kunita S, Takahashi S, Goto K, Koyama Y, Shioda S, Yanagisawa M. 2005. Input of orexin/hypocretin neurons revealed by a genetically encoded tracer in mice. Neuron 46:297–308.

Saper CB, Chou TC, Scammell TE. 2001. The sleep switch: hypothalamic control of sleep and wakefulness. Trends Neurosci 24:726–731.

Sassoe-Pognetto M, Fritschy JM. 2000. Mini-review: gephyrin, a major postsynaptic protein of GABAergic synapses. Eur J Neurosci 12:2205–2210.

Sassoe-Pognetto M, Kirsch J, Grunert U, Greferath U, Fritschy JM, Mohler H, Betz H, Wassle H. 1995. Colocalization of gephyrin and GABAA-receptor subunits in the rat retina. J Comp Neurol 357:1–14.

Sassoe-Pognetto M, Panzanelli P, Sieghart W, Fritschy JM. 2000. Colocalization of multiple GABA(A) receptor subtypes with gephyrin at postsynaptic sites. J Comp Neurol 420:481–498.

Sassoe-Pognetto M, Utvik JK, Camoletto P, Watanabe M, Stephenson FA, Bredt DS, Ottersen OP. 2003. Organization of postsynaptic density proteins and glutamate receptors in axodendritic and dendrodendritic synapses of the rat olfactory bulb. J Comp Neurol 463:237–248.

Semba K, Reiner PB, McGeer EG, Fibiger HC. 1989. Brainstem projecting neurons in the rat basal forebrain: neurochemical, topographical, and physiological distinctions from cortically projecting cholinergic neurons. Brain Res Bull 22:501–509.

Sheng M, Pak DT. 2000. Ligand-gated ion channel interactions with cytoskeletal and signaling proteins. Annu Rev Physiol 62:755–778.

Siegel JM. 2004. Hypocretin (orexin): role in normal behavior and neuropathology. Annu Rev Psychol 55:125–148.

Swanson LW. 1976. An autoradiographic study of the efferent connections of the preoptic region in the rat. J Comp Neurol 167:227–256.

Swanson LW, Sanchez-Watts G, Watts AG. 2005. Comparison of melanin-concentrating hormone and hypocretin/orexin mRNA expression patterns in a new parceling scheme of the lateral hypothalamic zone. Neurosci Lett 387:80–84.

Szymusiak R, McGinty D. 1986a. Sleep suppression following kainic acid-induced lesions of the basal forebrain. Exp Neurol 94:598–614.

Szymusiak R, McGinty D. 1986b. Sleep-related neuronal discharge in the basal forebrain of cats. Brain Res 370:82–92.

Szymusiak R, Alam N, McGinty D. 2000. Discharge patterns of neurons in cholinergic regions of the basal forebrain during waking and sleep. Behav Brain Res 115:171–182.